Geologic Excursions in the Overthrust Belt and Metamorphic Core Complexes of the Intermountain Region

GUIDEBOOK — PART I

The Geological Society of America
Rocky Mountain and Cordilleran Sections Meeting
Salt Lake City, Utah
May 2 - 4, 1983

WILLIAM P. NASH
General Chairman

GREGORY D. HARPER
Field Trip Coordinator

KLAUS D. GURGEL
Editor

UTAH GEOLOGICAL AND MINERAL SURVEY
a division of
Utah Department of Natural Resources and Energy

Special Studies 59 May 1983

GEOLOGIC EXCURSIONS IN THE OVERTHRUST BELT AND METAMORPHIC CORE COMPLEXES

Geologic Excursions in the Overthrust Belt and Metamorphic Core Complexes of the Intermountain Region

GUIDEBOOK — PART I

The Geological Society of America
Rocky Mountain and Cordilleran Sections Meeting
Salt Lake City, Utah
May 2 - 4, 1983

WILLIAM P. NASH
General Chairman

GREGORY D. HARPER
Field Trip Coordinator

KLAUS D. GURGEL
Editor

UTAH GEOLOGICAL AND MINERAL SURVEY
a division of
Utah Department of Natural Resources and Energy

Special Studies 59 May 1983

Editor's Note: The papers contained in this Guidebook were solicited by the organizers of the GSA Rocky Mountain and Cordilleran Sections and have been edited and given a common format; however, their style and content have not been formally reviewed by the Utah Geological and Mineral Survey.

Contents

Utah Geological and Mineral Survey Special Studies 59, 1983
Guidebook Part 1 — GSA Rocky Mountain and Cordilleran Sections Meeting
Salt Lake City, Utah — May 2 - 4, 1983

GEOLOGY OF THE ALBION-RAFT RIVER-GROUSE CREEK MOUNTAINS AREA, NORTHWESTERN UTAH AND SOUTHERN IDAHO

David M. Miller
U.S. Geological Survey, 345 Middlefield Road, Menlo Park, CA 94025

Richard L. Armstrong
Department of Geological Sciences, University of British Columbia, Vancouver, B. C., Canada

Robert R. Compton
Department of Geology, Stanford University, Stanford, CA 94305

Victoria R. Todd
U.S. Geological Survey, 345 Middlefield Road, Menlo Park, CA 94025

INTRODUCTION

The Albion, Raft River, and Grouse Creek Mountains and parts of adjacent ranges expose a large metamorphic terrane ("metamorphic core complex") composed of metamorphic and igneous rocks forming basement for structurally overlying unmetamorphosed upper Paleozoic and Tertiary strata. The terrane has been studied by Armstrong (1968, 1970a), Compton (1972, 1975, 1983), Todd (1975, 1980, 1983), Williams and others (1975), Compton and others (1977), Armstrong and others (1978), Miller (1980, 1983), Covington (1983), and Jordan (1983). These workers have established remarkably similar structural, metamorphic, and igneous histories for separate parts of the terrane. A schematic summary of these events is given in Figure 1. Despite the extensive work in the terrane and bordering regions and the similar histories that have been developed for the many parts of the terrane, no synthesis of the region has been undertaken. This lack of regional synthesis can be partly ascribed to incompletely understood aspects, such as: a) the timing and geometry of the detachment of cover rocks, b) the age and correlation of most of the metasedimentary rocks, c) the timing, kinematics, and distribution of Mesozoic deformation, d) the relation between Mesozoic and Cenozoic ductile deformation, e) the relation between ductile and brittle deformation during the Cenozoic , and f) the relation between plutonism and ductile deformation. In particular, the inability to correlate much of the metasedimentary sequence in the terrane with stratified rocks elsewhere in the region has proved to be a major hindrance for developing regional tectonic models.

Stratigraphic nomenclature used in this guidebook largely follows Armstrong (1968) and Compton (1972, 1975); the reader should refer to these works for detailed descriptions of units and stratigraphic relations. Because of the difficulty of correlating the metamorphic rocks of the terrane, equivalent rock units have been assigned different ages by different workers; these differences are reflected in this guidebook, and are particularly evident in the figures. For example, the lower three units of the Raft River Mountains sequence (defined in Miller, 1983) have been assigned to the Cambrian (Armstrong, 1968), the late Proterozoic (?) (Compton, 1975; Todd, 1980), and the early Proterozoic (Miller, 1978; Crittenden, 1979). Unpublished work by all of the authors of this guidebook, including tentative stratigraphic assignments that will be subject to change in upcoming formal publications, is included in this guidebook.

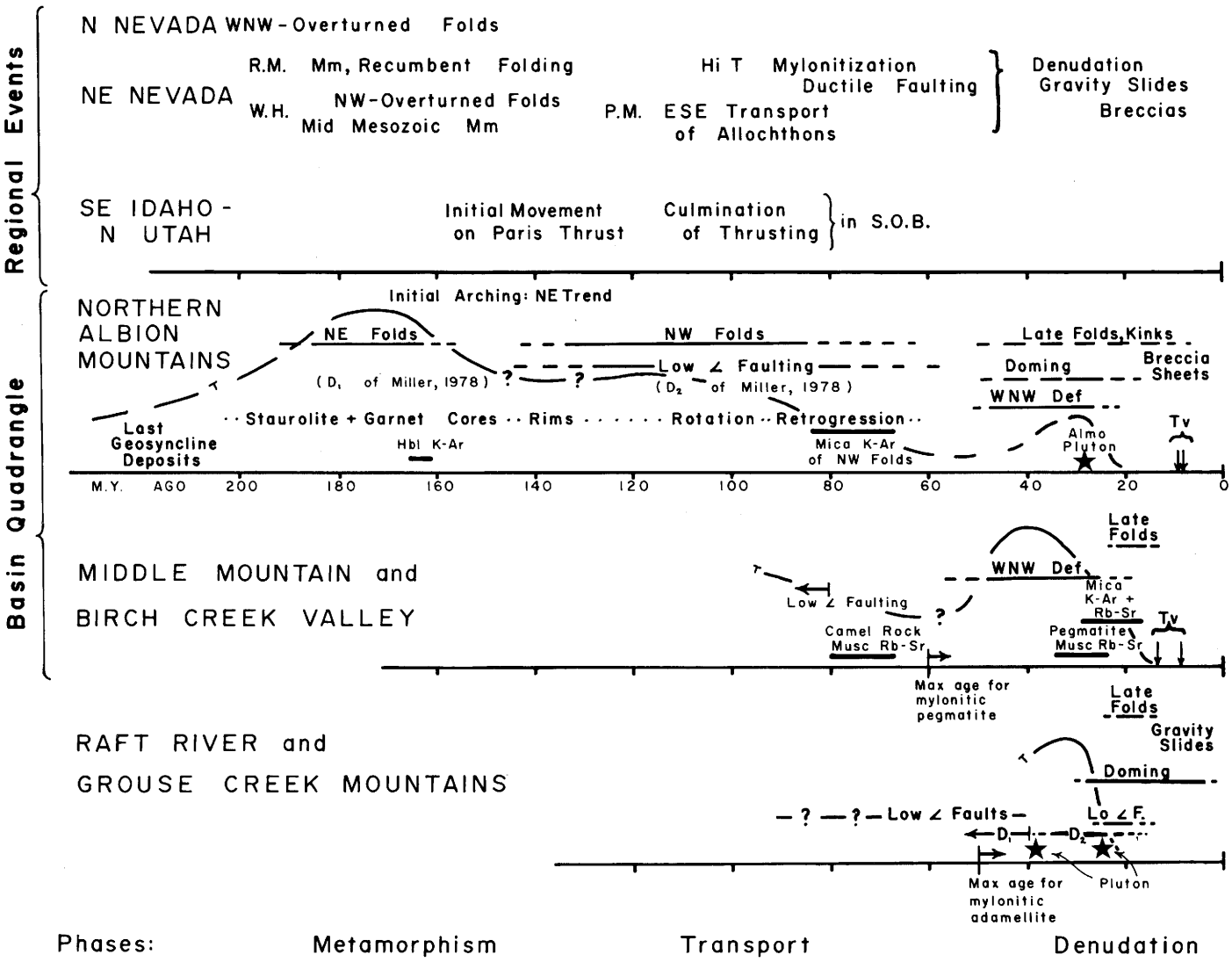

Figure 1. Comparison of the tectonic-metamorphic chronology of the region with the chronology for the Albion-Raft River-Grouse Creek Mountains metamorphic terrane. R. M. = Ruby Mountains, W. H. = Wood Hills, P. M. = Pequop Mountains, S. O. B. = Sevier Orogenic Belt; Tv = Tertiary volcanism.

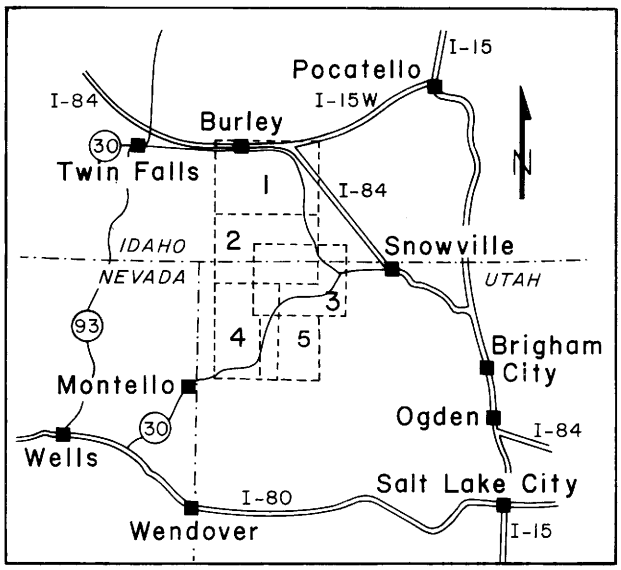

Figure 2. Location map showing maps of trip segments.

This field trip guidebook seeks to unify the studies done in disparate parts of the terrane, and focuses on broad relations such as structural sequence, character and timing of metamorphism, igneous history, and timing and geometry of middle to late Tertiary faulting. The guidebook is an expanded and updated version of one prepared for the Rocky Mountain Section meeting of the Geological Society of America, May 16-17, 1980 (Miller and others, 1980). Much of the area is not accessible without four wheel drive vehicles or long hikes. Some of the stops (Nos. 7, 8, 9, 10, 11, 13, and 14 of Day 1 and Nos. 4 and 5 of Day 2) described in this guide are reached via roads that are passable only during the summer months due to heavy snowfall in the mountains. Topographic maps showing the trip routes follow the text; they are indexed in Figure 2.

On the first day of this three-day trip we will examine metamorphic and igneous rocks in the Albion Mountains and discuss deformation styles and timing, the effects of intrusive rocks, regional stratigraphic problems, and Tertiary deformation and "detachment" faulting. Days 2 and 3 will be centered in the Raft River and Grouse Creek Mountains. On Day 2 we will examine the Archean basement in detail, discuss the general stratigraphic and structural relations in the Raft River Mountains, and then traverse much of a folded section of the thinned autochthonous and allochthonous rocks, examining structural styles and discussing correlation of the metamorphic rocks. On Day 3 the trip will focus on Miocene volcanic and sedimentary sequences and enclosed slices of upper Paleozoic strata, and the nature of their tectonic boundaries with the underlying metamorphic rocks of the core complex and sedimentary sequences around the margin of the metamorphic terrane.

FIELD TRIP ROAD LOG: FIRST DAY

Meet and organize at the Y-Dell Market at the eastern edge of Burley, Idaho, on U.S. Highway 30. Across from the market is Burley Airport. Begin mileage at the junction between U.S. Highway 30 and Idaho Route 81.

Mileage		Description
Incremental	Cumulative	
0.0	0.0	Turn Right on Rt. 81. As we drive east along the south side of the Snake River, which was a major barrier to immigrations during the 19th century, we can see a shield volcano to the NNE on the Snake River Plain. The Snake River Plain is a Miocene to Recent tectonic downwarp or graben filled with a thick sequence of mafic and felsic volcanic rocks and lesser sedimentary rocks. The Plain narrows to the northeast, and the age of initiation of volcanism youngs in that direction to the presently active Yellowstone area. To the south and southeast are the Albion Mountain. The range consists of two, broad, rounded mountains and several smaller hills, each physiographic culmination representing a structural dome underlain by resistant rocks. A low ridge extending north from the closest dome is underlain by metaquartzite with lesser marble and schist; most of these metamorphic rocks are of uncertain age. Also present are isolated low-angle fault-bounded slices of Mississippian, Permian, and

Triassic strata.

8.0 8.0 Turn Right (south) on Idaho Rt. 77 in town of Declo.

Burley is the Cassia County seat and is the center of a thriving agricultural area on the Snake River Plain. The town got its first boost near the turn of the century when it was decided that the railroad would be built through Burley rather than through Albion, the county seat at that time. In 1904 one of the Bureau of Reclamation's first major irrigation projects was initiated in this area, and Burley has prospered ever since. Ample evidence of the area's agricultural wealth is present in the fertile fields and new ranches on both sides of the road as we drive southward to the margin of the Snake River Plain.

4.8 12.8 We turn east as we climb the northern ridge of the Albion Mountains. Good road cuts here expose white, medium-grained metaquartzite that varies from orthoquartzite to micaceous quartzite and contains interbedded thick units of white-mica schist. Many small high-angle faults have caused considerable fracturing of the quartzite.

0.2 13.0 Boulders of black mylonite on the slope left of the road mark a low-angle fault trace. The fault juxtaposes the quartzite described above and thin-bedded, micaceous marble under the quartzite that is well-exposed farther up the road. The black mylonite locally contains breccia consisting of angular clasts of quartzite and chert. Foliated muscovite and garnet-bearing granite occurs in several dikes exposed in these road cuts.

2.8 15.8 **STOP 1**. Park on the right side of the road. On the left side of the road a Miocene rhyolite ash flow is exposed in the wash. This ash flow and underlying lava flows extend under the dry farm fields that surround us at this point and are equivalent to volcanic rocks of the Cotterel Mountains southeast across the Albion basin. Isolated exposures of these same volcanic rocks occur in numerous places in the Albion Mountains, indicating that the region must have been blanketed at one time by ash flows with only higher peaks protruding through aprons of volcanic ash. Removal of most of these aprons has exhumed prevolcanic topography. Uplift of the range with respect to surrounding lowlands has been minor in post-volcanic time.

In the wash adjacent to the road orange-weathered loess and ash are overlain by 1 m of bedded rhyolitic air-fall tuff and 2 m of a welded ash-flow tuff with a black glassy vitrophyre base. The welded tuff here caps a much thicker rhyolite flow that forms the resistant hogback of the Cotterel Mountains. The rhyolite flow and overlying low-potassium olivine basalt in the northern Cotterel Mountains have both been dated as 9.2 m.y. old (9.2 ± 1.5 m.y. for basalt; 9.2 ± 0.5 m.y. for rhyolite) and younger rhyolite ash flows, dated at localities west of the Albion Range, are about 8.5 m.y. old (Armstrong, 1975). These ash flows, typical of those on the southern Snake River Plain, are generally alkali rich rhyolite (~74% SiO_2 and ~5.0% K_2O) vitric tuffs with plagioclase, pyroxene (pigeonite and hypersthene) and

quartz as phenocyrsts. They must have been erupted at extremely high temperature. Source vents for the ash near Albion were probably in or near either the Jim Sage Mountains or southern Cotterel Mountains. Post-volcanic faulting and rotation has produced a gentle westward dip. The principal fault between the Cotterel Mountains and East Hills must dip gently eastward; it follows Marsh Creek north of Albion and wraps around the Big Bertha Dome through Connor Pass.

Even the volcanic rocks we see here may overlie a detachment fault with small displacement, peripheral to the major detachment surface underlying the Jim Sage and Cotterel Mountains and Raft River basin (Covington, 1983).

From the vehicles we can see a broad mountain, Mount Harrison, dominating the southern skyline (Figure 3). Its corresponding structural dome is Big Bertha Dome. The eastern ridge is largely a dip slope in Elba Quartzite. Dips are easterly along the eastern portion, horizontal on top, northerly on the slopes facing us, and northwesterly along the grassy western slopes. Overlying the autochthonous units (the Elba Quartzite and the schist of the Upper Narrows) are allochthonous quartzite and carbonate units that crop out in the tree-covered slopes farther west. The higher, western part of this dome consists of an overturned sequence of quartzite and schist of late Proterozoic or Paleozoic age. These west-dipping units lie on thin, faulted slices of Ordovician and Mississippian metamorphic rocks that in turn lie on autochthonous rocks of the western flank of Big Bertha Dome. The dome top is nearly flat and is a rounded triangular shape in plan view. A geologic map of the dome is shown in Figure 4.

0.9	16.7	Town of Albion. Proceed south on Rt. 77. Albion State Normal School, on the right side of the road at the north end of town, served as a teachers college from 1893 to 1946 and then as a church-run college until 1951. It was later leased by an outfit of dubious merit and stripped of furniture and other valuables and abandoned.

Albion was settled during the massive immigrations along the Oregon Trail in the middle part of the 19th century. An alternate route of the Oregon Trail looped through the verdent Marsh Creek Basin, where Albion is now located. Legend has it that a merchant's wagon, heavily laden with goods, bogged down in the swampy ground of Albion. Because the merchant could not drag his wagon out of the mire, he opened up shop on the spot and the town gradually grew around him. The town served as the Cassia County seat until early in the 20th Century.

6.0	22.7	Turn Right on gravel road marked "Pomerelle Ski Area."
1.0	23.7	**STOP 2**. Park on the roadside just beyond the National Forest sign. The schist of the Upper Narrows exposed in the roadcut is typically platy, quartzose, brown mica schist. It contains biotite, white mica, plagioclase, and quartz as major constituents with minor

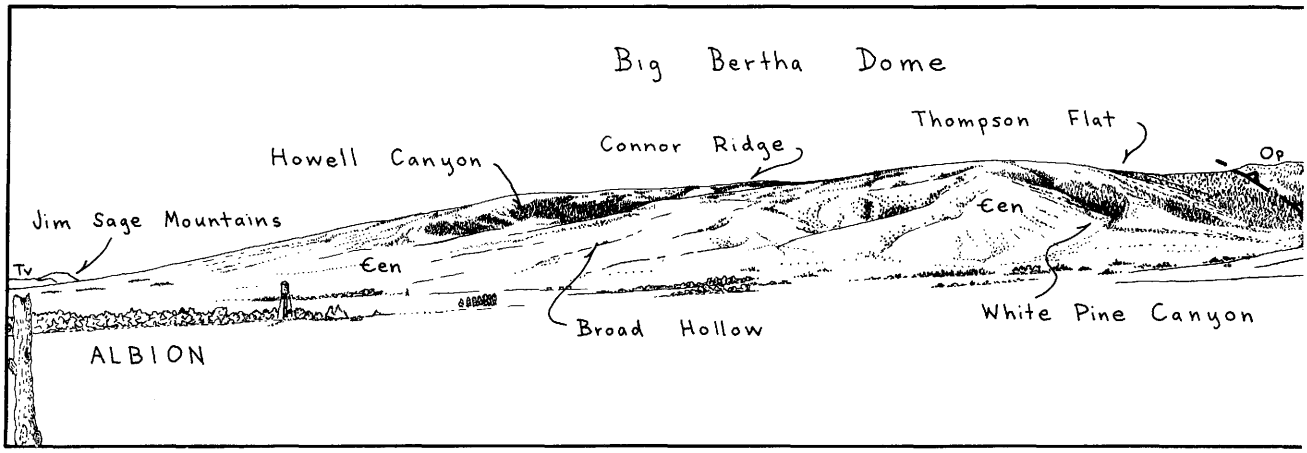

Figure 3. Looking southeast to west from STOP 1 (DAY 1) on the highway, 1 mile northwest of the town of Albion (visible on left hand side of the drawing). The Big Bertha Dome is expressed by grass-and sagebrush-covered dip-slopes composed of the Elba Quartzite and the schist of the Upper Narrows (Ꞓen). The Archean Green Creek Complex is exposed in erosional windows through the dome carapace in Howell Canyon, Broad Hollow, and White Pine Canyon. A zone of imbricate Raft River Mountains sequence rocks consisting of schist quartzite, carbonate (Op, mostly metamorphosed Pogonip Group(?), and black phyllite (Mm, metamorphosed Manning Canyon(?) Shale) underlies the ridge between the dome and Mount Harrison. Mount Harrison is composed of overturned Harrison

chloritoid, iron oxides, tourmaline, and detrital microcline. Lithologies range from impure quartzite to pelitic schist, but the typical schist in the northern Albion Mountains is quartzose. Rarely, cross-laminations are preserved. On this part of Big Bertha Dome, early structures are preserved unusually well. Foliation (S_1) and lineation (here a northeast-trending lineation, L_1) are prominent here. Commonly bedding is transposed and folded. F_1 folds trend northeast and are here overturned to the southeast; in most outcrops parallel F_1 folds are systematically overturned to the northwest. Quartzo-feldspathic segregations commonly are boudinaged. Locally in this roadcut, northwest-trending lineations and crenulation folds (L_2 and F_2) are present; F_2 and L_2 are better developed elsewhere on the dome.

1.0 24.7 **STOP 3**. We have driven downstructure to the base of the Elba Quartzite and are now on the geologic map shown in Figure 5. Here the top of the Archean Green Creek Complex of Armstrong and Hills, (1967) and Armstrong (1968) is white mica schist that is unconformably overlain by the pure, white, thin-bedded basal member of the Elba Quartzite (10 to 45 m thick). Commonly a thin-bedded white mica schist, locally pebbly, occurs at the base of the Elba Quartzite. At the top of the low hill south of the road we can observe outcrops of the conglomerate member of Elba Quartzite overlying the white basal member. The conglomerate is micaceous and feldspathic, and contains clasts of quartzite, vein quartz, and microcline crystals. It varies from 2 to 20 m thick on Big Bertha Dome. The conglomerate is overlain by brown to gray, poorly sorted, locally granule-rich, thick-bedded and cross laminated, micaceous and feldspathic quartzite 130 to 160 m thick.

Strain measured from

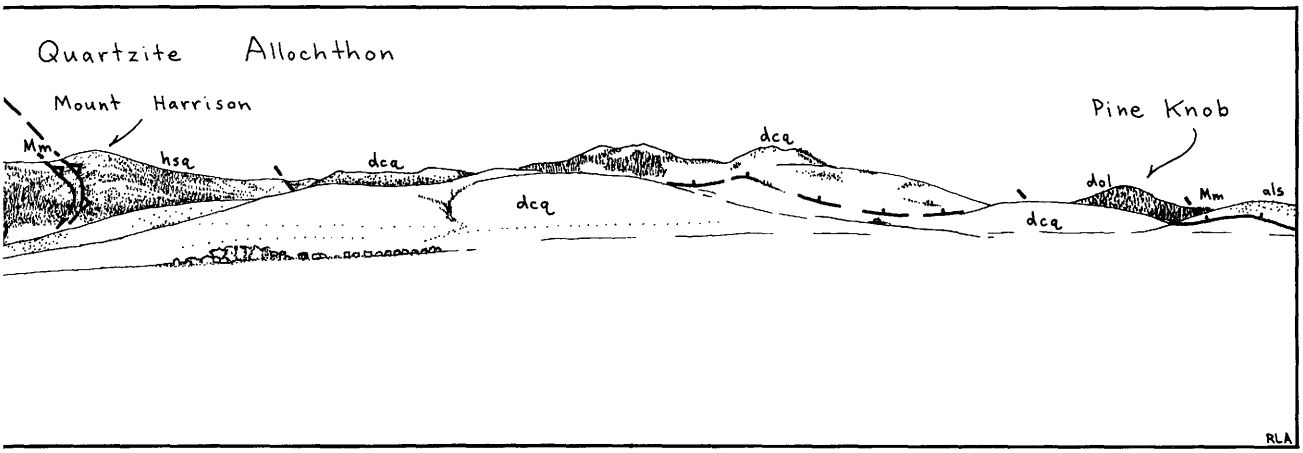

Summit Quartzite (hsq) of the quartzite assemblage. Much of the ridge continuing north, towards the observation point, is composed of Dayley Creek Quartzite of Armstrong (1968) (dcq), largely overturned thick tectonic slices of somewhat impure quartzite with minor schist lenses and partings. Pine Knob is pure massive dolomite marble (dol) structurally overlain by black phyllite and limestone marble (unit Mm), and other tectonic slices of metasedimentary rocks, such as the limestone of Albion (als) forming the northernmost hill in the panorama. Unit symbols follow those used for Views 1-3 in Miller and others (1980). Tv, Tertiary volcanic rocks.

pebble shapes in the conglomerate here is (1.33 0.16 0.63). The maximum shortening is perpendicular to foliation, which is subparallel to bedding, and maximum extension is nearly parallel to L_2 lineation (S. 59 E.). The pebble shapes here are to be compared with shapes elsewhere on the dome later today.

Across the canyon to the northwest in cliff exposures the Elba Quartzite dip northeast above hummocky slopes of the Archean schist and gneiss. Slump blocks of the Elba Quartzite have moved over the Archean rocks in several places. On the south side of the canyon, where the road curves sharply around a hill that projects into the canyon, we can see a slide block of the Elba Quartzite and the schist of the Upper Narrows. Bedding in the block dips about 30° southwest, suggesting rotation as a result of sliding from a position over 300 m higher, near the upper surface of the dome in the cliffs on the south side of Howell Canyon.

0.5	25.2	Drive over the slide block described above.
0.6	25.8	Cross glacial moraines that probably are end moraines from a glacier that extended down the Howell Canyon.
1.2	27.0	**STOP 4**. View northward towards East Hills and Cotterel Mountains. The northernmost exposures of the Raft River Mountains sequence occur in the East Hills. The top of the Elba Quartzite, overlain by the schist of the Upper Narrows, is found on the west side of Marsh Creek. Amphibolitic schist of Stevens Spring and graphitic garnet-staurolite schist of Mahogany Peaks are also identified and are quite similar to their stratigraphic equivalents in the Raft River and Grouse Creek Mountains. These familiar units occur in jumbled fault-bounded blocks and as windows where they poke through a cover of breccia

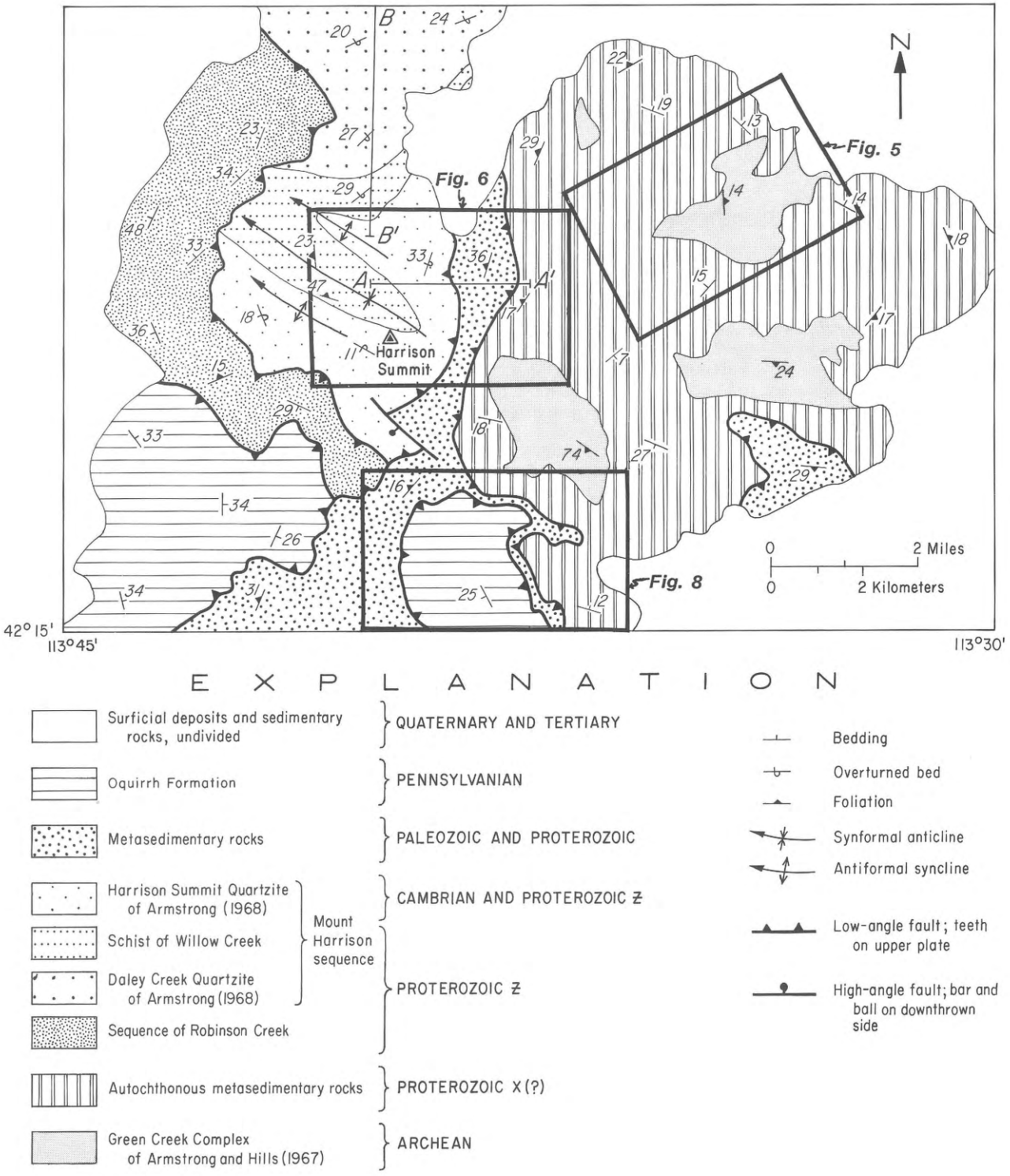

Figure 4. Generalized geologic map of Big Bertha Dome area, after Miller (1978, 1983). Detailed geologic maps are outlined.

sheets, Tertiary volcanic rocks, and quartzite or marble units of uncertain stratigraphic affinities. At the north end of the range, east of Declo, in low isolated exposures surrounded by loess, and presumably in fault contact with older rocks, are the unmetamorphosed Permian Rex Chert member of the Phosphoria Formation and the Triassic Dinwoody Formation. Both are well exposed in quarries developed for road metal and ditch lining material, respectively.

The breccia sheets that mantle the East Hills are composed of monolithologic quartzite breccia and monolithologic limestone breccia and mixed lithology breccias that are overlain by, but also interfinger with, the Tertiary volcanic rocks we examined in STOP 1. The breccias are thus believed to be relatively late features, mostly Miocene, corresponding in age to a time of rapid uplift of much of the Albion-Raft River-Grouse Creek metamorphic terrane.

The Cotterel Mountains are a west dipping hogback of volcanic rocks. The main portion is a thick, extensive rhyolite flow. Towards the south these strata are disrupted by rhyolite domes and thick viscous rhyolite flows, presumably because they are nearer to source vents. Older volcanic ash, flow, and agglomerate units are exposed near Connor Pass and on the out-of-sight east face of the Cotterel Mountains. At the north end of the range diatomite occurs between the previously discussed rhyolite flow and the capping basalt flow of similar K-Ar ages. The tilted volcanic rocks of the range plunge north under Pleistocene(?) basalt flows of the Snake River Plain.

1.1 28.1 **STOP 5**. Archean granitic gneiss here bears penetrative foliation defined by flattened quartz and aligned micas and concordant compositional layering. Potassium feldspar phenocrysts, common in many exposures of the Archean gneiss, are absent. Pegmatites are common. Similar gneiss locally intrudes schist and amphibolite elsewhere in the Albion Mountains and migmatitic mixing of granitic gneiss and schist is evident in a few exposures. The variation in the degree of development of fabrics in the Archean rocks corresponds closely to similar variation in overlying metasedimentary rocks, indicating that the entire sequence acquired the fabric simultaneously, although rarely an older, possible Archean, fabric can also be identified in these rocks.

0.6 28.7 **STOP 6**. Stop next to quaking aspens in a small canyon at the road side and climb the slope towards the northeast about 100 m to small cliffs of the conglomerate member of the Elba Quartzite. Compare the strain, (0.65 -0.06 -0.35), and maximum extension, S. 29 E.; with that of STOP 3. On Big Bertha dome there is a systematic increase of strain within the Elba from low values such as (0.61 -0.10 -0.31) in the apical region to high values such as (1.50 0.24 -0.69) near the adjoining basins. This variation indicates that strain due to doming was superimposed on presumably uniform strain resulting from earlier fold events. F_1 and F_2 folds are

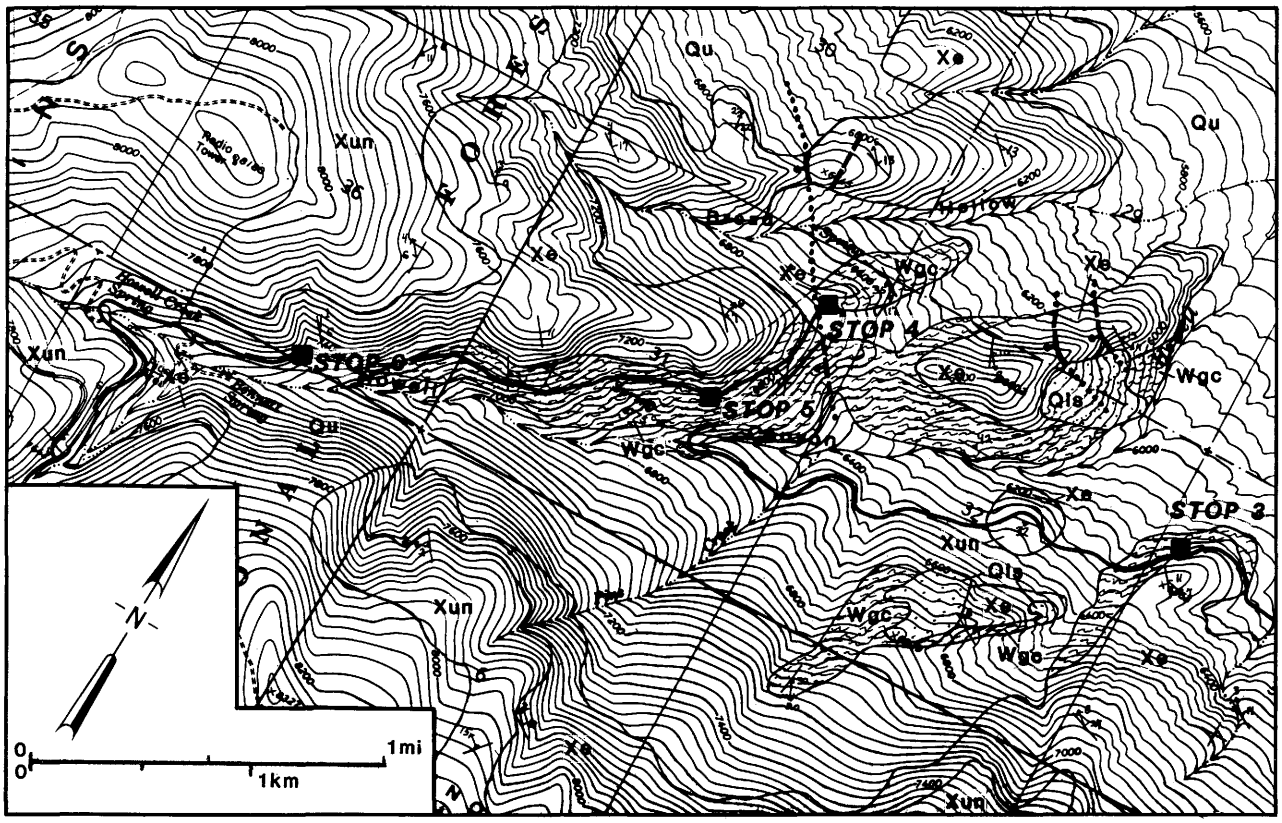

Figure 5. Geologic map of Howell Canyon area, after Miller (1978).

warped over the dome, while F_3 folds trend about parallel to the circumference of the dome and verge basinward, and therefore are probably related to doming.

Grassy bluffs with white boulders across the canyon are formed by the lower part of the Elba Quartzite and are the southward projection of the strata you now stand on. Archean rocks in the canyon below are poorly exposed due to a cover of glacial and slopewash deposits.

0.6 29.3 Bennett Springs, in the valley on your left, results from surfacing of groundwater flow within the till where it thins on shallowly buried Elba Quartzite.

0.5 29.8 The contact between the Elba Quartzite and the schist of the Upper Narrows is poorly exposed in road cuts on the right. We are at the top of the dome here, so the contact is nearly horizontal.

0.2 30.0 Turn Right at road junction. Left fork continues to Pomerelle Ski Area, located in a cirque floored by the schist of the Upper Narrows. Right fork continues to Thompson Flat, Cleveland Lake, and Mount Harrison summit.

Road cuts on the left (after the turn) expose schist of the Upper Narrows as we continue toward Thompson Flat.

1.4 31.4 Pass turnoff to Thompson Flat camp ground, an excellent campground in a quiet fir forest on glacial till. Plan ahead if you want to stay here - the

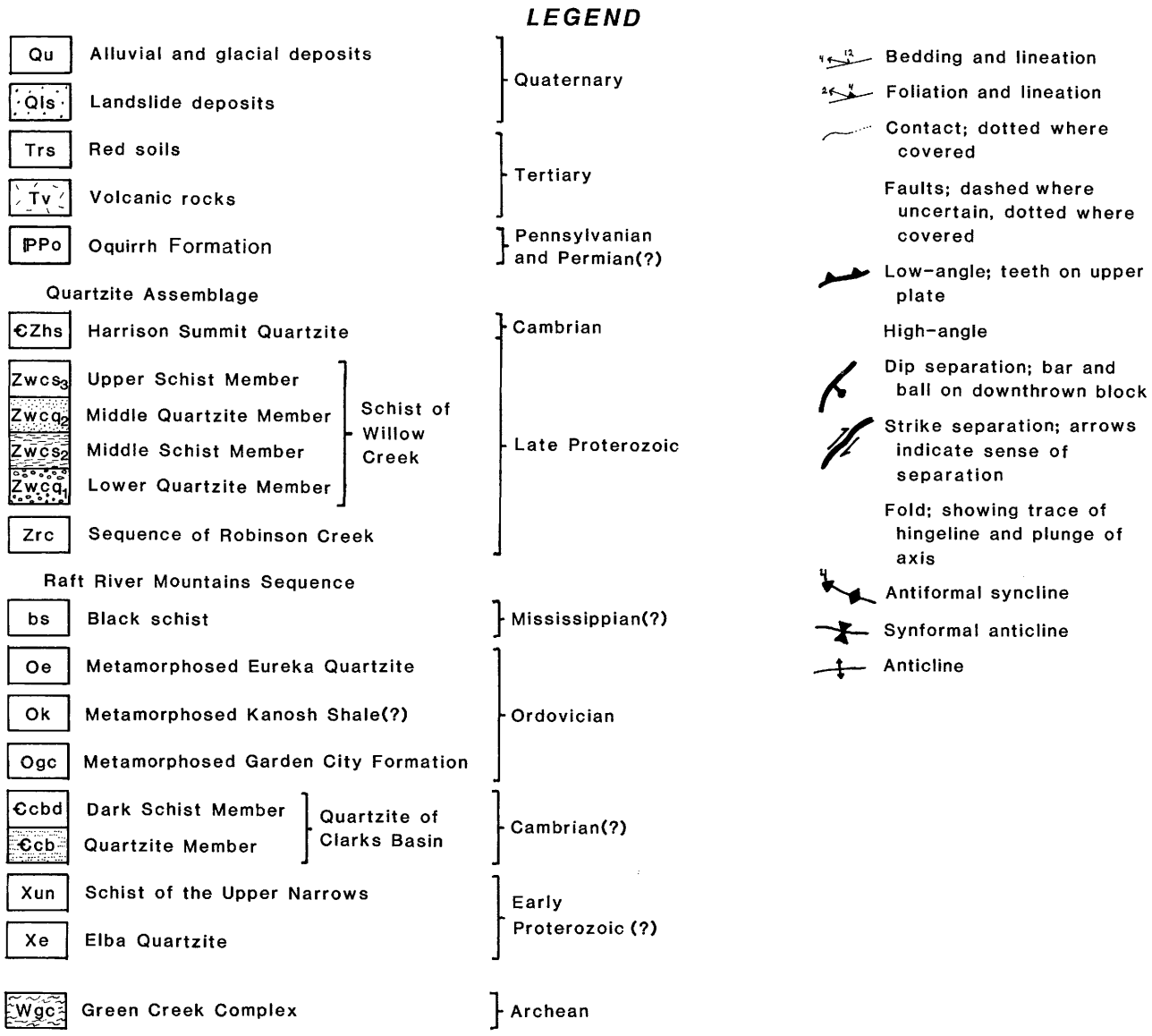

campground is typically crowded on summer weekends!

Refer to the geologic map (Figure 6) as we continue to the top of Mount Harrison.

0.2 31.6 **STOP 7.** The white, flaggy quartzite exposed in a prospect pit on the left side of the road is tentatively assigned to the quartzite of Clarks basin (Miller, 1980) on the basis of its micaceous partings and thin-bedded character. It overlies the schist of the Upper Narrows along a low-angle fault exposed in a borrow pit 50 m to the southeast. Well-developed F_2 folds and parallel L_2 lineations are present here. We are now on the western flank of the dome, as indicated by westerly dips in bedding in the schist of the Upper Narrows, the quartzite of Clarks basin, and overlying rocks exposed to the west.

We will walk west along the south side of the road to look at rock types typical of the upper part of the quartzite of

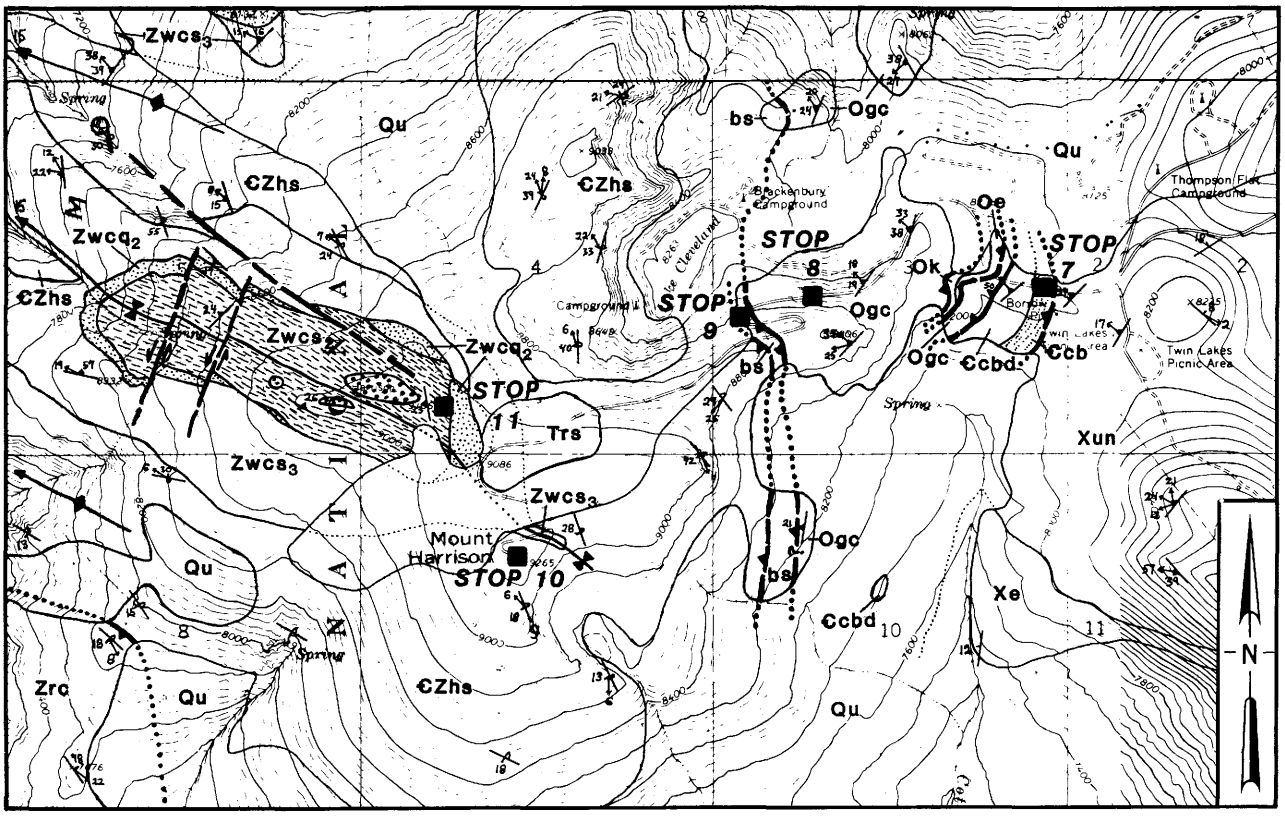

Figure 6. Geologic map of Thompson Flat and Mount Harrison summit region, after Miller (1978). Symbols and units described in Figure 5. Scale same as in Figure 5.

Clarks basin and then cross to the prominent white hill on the north side of the road. Proceeding west, we move through a low, poorly exposed, sage-covered area with quartzite and schist float. Better exposures in a grassy knoll about 30 to 50 m west of the prospect pit show the white, flaggy quartzite with interbeds of biotite and white mica schist typical of the dark schist member of the quartzite of Clarks Basin (Figure 6). The quartzite of Clarks Basin is of uncertain age, but it is probably Cambrian (Armstrong, 1968; Compton, 1972, 1975).

Cross the road to exposures of micaceous, brown-weathering marble considered to be metamorphosed limestone of the Ordovician Garden City Formation. The interbedded shale and limestone that probably formed the protolith of these metamorphic rocks are most similar to the Garden City Formation. A better exposure of these marbles can be found 40 m southwest in the cliffs on the west side of the gully. The ridge that continues west from that cliff also has good exposures of the overlying units. A low-angle fault occurs between the marble and overlying white, uniform orthoquartzite considered to be the metamorphosed Ordovician Eureka(?) Quartzite, exposed in this roadcut. The quartzite is in turn overlain by a very thin unit that contains a heterogeneous collection of lithologies including: am-

phibole schist, white-mica and dolomite-bearing quartzite; schistose dolomitic marble; dark phyllite; and white mica schist with retrograded garnet(?). Lehi Hintze (written communication, 1978) suggested that the most likely correlative of this unit is the Ordovician Kanosh Shale. Exposures southwest of this roadcut indicate that the metamorphosed Kanosh(?) Shale is overlain by marble of the metamorphosed Garden City(?) Formation, the reverse of the normal stratigraphic relations of these units. It is therefore possible that the sequence is overturned. Additional support for this hypothesis is found in the sequence of lithologies exposed in the metamorphosed Garden City Formation(?): clean, massive and thick-bedded marble is overlain by brown, micaceous, laminated marble, the reverse of the stratigraphy of unmetamorphosed sequences of the Garden City Formation and also the reverse of similar metamorphosed units in the Raft River Mountains (Compton, 1972, 1975). The overturned sequence here is probably part of a large overturned sequence that includes the remainder of the units we will pass through on Mount Harrison.

Return to the vehicles and proceed up the road.

0.7 32.3 Road to right leads to Lake Cleveland. Proceed straight (southwest) on main road. An excellent roadcut in marble of the folded Garden City Formation can be found at the bottom of the hill along the road to Lake Cleveland.

0.3 32.6 **STOP 8**. Metamorphosed Garden City Formation. The laminated, micaceous, calcite marble here is spectacularly folded. Orientations of F_2 fold axes vary greatly in this single outcrop, but because refolding cannot be established on the basis of two sets of folds or lineations, and because the axial plane foliation defined by micas is nearly constantly oriented, the folding probably reflects a complicated deformation gradient during a single event. Coarse micas are oriented uniformly at high angles to the axial plane foliation and represent a late (S_3) cleavage.

Lake Cleveland lies in the adjacent cirque. The west wall is composed of the Harrison Summit Quartzite. The glacier flowed northeast toward the town of Albion. A Little Ice Age moraine loop can be seen in the northeast side of the lake.

0.2 32.8 **STOP 9**. A "melange" of black schist, phyllite, and quartzite are exposed in the roadcut on the hairpin turn (black schist unit of Figure 6). These rock types probably represent the metamorphosed Mississippian and Pennsylvanian Manning Canyon Shale (metamorphosed Chainman-Diamond Peak Formation of the Utah portion of the metamorphic terrane); blocks of knobby dark schist assigned to the Cambrian(?) schist of Mahogany Peaks are also present. These blocks contain retrogressed staurolite with chlorite zone assemblages, suggesting that movement along this "melange" zone took place at lower metamorphic temperatures. The Harrison Summit Quartzite exposed a short distance above this zone

is not unusually deformed.

We now continue up the road, returning to marble of the Garden City Formation as we switch back, and then crossing the poorly exposed zone of dark phyllites once more. The Harrison Summit Quartzite is exposed only as felsenmeer along the road.

1.3 34.1 Pass red soil exposures on the left that may represent a Tertiary erosional surface that is now largly covered by Quaternary felsenmeer. Continue straight (west) at road junction.

0.4 34.5 **STOP 10**. Mount Harrison summit. Here, we are near the structural top of the Harrison Summit Quartzite. Crossbeds, exposed along the tops of the cliffs, demonstrate that the unit is overturned. An infold of dark schist exposed about 200 m east of the summit, along the cliff top, represents the structural base of the overlying unit, which consists largely of pelitic schist with interbedded marble but is quartzose near the contact with the Harrison Summit Quartzite. The Harrison Summit Quartzite is characterized by thick bedding and prominent cross laminations, is moderately micaceous to clean, and has coarse sand to granule-sized grains.

To the south can be seen Mount Independence and Cache Peak, the topographic expression of the Independence Lakes Dome, and west of this is Middle Mountain. The town of Elba lies northeast of Mount Independence and behind Elba are the Jim Sage Mountains, a north-trending arch of rhyolite lava flows correlative with those in the Cotterel Mountains. Beyond the Jim Sage Mountains are the Raft River Mountains, and northeast of these mountains are the Black Pine and Sublette Ranges. To the west, the Cassia Mountains form a broad dome beyond the Oakley basin. A few patches of unmetamorphosed Permian and Triassic strata show through the extensive Tertiary ash flow sheets and sedimentary rocks of this range (Mytton and others, 1983). Northward lies the Snake River Plain, across which the foothills and rugged mountains of central Idaho may be seen on a clear day.

Turn around and descend along the main road.

0.4 34.9 Turn left on dirt road. (WARNING: this rocky road may be impassable for passenger cars). Stay on the main track; avoid lesser used routes.

0.4 35.1 **STOP 11**. Schist and quartzite units that structurally overlie the Harrison Summit Quartzite are exposed in this vicinity. The unit names in the following description correspond to those on Figure 7, and are from Miller (1983); they differ from Armstrong's designations as indicated on Figure 7. Because both overlying and underlying quartzite units are overturned, the schist of Willow Creek is presumed to be overturned. East of the road is the middle quartzite member ($Zwcq_2$) in a highly fractured exposure that contains much secondary(?) silica. The unit is micaceous, coarse-grained and highly deformed. Northward the unit pinches out, and begins again in the patch of trees 100 m further north. It is structurally under-

lain by poorly exposed pelitic schist belonging to the upper schist member ($Zwcs_3$). Eastward and upstructure, float and a few outcrops of the middle, garnetiferous pelitic schist member ($Zwcs_2$) are exposed and are overlain by the lower quartzite member ($Zwcq_1$). Bedding/foliation relations are easily observed in the schist. Garnet grains have cores with inclusion trails oriented differently from those in the rims; pressure shadows are common. The overlying quartzite is typically "gritty" and micaceous with sparse pebbles distributed throughout. A few conglomerate beds can be observed, and a zone of rip-up clasts(?) of schist is also present. The ridge underlain by the lower quartzite member marks the axial trace of a large syncline with N. 60° W. trend and northeastern vergence that probably represents an F_2 structure.

Armstrong believes that the garnetiferous schist and grit and pebble-bearing quartzite belong to a structurally higher slice than the Harrison Summit Quartzite and the calcareous schist unit attached to it. On an unpublished map, he shows these exposures as part of a folded klippe. He considers these units to be Paleozoic on the basis of their similarity to a thrust sheet composed of middle Paleozoic flysch exposed in central Idaho. Miller (1983) considers these strata to be a continuous depositional sequence that correlates with late Proterozoic and Cambrian strata in the Pilot Range, Nevada and Utah, as shown in Figure 7.

Turn around and return to main road.

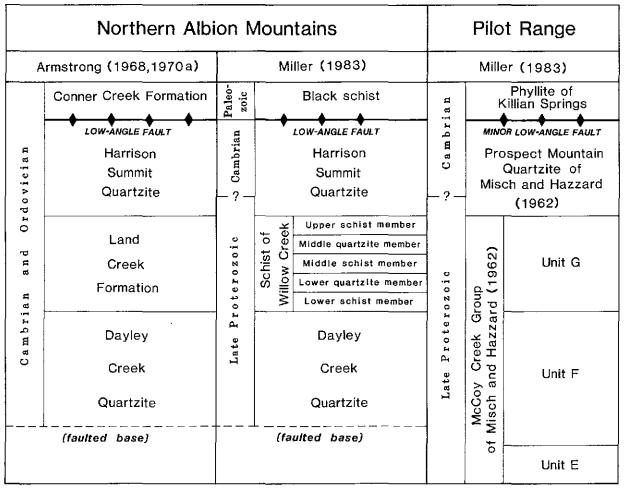

Figure 7. Structure sections of strata on Mount Harrison summit region showing stratigraphic nomenclature and structural interpretations, after Miller (1983).

0.2	35.3	Turn left. Return down the mountain to Rt. 77.
2.6	37.9	Pass turnoff to Thompson Flat Campground.
2.1	40.0	Turn left toward Rt. 77.
8.5	48.5	Turn right on Rt. 77.
1.8	50.3	Here in Connor Pass between the Cassia Creek drainage to the south and Marsh Creek to the north we can see the schist of the Upper Narrows extending down the flank of Big Bertha Dome on the west and Tertiary volcanic flows on the east. Quaternary deposits in the pass presumably cover a detachment fault that has a prominent geophysical signature north and south of here in the Elba and Marsh Creek basins (Mabey and Wilson, 1973). The fault probably dips shallowly eastward here and steepens both to the north and south; it flattens everywhere at depth, becoming parallel to the bedrock surface that projects under the Raft River basin (Covington, 1983).

3.6 53.9 Turn right to Elba and Almo. Cassia Creek here follows a possible strike-separation fault that offsets the two north-trending ranges of Tertiary volcanic rocks in a right-lateral sense. This fault may extend westward through metamorphic rocks in the syncline between Big Bertha and Independence Lakes Domes where the rocks are poorly exposed and bedding is nearly horizontal. Little evidence is to be found for the presence of this fault, however, leading to the alternative interpretation that the right lateral offsets are confined to structures in the detached block containing Tertiary sedimentary and volcanic rocks (Covington, 1983).

Armstrong interprets the offset of Tertiary ranges as a result of fault curvature and intersection of Basin and Range normal faults, without intervention of a strike separation fault.

South-facing dip slopes of the Elba Quartzite and overlying units are visible to the northeast. The major canyon in that area whose northern wall is composed of hummocky slopes floored by till and Archean schist, all topped by the massive cliffs composed of the Elba Quartzite, is named after Col. Patrick Connor. He led a group of California volunteers into many battles with the Bannock Indians, led by Chief Pocatello, in this area. The battles usually resulted from Indian raids on wagon trains passing along the California Trail on Cassia Creek here and southward toward Almo. Stories are told of Connor massacring the inhabitants of an Indian camp near Connor Corner, although one popular version has the Indians wiping out Connor's troops!

3.9 57.8 Turn right on gravel road into town of Elba.

0.9 58.7 Turn right on gravel road.

0.2 58.9 Turn left.

0.8 59.7 Turn right.

0.3 60.0 Turn left.

1.1 61.1 The Elba Quartzite is exposed on both sides of Clyde Creek here (see Figure 8). The white basal member and conglomerate member are exposed on the right. As we proceed up the road we climb slowly through the Elba Quartzite and the schist of the Upper Narrows to a low-angle fault-bounded plate of the quartzite of Clarks Basin. Overlying this thin plate is the limestone, chert, and sandy limestone unit of the Oquirrh Formation, undivided, here slightly metamorphosed and highly fractured.

2.1 63.2 **STOP 12**. Stop at the turnout on the left side of the road and walk back down the road about 50 m to a small roadcut. The Oquirrh Formation here is composed of sandy limestone. Elsewhere limestone with chert nodules and chert and sandstone beds are present. Microfossils indicate the unit here is Pennsylvanian (B. Skipp, oral commun., 1975). Return to cars and climb dirt track up hill to the east for a view.

To the north, across Clyde Flat, low hills of the Oquirrh Formation are exposed below extensive deposits of till and alluvium (Figures 8 and 9). West of these hills is a larger hill with brown outcrops of the

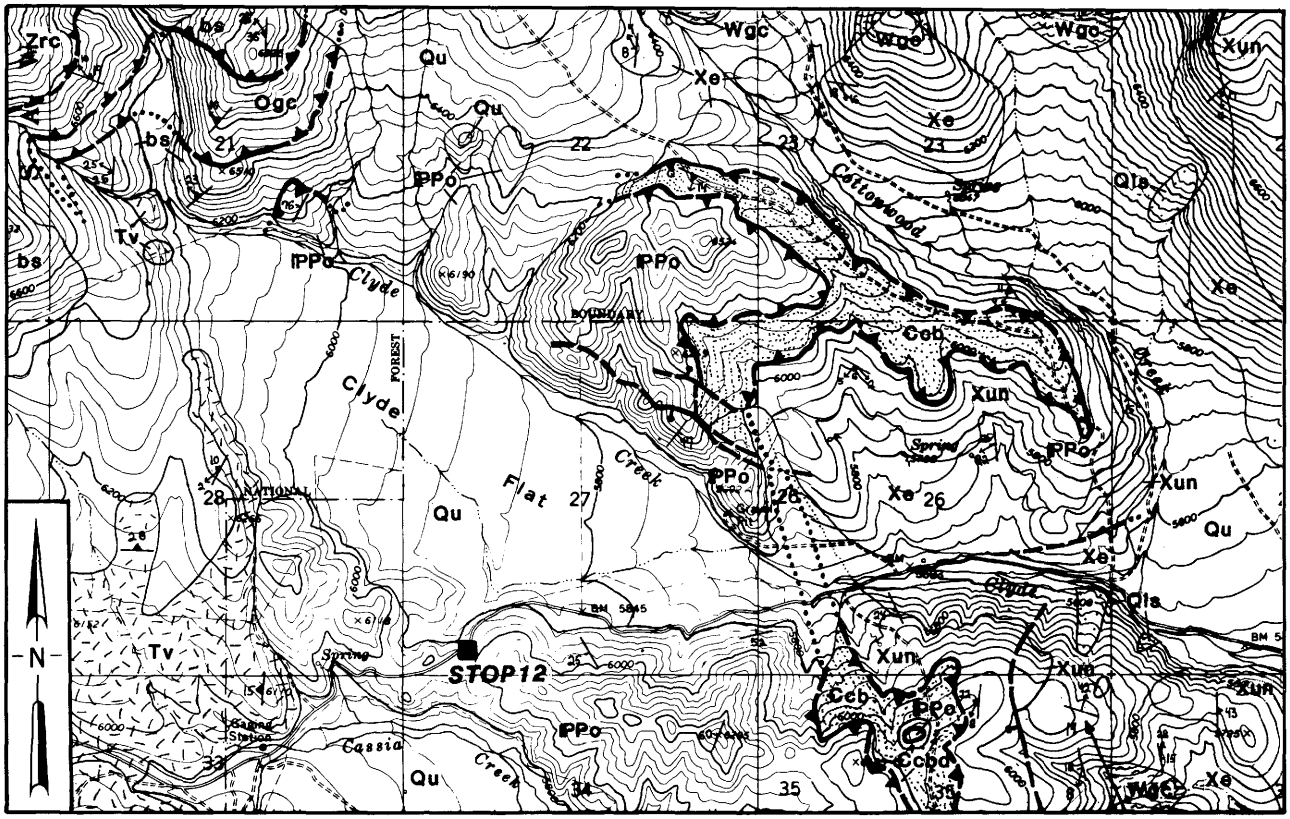

Figure 8. Geologic map of the Clyde Flat area, after Miller (1978). Units and symbols are as defined in Figure 5. Same scale as Figure 5.

schist of Mahogany Peaks, Ordovician(?) marble and the metamorphosed Manning Canyon Formation. The light-colored knob composed of the Oquirrh Formation nestled below the schist has uncertain relations with the schist; it may lie under or over the schist.

Southward, the north-facing dip slopes of the Elba Quartzite are prominent in the nearby grassy slopes and the intermediate forested ridge. The most distant ridge is made up largely of Archean rocks and represents the apex of the Independence Lakes Dome. Eastward along the distant ridge dip slopes of the Elba Quartzite overlie the Archean rocks.

0.7	63.9	Tertiary rhyolite ash flows, 8.5 ± 0.2 m.y. old (Armstrong, 1975) and similar to those seen at Stop 1, are exposed in bluffs to the right of the road.
0.3	64.2	Bear right on road to Oakley.
0.5	64.7	Bear left at junction.
1.5	66.2	We are now driving through an area of poorly exposed the schist of Mahogany Peaks-the black, knobby schist present in big slabs in the fields. The schist of Mahogany Peaks is faulted over the schist of the Upper Narrows. The ridge north of the road consists of unmetamorphosed sandstone of the Oquirrh Formation faulted over the schist of Mahogany Peaks and the metamorphosed Manning Canyon Shale.
1.6	67.8	**STOP 13.** White and gray marble units containing tremolite are exposed along the road

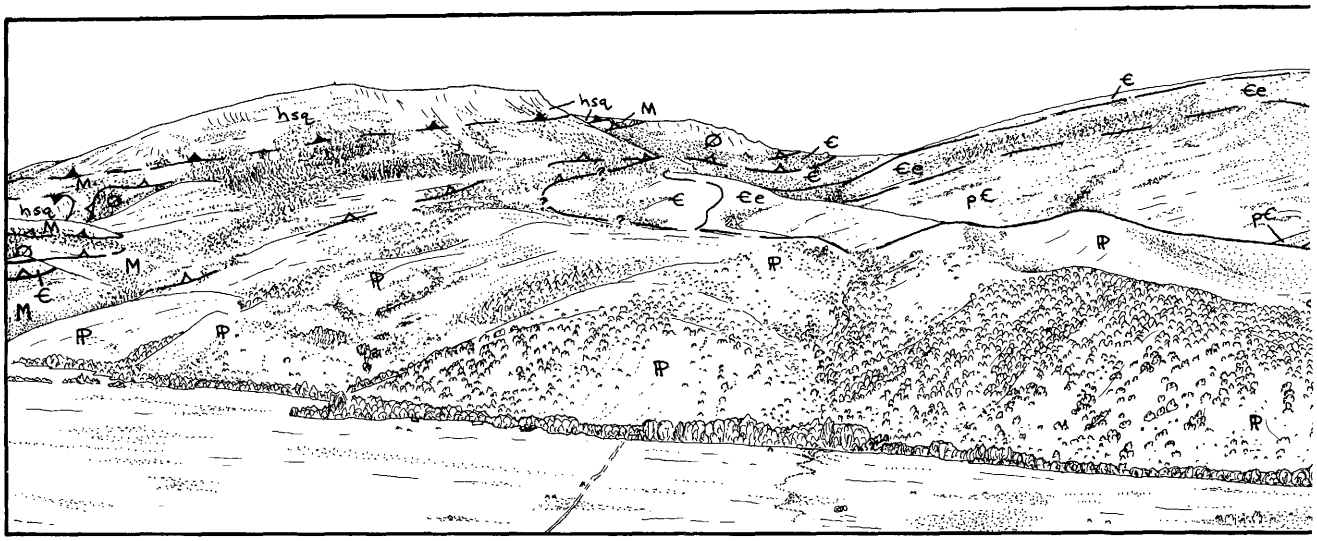

Figure 9. View north across Clyde Flat from above Elba-Oakley road, near STOP 12 (DAY 1), from Miller and others (1980). The Elba Quartzite (€e) unconformably overlies the Late Archean Green Creek Complex (p€) and outlines the structure of the Big Bertha Dome-center and right background. Various schists and thin quartzite units (€) that stratigraphically overlie the Elba form the remainder of the autochthon. Parautochthonous slices include white quartzite (wq) (probably either quartzite of Yost or quartzite of Clarks Basin), several schist and thin quartzite units (€), siliceous marble of the metamorphosed Pogonip Group (O), and the carbonaceous phyllite of the metamorphosed Manning Canyon Shale (M). Mount Harrison, left skyline, is composed of gently west dipping, overturned quartzite, the Harrison Summit Quartzite (hsp). This formation is not part of the Raft River Mountains sequence, and most likely represents rocks

here. This lens of marble and similar lenses of calcite marble, dolomite marble, and quartzite are tectonic "fish" in the black schist belonging to the schist of Mahogany Peaks and the metamorphosed Manning Canyon Shale. Crinoids have been recognized in one of these "fish." The "fish" perhaps originated as thin thrust plates or hinges of tight folds which were segmented during continued deformation.

0.1 67.9 **STOP 14**. Stop at the road junction beyond the cattle guard to examine the schist of Mahogany Peaks. The crinkly black schist contains abundant garnet and staurolite; although staurolite is not common at this location, it can be found in outcrops 30 m north next to the fence, and it is abundant a bit farther down the road towards Oakley.

The dark ridge in the basin west of this ridge is a fault block composed of Tertiary rhyolite ash flows. A water gap cuts the ridge.

Turn around and return to the paved road via Elba.

Optional continuation of Tour: Proceed west down switchbacks in road towards Oakley, crossing over good exposures of the schist of Mahogany Peaks. Around the first hairpin turn marble and then black phyllite are enountered in successively higher structural slices. On the following downgrade, additional outcrops of the schist of Mahogany Peaks are followed by poorly exposed brownish-weathering tremolite-bearing marble. Beyond the covered area around a spring and pump are black argillite and slate (metamorphosed Mississippian and Pennsylvanian Manning Canyon Shale) and where the road heads north after the last

of a more western site of deposition. The Harrison Summit is either Paleozoic, a siliceous facies correlative with the predominantly pelitic rocks of the Raft River Mountains sequence (interpretation of Armstrong), or it is Late Proterozoic and without equivalents in the Raft River Mountains sequence (interpretation of Miller). Low hills in the foreground are composed of limestone of the Pennsylvanian Oquirrh Group (IP) that is either a lensoid parautochthonous slice beneath other slices of the Raft River Mountains sequence and the overriding quartzite allochthon composed of Harrison Summit Quartzite (interpretation of Armstrong) or a klippe superimposed on the imbricate structure of the range (interpretation of Miller).

hairpin turn is tan-weathering light-gray dolomite (interlayered upslope with white quartzite), possibly equivalent to the Cassia Dolomite of Armstrong (1968), and belonging to the quartzite assemblage (discussed more completely at STOP 17). The road leaves the mountains headed on a westward route through calcareous sandstone of the Oquirrh Formation. The east-dipping layering of sandstone, calcareous sandstone, and clastic limestone can be seen on the opposite (north) side of the canyon. Return to STOP 14, then continue eastward to the paved road via Elba.

7.2 75.1 Continuation of tour: As we near Elba, we will have an excellent view of the white hogbacks composed of the quartzite of Clarks Basin to the northeast. The quartzite is highly folded and lies in low-angle fault contact on top of slices of the schist of Stevens Spring and the quartzite of Yost. These allochthonous units lie upon the autochthonous schist of the Upper Narrows. F_3 folds in the quartzite of Clarks Basin trend S. 30° W., approximately parallel to the circumference of the dome, and verge southeast. The folds are increasingly flattened downward and the quartzite appears mylonitic adjacent to the basal low-angle fault, leading Miller (1980) to suggest that the fault moved in association with development of F_3 folds, which are related to doming.

2.8 77.0 Turn right on paved road. We will follow the general route of the California Trail, established in 1843 by Joseph Walker, for the next 22 miles.

Exposed in the prominent

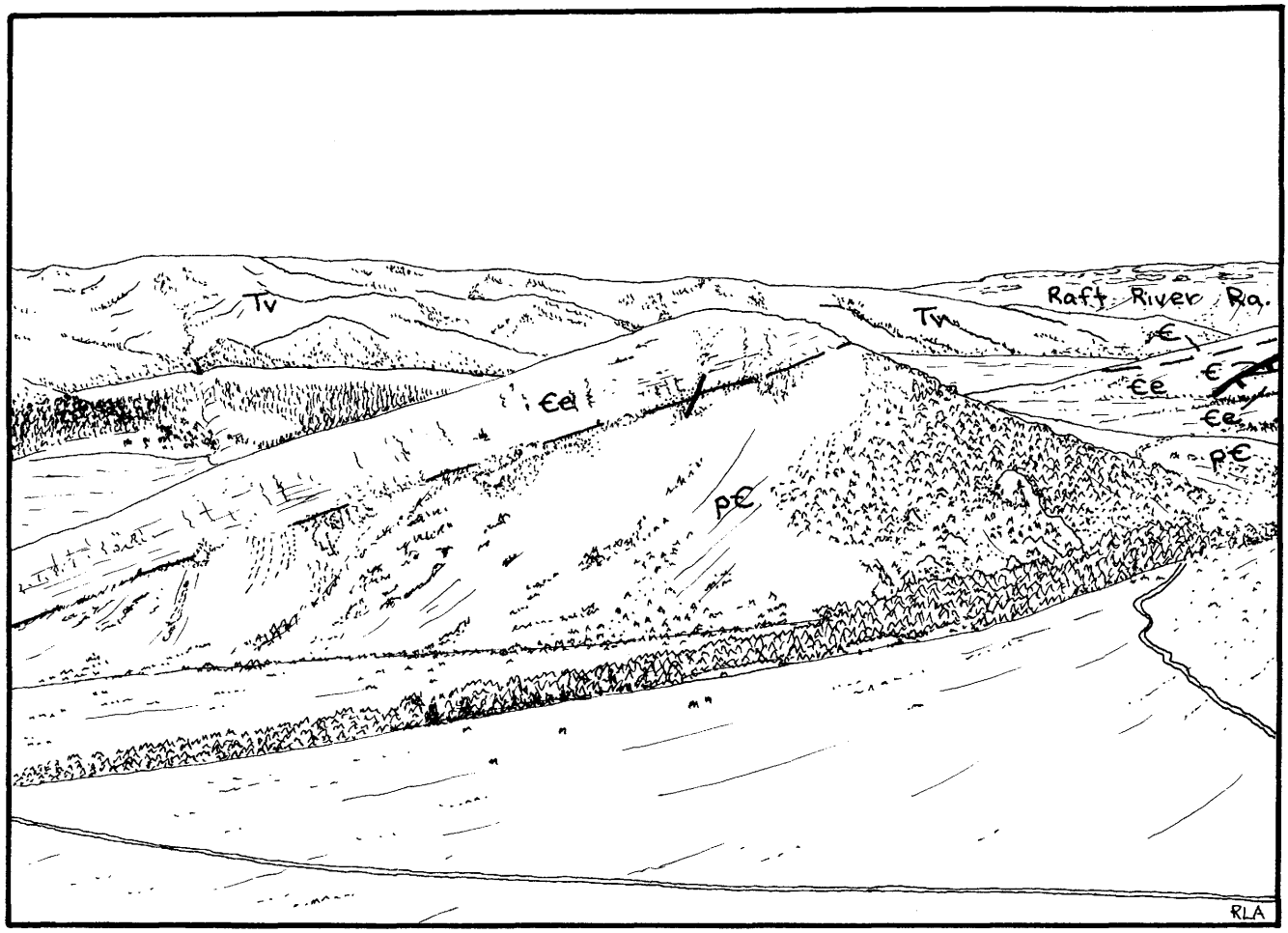

Figure 10. Looking southeast across Cassia Creek from the hills west of Elba. The Jim Sage Mountains form central and left skyline. The Raft River Mountains are visible in the right distance. Green Creek flows from right to left across foreground. The hogback in center of view shows Elba Quartzite (€e) unconformably overlying the Late Archean Green Creek Complex (p€). In the wooded slope massive recessively weathering biotite schist and more resistant dark pods of amphibolite are intruded by light gray porphyritic adamellite gneiss that stands as erosion-resistant rocky pinnacles. From Miller and others (1980).

hill close by to the west are Quaternary gravel deposits. Hogbacks farther to the west consist of the Elba Quartzite dipping northeast and east off Independence Lakes Dome.

One of these hogbacks is shown in Figure 10. An optional side trip follows the dirt road south of Elba, turning right to go up Cassia Creek and then left up the Green Creek fan to the base of the illustrated hogback. There, a variety of Archean lithologies can be observed in place at the type locality of the Green Creek Complex. Several Rb-Sr and K-Ar samples for dating the Green Creek Complex as Archean (2.44 b.y.) came from that location (Armstrong, 1976).

5.1 83.0 From this crest as we drive south towards Almo we can see the Raft River Mountains to the southeast across the Upper Raft River Valley. The mountains extend west to directly in front of us where the Dove Creek Mountains join the Raft River and Albion Mountains. North-facing dip

slopes of Elba Quartzite and other units can be seen in the Raft River Mountains. The topography typical of City of Rocks Adamellite of Armstrong and Hills (1967) is visible to the southwest surrounded by hogbacks of Elba Quartzite.

6.8 89.9 As we near Almo part of the City of Rocks pluton, Castle Rocks, is visible to the west.

0.2 90.0 Enter Almo. In the town of Almo is a historical plaque that reads, "Dedicated to the memory of those who lost their lives in a most horrible Indian massacre 1861. Only five escaped." The massacre occurred on the California Trail immediately southeast of Almo. The massacre evidently took place following days and days of Indian harrassment by the wagon train's sharpshooters. After four days and nights of repeated Indian attacks nearly 300 Missouri emigrants lay dead. The Indians camped in a grassy spot in the City of Rocks to the southwest.

0.2 90.2 Continue straight as paved road ends.

0.8 91.0 Turn right on gravel road to the City of Rocks. Forested hills are hogbacks of the Elba Quartzite. As we drive into the City of Rocks, Archean granitic gneiss can be seen on the slopes beneath the Elba Quartzite.

2.5 93.5 First view of the City of Rocks.

0.3 93.8 Pass the old stagecoach station on the Salt Lake City-Twin Falls stage route. It was vacated in 1878 when the stage route was changed. Vandals recently bombed this beautiful old stone building.

Predominantly Archean granitic gneiss is exposed in this vicinity.

1.4 95.2 **STOP 15**. Stop at road junction and carefully cross the fence on the east side of the road. Walk about 80 m to Register Rock, where wagon train members signed their names while en route to California in the mid-1800s. The granite is part of a 30 m.y. old pluton that forms the core of the City of Rocks Dome.

Return to vehicles and continue on the left fork of the road.

2.4 97.6 **STOP 16**. Twin Sisters (named by California trail emigrants). The tall spire west of the parking area is the Tertiary granite "sister" and the one south of it is the Archean granitic gneiss "sister." The Tertiary granite is Ksparplag-biot-qtz monzogranite that contains many muscovite-bearing aplite dikes. The Archean gneiss is similar in composition but megacrystic and strongly foliated, weathers somewhat darker and brownish, and is cut by dikes of the Tertiary intrusion.

The contact between plutonic rocks and gneiss can also be seen under the hogback of the Elba Quartzite to the northeast where light-colored cliffs of the pluton underlie the darker Archean gneiss. A northwards view of the City of Rocks from the Cedar Hills (south of Twin Sisters) is shown in Figure 11.

Great Stone Bird Rock is on the left side of the road as we return to vehicles to continue south.

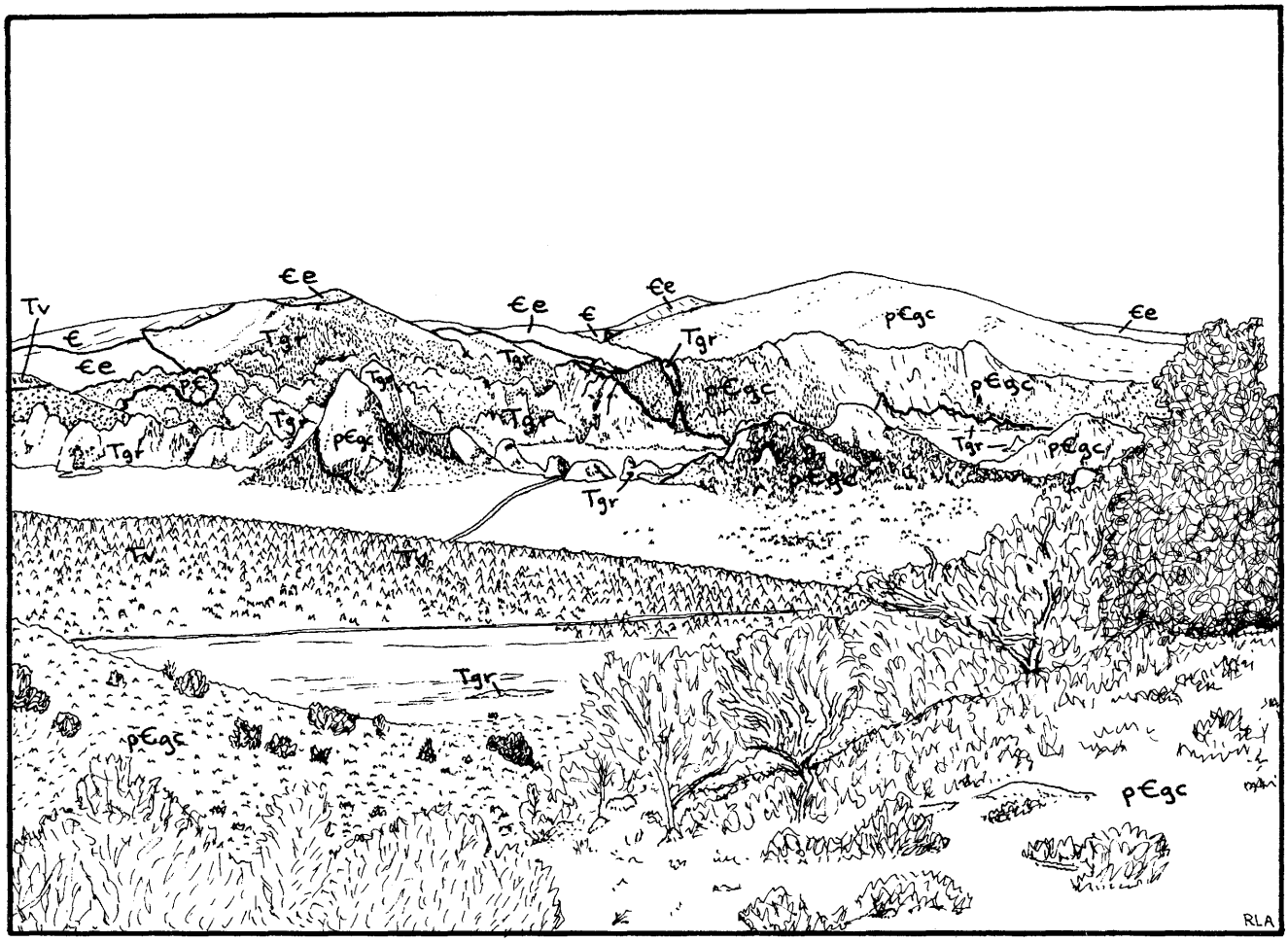

Figure 11. View north from south end of Albion Mountains across City of Rocks to Cache Peak (high point on skyline). Mount Independence is the skyline peak just left of Cache Peak, and Graham Mountain is the high point on the left skyline. Two granite pinnacles on the ridge crossing the middle view (just below Graham Mountain) are the Twin Sisters. The elongate gneiss domes cored by Green Creek Complex (pϵ) are outlined by the unconformably overlying Elba Quartzite (ϵe) that dip away to right and left and behind the gneissic core. Mount Independence is composed of the north-dipping Elba Quartzite, and a northwest plunging syncline developed in the Elba Quartzite separates the Cache and City of Rocks Domes. Intrusive into the core of the City of Rocks Dome is Tertiary Almo pluton (Tgr). On the left side the pluton intrudes Elba Quartzite and overlying schist units (ϵ). On the right the intrusive contact is with Green Creek Complex only. On the slopes below and behind Graham Mountain are large stoped xenoliths of country rock (not shown in view). The Twin Sisters are pinnacles of similarly weathering adamellite, but of greatly contrasting age. The nearer, more southerly pinnacle is composed of gneiss of the Green Creek Complex gneiss (flaser fabric, browner-weathering) cut by light-colored dikes of the younger intrusive body that forms the further, more northerly pinnacle. Patches of Miocene ash flow tuff (Tv) occur on the left side and middle foreground. From Miller and others (1980).

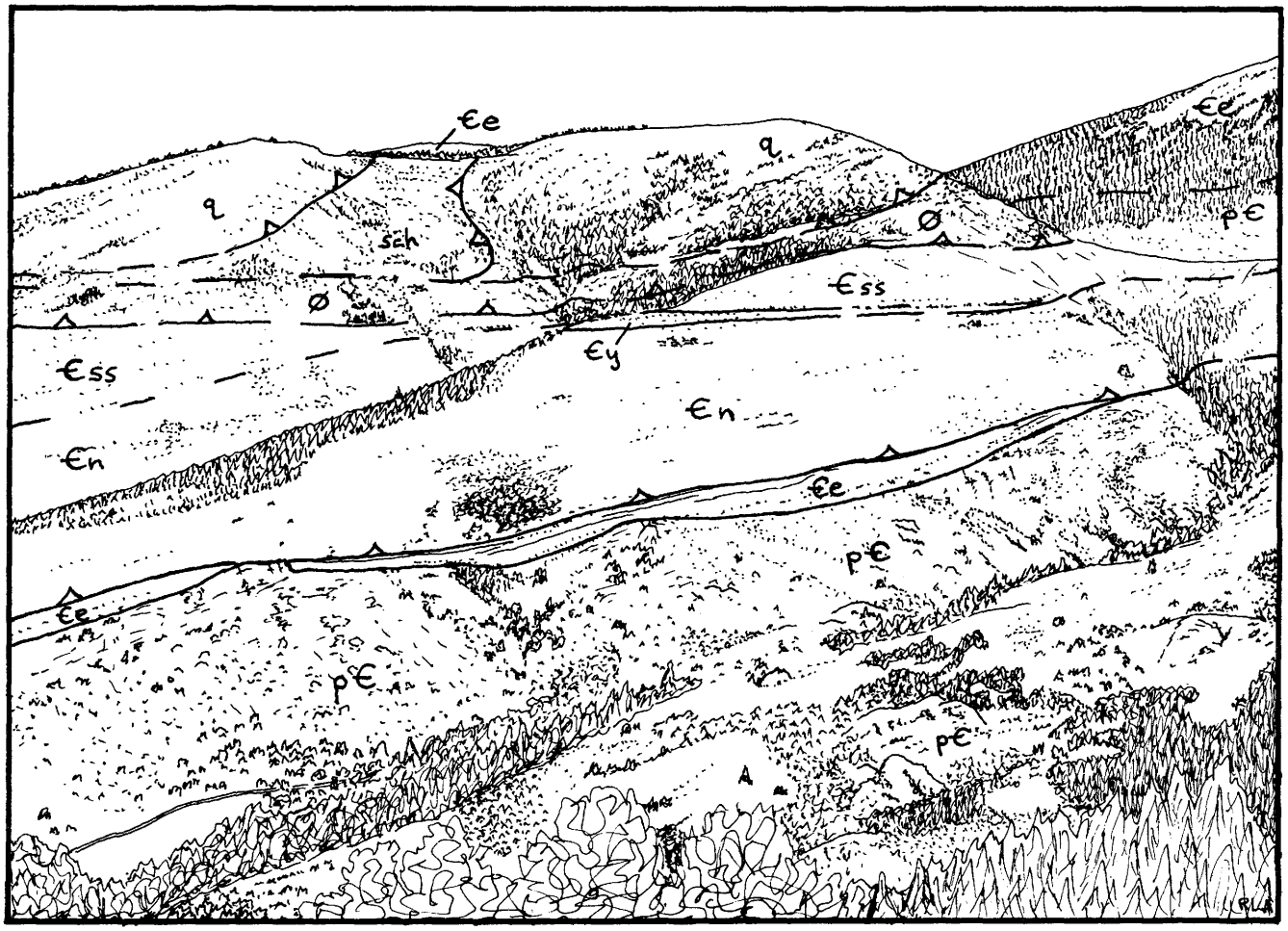

Figure 12. Looking northeast across Mill Creek. The north slope of Mount Independence is on the right skyline. The creek parallels the crest of a northwest-trending arch cored by the late Archean Green Creek Complex (pϵ). The Elba Quartzite (ϵe) is drastically thinned over this arch, but is overlain by a structurally simple sequence comprised of the schist of the Upper Narrows (ϵn), quartzite of Yost (ϵy), and schist of Stevens Spring (ϵss). A flat tectonic contact terminates the normal Raft River Mountains sequence (units pϵ, ϵe, ϵn, ϵy, and ϵss). Above that fault is a thin slice of middle Paleozoic dolomite (O), and above that are imbricate quartzite (q) and schist (sch) strata that cannot be assigned to any formation in the Raft River Mountains sequence. These strata belong to the quartzite assemblage. From Miller and others (1980).

1.2	98.8	Road on left to Emigrant Canyon; continue on main road.
2.7	101.5	Turn Right (north) at junction.
3.4	104.9	Lyman Pass.
0.6	105.5	Road on right to the City of Rocks and Almo. Glacial till lies on the slopes to the northeast. These slopes form the west flank of Independence Lakes Dome. A northwest trending nose of Archean gneiss extends from the Independence Lakes Dome along Mill Creek towards the community of Basin. A view of the structural complexities on the north side of Mill Creek is shown in Figure 12, in which the quartzite assemblage can be seen overlying schist units of the Raft River Mountains sequence. That same tectonic contact must lie buried by Quaternary deposits a bit to the west of this point in Birch Creek Valley and will be

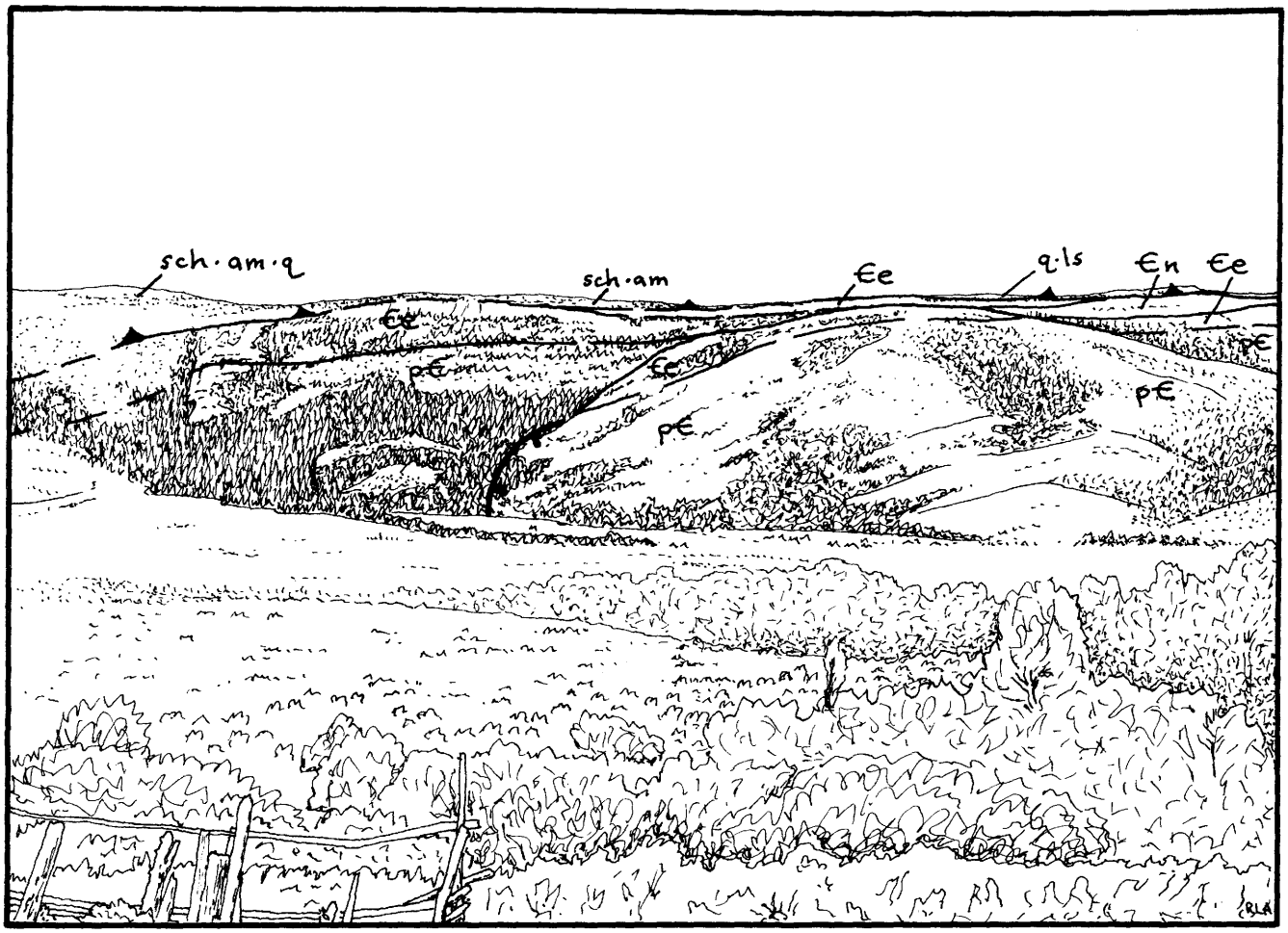

Figure 13. East slope of Middle Mountain. View west from approximately 2.7 miles north of Lyman Pass on Birch Creek Valley road. Elba Quartzite (∈e) and underlying late Archean Green Creek Complex (p∈) underlie the east facing mountain slope and a large rotated slump block (right of center). Schist of the Upper Narrows (∈n) overlies the Elba near the right skyline. Rocks on the skyline belong to the quartzitic assemblage-schist (sch), amphibolite (am), quartzite (q), and marble (ls). All units, and especially the structurally higher metasedimentary rocks, are invaded by granitic dikes and sills of the informally designated Middle Mountain injection complex. Metamorphism of these rocks is characterized by presence of sillimanite and diopside. From Miller and others (1980).

crossed before entering the gorge of Birch Creek.

2.1 107.6 **STOP 17**. View to the west of Middle Mountain. The Green Creek Complex and its cover units, the Elba Quartzite and the schist of the Upper Narrows, are exposed on the northeast face of Middle Mountain (Figure 13) in a structural culmination. The culmination results from a late stage (post D_2 and D_3) NNW-trending anticline and a suspected range-bounding normal fault (not exposed or provable from surface geology or physiography). Above these autochthonous units of the Raft River Mountains sequence is the quartzite sequence that makes up most of Middle Mountain. The entire range is distinct from the Albion Mountains in its higher metamorphic grade (sillimanite and diopside), injection by granitic material, and intense development of late mylonitic fabric with WNW-trending lineation (D_3)

in all rocks.

The rock units of the Raft River Mountains sequence at Middle Mountain are easily recognized: K-feldspar-porphyritic, biotite flaser gneiss with minor biotite schist and amphibolite pods and layers constitute the Archean Green Creek Complex; this lithologic identification has been confirmed isotopically (Armstrong, 1976). The overlying Elba Quartzite is cross-bedded, upright, massive and relatively pure, the schist of the Upper Narrows is well-foliated platy muscovite-and biotite-quartz schist. The structurally overlying rocks are not the schist units of the Raft River Mountains sequence but rather a thick succession of quartzite with subordinate carbonate rocks and minor schist. Deformation, pervasive invasion by granitic material, lack of distinctive horizons, and poor exposures prevented any stratigraphic or structural subdivision of this thick unit. On the northern part of Middle Mountain there are a number of quarries in flaggy quartzite; the quartzite is similar in appearance to the flaggy quartzite of Clarks Basin, but it is not sandwiched between schist units as in the Raft River Mountains sequence. This same flaggy quartzite extends into Utah in the northern Grouse Creek Mountains at least to the vicinity of Vipont where it has been mapped as the quartzite of Clarks Basin (Compton and others, 1977).

On the western edge of Middle Mountain siliceous limestone, white vitreous quartzite, and pure dolomite are inferred to be correlatives of Ordovician units (the metamorphosed Pogonip Group, the metamorphosed Eureka Quartzite, and the metamorphosed Fish Haven Dolomite). These appear to overlie the thick quartzite and they are less invaded by granite, lower in metamorphic grade (tremolite) and less deformed than the underlying quartzite and gneiss.

The thick quartzite, overlain by Ordovician(?) carbonate rocks and quartzite, is interpreted to be part of an allochthonous quartzite sequence. Too few examples of cross-bedding were found to indicate whether any large part of the quartzite succession is overturned. Overturned bedding was observed in one area in northern Middle Mountain; upright beds were seen in several exposures of the Elba Quartzite but not elsewhere. The fault that separates the Raft River Mountain sequence from the quartzite assemblage is at its lowest stratigraphic level in the Raft River Mountains sequence in Middle Mountain and the parautochthonous slices of the Raft River Mountains sequence are missing. This is consistent with an original geometry of the fault cutting upwards stratigraphically from west to east and presumably with transport from west to east in a thrust relationship.

Units of the Raft River Mountains and quartzite sequences are intruded by several large bodies of foliated monzogranite to granodiorite and innumerable dikes and sills of granitic and pegmatitic rocks. An initial impression in mapping is that most of the range is composed of granitic rocks because these rock types are com-

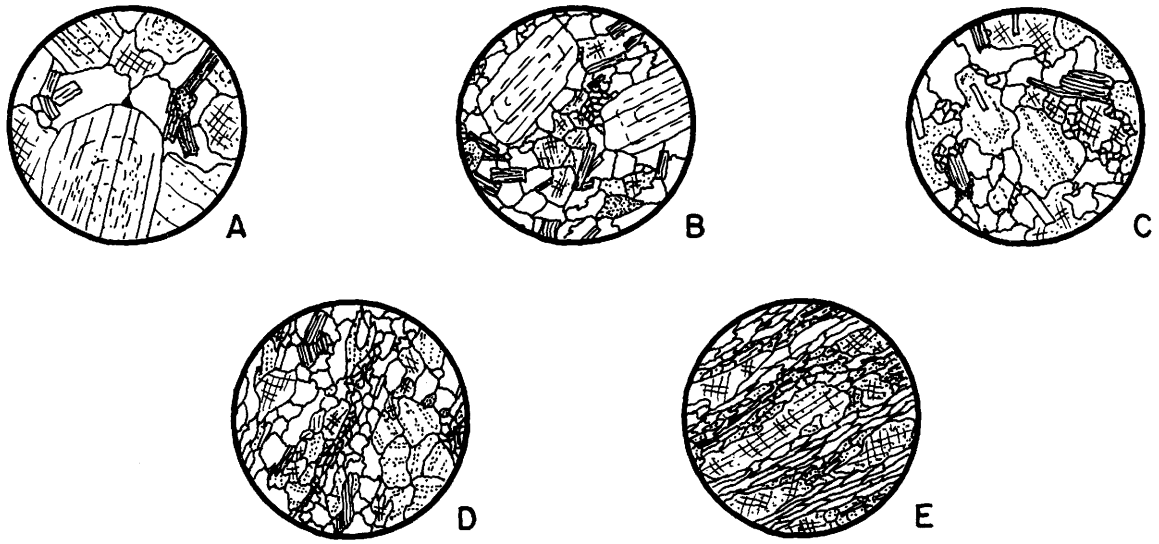

Figure 14. Progressive textural changes in adamellite between Almo pluton and mylonite of Middle Mountain. Plagioclase (twinned, zoned, and lightly stippled), K-feldspar (cross-hatched and lightly stippled), quartz (clear), biotite (heavily lined, rectangular shape), muscovite (lightly lined, rectangular), and accessory minerals (opaque and heavily stippled). A. The Almo pluton in the City of Rocks (YAG 797), hypidiomorphic granular muscovite and biotite adamellite. B. Birch Creek (YAG 795), strongly lineated protoclastic, relict-hypidiormophic granular, biotite adamellite gneiss. C. Middle Mountain (YAG 944), foliated and lineated protoclastic allotriomorphic biotite adamellite gneiss. Plagioclase zoning very weak, quartz poloygonized. D. Middle Mountain (YAG 943), mylonitic, strongly foliated and lineated biotite adamellite gneiss. E. Middle Mountain (YAG 948), mylonite derived from biotite adamellite. Well-developed quartz ribbons and bands of fine-grained, extremely foliated and polygonized mica, quartz, and feldspar enclosing anhedral K-feldspar megacrysts.

monly better exposed, but closer examination reveals that recessive and poorly exposed areas are typically underlain by metasedimentary rocks. The overall appearance of the Middle Mountain injection complex is duplicated in the Ruby Mountains in Nevada (Howard, 1971, 1980; Snoke, 1975, 1980).

The pegmatitic granitic rocks contain abundant coarse muscovite and scattered garnet, characteristic of S-type granites (Chappell and White, 1974). The granitic rocks contain anomalous radiogenic strontium, evidence of digestion of metasedimentary country rock (Armstrong, 1976; Compton and others, 1977). They have not been successfully dated by whole-rock Rb-Sr methods. One extremely Rb-rich granitic pegmatite cannot be older than 60 m.y.; a Mesozoic age is suspected for some of the gneissic granite (Armstrong, 1976). Mineral K-Ar and Rb-Sr dates range from 34 m.y. for coarse grained pegmatite muscovite to 16.5 m.y. for biotite. Tertiary metamorphic resetting was pervasive and has obscured any evidence of pre-Tertiary igneous episodes.

The granitic rocks of Birch Creek Valley and Middle Mountain are progressively more deformed from east to west. A complete gradation exists from undeformed granite, such as occurs in the Almo pluton, to mylonite (Figure 14). The intensity of deformation is locally variable with several generations of gneiss and pegmatite being evident in favorably exposed areas. In general the myloniti-

zation increases from east to west, reaching its most extreme development in the western part of Middle Mountain, where mylonitic gneiss hundreds of meters thick is exposed in valleys cutting across the range and at the north end of Middle Mountain. The metasedimentary rocks enclosed in gneiss are probably equally strained but the effects are less dramatic than in the mylonitic gneiss. All rocks in Middle Mountain are deformed, even the youngest pegmatite bodies. Foliation parallels layering in metasedimentary rocks (e.g., flaggy quartzite) and dips gently westward in most areas. Lineation-usually a mylonitic streaking in gneiss or streaking of micas on partings in quartzite-is well developed and invariably trends W to WNW.

At least some of this mylonitic fabric is Tertiary in age (Armstrong, 1976; Compton and others, 1977; Todd, 1980) and it is possible that it is entirely Tertiary but it is nearly coaxial with structure in metamorphic rocks of the Albion Mountains that is definitely Mesozoic. The fewest contradictions arise from the conclusion that distinct Mesozoic and middle Tertiary strain episodes (D_2 and D_3, respectively) were nearly coaxial as a result of inherited boundary conditions. The strain observed is one of intense stretching in a WNW direction and flattening parallel to layering in strata which were presumably near horizontal at the time of deformation (Compton, 1969; Todd, 1980; Compton and others, 1977). Later deformation has produced the west tilt of the range and open, upright NNW-to N-trending folds west of Lyman Pass. Similar late structures are recognized in Utah (Compton and others, 1977).

2.3 109.9 **STOP 18**. Relations between granitic gneiss and quartzite are well exposed in the road cut. Well-foliated and lineated granitic gneiss intrudes clean, prominently cross-bedded quartzite that is completely recrystallized and has rare tight folds. Pegmatite dikes cross-cut gneiss and are also foliated. Uncommon schist layers occur in the quartzite. The quartzite here is not typical of any of the quartzite units in the Raft River Mountains sequence and thus is included in the quartzite assemblage along with the Harrison Summit Quartzite (Armstrong's interpretation) and the thick quartzite-dominated section on Middle Mountain. The gneiss is transitional between the Almo pluton and gneiss units of Middle Mountain (Figure 14) and has been included with the transitional, and definitely Mesozoic, gneiss of Camel Rock in a discussion of the geochronometry (Armstrong, 1976). A paleovalley filled with Tertiary volcanic rocks is crossed twice by the canyon in the next few miles downstream.

2.5 112.4 A collapsed quarry on the right provides access to flaggy quartzite. Cliffs composed of Tertiary volcanic flows are prominent as we proceed northward.

5.5 117.9 Bear left at fork in road.

0.8 118.7 Turn right on Rt. 27 in center of Oakley.

7.6 126.3 Fault blocks composed of

Tertiary volcanic flows here create hills on the otherwise flat Snake River Plain. Several basaltic shield volcanos are visible in the distance to the northeast and northwest.

12.8 139.1 Burley City limits.

FIELD TRIP ROAD LOG: SECOND DAY

Mileage Incremental	Mileage Cumulative	Description
0.0	0.0	Meet at Y-Dell Market, same location as for Day 1. We will proceed east beyond the northern end of the Albion Mountains, and south through the Raft River Valley to the Raft River Mountains. Turn right on Rt. 81 towards Declo, as for Day 1.
8.0	8.0	Continue straight on Rt. 81 at junction with Rt. 77 in Declo.
3.3	11.3	Hill on right is flaggy, micaceous quartzite that probably was emplaced as a monolithologic breccia or slideblock during the Tertiary. The Permian Phosphoria and the Triassic Dinwoody Formations are poorly exposed in the low slopes about a mile south from here, where they are separated from the underlying metamorphic rocks by inferred low-angle faults.
3.0	14.3	We are climbing a gentle fan at the north end of the Cotterel Mountains. Miocene (9 m.y. old) basalt flows are visible in the railroad cuts adjacent to the road. They lie on rhyolite of the north end of the Cotterel Mountains. A Quaternary shield volcano is visible 3 km northeast of the road as we turn south along the eastern side of the Cotterel Mountains. Several Quaternary shield volcanoes lie a mile southwest of the road 2 miles farther along Rt. 81. A zone of north-trending normal faults southwest of here have downdropped the volcanic flows several hundreds of meters into the basin.
19.8	34.1	Continue straight at junction with Rt. 77 in Malta. The California Trail crossed near Malta en route to Elba and Almo.
10.1	44.2	The Raft River Geothermal pilot plant is being erected 1 km west of here. It is tapping 150°C water that is heated by circulation in a northeast-striking fault system in basement rocks (Williams and others, 1975). Approximately 1500 m of Tertiary sedimentary and volcanic rocks of the Salt Lake Formation lie within this basin (Covington, 1983). Structurally underlying these Miocene and younger rocks are metamorphic units correlated with schist of the Upper Narrows, Elba Quartzite and Archean gneiss on the basis of well cuttings and drill cores. A maximum dip of 7.5° to the southeast is indicated for the strata by drill data. On the basis of detailed geophysical and well-log studies, Covington (1983) has interpreted these relations as due to listric faulting of Tertiary rocks onto the metamorphic rocks.
10.8	55.0	Hill on right is a dome of Miocene rhyolite.
2.0	57.0	Turn right on oiled gravel road toward Yost and Grouse Creek. A well drilled near this road intersection cut through nearly 400 m of the Salt Lake

Formation above sandstone of the Oquirrh Formation about 330 m thick; the well then passed through metamorphic strata for its remaining 1600 m. A possible designation of the metamorphic units (from top to bottom) is Ordovician and Silurian(?) marble and quartzite (550 m); the quartzite of Clarks Basin(?) rock types (dolomitic micaceous quartzite) (65 m); a sequence of dolomitic and calcareous mica schist, quartzose schist, schistose marble and quartzose marble that is not recognizable in surface exposures in Raft River Mountains (70 m); the schist of Stevens Springs with additional minor calcareous schist accompanying typical lithologies (100 m); the quartzite of Yost(?) lithologies (carbonate-rich white quartzite) (130 m); quartzose dolomite of uncertain correlation (140 m); and feldspathic schist, quartzose schist and pelitic schist possibly correlative with the schist of the Upper Narrows (500 m). In general the metamorphic rocks contain much more carbonate than the rocks known in surface exposures, perhaps due to the presence of additional strata or to a transition from the pelitic- and clastic-dominant Raft River Mountains sequence to carbonate-dominant miogeoclinal strata seen in the Deep Creek Range and ranges farther east.

3.3	60.3	Turn left on gravel road to Clear Creek campground.
1.0	61.3	Continue past road on right. Hills one mile away on the right (west) at 3:00 are limestone of the Oquirrh Formation lying in fault contact on marble of the metamorphosed Pogonip Group. Beyond the hills and forming the mountain slope is the Elba Quartzite. Straight ahead are north-facing dip slopes of Archean gneiss and schist capped at the ridge crest by the Elba Quartzite and about eight klippe of metamorphosed Ordovician rocks.
0.9	62.2	Continue straight past roads on right and left.
0.3	62.5	Continue past road on left.
0.6	63.1	Turn left to Clear Creek Campground. The Elba Quartzite forms the prominent cliffs that overlie Archean gneiss and schist to the northwest. We are driving on a thin alluvial cover, through which Archean rocks and the Elba Quartzite poke here and there.
2.6	65.7	Cross bridge over Clear Creek.
0.7	66.4	**STOP 1**. Park at campground entrance. The cliffs north of here beautifully expose the upper portion of the Archean rocks and the lower Elba Quartzite. The dark bands in the white quartzite cliffs are feldspathic and micaceous quartzite sub-units. We will proceed up the steep slope to the north to the base of the cliffs composed of the Elba Quartzite, a total climb of 160 m. For those who prefer to avoid this hard climb, the rock types may all be found in float near the road. Start on a course heading east and north toward a small prominence of schistose trondhjemite well below the cliffs. These rocks are highly deformed, as indicated by strong schistosity created by parallel micas and flattened

and elongated quartz grains. Potassium feldspar megacrysts and quartz veins are fractured. Proceed directly upslope from this point. Units of foliated and lineated hornblende-biotite schist outcrop within the trondhjemite. Much of the slope consists of float of the brown, micaceous older schist unit of Compton (1975), here a hornblende gneiss. Micaceous white quartzite lying on the older schist unit marks the unconformity between Archean rocks and Elba Quartzite. Above the unconformity is a thick unit of spectacularly stretched cobble conglomerate. Elongation of the pebbles is approximately easterly, parallel to prominent lineations in white quartzite above the conglomerate. These lineations record the younger of two metamorphic deformations that are expressed in the Raft River and Grouse Creek Mountains.

A large number of strain and petrofabric measurements have been made on the lineated Elba Quartzite, chiefly from localities 5 km SW and 8 km SSE of our position (Compton, 1980). The results indicate simple horizontal extension in an east-west direction, with consequent vertical shortening. The strains took place during and after low-temperature metamorphism that ended during the Miocene (Compton and others, 1977).

Looking south, the outcrop of Archean rocks extends up to the prominent cliff of the Elba Quartzite that is almost on the skyline. The smooth erosion surface just above the cliff is topped by several low knobs that are klippen of Ordovician and Pennsylvanian strata—relics of two major allochthonous sheets that once formed a broadly arched cover on the autochthonous core of the range.

Return to vehicles and retrace route to Rt. 81.

9.3	75.7	Turn right on Rt. 77 through abandoned town of Strevell with picturesque remants of buildings.
1.3	77.0	Enter State of Utah.
1.8	78.8	Limestone of the Oquirrh Formation is exposed in road and railroad cuts here. As we leave the Oquirrh Formation roadcuts a sweeping panorama of the Pleistocene Lake Bonneville basin comes into view, with its many ranges that were islands during the high stand of the lake. The lake nearly crested this pass, reaching to only 35 m below the pass at high stand!
5.6	84.4	Turn right on Rt. 30 to Park Valley, Grouse Creek, and Elko. Note the scenic view of abandoned cars and their messages as we begin west on Rt. 30. Approximately 8 km east and southeast from here three wells encountered Devonian, Mississippian, and Pennsylvanian rocks in faulted and slightly metamorphosed sections (Peace, 1956).
2.2	86.6	The gravel pit on the left side of the road is in Lake Bonneville shoreline gravel deposits. The shore terraces in this area were left by several stands of the lake and are largely composed of well-sorted gravel deposits.
7.9	94.5	Basalt flows with Bonneville lake terraces etched along their sides are exposed north and

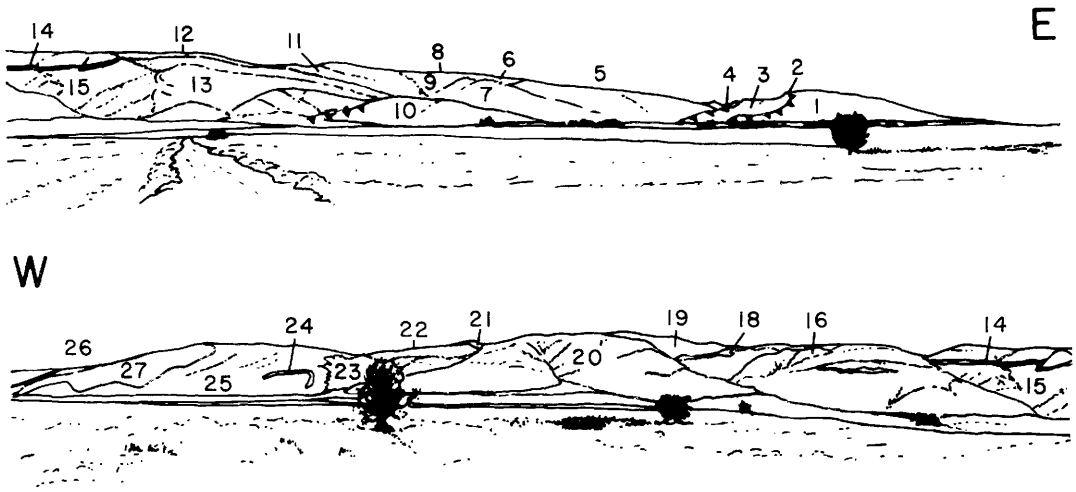

Figure 15. Panorama of Raft River Mountains, from the main highway about 3 km (2 mi) west of Park Valley (STOP 2, DAY 2). Numbers refer to descriptions in the text.

south of the highway. Similar basalt flows along strike with these are about 3 m.y. old by K-Ar (W. C. Hoggatt, U.S. Geological Survey, written communication, 1978; Todd, 1983). White deposits in the valleys are composed of calcareous silt from the floor of Lake Bonneville. As we top the rise another pit in shoreline gravel deposits shows on the left. White, south-facing dip slopes in the Raft River Mountains are the Elba Quartzite; they overlie darker slopes formed of Archean rocks. At the base of the range many klippe of younger rock units overlie the Elba Quartzite. Low-angle fault-bounded klippe on top and on the flanks of the mountains presumably once covered the older rocks. Strata in the klippe are mainly Ordovician units and the Oquirrh Formation.

3.9 98.4 Bonneville Shorelines have cut bluffs at the highest stand of the lake.

4.4 102.8 This north-trending ridge is composed of tuffaceous mudstone, sandstone, and conglomerate of the Salt Lake Formation of Tertiary (Miocene and Pliocene) age.

0.7 103.5 Park Valley, one of the centers of commercial exploitation of the beautiful flagstone occurring in the Raft River Mountains.

2.1 105.6 **STOP 2.** Stop at gravel road on right side of highway for a view of Raft River Mountains (Figure 15). Generally, we are looking north at the south-dipping limb of the broad anticline that makes up the mountain range. Most of the white exposures are composed of the Elba Quartzite, which conforms in a general way to the form of the anticline. The allochthonous sheets that also conform with the anticlinal arch are well exposed to the far right (east) on Bald Knoll, which consists of the Oquirrh Formation (1) lying along a low-angle fault (2) on Cambrian(?) and Ordovician units (3) of an allochthon with underlying fault at 4. Beneath

this fault are the schist of the Upper Narrows and the Elba Quartzite (5), which here define a nearly recumbent anticline (7) with hinge visible at 6. The underlying syncline is defined by the schist of the Upper Narrows at 9. The allochthonous sheets form another major exposure in hills at 10 and small klippen of Ordovician strata at 8 and of Pennsylvanian rocks at 11 and 12. The Elba Quartzite makes up the spur at 13 and the thin white band under the skyline (14). Above this band is more schist of the Upper Narrows and below it are Archean rocks of the range core (15). Continuing on the right half of the view, a syncline developed in the schist of the Upper Narrows (16) is surrounded by the Elba Quartzite that lies on Archean rocks (17) and picks up again, greatly thinned, in the low white cliff (18) beneath the schist of the Upper Narrows (19). Passing farther westward, similar relations are seen between the Elba Quartzite (20, 22, 25, 26), the overlying schist of Upper Narrows (21, 24) and the Archean rocks (23, 27). Out of sight at the east and west ends of the range, all of the units, including the allochthonous sheets, plunge downward beneath younger strata.

2.4	108.0	Rosette.
12.9	120.9	Hills on the left are just above the high stand of Lake Bonneville. They contain tuffaceous siltstone and vitric tuffs of the Salt Lake Formation. On the right the Grouse Creek Mountains form the skyline.
5.3	126.2	Turn right on gravel road marked "Immigrant Trail."
1.3	127.5	Continue past road on right.
0.7	128.2	Continue straight through crossroads.
0.1	128.3	Turn left at fork in road, on the Immigrant Trail.
1.7	130.0	Jeep trail on right leads 0.3 mi to low exposures of thinned units of the Elba Quartzite, the quartzite of Clarks Basin, and Ordovician units.
0.8	130.8	Turn right on dirt road used for flagstone quarrying (see Figure 16 for our location).
0.2	131.0	Turn left at fork.
0.5	131.5	Turn right at fork.
0.5	132.0	**STOP 3**. Park in the saddle on micaceous marble of the metamorphosed Pogonip Group. Walk southeast uphill through a thin slice of quartzose dark schist of Mahogany Peaks to the quartzite of Clarks Basin at the ridge crest. The units here dip steeply west on the steepened limb of a north-trending anticline. Near the ridge top, bedding changes to shallowly southeast dipping on the upright limb of the westward-verging fold. To the southeast are three oval outcrop patterns of marble of the Pogonip Group marking synclines (Figure 16). We will next walk northwest, beyond the vehicles, along the ridge of the metamorphosed Pogonip Group to a prominent white knob of the quartzite of Clarks Basin in another fold "core" and then on to the saddle in the middle distance and up the slope left of that saddle where

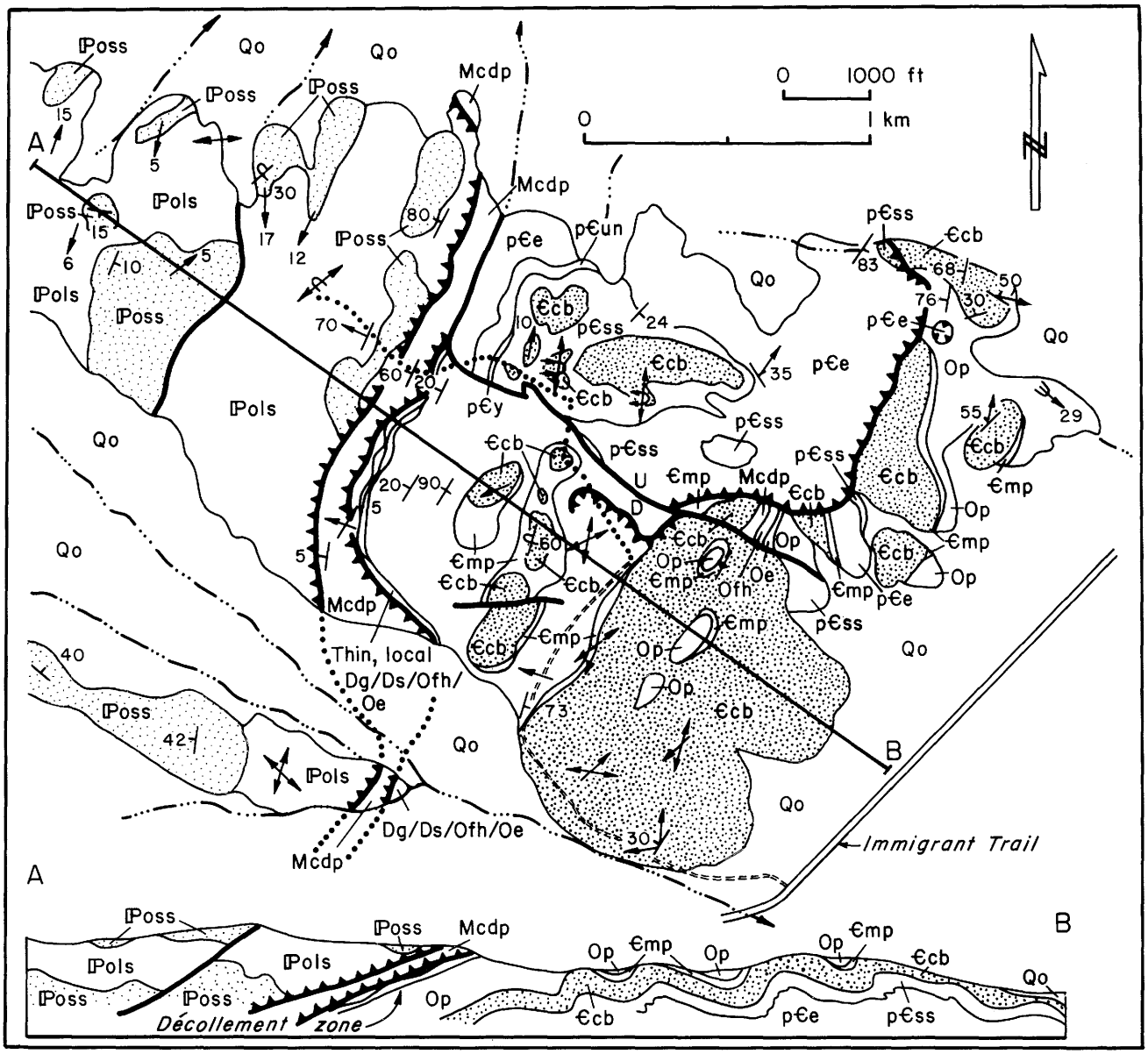

Figure 16. Geologic map and cross section for STOP 3, south of Rosebud Creek. pЄe, Elba Quartzite; pЄun, schist of the Upper Narrows; pЄy, quartzite of Yost; pЄss, schist of Stevens Spring; Єcb, quartzite of Clarks Basin; Єmp, schist of Mahogany Peaks; Op, metamorphosed Pogonip Group; Oe, metamorphosed Eureka Quartzite; Ofh, metamorphosed Fish Haven Dolomite; Ds, metamorphosed Simonson Dolomite; Dg, metamorphosed Guilmette Formation; Mcdp, metamorphosed Chainman-Diamond Peak Formation; IPols, limestone of the Oquirrh Formation; IPoss, sandstone of the Oquirrh Formation; Qo, older alluvium. From Miller and others (1980).

fault slices of Devonian, Mississippian, and Pennsylvanian rocks overlie the metamorphosed Pogonip Group (refer to Figure 16). The total distance of this traverse is about 3 km.

Return downslope to the vehicles now and walk northwest along the ridge underlain by the metamorphosed Pogonip Group marble. The metamorphosed Pogonip Group here consists of gray, white, and blue-gray, fine-grained dolomite marble, and coarse-grained, micaceous, laminated calcite marble. The schist of Mahogany Peaks is very thin near the vehicles. As we near the white quartzite knob, the schist of Mahogany Peaks appears near a bulldozed road. Here it is silvery, biotite-white mica schist that contains garnet and staurolite. The quartzite of Clarks Basin is thin-bedded, white quartzite with micaceous partings. It is strongly lineated and folded here.

To the south, doubly plunging anticlines developed in the quartzite of Clarks Basin are visible. The ridge about one mile distant south of us exposes metamorphosed Devonian strata overlain westward by Mississippian strata. The low ground beyond that ridge is underlain by a 38 m.y.-old pluton which cuts F_1 folds (Compton and others, 1977). Above and beyond the pluton is Bovine Mountain, which is composed of folded and overturned rocks of the Oquirrh Formation. The ridge immediately north of our position contains generally horizontal strata ranging from the Elba Quartzite to the quartzite of Clarks Basin. In the intervening saddle is a high-angle fault of about N. 60° W. strike with north side up relative to the south.

Walk down to the saddle and climb a short distance up the ridge beyond to examine the Elba Quartzite, and then follow the fault trace northwest where it juxtaposes the metamorphosed Pogonip Group marbles in the south block with the schist of Stevens Spring in the north block. Brecciated and highly fractured marble is common near the fault. The Elba Quartzite is unusual in that it is mainly thin-bedded and poorly schistose. Well-developed folds and lineations are present, and cross-laminations may still be found despite the highly deformed appearance of the rock. The schist of Stevens Spring is silvery, biotite-white mica schist that contains thin beds of white quartzite and calcite marble.

Walk back to the southern fault block of the metamorphosed Pogonip Group marble which forms a saddle, and climb the opposite slope through fault slices of metamorphosed middle and upper Paleozoic strata. Lenticular slices of the metamorphosed Eureka Quartzite, the metamorphosed Fish Haven Dolomite, the metamorphosed Guilmette Formation limestone, and Mississippian schist crop out on this slope. Exposed along the ridge crest is about 10 m of the metamorphosed Chainman-Diamond Peak Formation: black mica schist with dark gray and brown calcite marble beds. The top of these beds is marked by a small cliff exposure of the spectacularly folded and brec-

ciated limestone of the Oquirrh Formation. This thin slice is recrystallized and deformed, as indicated by deformed crinoid fragments. Conformably overlying the limestone in a small syncline is a thick sequence of calcareous sandstone of the Oquirrh Formation. The units we have traversed are largely bounded by low-angle faults, as shown on the geologic map (Figure 16).

Proceed to the ridge crest (marked X on the map) where the central part of Grouse Creek Mountains lies to the north (Figure 17). The high ridge at the end of Rosebud Creek Valley on the left is underlain by autochthonous rocks consisting of adamellite that is approximately 2.5 b.y. old on the basis of U-Pb and Rb-Sr methods (Armstrong, 1976; Compton and others, 1977), unconformably overlain by Elba Quartzite and schist of Stevens Spring. Two, and probably three, allochthonous sheets once covered this autochthon; remnants of the lower and middle sheets are present on all sides of the range, whereas parts of the uppermost allochthon lap onto the range on the west and south. The structural arrangement reflects what was probably the original stratigraphic sequence in the region, i.e., successively higher allochthons consist of progressively younger strata, with some formations tectonically cut out. Eastward-dipping high-angle faults (Basin and Range) have broken this layered structure on the east side; the Grouse Creek Mountains have been raised and tilted westward. East of the main ridge, we see three hills-probably all fault-bounded, in which the upper part of the original layered structure is preserved. These three hills are small horsts within the eastern downdropped block. The original distribution of autochthonous and allochthonous rocks cannot be determined unambiguously, but it appears to be similar to the domes of the Albion Mountains, part of which we saw yesterday.

The Archean adamellite is strongly gneissic throughout about 1 km of vertical exposure; mineral foliation and compositional layering in the gneiss are nearly parallel to the overlying low-angle faults, and to unit contacts and bedding within the autochthon and allochthons; all are gently dipping. Return to the vehicles and retrace the route to the main gravel road (Immigrant Trail).

1.1	133.1	Turn left on gravel road.
2.5	135.6	Turn left on the road following Rosebud Creek. Avoid side roads that leave the drainage.
0.7	136.3	We cross the high stand of Lake Bonneville.
4.7	141.0	Metaquartzite of the Oquirrh Formation crops out next to the road. The hill on our right is a north-trending horst (one of the three we saw from the last stop) which exposes the Chainman-Diamond Peak Formation and the Oquirrh Formation rocks of the middle allochthon, in low-angle fault contact over the quartzite of Clarks Basin, schist of Stevens Spring, Elba Quartzite and Archean adamellite. The rocks of the middle sheet occur in two or more large, near recum-

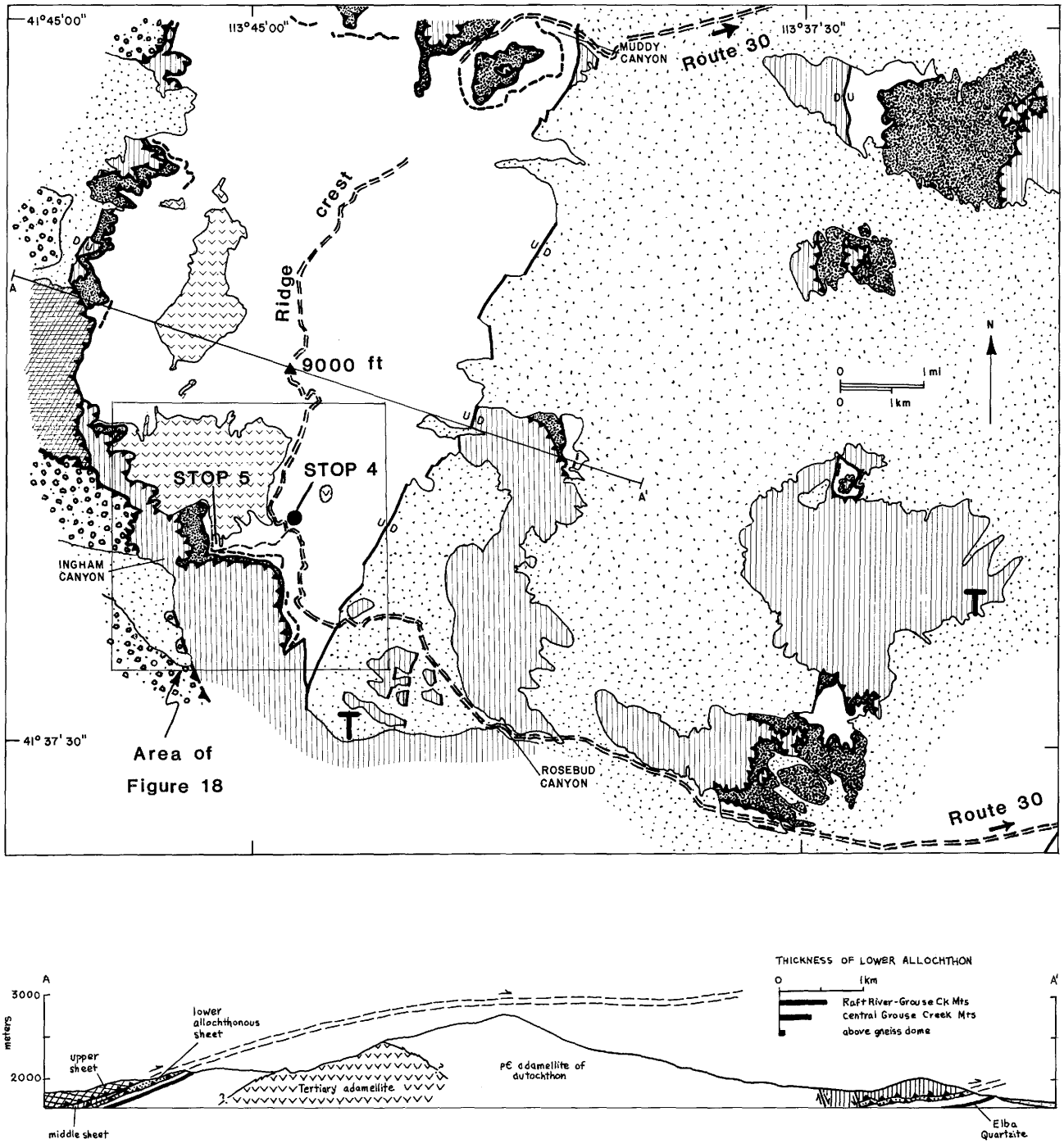

Figure 17. Generalized structure map and vertical cross section of central Grouse Creek Mountains. Cross section A-A′ has equal horizontal and vertical scales and is enlarged relative to the map. Thicknesses of rock units in lower sheet are maximal for region after metamorphism. Miocene rocks and upper allochthonous sheet comprise a complex uppermost allochthon (Compton, 1983). Possible Miocene rocks in the eastern Grouse Creek Mountains not shown. (After Todd, 1980).

EXPLANATION

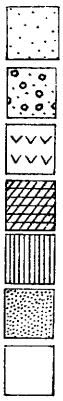

Pliocene and Quaternary rocks

Miocene rocks

Tertiary adamellite

Upper allochthonous sheet

Middle allochtonous sheet

Lower allochtonous sheet

Autochthon, chiefly Precambrian adamellite

Contact

Low-angle fault, teeth on upper plate

U/D High-angle fault; U on upthrown side, D on downthrown side

Elba Quartzite; indicates approximate location of intrusive contact between remobilized Precambrian adamellite and upper Precambrian(?) metasedimentary rocks of autochthon

T Allochthonous sheets on Tertiary beds

bent, southeast-and east-verging folds which were broken by low-angle faults. Hinges of two folds should be visible in the southwest side of the hill as we drive up the alluvial fan toward the range. A major low-angle fault has brought the low-grade Oquirrh metaquartzite and metamorphosed sandy limestone over metamorphosed Chainman-Diamond Peak Formation. Much of the Oquirrh marble has been cut out by the fault; it occurs as a thin layer between quartzite and the Chainman-Diamond Peak.

0.3 141.3 Turn right to Ingham Pass.

1.0 142.3 Turn left parallel to fence. Knolls south of here in this north-trending graben consist chiefly of the upper thinly bedded limestone and sandstone sub-unit of the Oquirrh Formation. Recent mapping by R. R. Compton and Stanford University field classes shows that the thinly bedded Oquirrh Formation rocks overlie the Tertiary Salt Lake Formation over an area of at least several square miles. This thin allochthon of upper Oquirrh Formation rocks is in low-angle fault contact with an apparently allochthonous lens of tuffaceous sandstone that dips up to 43°. These thin allochthons lie between the middle and upper allochthonous sheets of the Grouse Creek Mountains and probably moved at the same time as the upper allochthon.

0.7 143.0 The knoll next to the road is composed of Chainman-Diamond Peak Formation and possibly older Paleozoic formations down-dropped against Archean gneiss of the main range. Just beyond the knoll we will cross the frontal fault (here covered by alluvium). Along the road for the next 0.7 miles we will see abundant float from the Chainman-Diamond Peak Formation including stretched pebble conglomerate.

0.5 143.5 We are driving on poorly exposed Archean gneiss of the autochthon. The road continues in this unit up the steep eastern face of the Grouse Creek Mountains to the crest.

1.4 144.9 **STOP 4**. Park on the flat here and walk south along the ridge.

We will be walking up-section through gneissic meta-adamellite and less abundant meta-tonalite, amphibolite, and leucocratic rock toward the contact between the Archean adamellite and the Elba Quartzite (Figure 18). In most places the adamellite becomes increasingly schistose as the contact is approached due to recrystallization and hydrolysis reactions involving conversion of K-feldspar and, to a lesser extent, plagioclase and biotite to phengitic white mica and quartz. In its most extreme form, the end-product is phengite-quartz-albite schist. This transformation is the culmination of an upward increase in deformation and recrystallization and corresponding decrease in grain size seen throughout the 1 km vertical thickness of the Archean adamellite that is exposed in the central Grouse Creek Mountains. As we approach the contact, L_2 (northwest-trending aligned micas) becomes the predominant or the only lineation; closer to the vehicles, both L_1 (north to northeast-trending) and L_2 are present. The predominance of L_2 (and F_2) and the retrograde metamorphic reactions suggest that deformation was intensified in the upper part of the Archean adamellite in a late stage of metamorphism at a time when L_2 and F_2 structures were still forming.

At the upper contact of the adamellite which here dips gently to moderately to the southwest, we see greatly thinned units of the lower allochthon and upper part of the autochthon-Elba Quartzite, schist of Stevens Springs, quartzite of Clarks Basin, schist of Mahogany Peaks, and Pogonip Group marble. Although all of these units are tectonically attenuated, the schist of Mahogany Peaks and the Pogonip Group are locally missing, and are present only as slivers along the major low-angle fault. In contrast, the middle allochthon (the dark-colored hill above us to the south) is much thicker here than it is to the north; the dark rocks have been called the Chainman-Diamond Peak Formation, although lithologies with Diamond Peak affinities probably predominate. A variety of metamorphosed rock types are present, with carbonaceous quartzose rocks predominant over black phyllite and black marble. Thin beds of meta-conglomerate are also present. Molds and fragments of Mississippian shells were found in a float block from this hill (M. Gordon Jr., U.S. Geological Survey, written commun.). Both allochthons dip off the adamellite to the southwest. Elsewhere in the Raft River-Grouse Creek Mountains area, the lower of the two major low-angle faults occur within the schist of Stevens Spring, so that part of that unit and the Elba Quartzite are autochthonous. Here, however, the deformation was so intense that there was probably more than one fault within the upper Precambrian(?) and lower Paleozoic metasedimentary strata. Locally, the Elba Quartzite is brecciated and well-cemented and the base of the middle allochthon is strongly folded and brecciated.

The extreme attenuation of the Paleozoic section in the lower and middle allochthons in the central Grouse Creek

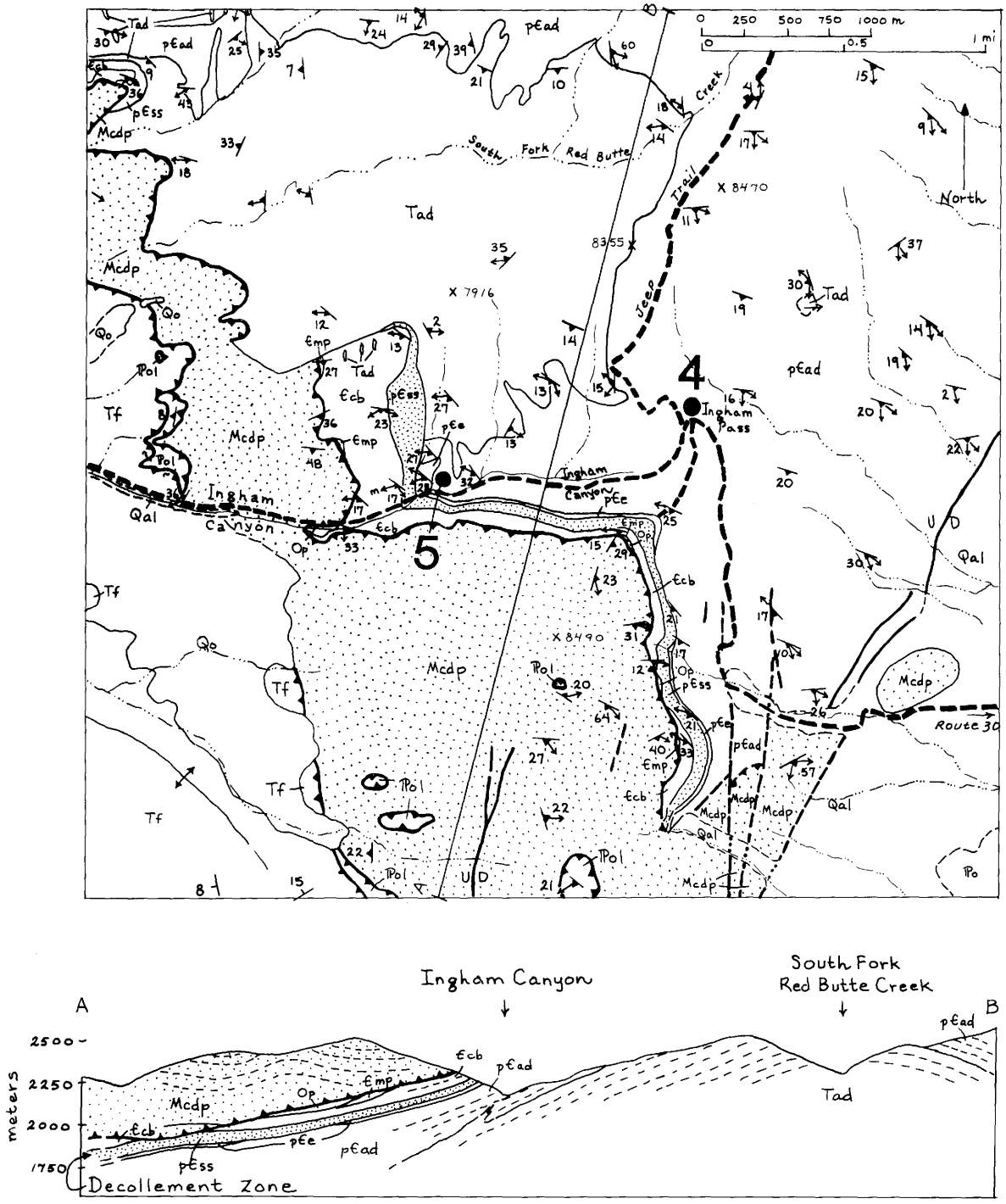

Figure 18. Geologic map and cross section for STOPS 4 and 5 (DAY 2), Ingham Pass area. pЄad, metamorphosed adamellite; pЄe, Elba Quartzite; pЄss, schist of Stevens Spring; Єcb, quartzite of Clarks Basin; Єmp, schist of Mahogany Peaks; Op, metamorphosed Pogonip Group; Mcdp, metamorphosed Chainman-Diamond Peak Formation; PPo, metamorphosed Oquirrh Formation, undivided; PPol, metamorphosed limestone of the Oquirrh Formation; Tad, adamellite; Tf, conglomerate and tuffaceous sedimentary deposits; Qo, older alluvium; Qal, modern alluvium. Low-angle faults in lower plate and Paleozoic rocks omitted for clarity. (After Todd, 1973).

Mountains (approximately 1/5 their original thickness) is spatially associated with the upward increase in synkinematic recrystallization in the underlying autochthon. Attenuation is also associated with outcroppings of a 25 m.y. old pluton (Red Butte stocks) (Figure 17) which appears to have an aureole in the Archean adamellite in which metamorphic reactions and fabrics are intensified (L_2 and F_2 predominant). This association of metamorphism, penetrative deformation, and low-angle faulting together with the presence of a broad welt of the Archean adamellite in the central Grouse Creek Mountains and local intrusive relations between the schistose (remobilized) adamellite and the Elba Quartzite indicates that a gneiss dome formed in the area about 25 m.y ago (Todd, 1980). Here the penetrative gneissic fabric and associated folds and lineation have been superimposed upon the Archean basement as late as the middle Tertiary.

Return to the vehicles and drive west on the road down Ingham Creek.

1.1 146.0 **STOP 5**. Park on the flat area where the road crosses the creek. Elba Quartzite is exposed in the canyon bottom immediately downstream and is underlain by Archean gneiss in the north side of the canyon. Walk 300 to 400 m up the side canyon on the north side of the stream into granitic rocks of the Red Butte pluton (Figure 18). The Tertiary adamellite pluton, which has been dated by Rb-Sr whole rock method as 24.9 ± 0.5 m.y. (Compton and others, 1977), crops out in two stocks after the Red Butte and Big Red Butte Creeks on the west side of the Grouse Creek Mountains. The outcrops here are weakly foliated and lineated (L_2, west-northwest-trending), reflecting mild cataclasis and minor recrystallization; elsewhere near the margins of the stocks, the Tertiary adamellite is more strongly foliated and lineated, and in Big Red Butte Creek (the next east-trending canyon to the north) the outermost 2 to 3 m of the stock is mylonitic beneath the middle allochthon and has strong west-northwest lineation (L_2). This fabric dies out through 400 m in the direction of the interior parts of the stocks. The foliation (defined chiefly by aligned biotite grains and aggregates) and lineation (marked by linear groups of quartz and biotite grains) are concordant with low-dipping foliation and L_2 in the surrounding Archean gneiss and metamorphosed allochthons. A broad aureole of metasomatic reactions and intensified F_2 -L_2 structures in the Archean adamellite suggests that the range is underlain by an extensive late Oligocene to Miocene pluton. The abundant leucocratic rocks, of probable Tertiary age, which occur in the Archean gneiss in both concordant and discordant bodies appear to have originated in two ways; directly, by intrusion, and indirectly, by metasomatic alteration of Precambrian adamellite by late-stage fluids. Walk north to the top of the ridge for a view of the west side of the range. The reddish, craggy outcrops of the Tertiary stocks are clearly visible; the surrounding Archean gneiss

forms smooth slopes with low white outcrops.

The high ridge of the Grouse Creek Mountains exposes fresh rocks, probably due to glaciation. Beautiful exposures of fine-to medium-grained adamellite gneiss of the upper part of the dome; kyanite-and staurolite-bearing pelitic schist inclusions; large amphibolite-trondhjemite bodies; and isoclinally folded gneiss (F_1 and F_2 with nearly horizontal axial planes) of the highly deformed upper part of the gneiss dome all can be seen in a 5- to 6-km traverse northward along the top of the range. The north wall of Muddy Canyon, on the east side of the range, is the best place to see schistose Precambrian adamellite intruding the Elba Quartzite (Figure 17).

Turn around and return to Rt. 30.

12.4	158.4	Turn right on Rt. 30 and proceed to our lodging in Montello, Nevada.
24.0	182.4	Crossroads. Continue straight on paved highway.
19.8	202.2	Montello.

FIELD TRIP ROAD LOG: THIRD DAY

Today we will examine upper Paleozoic and Tertiary strata and their low-angle fault relations with underlying metamorphic rocks to obtain a general picture of the styles and timing of the faulting in cover rocks of the terrane.

Mileage		Description
Incremental	Cumulative	
0.0	0.0	Leave Montello, head east on the main highway (Rt. 30).

Montello is an old railroad town, first settled in the 1800s when the original east to west railroad line was built. Its population has fluctuated from several thousands to less than a hundred, and it presently is slowly growing.

We drive east through Tecoma Valley, which was a broad, relatively shallow (100 m deep at highstand) arm of Lake Bonneville. The fine-grained lake deposits around us locally form sand dunes due to reworking by wind following the recession of the lake. To the west rise the Leach Mountains, predominantly composed of Permian through Triassic strata. The Permian strata in the southern part of the range are unusually thick (greater than 2150 m) and are thrust over Triassic deposits on east-and southeast-directed low-angle faults (Fedewa, 1980; Martindale, 1981). The Permian strata are structurally detached from fragments of Mississippian clastic rocks, and no older rocks crop out in the Leach Mountains. Permian rocks exposed in the northern part of the Leach Mountains apparently exceed 3000 m in thickness. There, the Permian section apparently lies unconformably on Mississippian clastic rocks (Le Compte, 1978). North of us are complexly faulted hills composed of upper Paleozoic strata and Tertiary sedimentary and volcanic rocks. South and east of us is the Pilot Range, which exposes a nearly complete section of sedimentary rocks of Late Proterozoic to Permian age, granitic rocks of Mesozoic and Cenozoic age, and volcanic rocks and intercalated sedimentary rocks of Oligocene

and Miocene age. The lower part of the prominent butte at the northern end of the Pilot Range is composed of white, non-resistant 9.6 m.y. old tuff and tuffaceous waterlain sedimentary rock. The butte is capped by a thick rhyolite flow with a basal vitrophyre. The rhyolite, slightly discordant on the sedimentary rocks, is 8.4 to 8.8 m.y. old (Armstrong, 1970b; Miller and Hoggatt-Hillhouse, 1983). Nearby black basalt is younger than the rhyolite, but undated as yet.

11.1	11.1	Enter state of Utah. During the next two miles we pass close by Permian rocks in the hills on our left and Ordovician rocks in Gartney Mountain on the right.
8.7	19.8	Crossroads; Grouse Creek to the left and Lucin to the right. We are now in the southwest corner of Map 4. Permian strata are exposed in the nearby hills to the south and Miocene rhyolite plugs are present to the north.
6.7	26.5	Turn left (north) on a small dirt road marked by a B.L.M. sign to Immigrant Pass and Rosebud Station (if approaching from the east, the turnoff is 4 miles west of the southernmost tip of Grouse Creek Mountains). Turn off is at southern edge of area shown in Figure 19. We will drive a short distance north on the dirt road and stop to view the surrounding features, the most prominent of which are four buttes to the west and northwest of the road. These are separate rhyolite plugs that are cut by high shorelines of Lake Bonneville; the plugs were dated by W. C. Hoggatt-Hillhouse and V. R. Todd as 11.7 m.y. in age. The plugs intrude a thick sequence of middle Miocene tuffs and interstratified sedimentary rocks that form white outcrops to the west of the road and underlie the smooth-surfaced hills rising to the northeast of the road. At localities 8 km to the north, the Miocene sequence ranges in age from approximately 15 m.y. to approximately 11.5 m.y. The Miocene rocks are in fault contact with the older rocks of the range at the break in slope where the smooth hills meet the more rugged slopes of Bovine Mountain. The fault here dips approximately 25° west-southwest. The same fault has been mapped continuously for 40 km to the north and from that point it has been mapped discontinuously to the Idaho State Line, a total distance of 65 km. The Miocene rocks 8 km to the north are tectonically intercalated with Triassic and Permian(?) rocks, and these rocks together comprise a detachment sheet along the western side of the Raft River-Grouse Creek core complex (includes the uppermost allochthonous sheet of Compton and others, 1977).
2.8	29.3	**STOP 1**. We will stop briefly to examine a large outcrop of Miocene conglomerate on the east side of the road. It dips 16° northeast, which is approximately the attitude of the other rocks underlying the smooth hills.
1.5	30.8	**STOP 2**. Stop near the large outcrop of white tuff on the east side of the road. The outcrop is typical of the Miocene tuffs, which here dip northeast-

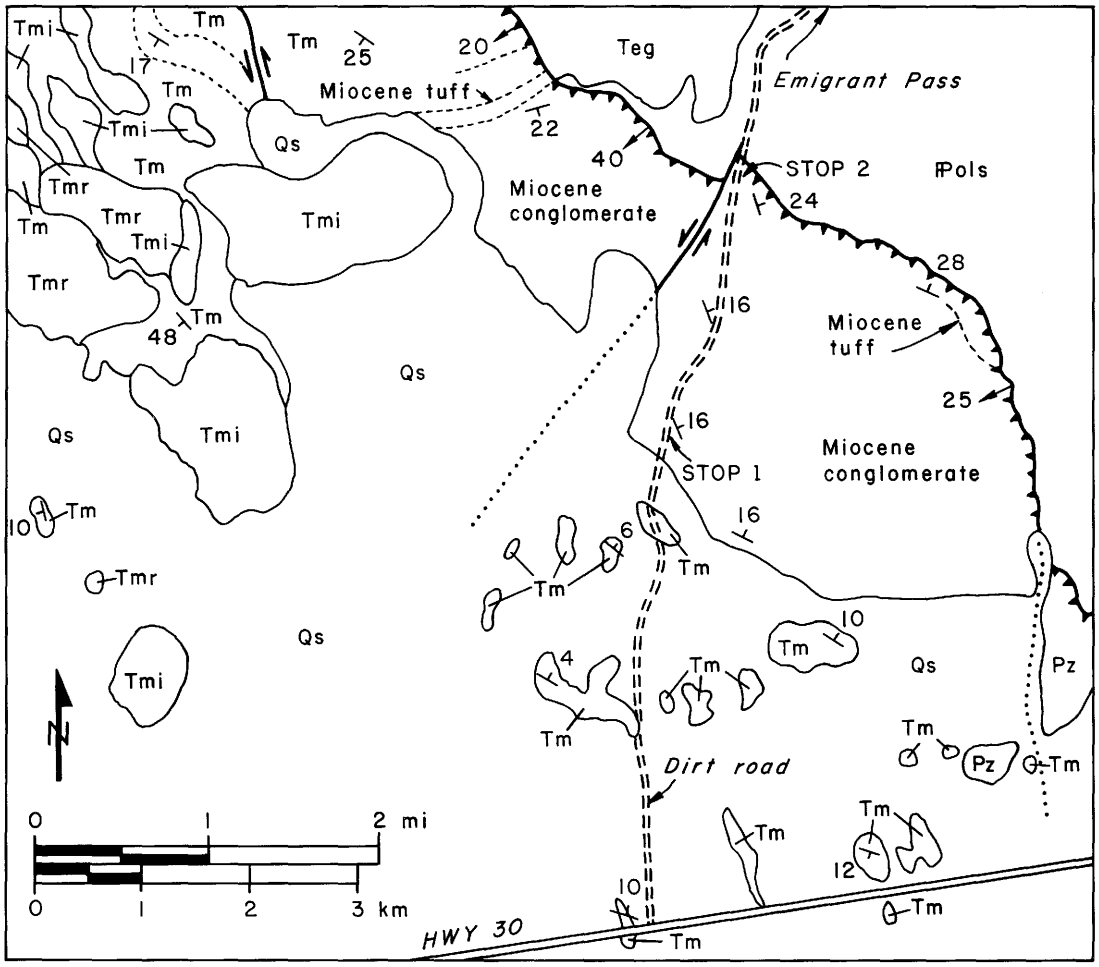

Figure 19. Geologic map of area between Highway 30 and Emigrant Pass. Pz, unmetamorphosed Paleozoic sedimentary rocks; Pols, mainly limestone of the Oquirrh Formation; Teg, Eocene granodiorite (38.1 ± m.y.; Compton and others, 1977); Tm, Miocene tuff and conglomerate; Tmr, Miocene rhyolite flows; Tmi, intrusive Miocene rhyolite; and Qs, Quaternary alluvium and Lake Bonneville sedimentary deposits.

ward into the low-angle fault that delimits the core complex. The foot-wall rocks are limestone of the Oquirrh Formation (Pennsylvanian); they are exposed adjacent to the fault surface near the tuff. Fragments of the rhyolite that makes up the plugs can be found in the fault zone, indicating displacement since 11.7 m.y. ago. Walk north-northwest (back across the road) to where the bedded tuff abuts more outcrops of the Oquirrh Limestone. This contact is apparently a strike-slip fault that offsets the plate composed of Miocene rocks. The structural relations are shown on the accompanying map (Figure 19).

Return to main highway.

4.3	35.1	Turn left (east) on main highway.
1.3	36.4	Miocene vitric waterlaid tuff is well exposed in natural outcrops and a quarry on the left (north) side of the road. The beds are folded on roughly west-trending axes and dips are at low angles (12 to 20°) to the north and south.

2.2 38.6 **STOP 3**. We will stop briefly to view the south end of the Grouse Creek Mountains, either at this first left-hand bend or nearby. The high mountain mass is called Bovine Mountain; its geology has been studied in detail by Jordan (1983). It exposes an unusually thick sequence of the Oquirrh Formation that has been deformed broadly by folding on east-verging recumbent folds that predate the 38 m.y. old pluton. Most of the exposures on the mountain are in an overturned limb, and dip at moderate angles to the west. The pale gray rocks around the base of the mountain are another structural element — a plate of an unnamed limestone member of the overturned Oquirrh Formation, lying on a low-angle fault that dips toward the highway. The fault parallels bedding in the limestone member but clearly cuts across bedding in sandstone of the Oquirrh Formation (brownish outcrops) that forms the main ridge immediately to the north. A third structural element is exposed in the low, dark (desert-varnished) outcrops that extend from near the highway for about 1 km to the north. These are overturned Ordovician and Silurian strata that are unique within the entire area of the core complex and its cover in being unmetamorphosed and texturally unstrained. These rocks are separated from the Oquirrh Formation limestone by a fault that parallels bedding in both fault blocks and that is folded by northeast trending folds that are apparently of mid-or late-Cenozoic age.

Continue northeast on the highway.

2.3 40.9 Just beyond left-hand bend in highway is a prominent outcrop of unmetamorphosed Silurian Laketown Dolomite, with bedding dipping 60° or so to the northeast.

2.0 42.9 The craggy outcrops to the left (northwest) are of granodiorite that is in intrusive contact with the Oquirrh Formation strata. The outcrops are part of a pluton that extends for 5 km to the north and 14 km to the west, and was dated by R. Zartman as approximately 38 m.y. old by the Rb-Sr method (Compton and others, 1977). Also visible are the high wave-cut benches of Lake Bonneville and a level-topped boulder bar that extends from the main front northeast to a low, craggy spur exposing granodiorite.

9.8 52.7 Turn right on gravel road that crosses main highway and has, on the left-hand side, a sign to Immigrant Trail and Rosebud Station.

1.0 53.7 Continue straight on Immigrant Trail at junction.

1.8 55.5 Turn left on dirt road.

0.3 55.8 Turn right on jeep trail (watch for boulders!).

0.5 56.3 **STOP 4**. In the Matlin Mountains, we will look at structural relations 5 to 10 km east of the core complex in a complex allochthon that was emplaced in the same approximate time span (middle to late Miocene) as the upper allochthon of the Grouse Creek Mountains, part of which we viewed at STOP 2. The Matlin

Mountains, named for a water stop of the first transcontinental railroad, were islands in the northwestern part of Lake Bonneville and are surrounded by, and partly covered by, lacustrine sedimentary deposits. They expose a sequence of five thin displaced sheets that consist of upper Paleozoic and lower Mesozoic rocks and Tertiary strata. This displaced sequence rests in low-angle fault contact on a rooted upper Paleozoic section to the east (Figure 20). The thickness of the displaced sheets is typically less than 200 m and the exposed extent of individual sheets is roughly 10 to 20 km from north to south and 5 to 10 km from east to west. The entire displaced sequence appears to dip gently westward toward the Grouse Creek Mountains. Two of the five low-angle faults that form the boundaries of the displaced sheets divide the displaced terrane into two composite plates which appear to have had different histories and to have moved separately. One of these faults, the East Fault, is the basal fault which separates the displaced terrane from the rooted section. The other, the West fault, probably dips westward and joins the basal fault at depth (Figure 20). These two faults juxtapose plates that differ significantly in lithology, metamorphism and structural character and they probably have the largest displacements of the faults in the Matlin displaced terrane.

The dark knoll immediately to our north exposes one of the displaced sheets (sheet IV) which comprises the structurally higher of the two composite plates (Figure 21). Sheet IV consists of the marble and metaquartzite of the metamorphosed Oquirrh Formation with lesser metamorphosed Chainman-Diamond Peak Formation. It rests on a sequence of approximately 2,000 m of northwest-dipping Tertiary strata which contains an 11.1 to 10.5 m.y. old vitric tuff in its upper part. The knoll is the southern end of a northeast-trending hill (affectionately named "Big Pink") that consists of Tertiary strata overlain by the metamorphosed Oquirrh Formation and unconformably overlying Lower Permian rocks, the metamorphosed Kaibab Limestone and the metamorphosed Arcturus or Pequop Formation. These rocks were heated to 400°C based on conodont alteration (Todd, 1983). The southeastern flank of the hill is bordered by a northwest-dipping reverse fault along which the hill has been uplifted.
uplifted.

We will walk across the knoll to the northeast and look at the highly brecciated marble and metaquartzite of the metamorphosed Oquirrh Formation in displaced sheet IV. The underlying Tertiary strata are virtually undisturbed as we will see on the northeast side of the knoll where the contact is exposed. Locally, sandstone dikes containing rounded cobbles of Oquirrh(?) rocks extend upward from the Tertiary beds into the base of the brecciated Oquirrh sheet (Figure 20). The brecciated sheets are not monolithologic; in spite of pervasive fracturing of a given sheet (reconstructed by island-hopping) it typically preserves a recognizable stratigraphy. When mapped in

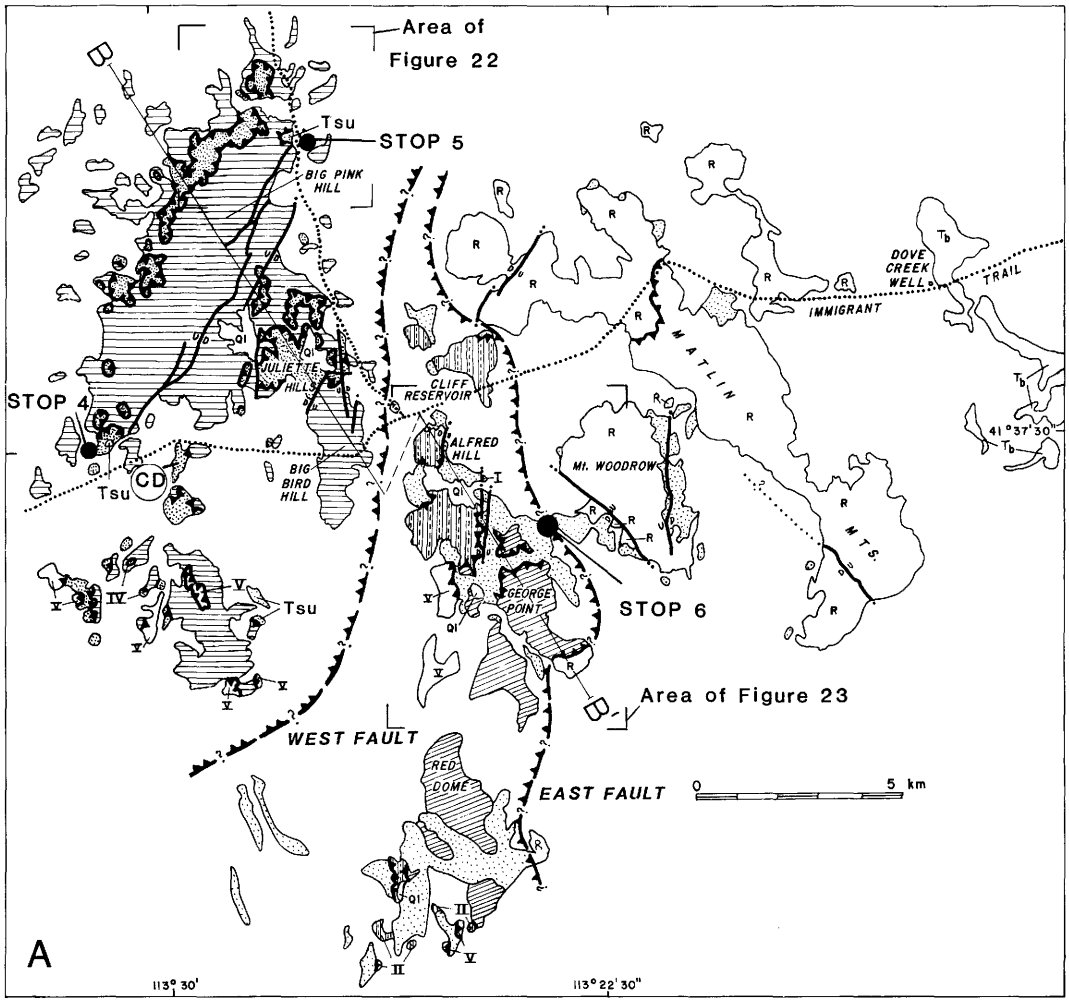

Contact

High-angle fault (u=upthrown block, d=downthrown block, dotted where covered)

Low-angle fault (teeth on upper plate, queried where inferred)

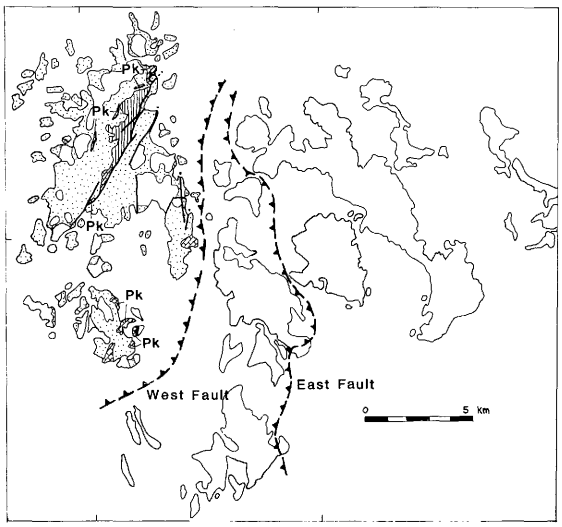

EXPLANATION

Interbedded fanglomerate and tuffaceous sandstone (Big Pink section) (Upper Miocene)

Kaibab Limestone (Lower Permian)

Arcturus or Pequop Formation (Lower Permian)

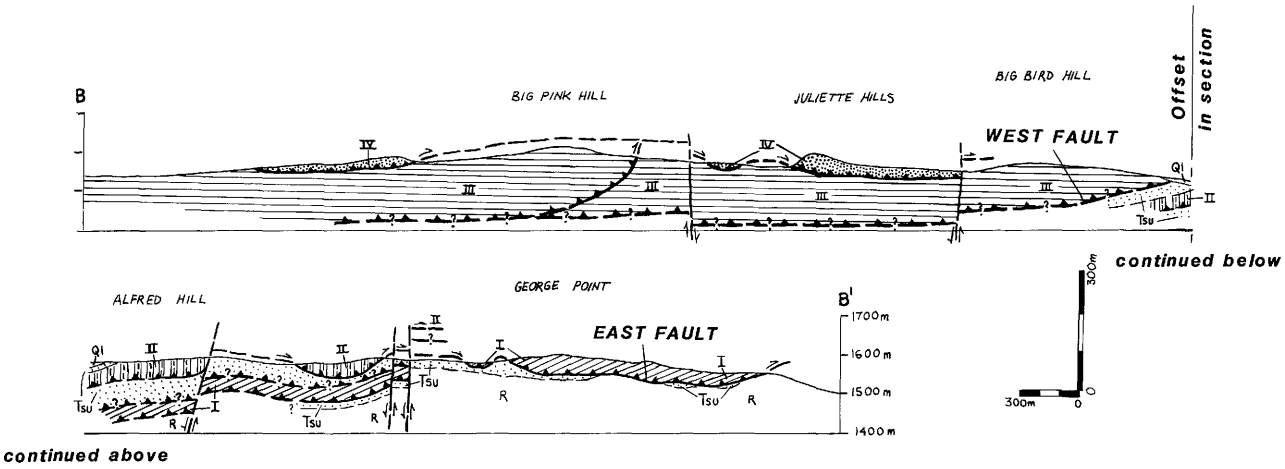

B

EXPLANATION FOR FIGURE 20A,B

Ql	Lake Bonneville deposits (Quaternary)
Tb	Basalt (Tertiary)
Tsu	Sedimentary rocks, undivided (Tertiary)
V	Displaced sheet V, consists of Permian and Triassic (?) sedimentary rocks
IV	Displaced sheet IV, consists of Paleozoic sedimentary rocks
III	Displaced sheet III, consists of Permian and Upper Miocene sedimentary rocks
II	Displaced sheet II, consists of Permian sedimentary rocks
I	Displaced sheet I, consists of Permian and Triassic (?) sedimentary rocks
R	Rooted section, consists of Pennsylvanian and Permian sedimentary rocks

Figure 20. Generalized structural map and cross section of Matlin Mountains showing distribution of displaced sheets I-V, rooted Paleozoic rocks, and Tertiary rocks. Dashed queried faults are inferred low-angle faults between displaced and rooted terranes (East fault), and between two composite plates of the displaced terrane (West fault). CD = clastic dikes. Insert shows distribution of Paleozoic and Tertiary rocks in sheet III. Pk, Kaibab Limestone. (After Todd, 1983).

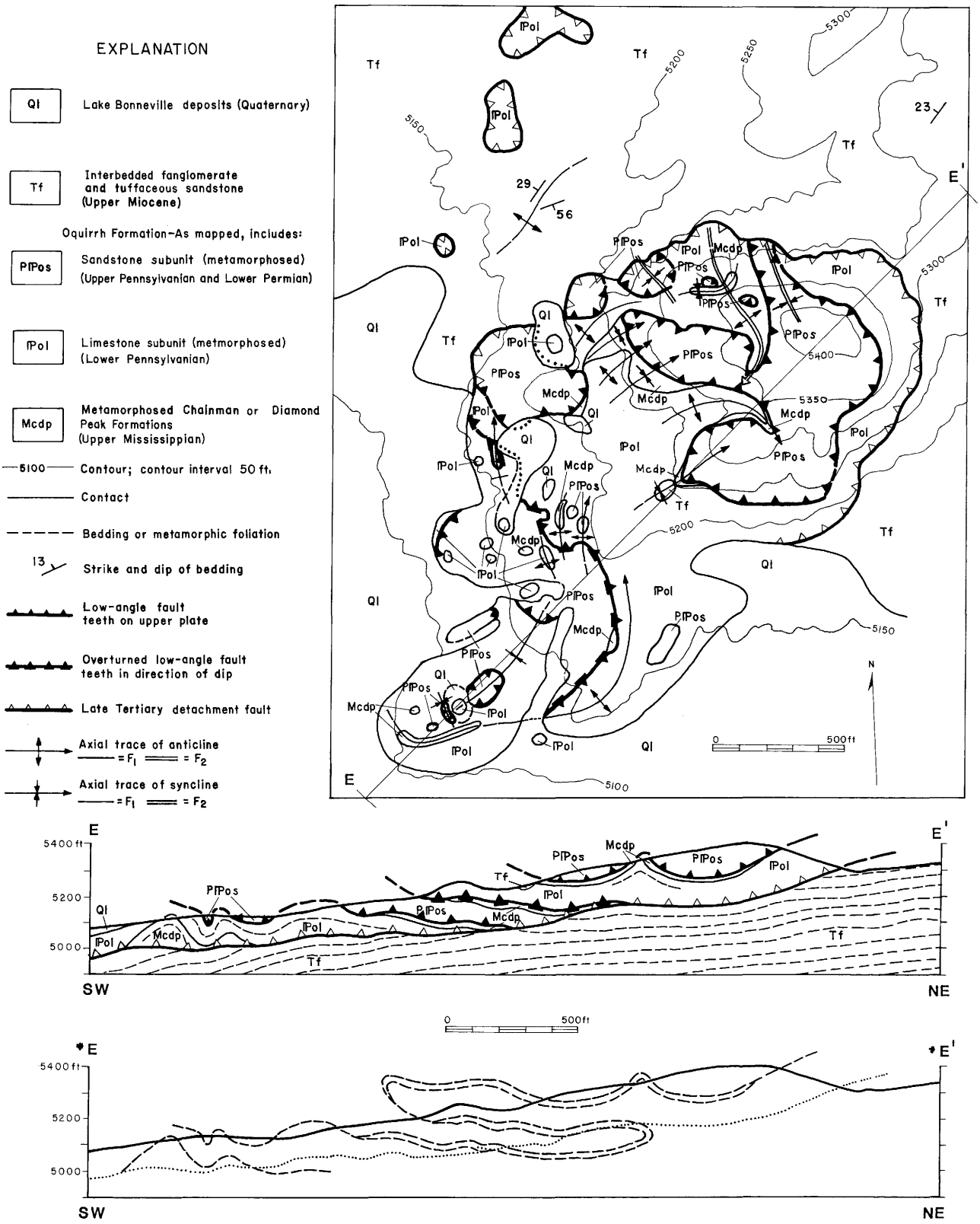

Figure 21. Detailed geologic map and cross section of area in displaced sheet IV (STOP 4, DAY 3, Figure 20). F1= northeast-trending folds; F2 = later, northwest-trending folds. Cross section E-E′ has equal horizontal and vertical scales; *E-*E′ is interpretive cross section. (From Todd, 1983).

detail, the rocks of sheet IV in this knoll and surrounding hills to the south compose an isoclinally folded (recumbent) thrust of quartzite over(?) marble, the two separated by a thin, discontinuous slice of black quartzite and phyllite (metamorphosed Chainman-Diamond Peak Formation). This structure was subsequently doubly folded in upright folds and brecciated, possibly during its emplacement over Tertiary sedimentary rocks.

If we look south from the top of the hill, we will see well-developed wave-cut terraces on the nearest "islands". Directly to the east is a well-developed shoreline; those immediately below us to the south and west are not as obvious; presumably the lake was shallower in this area.

The Tertiary beds here consist predominantly of fine-grained, fresh water tuffaceous lake deposits in the upper part and sandstone, lakeshore gravel and fanglomerate deposits in the lower part. The basal unconformity over the Lower Permian marble units is exposed about 1.5 km to the north (Figure 20). From a distance, the tuffaceous beds appear white, and the fanglomerate deposits appear as dark-brown, resistant layers. The red color of the hill underlain by Tertiary deposits to the north is due to abundant red-weathering meta-sandstone clasts. The lithic clasts provide a stratigraphy for the Big Pink Tertiary strata which is the reverse of the "structural stratigraphy" of the Grouse Creek Mountains: unmetamorphosed chert, carbonate rocks and argillite in the lower part, and metamorphosed carbonaceous phyllite, metacarbonate rocks and micaceous quartzite in the upper part. A sizeable proportion of the clasts in the upper part are lineated similarly to rocks we saw in the previous day's stops, and therefore these Miocene fanglomerate deposits were deposited during the unroofing of a part of the metamorphic terrane to the west.

Walk north about 2.5 km along the ridge crest to the high Tertiary hill to examine the Big Pink section. From this peak we can see dark hill caps to the north, remnants of displaced sheet IV lying in flat contact over light-colored truncated Tertiary strata. To the east, in informally named Juliette Valley, we can see more dark caps of sheet IV, there consisting of metamorphosed Kaibab Limestone over Tertiary strata. The Tertiary strata of Juliette Valley are continuous with the Big Pink section.

Drop downhill to the east to examine the unconformity (uplifted and exposed by the reverse fault) between the Big Pink section and lower Permian units, here possibly including some Oquirrh Formation rocks. The Big Pink section and underlying lower Permian rocks are interpreted to comprise displaced sheet III (Figure 20).

Continue eastward and cross the reverse fault which, on the basis of restoration of cross sections, is believed to have begun to form in a strongly folded part of the Big Pink section before it broke through as an upthrust. As we cross to the east side of the fault, we will be in the footwall — "Big Pink" strata overlain by sheet IV,

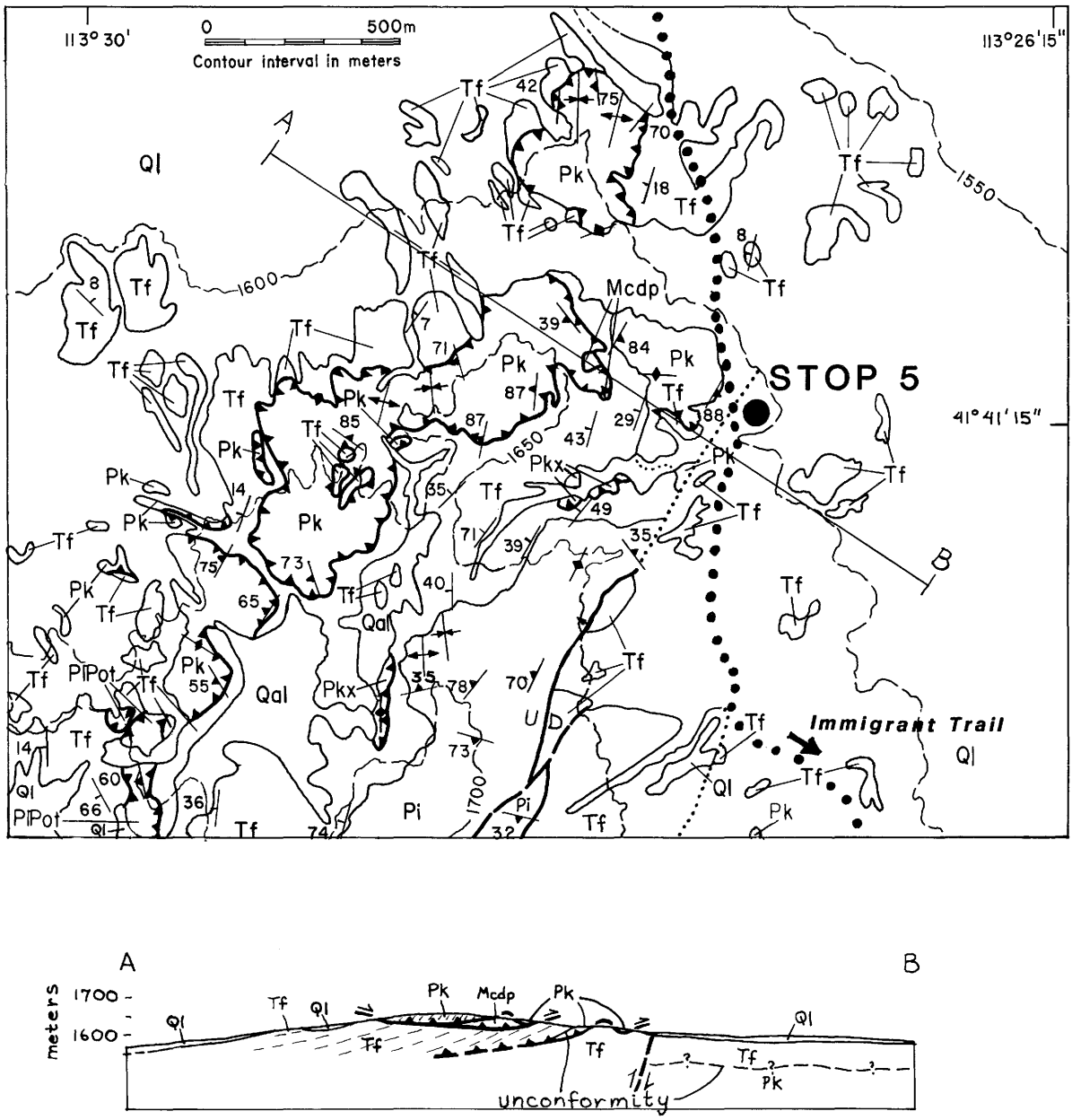

Figure 22. Geologic map and cross section for STOP 5, DAY 3, north end of Big Pink Hill. Pi probably equivalent to Arcturus or Pequop Formations. (After Todd, 1983).

EXPLANATION

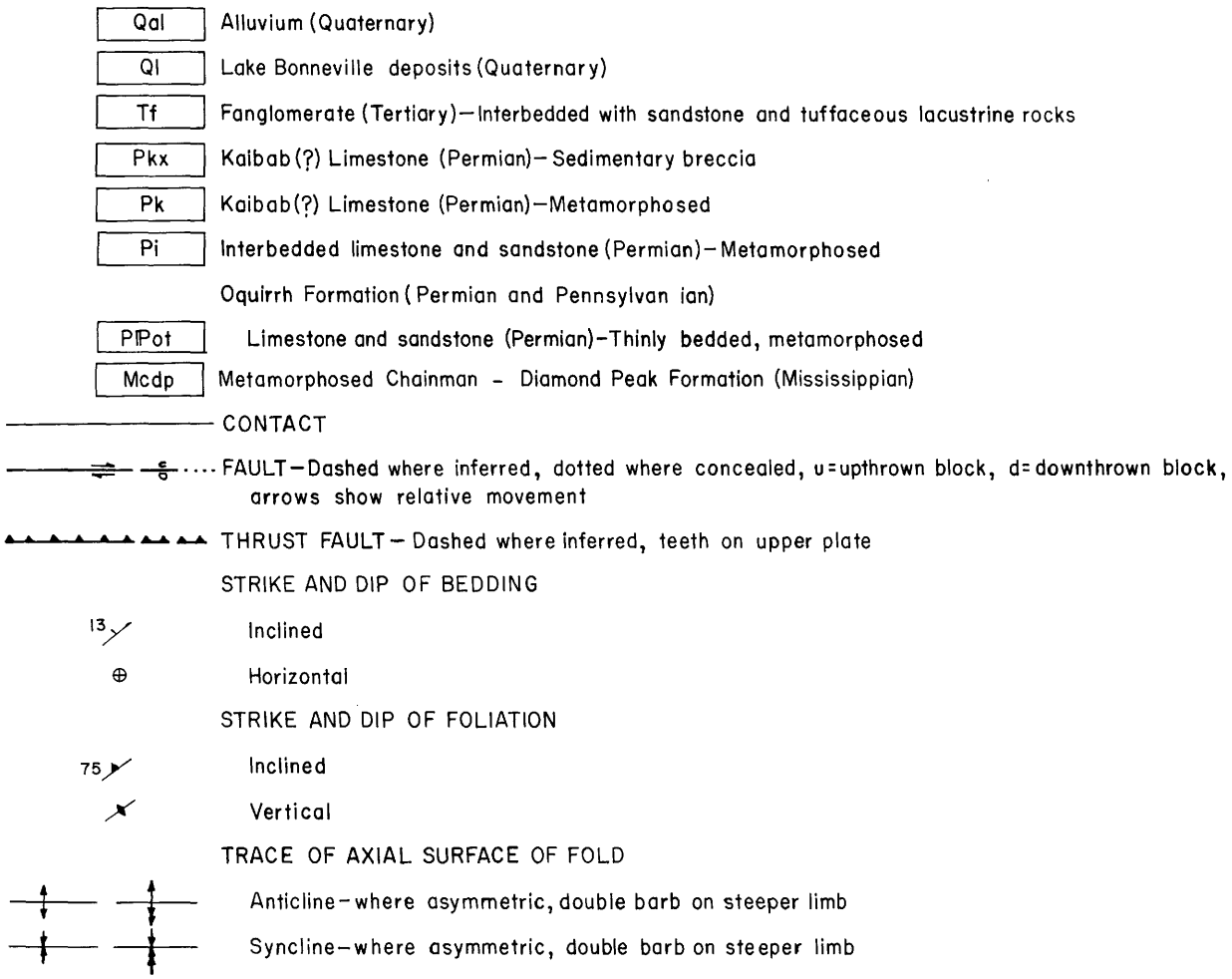

both offset by several short, straight Basin and Range faults. As the cross section of Figure 20 implies, the reverse fault does not offset sheet IV. The dashed line representing the restored base of sheet IV is controlled by small klippen not shown in Figure 20. The reverse fault may have been reactivated during Basin and Range faulting.

Walk south across down-dropped "Big Pink" strata to the old jeep trail; go right at the jeep trail and return to vehicles.

Return to Immigrant Trail and turn left; continue eastward on Immigrant Trail.

1.2	57.5	Pass dark outcrops of metamorphosed Oquirrh Formation on the right; the low-lying patches of Tertiary tuffaceous sandstone and conglomerate that surround each dark hill are part of the underlying "Big Pink" section.
1.1	58.6	On the left are east-northeast-dipping strata of the

eastern part of the "Big Pink" section exposed in a small horst informally named Big Bird Hill. The section here consists of somewhat finer-grained conglomerate interbedded with sandstone and tuffaceous siltstone. Patches of sheet IV overlie the north end of this hill, and a lens of brecciated metamorphosed Lower Permian Limestone that is interbedded with the Tertiary strata crops out spottily on the west side of the hill and just ahead in the road. Similar concordant breccia lenses are enclosed within the northwest-dipping Tertiary strata of Big Pink Hill, and one of these may have been continuous with the breccia lens of Big Bird Hill. These concordant breccia lenses are interpreted to be landslide deposits that formed during the accumulation of the "Big Pink" section. Unlike the displaced sheets, they are small, totally brecciated, and concordant with the enclosing sedimentary strata; they probably had the same source as displaced sheets III and IV.

The road continues on a Lake Bonneville shoreline; go straight past a jeep trail turnoff to the right.

1.3 59.9 Turn left onto jeep trail. Continue for approximately 4.5 mi to the northern end of Big Pink Hill, and past outcrops of sheet IV overlying Tertiary strata. Stay on main jeep trail; do not take side trails.

4.5 64.4 **STOP 5**. Examine exposures of the base of displaced sheet III (Figure 22). Brecciated metamorphosed Kaibab Limestone overlies Tertiary tuffaceous strata in low-angle fault contact. Walk westward (structurally up section) across the unconformable contact between the overlying "Big Pink" strata and this brecciated Kaibab Limestone, to the fault contact between the "Big Pink" strata and sheet IV (Figure 22). Lenses of the Chainman-Diamond Peak Formation lie along the base of sheet IV.

The base of sheet III is poorly exposed near the southern end of the sheet's extent (Figure 20). Even without these two exposures of the basal fault, the clast stratigraphy of the "Big Pink" section indicates that these rocks were not deposited here and that the section is allochthonous. The upper part of the section includes metamorphic clasts from formations of the core complex that were still buried to metamorphic depths in late Miocene time.

4.5 68.9 Return to the Immigrant Trail, turn left; proceed eastward on Immigrant Trail.

0.5 69.4 Turn right on jeep trail, and bear left almost immediately at junction of two jeep trails.

Somewhere between Big Bird Hill and the dark hill immediately ahead of us (informally named Alfred Hill), we crossed the West fault, the inferred westward-dipping low-angle fault which separates the displaced sheets that consist of metamorphosed Mississippian to lower Permian rocks and the "Big Pink" section on the west from displaced sheets of unmetamorphosed Permian and Triassic rocks and associated Tertiary sedimentary rocks on the east (Figure 20). The eastern displaced Tertiary rocks consist of tuffaceous

sandstone and fanglomerate that are as yet undated but are lithologically similar to the "Big Pink" section. The highest displaced sheet V occurs in the southern part of the Matlin Mountains on both sides of the West fault; presumably, it was emplaced after both higher (west) and lower (east) composite plates were in their present position. The fault contact between metamorphosed Kaibab Limestone and underlying Tertiary rocks (base of sheet III) which we viewed at STOP 5 maybe an exposure of the West fault.

Alfred Hill and small islands to the south expose unmetamorphosed Permian Gerster Formation which is overlain by fanglomerate and in turn overlies fanglomerate similar to that in the lower part of the "Big Pink" Tertiary section (Figure 23). This structurally lower fanglomerate lies in low-angle fault or depositional contact on unmetamorphosed Upper Permian and Triassic strata which in turn overlie red-weathering Tertiary conglomerate in low-angle fault contact. In the eastern Matlin Mountains, this red conglomerate conformably overlies an unmetamorphosed Pennsylvanian and Permian terrane that has a normal depositional cover of tuffaceous Tertiary sedimentary rocks (rooted section) (Figure 20). The basal low-angle fault (East fault) that separates the rooted section from the western displaced terrane can be traced discontinuously for 1 to 2 km from east to west and is inferred to join the West fault at depth.

1.6 71.0 Continue straight through junction with jeep trail on right.

0.6 71.6 **STOP 6**. Park where two jeep trails cross. Walk approximately 600 m southwest to the top of a hill underlain by Tertiary fanglomerate that overlies Plympton Formation of displaced sheet I (Figure 23). To the northwest is informally-named Mount Woodrow, which is underlain by a rooted, gently to moderately northwest-dipping section of unmetamorphosed Kaibab Limestone grading into Plympton Formation. These units were uplifted along a steep northwest-trending Basin and Range fault that occurs at the break in slope. The low ridges southwest of the fault consist of Lake Bonneville gravel deposits which overlie poorly exposed pale buff-white fine-grained tuffaceous sandstone with conglomeratic interbeds whose clasts appear to be derived from the rooted section. Patches of red-weathering Tertiary conglomerate consisting chiefly of clasts of Lower Triassic Dinwoody and Thaynes Formations conformably overlie the buff sandstone around the southern and eastern flanks of Mount Woodrow. The East fault must lie beneath lake gravel in the bottom of the valley between us and Mount Woodrow. A low-angle fault located about 3 km to the south has brought Plympton Formation (sheet I) over Kaibab Limestone; this fault, which dips about 20° to the northwest, is probably the East fault.

The valley to the northwest was an embayment of Lake Bonneville. If we were to continue south on the main jeep trail we would see a well-

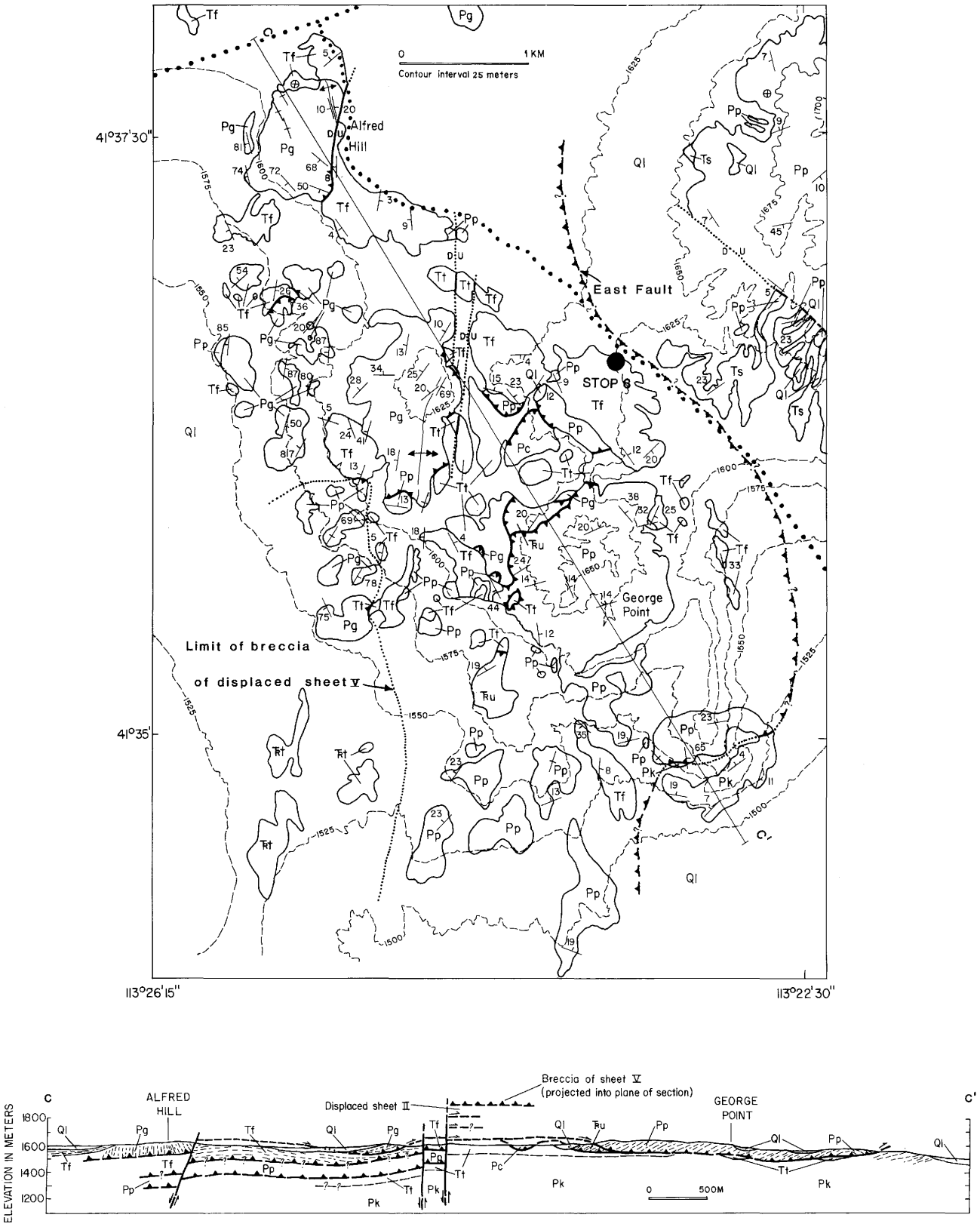

Figure 23. Geologic map and cross section for STOP 6, DAY 3, Alfred Hill-George Point area. (After Todd, 1983).

EXPLANATION

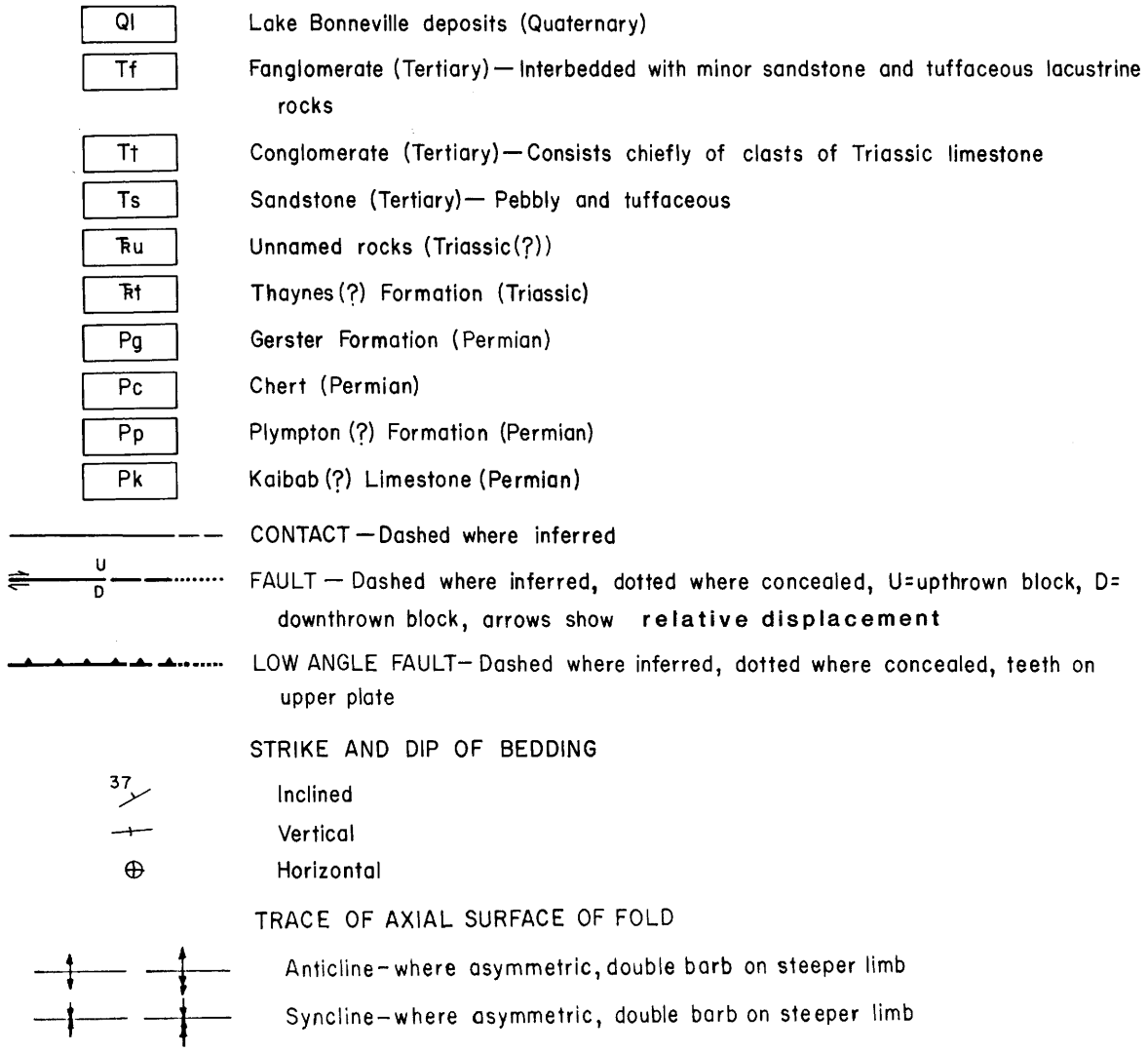

developed beach, gravel spit, and wave-cut sea cliff. These features are spectacularly well-developed in the large embayment and ridge (south Matlin) east of Mount Woodrow.

The valley to the southwest forms a window through displaced sheet I, exposing the red conglomerate of the rooted section. The true nature of the "red mounds" was debated back and forth until unambiguous outcrops of Gerster Formation were seen to underlie red mounds on the east side of Mount Woodrow. The black-colored mound of black chert is probably a tectonic sliver related to the fault at the base of sheet I; a similar sliver of Gerster Formation appears to lie between the red conglomerate and the Plympton Formation of sheet I in the large hill to the south (informally named George Point). Probable Middle and Upper Triassic carbonate rocks are infaulted with the Plympton Formation on George Point. To the west is a hill consisting of the Ger-

ster Formation overlying Tertiary fanglomerate; the latter is essentially continuous with the fanglomerate we are now standing on. The Gerster rocks are part of the structurally higher displaced sheet II, and they are essentially continuous with the outcrops of Alfred Hill to the north (Figure 23).

At this stop, we will walk southwest, down across the poorly exposed contact between Plympton Formation and the red conglomerate, and into the valley to examine the red mounds. Then we'll walk north, cross buried steep faults which have apparently brought sheet I and the rooted section up on the east against sheet II, and examine a small outcrop of the fanglomerate at the base of displaced sheet II. Return to the Immigrant Trail; turn left and return to Route 30.

3.5 75.1 Route 30. Turn left for return trip to the Lucin crossroads, 24 miles distant and near the Nevada border, where a left turn will place us on a graded main road following the eastern flank of the Pilot Range. Stay on the main road the entire length of the range, connecting with Interstate 80 just east of Wendover at the Bonneville Salt Flats exit. From there drive east to Salt Lake City.

END OF FIELD TRIP.

REFERENCES

Armstrong, R. L., 1968, Mantled gneiss domes in the Albion Range, southern Idaho: Geological Society of America Bulletin, v. 79, p. 1295-1314.

_____, 1970a, Mantled gneiss domes in the Albion Range, southern Idaho: A revision: Geological Society of America Bulletin, v. 81, p. 909-910.

_____, 1970b, Geochronology of Tertiary igneous rocks, eastern Basin and Range province, western Utah, eastern Nevada, and vicinity, U.S.A.: Geochimica et Cosmochimica Acta, v. 34, p. 203-232.

_____, 1975, The geochronometry of Idaho, Part I: Isochron/West, No. 14, p. 1-50.

_____, 1976, The geochronometry of Idaho, Part II: Isochron/West, No. 15, p. 1-33.

Armstrong, R. L., and Hills, F. A., 1967, Rb-Sr and K-Ar geochronologic studies of mantled gneiss domes, Albion Range, southern Idaho, U.S.A.: Earth and Planetary Science Letters, v. 3, p. 114-124.

Armstrong, R. L., Smith, J. F., Jr., Covington, H. R., and Williams, P. L., 1978, Preliminary geologic map of the west half of the Pocatello 1°x 2° quadrangle, Idaho: U.S. Geological Survey Open-File Report 78-533.

Chappell, B. W., and White, A. J. R., 1974, Two contrasting magma types: Pacific Geology, v. 8, p. 173-174.

Compton, R. R., 1969, Thrusting in northwest Utah: Geological Society of America Abstracts 1969, pt. 5, p. 15.

_____, 1972, Geologic map of the Yost quadrangle, Box Elder County, Utah, and Cassia County, Idaho: U.S. Geological Survey Miscellaneous Geologic Investigations Map I-672.

_____, 1975, Geologic map of the Park Valley quadrangle, Box Elder County, Utah and Cassia County, Idaho: U.S. Geological Survey Miscellaneous Geologic Investigations Map I-873.

_____, 1980, Fabrics and strains in quartzites of a metamorphic core complex, *in* Crittenden, M. D., Jr., and others, eds., Cordilleran metamorphic core complexes: Geological Society of America Memoir 153, p. 385-398.

_____, 1983, Displaced Miocene rocks on the west flank of the Raft River-Grouse Creek core complex, Utah, *in* Miller, D. M., and others, eds., Tectonic and stratigraphic studies in the eastern Great Basin: Geological Society of America Memoir 157 (in press).

Compton, R. R., Todd, V. R., Zartman, R. F., and Naeser, C. W., 1977, Oligocene and Miocene metamorphism, folding, and low-angle faulting in northwestern Utah: Geological Society of America Bulletin, v. 88, p. 1237-1250.

Covington, H. R., 1983, Structural evolution of the Raft River basin, Idaho, *in* Miller, D. M., and others, eds., Tectonic and stratigraphic studies of the eastern Great Basin: Geological Society of America Memoir 157 (in press).

Crittenden, M. D., Jr., 1979, Discussion on Oligocene and Miocene metamorphism, folding, and low-angle faulting in northwestern Utah: Geological Society of America Bulletin, v. 90, p. 305-309.

Fedewa, W. T., 1980, Stratigraphy and phosphate resources of the Murdock Mountain area, Elko

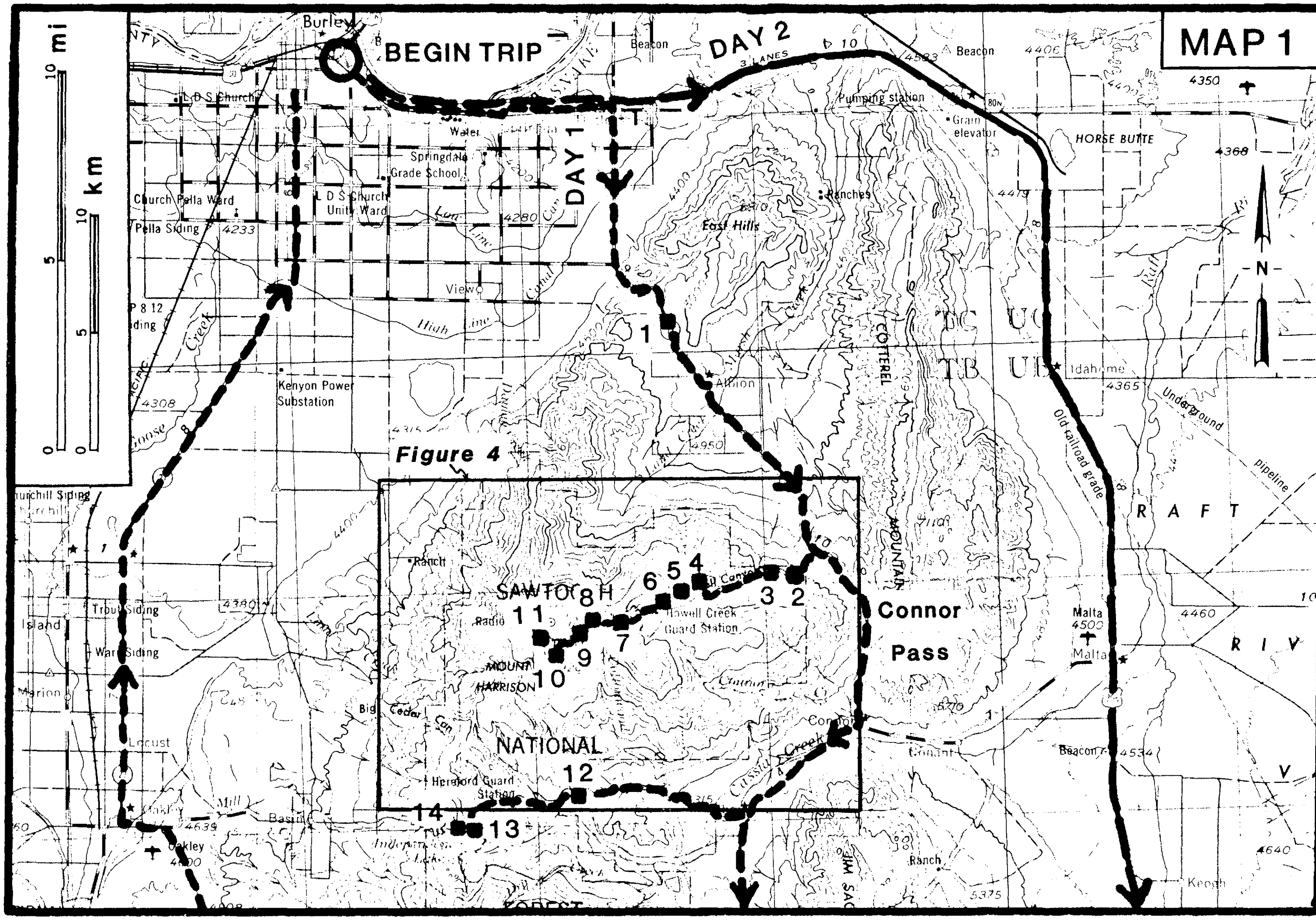
MAP 1
BEGIN TRIP
DAY 1
DAY 2
Burley
Beacon
Pumping station
Grain elevator
HORSE BUTTE
Springdale Grade School
L D S Church
L D S Church Unity Ward
Church Pella Ward
Pella Siding
East Hills
Ranches
Albion
Kenyon Power Substation
COTTEREL MOUNTAIN
Idahome
Old railroad grade
Underground pipeline
RAFT RIV
Figure 4
SAWTOOTH NATIONAL FOREST
MOUNT HARRISON
Howell Creek Guard Station
Connor Pass
Hereford Guard Station
Malta
Conant
Trout Siding
Ward Siding
Island
Marion
Locust
Oakley
Basin
Ranch
Keogh
0 5 10 mi
0 5 10 km
N

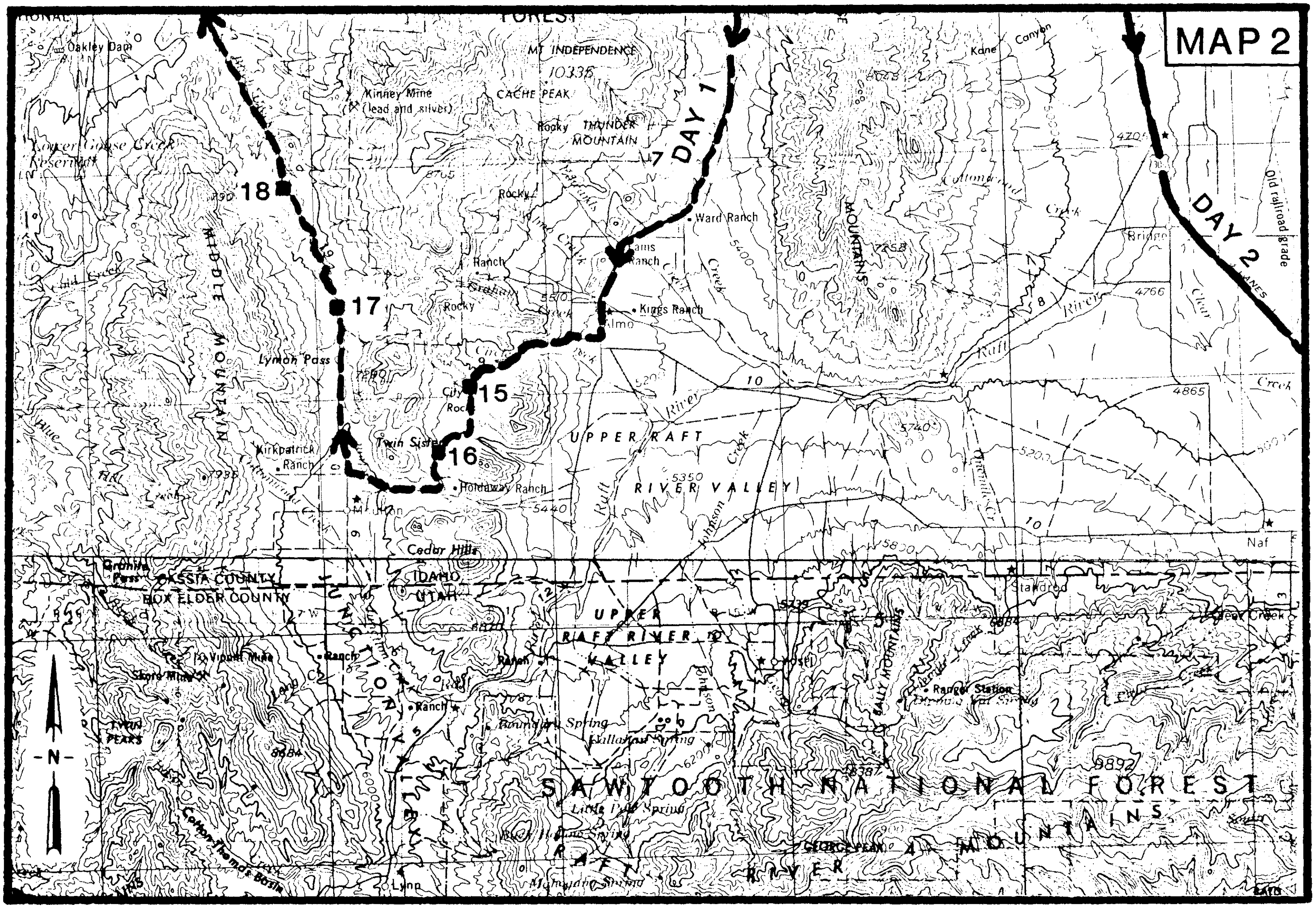
MAP 2
DAY 1
DAY 2
Oakley Dam
MT INDEPENDENCE
10335
Kinney Mine
(lead and silver)
CACHE PEAK
THUNDER MOUNTAIN
Ward Ranch
Kings Ranch
Almo
Lyman Pass
City Rock
Twin Sisters
Kirkpatrick Ranch
Holdaway Ranch
Cedar Hills
MIDDLE MOUNTAIN
UPPER RAFT RIVER VALLEY
CASSIA COUNTY
BOX ELDER COUNTY
IDAHO
UTAH
Standrod
Naf
Old railroad grade
SAWTOOTH NATIONAL FOREST
RAFT RIVER MOUNTAINS
GEORGE PEAK
Ranger Station
Lynn
Vipont Mine
Twin Peaks
Little Pole Spring
Bridge
Kane Canyon
18
17
15
16
-N-

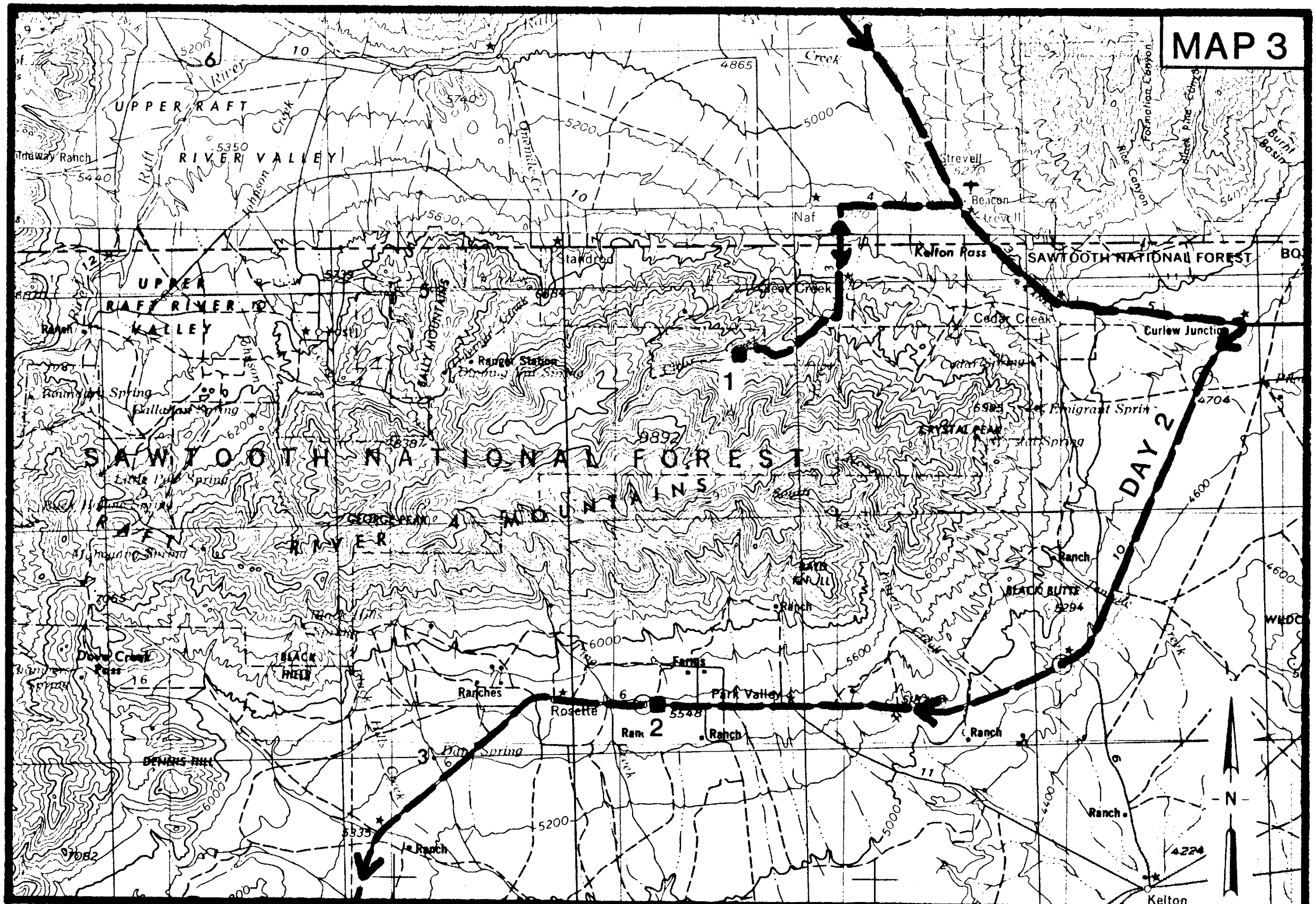
MAP 3
UPPER RAFT RIVER VALLEY
UPPER RAFT RIVER VALLEY
SAWTOOTH NATIONAL FOREST
RAFT RIVER MOUNTAINS
SAWTOOTH NATIONAL FOREST
DAY 2
Strevell
Naf
Standrod
Kelton Pass
Curlew Junction
Cedar Creek
Ranger Station
Rosette
Park Valley
Ranches
Farms
Ranch
Kelton
Black Butte
Crystal Peak
George Peak
Dove Creek Pass
Black Hills
Emigrant Spring
Cedar Spring
N
1
2
3
4
5
6

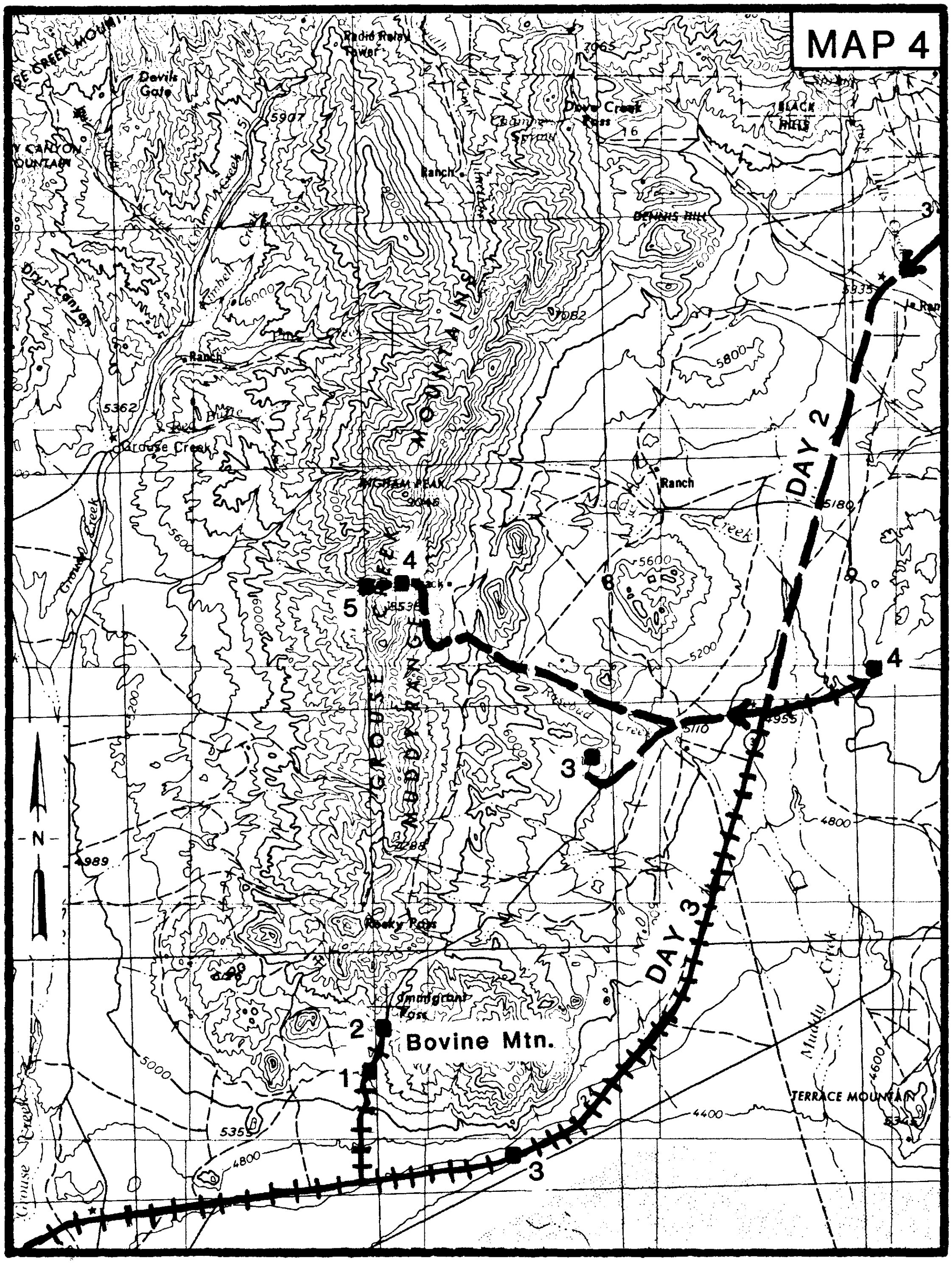
MAP 4
Devils Gate
Radio Relay Tower
Dove Creek Pass
BLACK HILLS
DENNIS HILL
Ranch
Grouse Creek
BIGHAM PEAK
GROUSE CREEK MOUNTAINS
MUDDY RANGE
Rocky Pass
Immigrant Pass
Bovine Mtn.
TERRACE MOUNTAIN
DAY 2
DAY 3
N
Muddy Creek

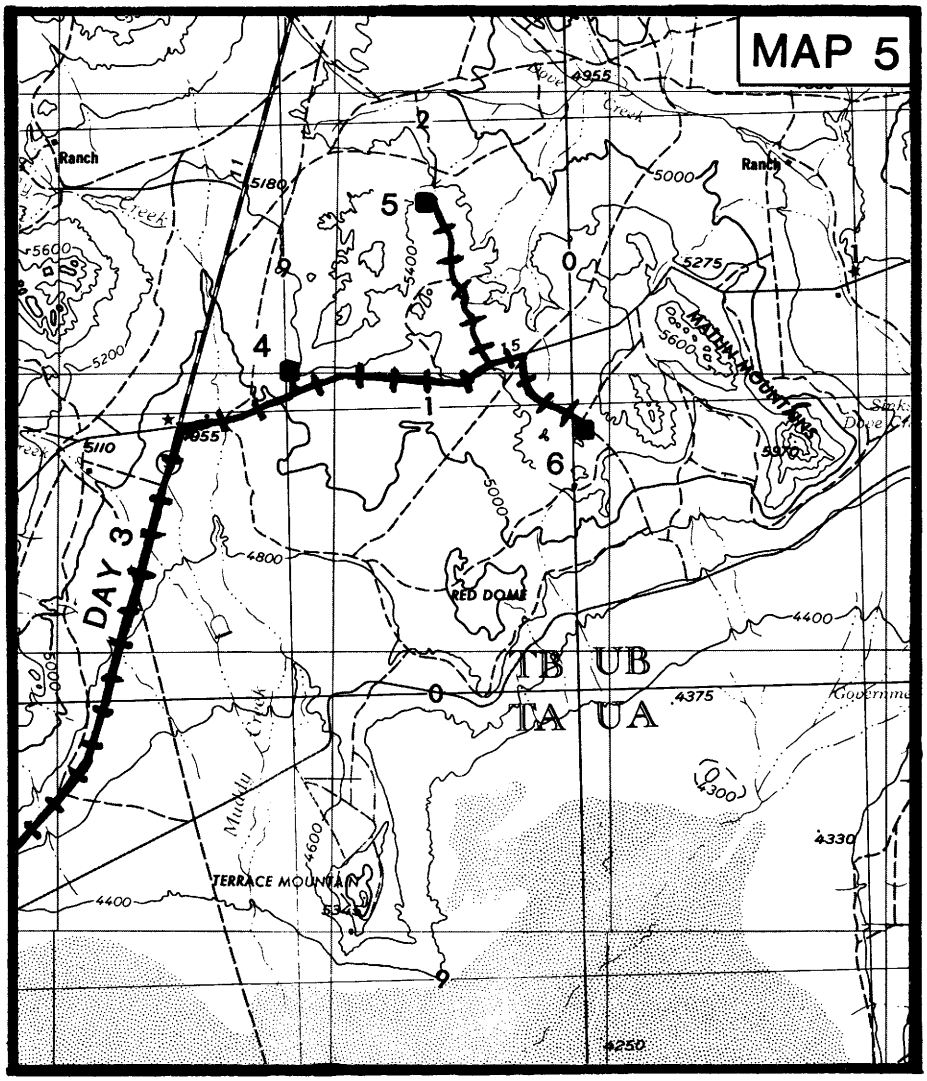
MAP 5
Ranch
Ranch
5180
5000
5600
5400
5275
5200
5600
MATHIN MOUNTAINS
5110
5055
5970
5000
4800
RED DOME
4400
DAY 3
TB UB
TA UA
4375
4300
4330
4600
TERRACE MOUNTAIN
5345
4400
4250

County, Nevada: Unpublished M.S. thesis, San Jose State University, 98 p.

Howard, K. A., 1971, Paleozoic metasediments in the northern Ruby Mountains, Nevada: Geological Society of America Bulletin, v. 82, p. 259-264.

Howard, K. A., 1980, Metamorphic infrastructure in the northern Ruby Mountains, Nevada, *in* Crittenden, M. D., Jr., and others, eds., Cordilleran metamorphic core complexes: Geological Society of America Memoir 153, p. 335-347.

Jordan, T. E., 1983, Structural geometry and sequence, Bovine Mountain, northwestern Utah, *in* Miller, D. M., and others, eds., Tectonic and stratigraphic studies in the eastern Great Basin: Geological Society of America Memoir 157 (in press).

LeCompte, J. R., 1978, Geology of the northwestern part of the Leach Range, Elko County, Nevada: Unpublished M.S. thesis, San Jose State University, 71 p.

Mabey, D. R., and Wilson, C. W., 1973, Regional gravity and magnetic surveys in the Albion Mountains area of southern Idaho: U.S. Geological Survey Open-File Report.

Martindale, S. G., 1981, Stratigraphy and structural geology of the southern part of the Leach Range, Elko County, Nevada: Unpublished M.S. thesis, San Jose State University, 117 p.

Miller, D. M., 1978, Deformation associated with Big Bertha Dome, Albion Mountains, Idaho: Unpublished Ph.D. dissertation, University of California, Los Angeles, 255 p.

———, 1980, Structural geology of the northern Albion Mountains, south-central Idaho, *in* Crittenden, M. D., Jr., and others, eds., Cordilleran metamorphic core complexes: Geological Society of America Memoir 153, p. 399-423.

———, 1983, Allochthonous quartzite sequence in the Albion Mountains, Idaho, and proposed Proterozoic Z and Lower Cambrian correlatives in the Pilot Range, Utah and Nevada, *in* Miller, D. M., and others, eds., Tectonic and stratigraphic studies in the eastern Great Basin: Geological Society of America Memoir 157 (in press).

Miller, D. M., and Hoggatt-Hillhouse, W. C., 1983, Geometry and age of Cenozoic low-angle faults, Pilot Range, Utah and Nevada: Geological Society of America Abstracts with Programs, v. 13 (in press).

Miller, D. M., Todd, V. R., Armstrong, R. L., and Compton, R. R., 1980, Geology of the Albion-Raft River-Grouse Creek Mountains area, northwestern Utah and southern Idaho: Field trip guidebook for Rocky Mountain section, Geological Society of America, May 16-17, 1980, 33 p.

Misch, P., and Hazzard, J. C., 1962, Stratigraphy and metamorphism of late Precambrian rocks in central northwestern Nevada and adjacent Utah: American Association of Petroleum Geologists Bulletin, v. 46, p. 289-343.

Mytton, J. W., Morgan, W. A., and Wardlaw, B. R., 1983, Stratigraphic relations of Permian units, Cassia Mountains, Idaho, *in* Miller, D. M., and others, eds., Tectonic and stratigraphic studies in the eastern Great Basin: Geological Society of America Memoir 157 (in press).

Peace, F. S., 1956, History of exploration for oil and gas in Box Elder County, Utah, and vicinity: Utah Geological Society Guidebook to the Geology of Utah, No. 11, Geology of parts of northwestern Utah, p. 17-31.

Snoke, A. W., 1975, A structural and geochronological puzzle: Secret Creek gorge area, northern Ruby Mountains: Geological Society of America Abstracts with Programs, v. 7, p. 1278-1279.

———, 1980, Transition from infrastructure to suprastructure in the northern Ruby Mountains, Nevada, *in* Crittenden, M. D., Jr., and others, eds., Cordilleran metamorphic core complexes: Geological Society of America Memoir 153, p. 287-333.

Todd, V. R., 1973, Structure and petrology of metamorphosed rocks in central Grouse Creek Mountains, Box Elder County, Utah: Unpublished Ph.D. dissertation, Stanford University, 316 p.

———, 1975, Late Tertiary low-angle faulting and folding in Matlin Mountains, northwestern Utah: Geological Society of America Abstracts with Programs, v. 7, p. 381-382.

———, 1980, Structure and petrology of a Tertiary gneiss dome in northwestern Utah, *in* Crittenden, M. D., Jr., and others, eds., Cordilleran metamorphic core complexes: Geological Society of America Memoir 153, p. 349-383.

———, 1983, Miocene displacement of pre-Tertiary and Tertiary rocks in Matlin Mountains, northwestern Utah, *in* Miller, D. M., and others, eds., Tectonic and stratigraphic studies in the eastern Great Basin: Geological Society of America Memoir 157 (in press).

Williams, P. L., Mabey, D. R., Zohdy, A. R., Ackermann, H., Hoover, D. P., Pierce, K. L., and Oriel, S. S., 1975, Geology and geophysics of the southern Raft River Valley geothermal area, Idaho, U.S.A.: U.S. Geological Survey Open-File Report 75-322.

Utah Geological and Mineral Survey Special Studies 59, 1983
Guidebook Part 1 — GSA Rocky Mountain and Cordilleran Sections Meeting
Salt Lake City, Utah — May 2 - 4, 1983

MESOZOIC AND EARLY TERTIARY STRUCTURE AND SEDIMENTOLOGY OF THE CENTRAL WASATCH MOUNTAINS, UINTA MOUNTAINS AND UINTA BASIN

Ronald L. Bruhn, M. Dane Picard, and Susan L. Beck[1]
Department of Geology and Geophysics, University of Utah, Salt Lake City, UT 84112

ABSTRACT

During latest Cretaceous - Eocene time, 5,000 m of beds were deposited in central and northeast Utah. In the Late Cretaceous, sediment derived from the Sevier-Laramide thrust belt was transported to the east and southeast. Southerly paleocurrent directions in the base of the Currant Creek Formation (Maestrichtian) raise the possibility that uplift of the Uintas may have begun by then. The thrust belt continued as a major highland during the early Paleocene and major uplift of the Uintas occurred. By the middle Paleocene there was an extensive lake which regressed during the late Paleocene as uplift of the Uintas continued. Lake Uinta reached its maximum size during the middle Eocene. During the late Eocene, Lake Uinta regressed and, near the end of the epoch, the lake expired. Major sediment influx was from the east and southeast. Lower (early Duchesnean) and upper (late Duchesnean) conglomeratic intervals record major episodes of uplift in the Uintas during latest Eocene.

Structurally, the Wasatch Mountains are part of a marginal foreland fold and thrust belt. In the northern Wasatch Mountains, pre-Late Cretaceous thrust fault plates were folded in part of a large, ramp-anticline that is cored by allochthonous, crystalline basement. Foreland thrust-belt structures in the central Wasatch Mountains were folded about the east-trending Uinta axis as the Uinta Mountains formed. Eastward movement on the Hogsback thrust in the Paleocene was transferred onto the adjacent Uinta axis and Uinta Mountains structure, causing about 20 km of sinistral-slip in the western Uinta Mountains. Deformation in the Uinta Mountains continued following cessation of movement on the Hogsback thrust system. A south-dipping fault-ramp was located beneath the Uinta Mountains and extended to depths of 15-20 km. Oblique-slip on this ramp probably resulted in about 20 km of crustal shortening perpendicular to the trend of the mountains.

[1]Present address: Department of Geological Sciences, University of Michigan, Ann Arbor, MI 48109

INTRODUCTION

The Mesozoic and early Tertiary structure and sedimentology of the central Wasatch Mountains, Uinta Mountains, and Uinta Basin reflect a long and complex history of compressional deformation and synorogenic erosion and deposition. The Wasatch Mountains contain several major thrust plates that developed during eastward-directed thrust faulting in the Sevier-Laramide orogeny. In the central Wasatch Mountains, early Tertiary thrust faulting overlapped in space and time with development of the Uinta Mountains, a major east-trending Laramide mountain range that developed on the site of a Precambrian aulacogen (Figure 1). To comprehend the interaction between the north-trending thrust belt structures and the Uinta Mountains is one of the fundamental tectonic problems in this part of the Sevier-Laramide orogenic belt. Much of the information that makes it possible to approach this problem in a unified way comes from knowledge of the sedimentary strata exposed in the mountains and present in adjacent basins. Through this classic approach we attempt to present a consistent explanation of the structural and sedimentologic history.

MESOZOIC AND TERTIARY STRATA

Mesozoic and Tertiary rocks in northeastern Utah are dominantly nonmarine (Table 1). About ¾ of the stratigraphic section was deposited in this

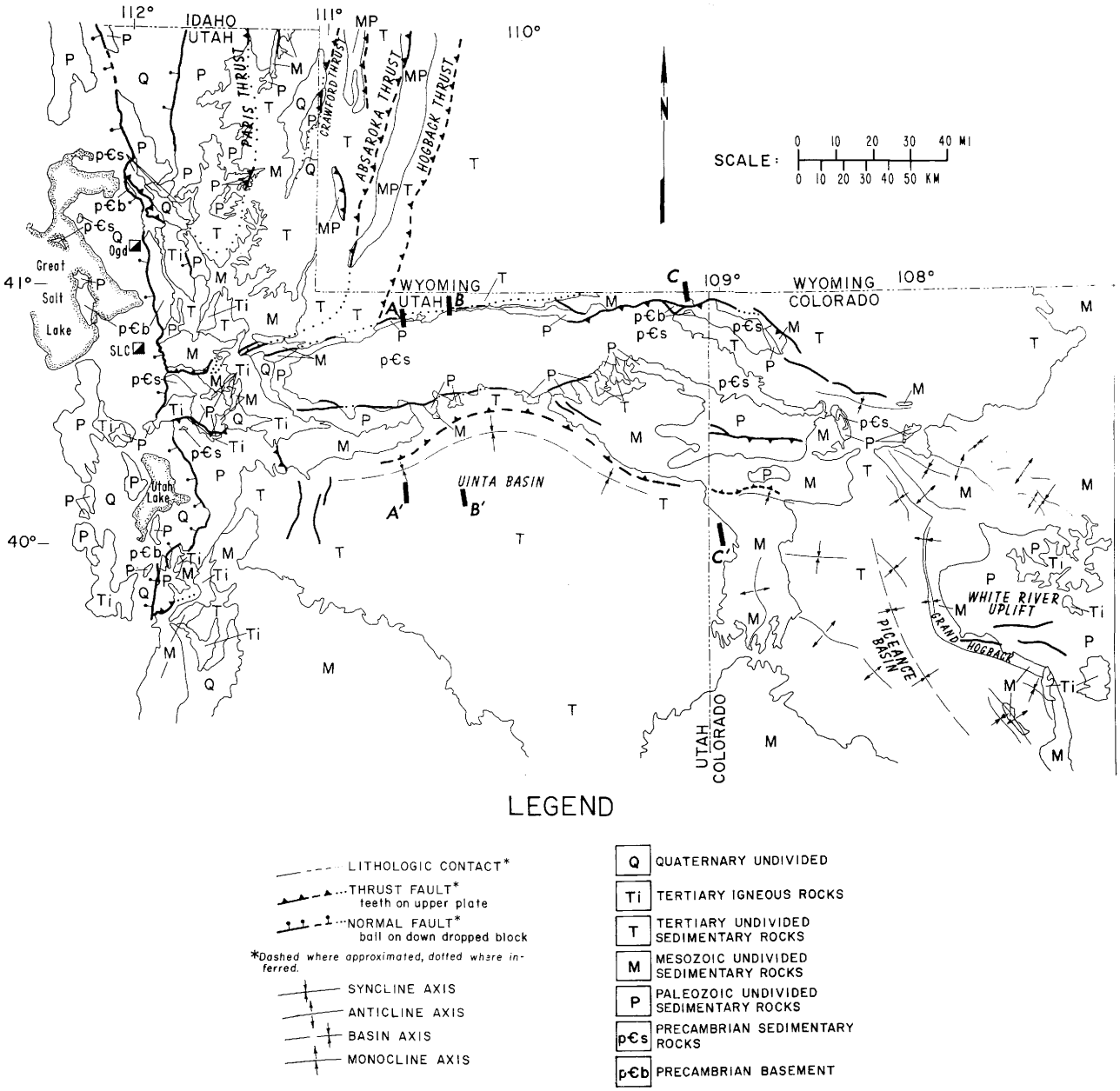

Figure 1. Generalized geologic map of northeastern Utah, western Wyoming and western Colorado.

setting. The marine rocks, except for the Cretaceous Mancos Shale, are shallow marine deposits.

The order of abundance of nonmarine rock types by stratigraphic thickness is sandstone (most abundant), fine-grained rocks (siltstone and claystone), carbonate rocks — dominantly in the early Tertiary Green River and Flagstaff Formations — and conglomerate. Conglomerate is volumetrically concentrated in synorogenic deposits of the Price River-North Horn, Currant Creek, and Duchesne River Formations.

Red beds and varicolored sequences are characteristic of these rocks (Table 1). Principal red formations are the Woodside, Ankareh, Nugget, lower Twin Creek (Gypsum Spring Member), Entrada, Currant Creek, and Duchesne River. Pigmentation occurred in these beds primarily during diagenesis. A persistent, oxygenating environment of burial is indicated by the red pigment (Van Houten, 1973, p. 51).

The varicolored rocks are mainly the fine-grained parts of alluvial and lacustrine formations — Popo

Table 1. Mesozoic and Tertiary Sequence, Southwestern Uinta Mountains and Central Uinta Basin. (Rock types: Cgl, conglomerate; SS, sandstone; F, siltstone and claystone; Carb, carbonate rocks; E, evaporites; R, red beds or varicolored rocks; C, coal; V, volcanic or volcaniclastic rocks.)

Age	Formation	Thickness (m)	Depositional Environment	Rock Type
Eocene-Oligocene	Duchesne River	1,140	Alluvial	Ss, Cgl F, V, R
Eocene	Uinta	600	Alluvial, lacustrine	Ss, F, V, R
Paleocene-Eocene	Green River	1,650	Lacustrine, alluvial, delta	Ss, Carb, F, C, V, R
Cretaceous-Paleocene	Wasatch	1,350	Alluvial, lacustrine	Ss, F, Carb, R, V
Cretaceous	Mesaverde Group	300	Delta, marine clastic shoreline	Ss, F, Cgl, C
	Mancos	750	Offshore marine	F
	Frontier	135	Delta, marine clastic shoreline, offshore marine	Ss, F, C
	Mowry	75	Marine	F, V, C
	Dakota	55	Alluvial, marine reworking	Ss, F, R
	Cedar Mountain	40	Alluvial	F, Ss, R
Jurassic	Morrison	435	Alluvial, lacustrine	F, Ss, Cgl, V, R
	Curtis	50	Shallow marine shelf	Ss, F, Carb
	Entrada (Preuss)	210	Eolian, shallow marine, alluvial	Ss, F, R
	Twin Creek	225	Shallow marine shelf	Carb, F, Ss, E
	Nugget	400	Eolian, lacustrine	Ss, F, Carb, R, E
Triassic	Popo Agie (Chinle)	125	Alluvial, lacustrine	F, Ss, V, R
	Gartra	15	Alluvial	Ss, Cgl, F, R
	Ankareh	220	Paralic, shallow marine	F, Ss, E, R
	Thaynes	115	Shallow marine	F, Carb, Ss
	Woodside	245	Tide-dominated shelf	F, Ss, E, R
	Dinwoody	25	Shallow marine	F, Ss, Carb
Permian	Park City-Phosphoria			

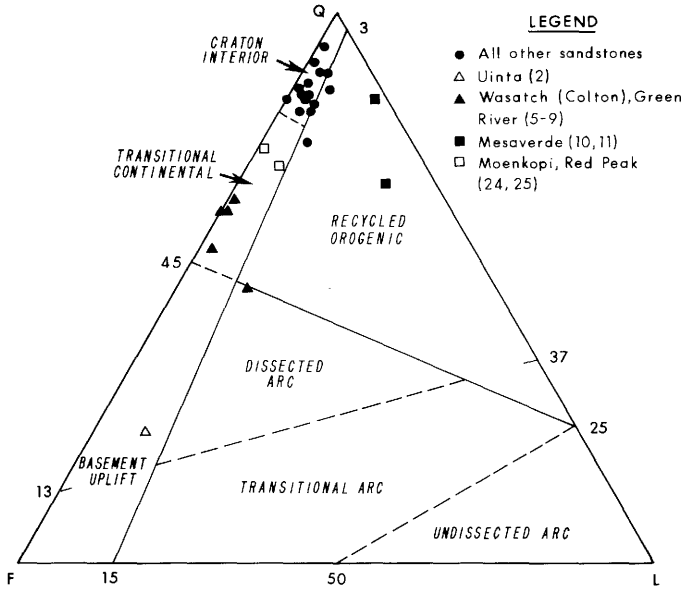

Figure 2. QFL plot of Mesozoic and Tertiary sandstone in northeastern Utah and vicinity. Q, total quartzose grains including chert; F, monocrystalline feldspar grains; L, unstable polycrystalline lithic fragments. Provenance terranes are those of Dickinson and others (in press).

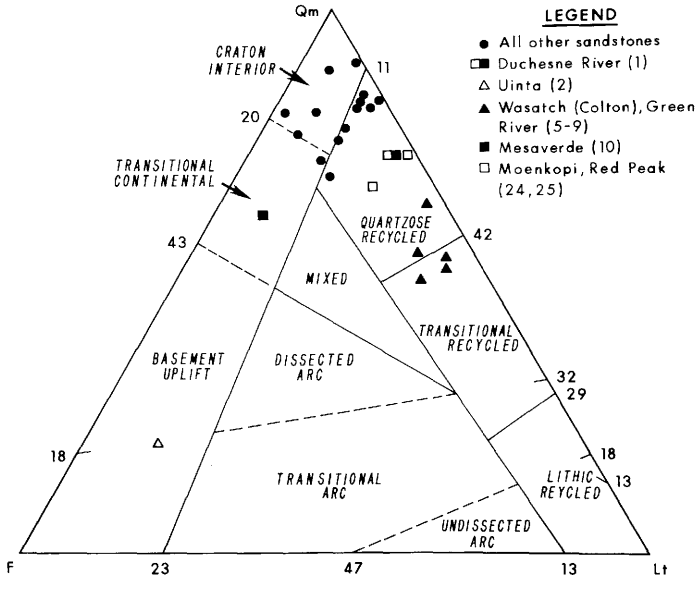

Figure 3. QmFLt plot of sandstone summarized in Table 2. Qm, monocrystalline quartz; F, feldspar; Lt, total polycrystalline lithic fragments.

Agie, Morrison, Cedar Mountain, Dakota, Wasatch, Green River, and Uinta. Common colors are dark and dusky red, olive, greenish yellow, olive gray, gray, and dusky green. The characteristic, laterally uniform red color — for hundreds of meters or kilometers — of the red beds is lacking in the varicolored rocks. Instead, color changes are frequent.

The red parts of the varicolored deposits inherited essentially the same grains and matrix as did the non-red parts. Color differences developed principally during deposition and diagenesis. The initial sediment of the alluvial beds contained soil-derived, brown ferric oxide that was concentrated into the fine-grained parts of upward-fining cycles during deposition.

Principal unconformities in the Triassic and Jurassic rocks are given in Pipiringos and O'Sullivan (1978). For the Cretaceous, the field guide edited by Kauffman (1977) is recommended.

SANDSTONE PETROGRAPHY

Dickinson and others (1983) have suggested that framework modes of terrigenous sandstone reflect provenance that depends upon plate tectonic setting. They divide triangular QFL and QmFLt compositional diagrams into three main fields termed continental blocks, magmatic arcs and recycled orogens. Based on study of 233 Phanerozoic suites from North America, they believe their classification could lead to important conclusions about the timing and nature of major tectonic events. Certainly, sandstone petrography yields useful information about provenance.

Plots of Mesozoic and Tertiary sandstone, similar in style to those in Dickinson and others (1983), are given in Figures 2 and 3. Each sandstone is listed in Table 2. Space is too limited to list all sources; we will send specific references to those who request them.

Nearly all of the sandstone shown in the QFL diagram (Figure 2) falls in the field of continental blocks — quartzo-feldspathic sandstone low in lithic fragments. Sediment sources are generally considered to be either on stable shields and platforms, or in uplifts that mark plate boundaries and trends of intraplate deformation that transect the continental blocks (Dickinson and others, 1983). Some of the sandstone that plots in the craton interior subfield is multi-cycle sandstone whose grains were dominantly derived from sedimentary rocks very low in lithic fragments (for example, nos. 3, 4, 12 to 14, 17 to 21; Table 2). In other sandstone that is low in lithic

Table 2. Framework Modes of Mesozoic and Tertiary Sandstones.

Formation	N	QFL	QmFLt	Unit, Location
1. Duchesne River	46	87-2-11	73-2-25	Northern Uinta Basin
2. Uinta	21	24-68-8	20-68-12	Saline facies, central Uinta Basin
3. Green River	15	94-5-1	89-5-6	Lacustrine beds in Parachute Creek Member, NE Uinta Basin
4. Green River	6	85-12-3	72-12-16	Same (fluvial beds)
5. Green River	20	66-33-1	64-33-3	Douglas Creek and Garden Gulch Members, SE Uinta Basin
6. Green River	14	57-41-2	54-41-5	Same (fluvial beds)
7. Wasatch (Colton)	6	64-35-1	52-42-6	Southeast Uinta Basin
8. Wasatch (Colton)	25	50-39-11	50-39-11	Sunnyside area, southern Uinta basin
9. Green River	10	64-36-0	55-36-9	Black shale facies, southern Uinta Basin
10. Tuscher, Farrer	23	69-8-23	62-8-30	Formations of Mesaverde Group, Uinta Basin
11. Neslen	13	84-2-14	81-2-17	Same
12. Emery	31	84-12-3	78-13-9	Member of Mancos Shale, central Utah
13. Frontier (v. f. ss)	38	89-7-4	81-7-12	Uinta Mountains, northeast Utah
14. Frontier (f. ss)	35	86-6-6	77-6-17	Same
15. Morrison	124	82-13-5	76-13-11	Southeast Utah
16. Entrada	37	89-8-3	89-8-3	Uinta Mountains, NE Utah and NW Colorado
17. Arapien	19	85-13-2	83-13-4	Central Utah
18. Nugget	9	82-16-0	82-13-5	Uinta Mountains, NE Utah
19. Nugget	11	84-16-0	83-16-1	Southwest Wyoming
20. Navajo-Nugget	8	82-15-3	82-15-3	Uinta Mountains, NE Utah
21. Navajo	35	84-13-3	84-13-3	Central Utah
22. Gartra	40	91-8-1	90-8-2	Uinta Mountains, NE Utah and NW Colorado
23. Crow Mountain	18	86-13-1	83-13-4	Formation of Chugwater Group, west-central Wyoming
24. Red Peak	6	75-24-1	73-24-3	Same
25. Moenkopi	131	72-23-5	67-23-10	Utah

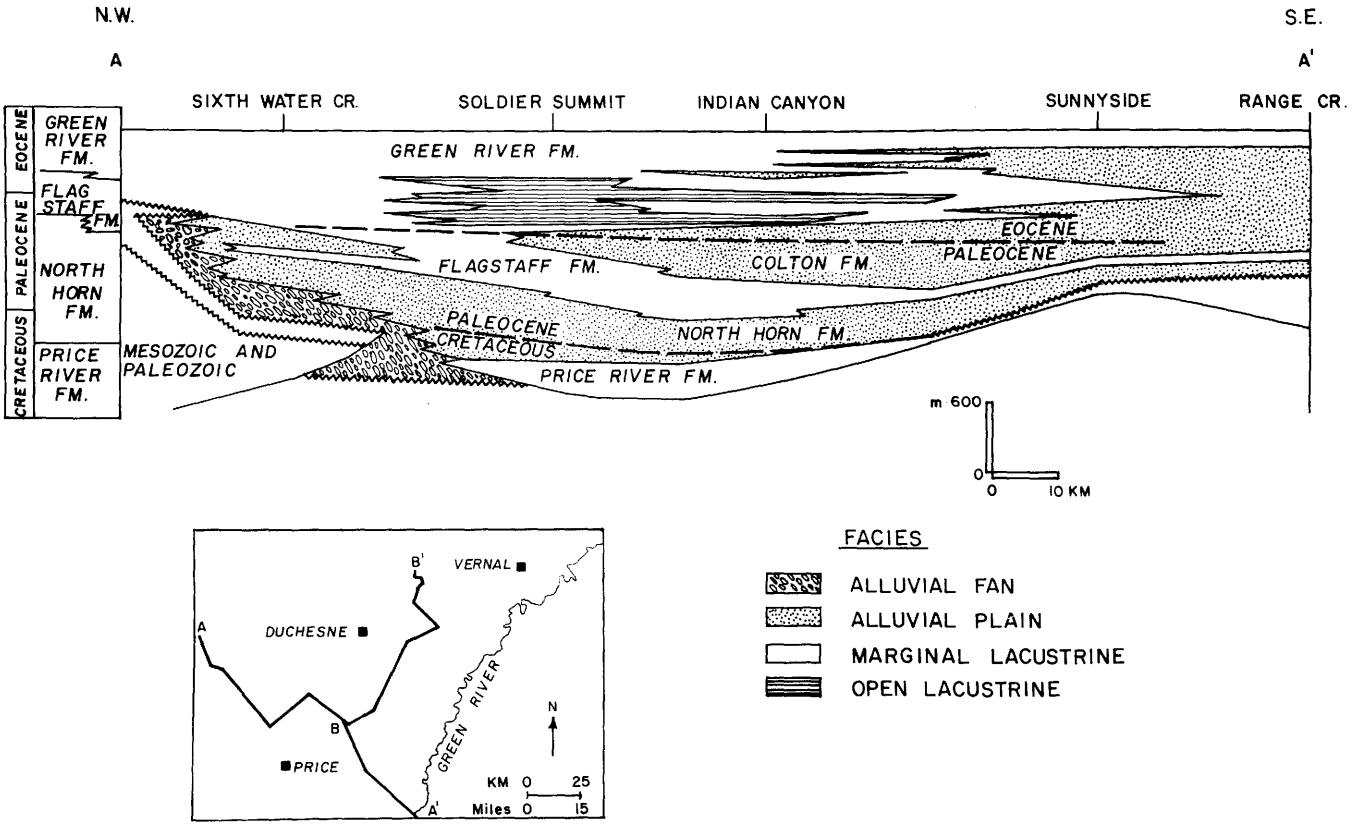

Figure 4. Stratigraphic section along outcrops of southwest flank of Uinta Basin, Utah. Datum is middle of Green River Formation (section after Ryder and others, 1976).

fragments, grains were recycled from sedimentary sources, but there was also a first-cycle contribution of grains from igneous source rocks (15, 16, 22, 23 to 25). Duchesne River sand-size grains (no. 1) were derived from sedimentary source rocks in the Uinta Mountains that were high in lithic fragments. In contrast, the Uinta arkose (no. 2) is a volcaniclastic sandstone derived from western and southwestern Colorado. There also is considerable authigenic feldspar in the Uinta Formation, a further petrographic complication.

LATE CRETACEOUS-EOCENE PALEOGEOGRAPHY

Introduction

During latest Cretaceous through Eocene time, nearly 5,000 m of sedimentary rocks accumulated in central and northeastern Utah. The late-orogenic molasse basins are intermontane in type (Picard, 1980, p. 76). The lacustrine depositional centers — lakes Flagstaff and Uinta — formed after the eastward retreat of the Late Cretaceous seaway and were localized within regional tectonic depressions where subsidence rates exceeded depositional rates. Lake Uinta coincided approximately with the structural axis of the Uinta Basin, and Lake Flagstaff was situated in the structural basin between the Sevier-Laramide orogenic belt and the San Rafael Swell (Ryder and others, 1976). The lacustrine facies were preceded by alluvial facies, surrounded by them, and finally, succeeded by younger alluvial facies. This Late Cretaceous-Eocene sequence of beds — deposited from about 70 to 35 m.y.a. — records the late-orogenic episodes of the Sevier-Laramide orogeny.

Distribution of Facies

The major lower Tertiary facies and associated nomenclature are illustrated in Figures 4 and 5 which are modified from Ryder and others (1976). Figure 4 shows stratigraphic relations along the southwest flank of the Uinta Basin, including Indian Canyon. Figure 5 shows similar relations into the basin from the Nine Mile Canyon surface section to the Bluebell oil field. Alluvial fan deposits are principally thick, synorogenic conglomerate and interbedded conglomeratic sandstone. Bedding is crude in the conglomerate, but there is some horizontal

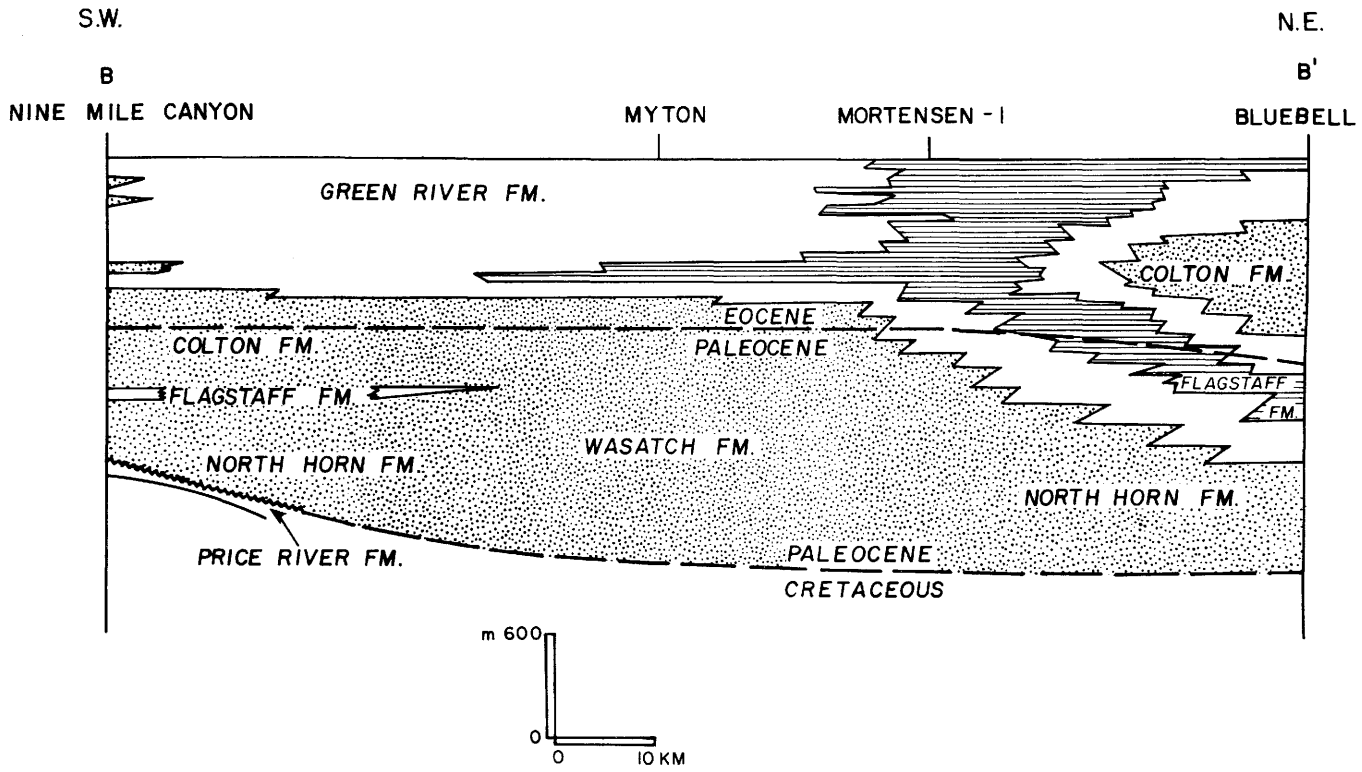

Figure 5. Stratigraphic section between Willow Creek-Indian Canyon surface section and the Altamont oil field. Same datum as Figure 4. Modified from Ryder and others (1976).

stratification, cross-stratification and imbrication of clasts. Associated sandstone is characterized by horizontal stratification, cross-stratification and parting lineation. Such beds were dominantly deposited in braided streams. Alluvial plain deposits include 10 to 30 m thick channel-form sandstone units and interbedded thinly bedded sandstone, siltstone and varicolored claystone. These beds formed in braided, meandering and floodplain settings. Marginal lacustrine facies include gray and green claystone, siltstone, sandstone and carbonate rocks. Open lacustrine facies are dark gray to brown dolomicrite, algal beds, micrite and limy siltstone.

Late Cretaceous Paleogeography

During the Late Cretaceous the Sevier-Laramide orogenic belt was high and sediment transport was primarily to the east and southeast (Figure 6). Clast imbrication west and north of Coalville, Utah, in the Echo Canyon Conglomerate indicates that current flow was to the northeast in that region (Beutner, 1977).

Transport directions in the Currant Creek Formation in the Currant Creek area (sec. 33, T. 1 S., R. 10 W.) are to the south and east (Figure 7). Farther east in the Red Creek area (secs. 23, 25, T. 1 S., R. 9 W.) in the basal sandstone unit they are also to the south and east. Younger sandstone lenses within a conglomerate sequence in the same area show transport almost entirely to the east — from 61° to 120°. North of Tabiona, Utah, and east of Red Creek (sec. 18, T. 1 S., R. 7 W.), dominant directions are to the south (151° to 240°). There is a decrease in the maximum size of clasts in the conglomerate from west to east: Currant Creek, > 1 m; Red Creek, > 50 cm; Duchesne River, > 10 cm. This has led to the idea that coarse clasts (conglomerate-sized material) may have been dominantly transported from west to east while finer material (sand-size grains) was primarily transported from north to south.

The base of the formation has been dated as Maestrichtian on the basis of ostracodes and pollen (Bruce Bryant, personal communication, 1982). The depositional time range of the formation is unknown. It is difficult to pinpoint the contact between the Currant Creek and the overlying Duchesne River Formation. A younger surge of gravel, some of it as much as 1 m in diameter, was deposited in the uppermost part of the Currant Creek Formation in the Duchesne River area. Some of these clasts are Cretaceous in age, possibly

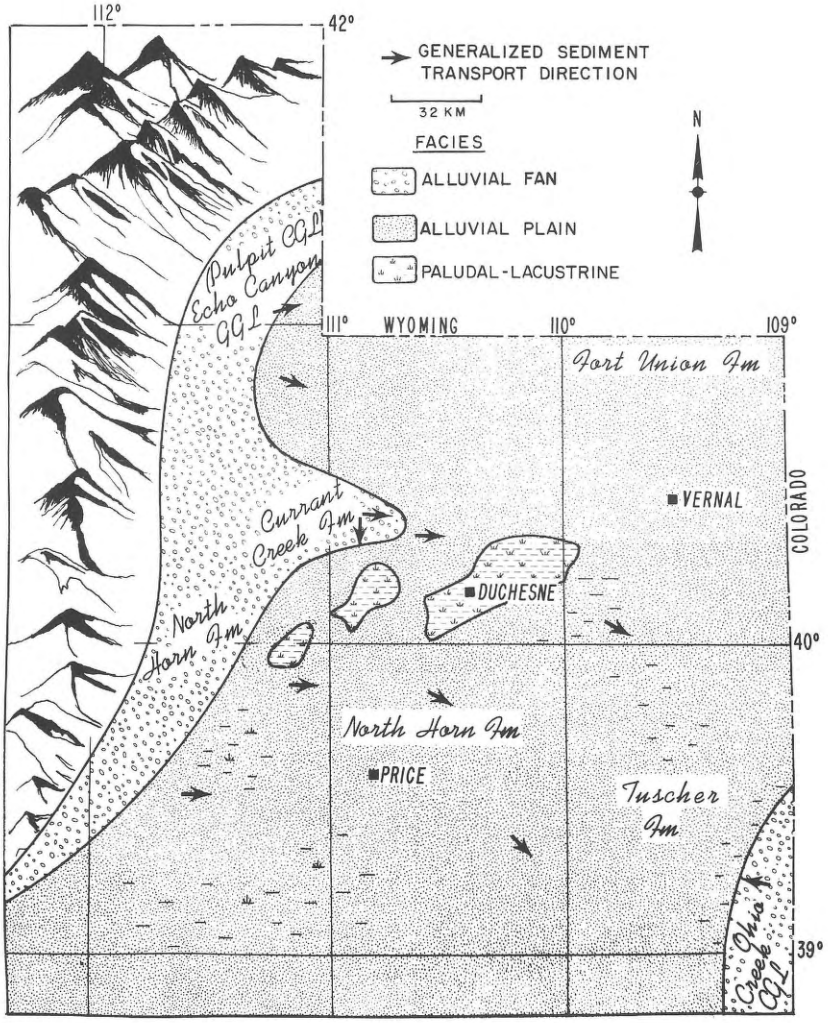

Figure 6. Late Cretaceous paleogeography, northeastern Utah.

Frontier sandstone, and contain marine bivalves. Although apparently small in extent, this younger conglomerate may represent still another synorogenic episode or a continuation of the episode characterized by the thick conglomerate units in the lower part of the formation.

We do not show the Uinta Uplift (Figure 6) on the paleogeographic map. The southerly paleocurrent directions in certain intervals of the Currant Creek Formation do, however, give one pause. These measurements and indications from structural studies raise the possibility that the uplift of the Uintas may have begun in latest Cretaceous time.

Early Paleocene Paleogeography

Major thrust faulting affected central Utah in late Albian or Cenomanian and was continuous until deformation ended in the late Campanian (Lawton, 1982, p. 199) or possibly, early Maestrichtian. Still, the Sevier-Laramide orogenic belt was a major sediment source area during the early Paleocene as indicated by alluvial fan, conglomeratic braided stream, and sandy braided stream deposits in the North Horn Formation (Maestrichtian-late Paleocene). Folding continued in the area after late Campanian and there may have been local thrusting. Conglomerate in the North Horn is dominantly composed of pebbles, cobbles and boulders of Precambrian and Cambrian quartzite and Paleozoic carbonate rock. Clasts were eroded from source terranes in the Sevier-Laramide orogenic belt and from Cretaceous (Cenomanian (?)- Maestrichtian) Indianola conglomerate exposed in anticlines (Stanley and Collinson, 1979, p. 315). Streams flowed toward the east and southeast depositing coarse detritus in a large, wedge-shaped alluvial fan

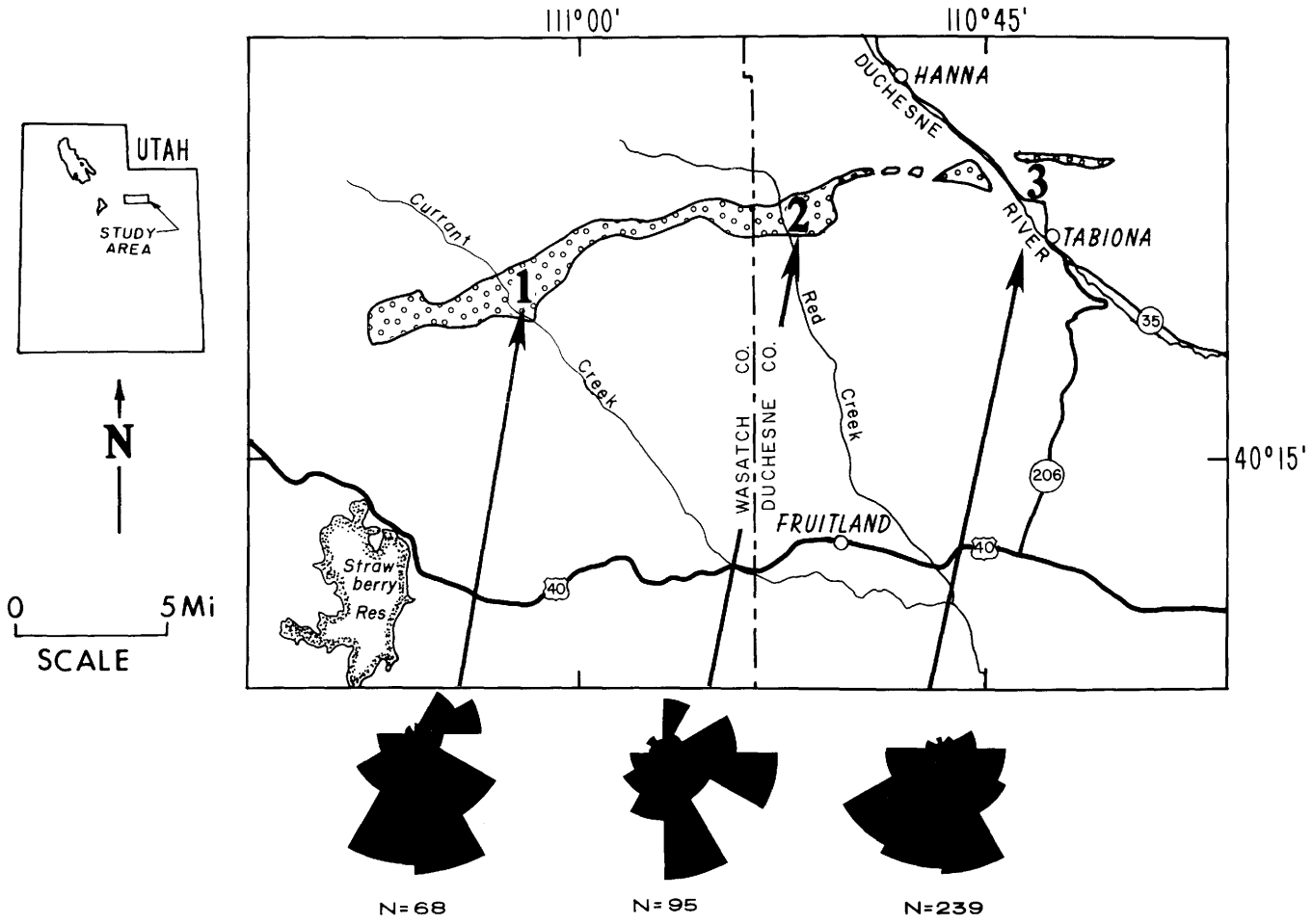

Figure 7. Paleocurrent pattern in the Currant Creek Formation. Information from John Isby.

(Figure 8) characterized by fan and braided stream deposits. Locally, streams were diverted because of uplift of the Sanpete Valley anticline and sediment was dispersed both to the northwest and to the east and southeast (Stanley and Collinson, 1979, p. 313).

North Horn sandstone eroded from the Sevier-Laramide orogenic belt and from local anticlines reflects the composition of Cretaceous (note nos. 10-14, Table 2) and older sedimentary rocks — mostly quartz with lesser amounts of chert and sedimentary rock fragments and less than 3 percent feldspar (Birsa, 1974). In contrast, Ryder and others (1976, p. 510) note that feldspar-rich sand was supplied to the south flank of the Uinta Basin by latest Cretaceous time.

The paludal-lacustrine facies centered at Duchesne (Figure 8) may represent a lake or several lakes that extended southwest between the San Rafael Swell and the lobe of coarse clastics from the Sevier-Laramide orogenic belt. Position of the southwestern margin of the basin is uncertain. If North Horn beds once extended onto the San Rafael Swell, the evidence has been removed by erosion. North Horn beds onlap the Uncompahgre uplift, suggesting that the uplift was low-lying during the early Paleocene.

Sedimentologic information from the northern part of the basin is scarce. There are no outcrops. Deep wells into this sequence are few. The Currant Creek Formation probably contains early Paleocene intervals.

Late Paleocene Paleogeography

By middle Paleocene time there was an extensive lake (Figure 9). Near the present Green River, a large deltaic and lower deltaic-plain system extended northwest into Lake Uinta and supplied it with prodigious quantities of feldspar-rich sand. At the northern perimeter of this alluvial and deltaic complex, shallow water lacustrine carbonate was

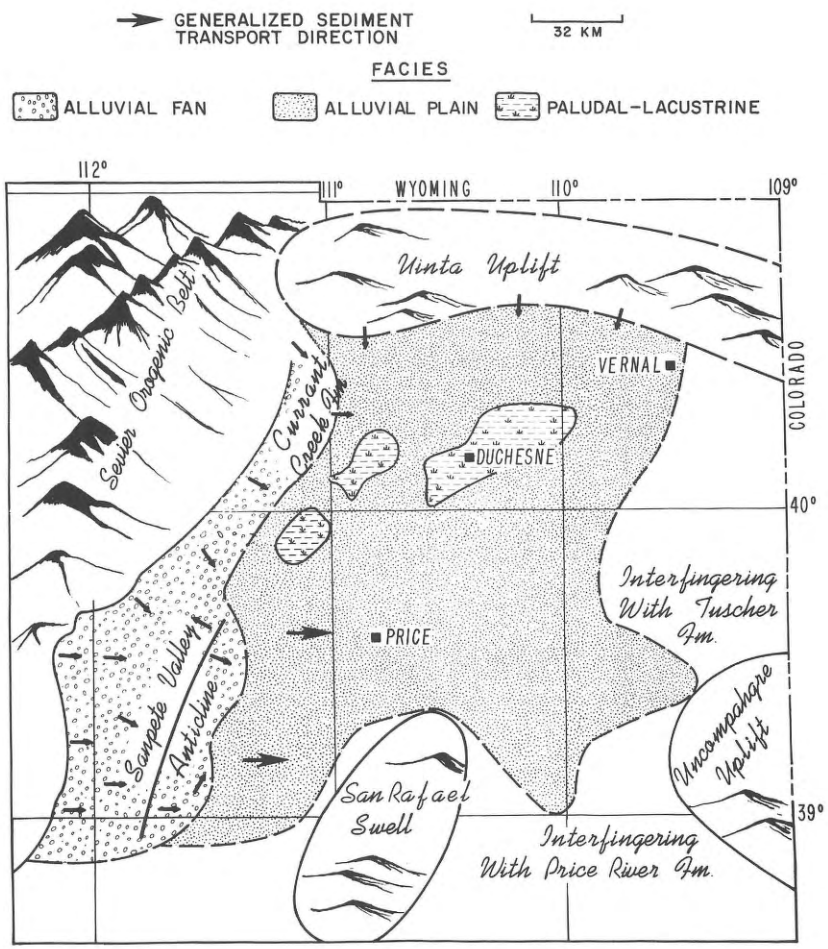

Figure 8. Early Paleocene paleogeography, North Horn Formation, northeastern Utah.

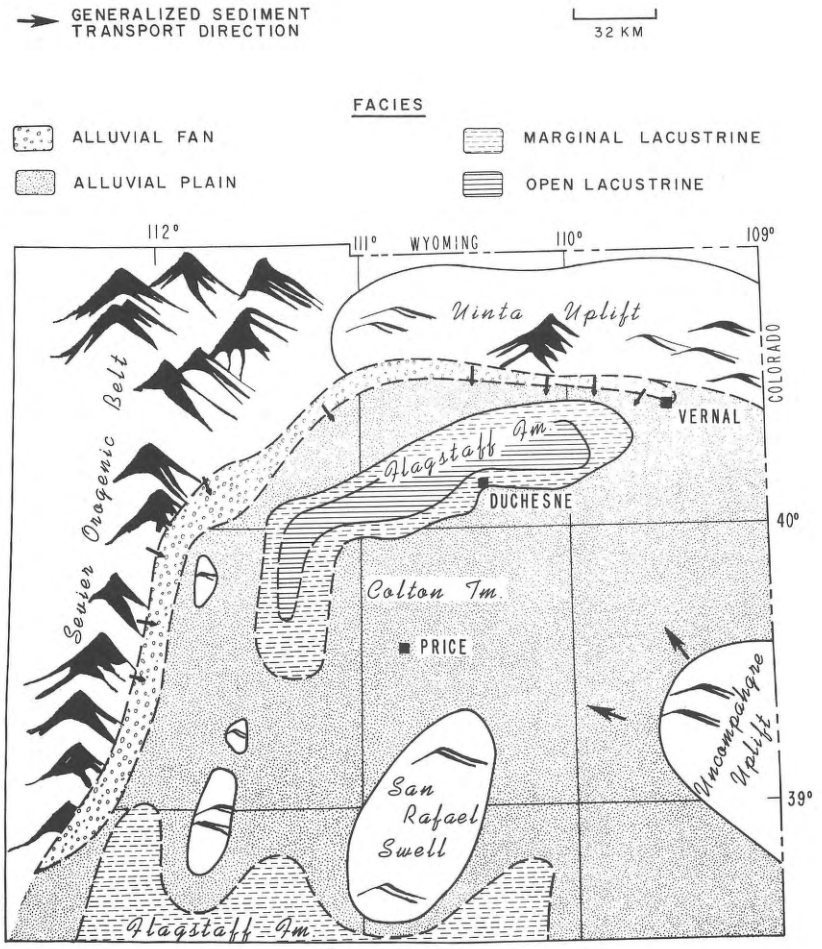

Figure 9. Late Paleocene paleogeography, northeastern Utah.

deposited. This major, varicolored complex and its successors near the Sunnyside area form the thick, clastic wedge assigned to the Colton, North Horn, and Wasatch Formations (see Ryder and others, 1976, p. 510).

Lake Uinta regressed from its margins during the late Paleocene and alluvial deposition extended well into the basin (Figure 9). In the Sunnyside area, north of the San Rafael Swell, paleocurrent directions in the Colton Formation show current flow to the northeast. The feldspar-rich sandstone (nos. 7, 8 and 9, Table 2) could not have been eroded from the San Rafael Swell. Petrographic studies indicate a mixed crystalline and sedimentary provenance. It is likely that primary crystalline detritus was derived from southwestern Colorado and sedimentary detritus from locally adjacent Colorado Plateau uplifts (Banks, 1981). The San Rafael Swell probably diverted major streams from the south and southeast to the northeast into the basin.

Quartz-rich sand was eroded from the Sevier-Laramide orogenic belt and from the growing Uinta uplift. Such sandstone is composed dominantly of recycled grains from sedimentary rocks that cropped out on the north and west. The Uncompahgre uplift on the southeast was probably low-lying during late Paleocene time.

Middle Eocene Paleogeography

Lake Uinta reached its maximum size during the middle Eocene (Figure 10). Similar beds of this age are present in the Piceance Creek Basin of northwestern Colorado. The ancient lake transgressed — beginning in the early Eocene — to its maximum extent in northeastern Utah and over the Douglas Creek arch on the east. Expansion of the lake led to great organic productivity and to the formation of the Mahogany zone and other rich, oil shale deposits. The areal extent of both open lacustrine and marginal lacustrine rocks — oolite, algal beds and ostracodal carbonate beds — is most extensive during this time. Alluvial deposits formed in a thin band on the north during early and middle Eocene time. The situation on the south and west is uncertain, but alluvial deposition was much less extensive than during the Late Cretaceous, Paleocene, and early Eocene. This major transgression and many minor pulses on it may be related to climatic changes, but there may also have been a change in basinal subsidence rate. The depositional axis of the Uinta Basin closely parallels the structural axis of the Uinta uplift.

Sandstone primarily derived from the Uinta uplift is quartz-rich (nos. 3 and 4, Table 2) but contains some first-cycle feldspar that probably originated in source areas on the southeast (Picard and High, 1972, p. 2697). Relief between the Uinta Basin and the Uinta uplift was less than it is today. In the southeast part of the Uinta Basin the sandstone contains much more feldspar which was eroded from highlands on the southeast in southwestern Colorado (Picard, 1971).

Late Eocene Paleogeography

During the late Eocene, Lake Uinta regressed markedly from the basin margins (Figure 11) and, near the end of the Eocene, the lake expired. Two facies of the Uinta Formation — saline, sandstone and limestone — record the regression and last several million years of lacustrine deposition in this long-lived lake. Major sediment influx into the basin was from the east and southeast from highlands in northcentral and southwestern Colorado. Much volcanic material entered the basin as stream sediment and air falls.

The Uinta and Uncompahgre uplifts and the San Rafael Swell were apparently low-lying. Similarly, based on limited drilling in the western Uinta Basin, the Sevier-Laramide orogenic belt did not contribute appreciable clastic material to the basin. Major detritus came from beyond the highlands bordering the basin.

The Duchesne River Formation, which unconformably overlies the Uinta Formation, contains evidence of latest Laramide deformation in the Uinta Mountains area. Fossiliferous parts of the Duchesne River are latest Eocene in age. The uppermost part of the formation (Starr Flat Member) is undated and may be Oligocene (Andersen and Picard, 1972). The characteristic alluvial deposits consist of heterogeneous, laterally discontinuous sandstone lenses with varying amounts of conglomerate and poorly stratified fine-grained rocks. Deposition was in relatively small, rapidly aggrading, southward-flowing streams (Figure 12). Most stream channels were braided with high gradients and high velocities of flow. Composition of sandstone in the Duchesne River Formation (no. 1, Table 2) reflects the abundance of sedimentary source rocks in the Uinta Mountains. Lower (early Duchesnean) and upper (late Duchesnean) conglomeratic rock units record two major episodes of uplift, each composed of several smaller events (Andersen and Picard, 1974). Volcanic ash deposits accumulated during the time (middle Duchesnean) between major uplifts. Altered volcaniclastic rocks probably originated in eruptive centers on the west.

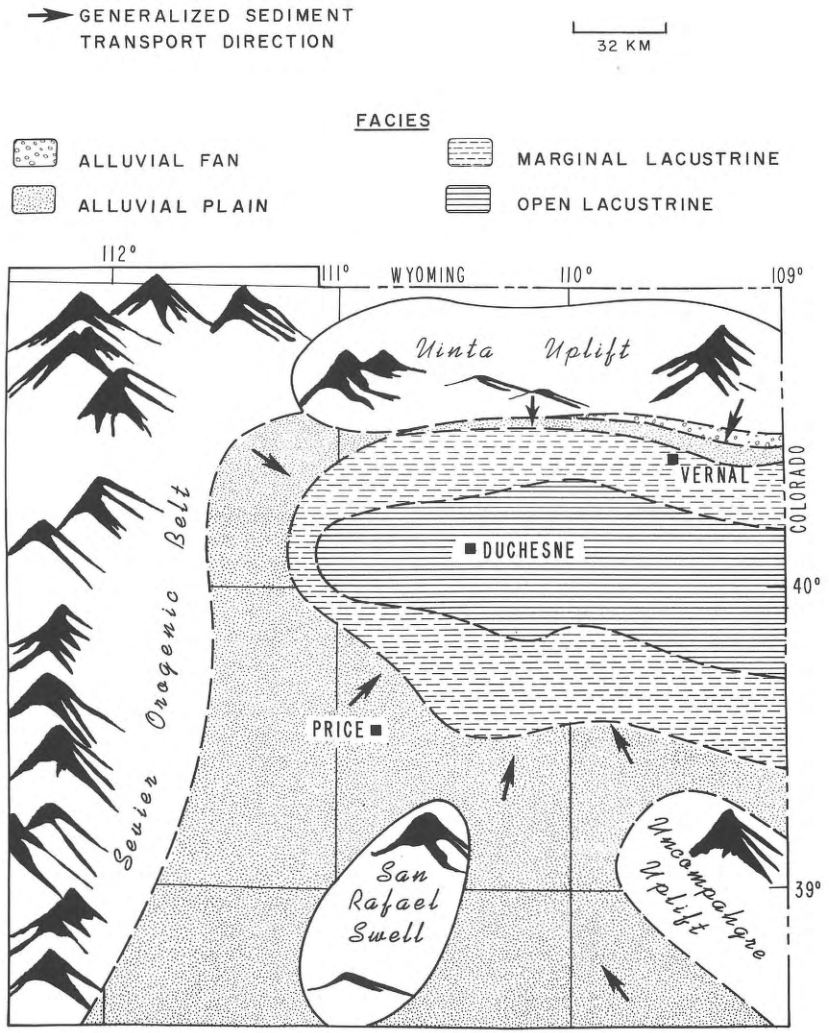

Figure 10. Middle Eocene paleogeography, Upper Parachute Creek, Green River Formation, northeastern Utah.

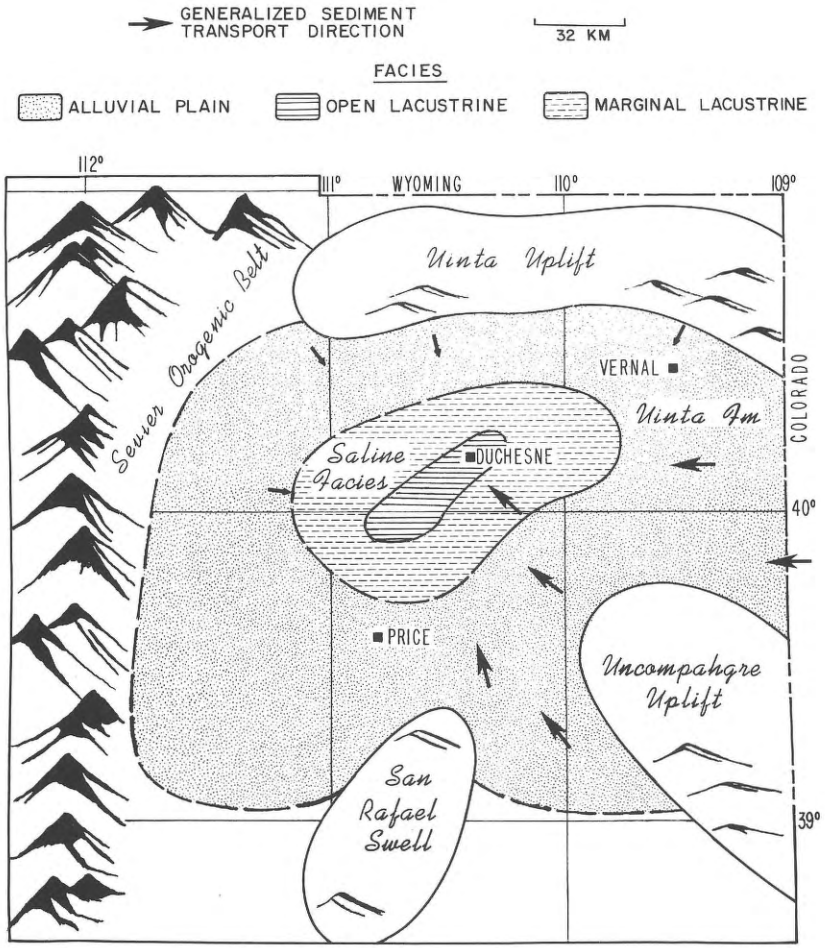

Figure 11. Late Eocene paleogeography, northeastern Utah.

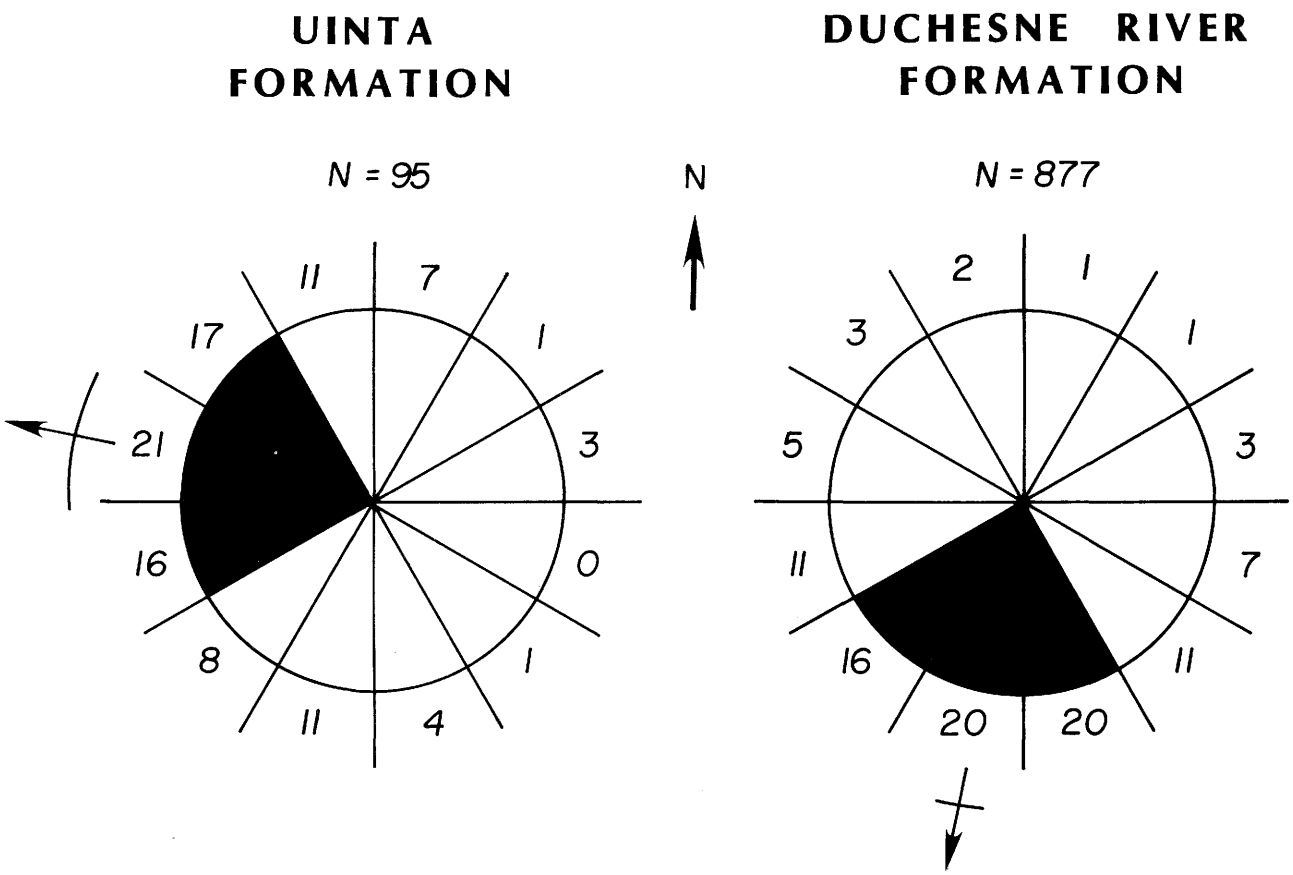

Figure 12. Compass diagrams of paleocurrent measurements from the Uinta and Duchesne River Formations. Numbers around circles represent percent of measurements in each 30° sector. Shaded sectors are modes. Vector resultant directions and 95 percent confidence limits are shown.

STRUCTURAL GEOMETRY OF WASATCH MOUNTAINS

There are four major thrust fault systems in northeastern Utah and western Wyoming: the Paris, Crawford, Absaroka, and Hogsback (Figure 1). These thrust systems formed over an extended period of time between Late Jurassic and Paleocene as the basal decollement propogated eastward from the metamorphic hinterland of the orogenic belt in western Utah and Nevada (Figure 13; Armstrong, 1968; Armstrong and Oriel, 1972; Royse and others, 1975). Consequently, the oldest thrust plates crop out in the western part of the range where they overlap younger and structurally lower plates to the east (Figure 14).

The position of the basal decollement varied throughout the history of thrust faulting. The oldest faults in this part of the orogenic belt are the Paris and Crawford thrust faults (Figure 1). Movement on the Paris thrust is dated as latest Jurassic to Early Cretaceous while the Crawford fault is Middle Cretaceous in age (Armstrong and Oriel, 1965). According to Royse and others (1975), these thrusts share the same structural position in the northern Wasatch Mountains where they occur as a zone of east-dipping faults that are folded into part of a large ramp-anticline that formed during the Late Cretaceous. These faults form a complex zone of deformation characterized by ductile and brittle faulting. Large-scale, ductile deformation is confined to rocks in a 1 to 2 km thick zone directly above the Willard thrust fault while deformation beneath the fault is characterized by brittle faulting and flexural-slip folding.

The upper plate of the Willard thrust fault consists of a thick section of Paleozoic and late Precambrian strata. Tectonic slices of older, Precambrian schist, phyllite and quartzite crop out sporadically near the base of the thrust plate. Precambrian rocks in the basal 2 km of the plate were ductilely deformed and metamorphosed to greenschist facies during thrusting. The rocks are cleaved and tight to isoclinally folded with ductile thrust faults (tectonic slides) separating the major folds (Figures 15 and

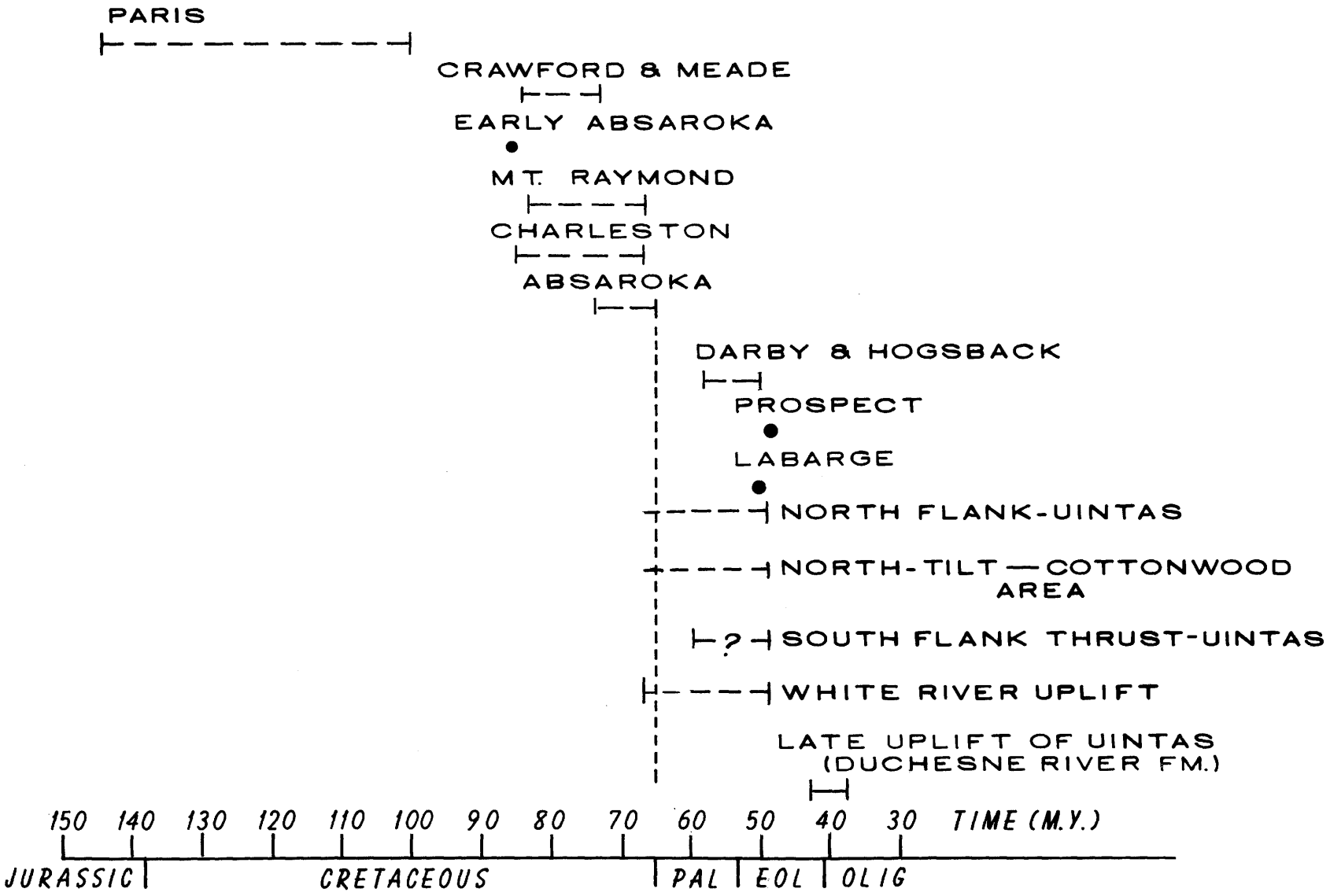

Figure 13. Estimated ages of major thrust faults in the Wasatch Mountains and timing of deformation in the Uinta Mountains region.

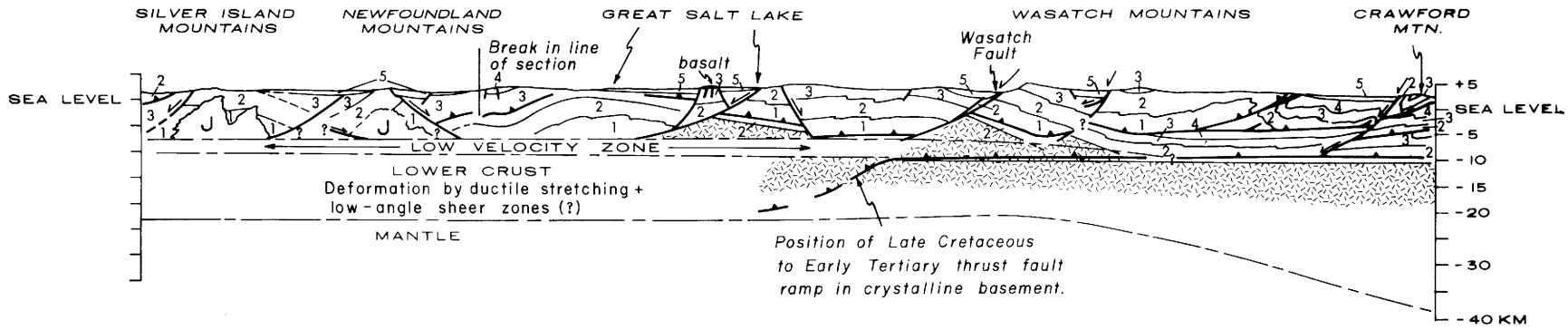

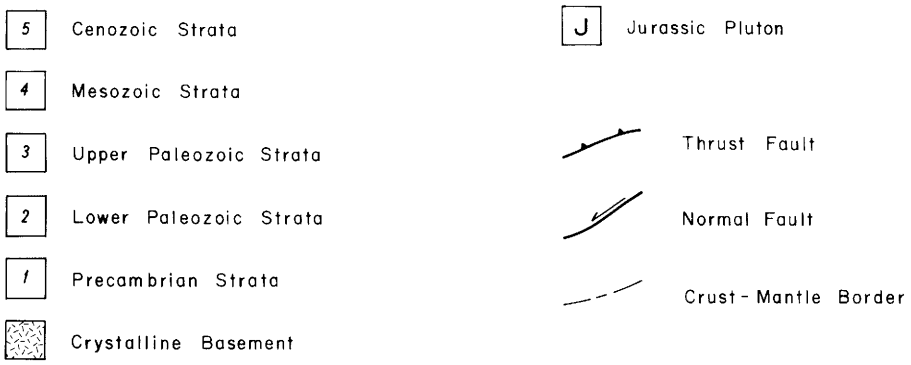

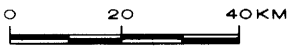

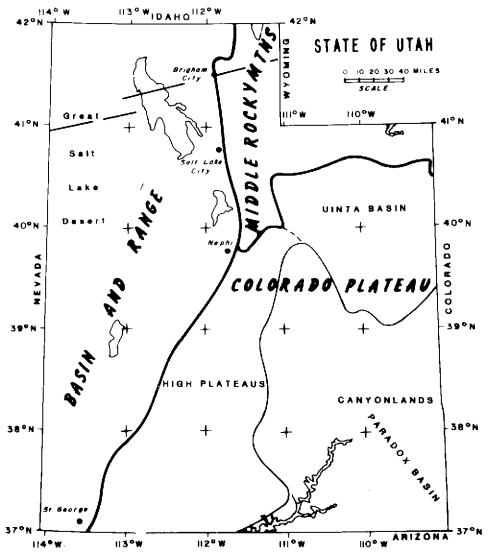

Figure 14. Regional cross-section of northern Utah between 41° N and 42° N. Line of section is shown on the state map.

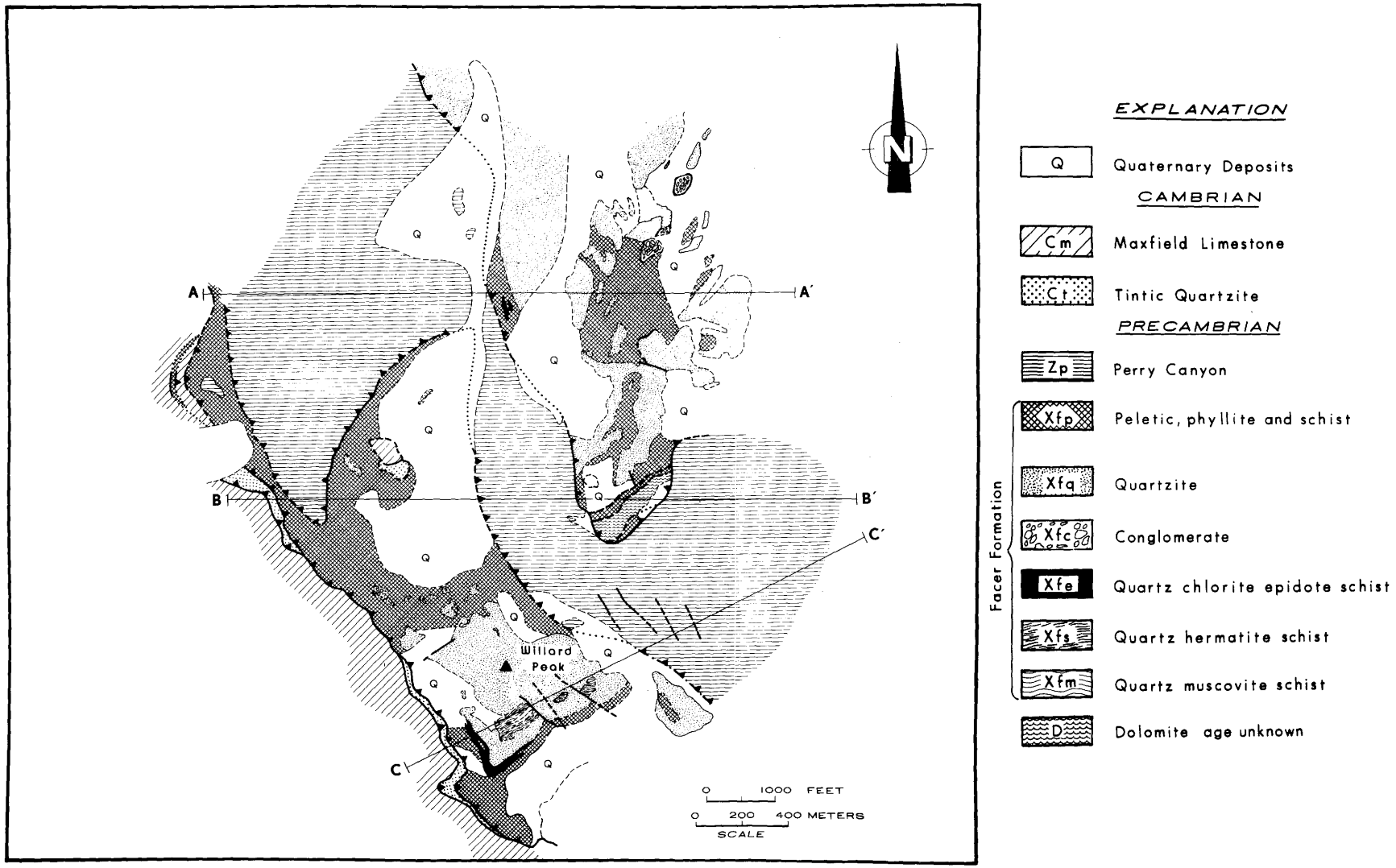

Figure 15. Geologic map of the Willard Peak area in the northern Wasatch Mountains. Location of figure is shown on index map in Figure 16 (from Beck, 1982).

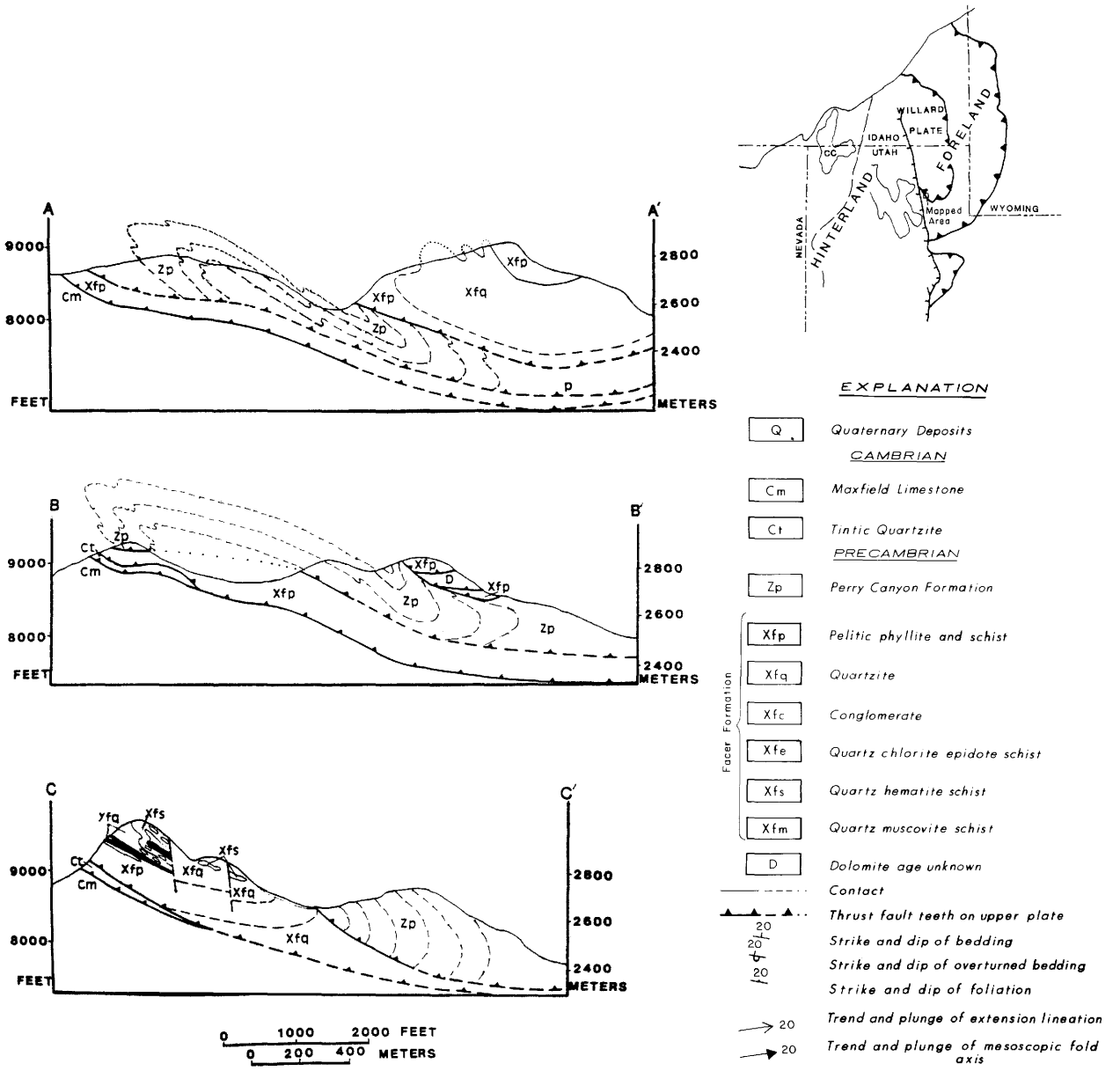

Figure 16. Cross-sections of the Willard thrust fault. Location of sections is shown in Figure 15 (from Beck, 1982).

16). Syntectonic mineral assemblages suggest that ductile deformation occurred at a temperature of about 300 to 350°C, corresponding to a depth of about 16 km (Hansen, 1980; Beck, 1982).

Deformation in the Cambrian strata and crystalline basement of the imbricated lower plate is characterized by thin, discrete thrust faults and flexural-slip folds which is in marked contrast to the penetrative deformation seen in the base of the upper plate. At some locales, upper plate phyllite is in fault contact with brecciated Paleozoic limestone along the Willard fault. Spaced cleavage — presumably caused by pressure solution — is locally developed and even has a "slaty" aspect, particularily in limestone. The thrust faults form a complex anastomosing pattern that in some areas has the geometry of an east-dipping duplex zone (Figure 17). Two of these thrusts, the Ogden and Taylor faults, cut crystalline basement (Figures 18 and 19; Eardley, 1944; Sorenson and Crittenden, 1972; Bruhn and Beck, 1981).

The geometry and structures of this zone of thrust faulting are useful in deducing a deformational sequence even though the ages of the events are

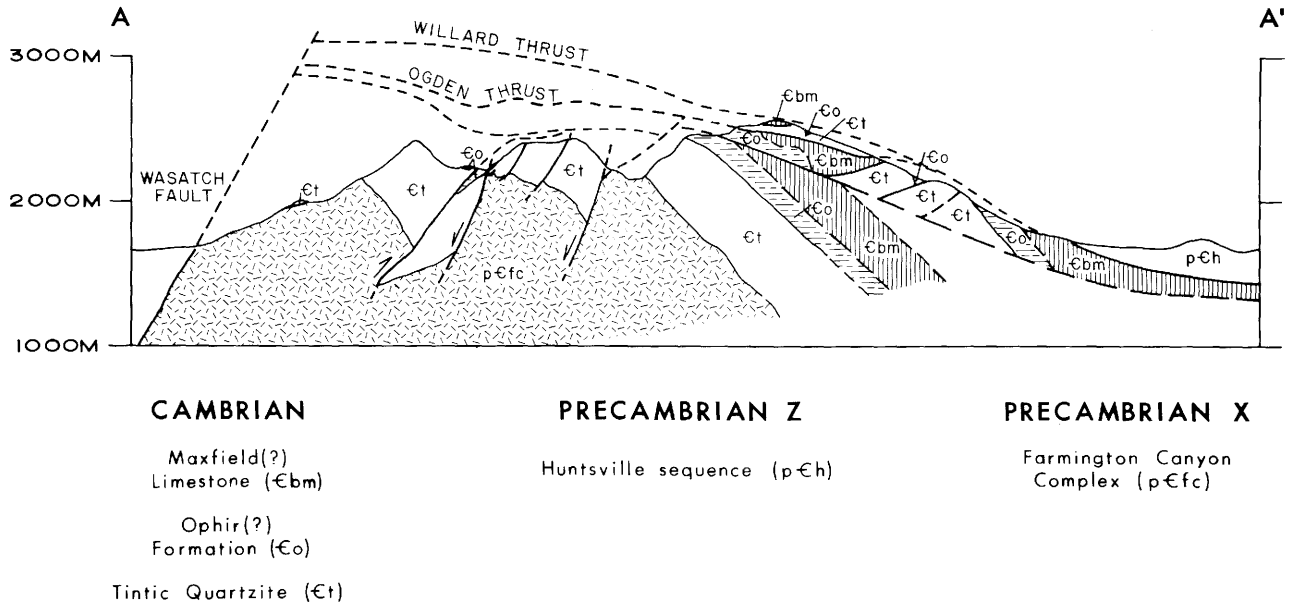

Figure 17. Geologic cross-section of part of the Wasatch Mountains immediately north of south Ogden Canyon. Notice the duplex geometry of the faults (after Sorenson and Crittenden, 1972).

not well constrained. The Willard thrust fault abruptly cuts upsection towards the east, rising in level from Lower Cambrian to Mississippian rocks in the westernmost Wasatch Mountains (Figure 17). The fault in this area therefore represents a large fault-ramp that was folded following movement on the Willard thrust fault. The penetratively deformed, greenschist facies rocks in the base of the upper plate presumably developed early in the history of faulting at a confining pressure close to 400 MPa and a temperature of about 300 to 350°C (Beck, 1982). These rocks subsequently encountered the fault-ramp and must have been uplifted as the upper plate moved eastward over the ramp. This uplift presumably resulted in a decrease in pressure and temperature at the base of the plate and a transition from a ductile to more brittle style of deformation.

We have no radiometric dates for the age of the greenschist metamorphism, nor do we know the exact time when the upper plate was faulted into its final position on the fault-ramp. Brittle faulting in the ramp region clearly predates formation of the large, Late Cretaceous anticline over which the ramp is folded. Royse and others (1975) infer that the thrust faults in the Cambrian rocks correspond to the decollement of the Crawford thrust system. They correlate the structurally overlying Willard fault with the older Paris system. This means that the deformation may range in age from latest Jurassic to Middle Cretaceous with final emplacement of the upper plate during movement on the Crawford thrust system in the Middle Cretaceous. While this interpretation is reasonable, it should be noted that the duplex-like geometry of the thrust faults makes it difficult to convince oneself as to which faults developed during movement on the Paris thrust system and which developed later as part of the Crawford thrust system (Figure 17).

The Late Cretaceous structure of the northern Wasatch Mountains is dominated by a large anticline that was partly dismembered by normal faulting during the Late Tertiary. The fold is cored by crystalline basement of the Farmington Canyon Complex in the mountain front between Salt Lake City and Ogden City (Figures 1 and 14). East of the large exposure of crystalline basement, the entire Paleozoic section and most of the lower Mesozoic section dips eastward in the steep fore-limb of the anticline. This limb contains numerous parasitic folds and bedding-plane faults that developed as the result of flexural-slip during folding. Synorogenic conglomerate of the Evanston Formation rests unconformably on Jurassic strata in the easternmost part of the steep limb near Devils Slide on Interstate Highway I-80. The Evanston Formation is Maestrichtian in age and presumably constrains the age of the fold itself.

North of Ogden City, the anticline plunges northward. Precambrian and Paleozoic rocks in the upper plate of the Willard thrust fault crop out in the crest region of the fold (Figure 14). The fold's

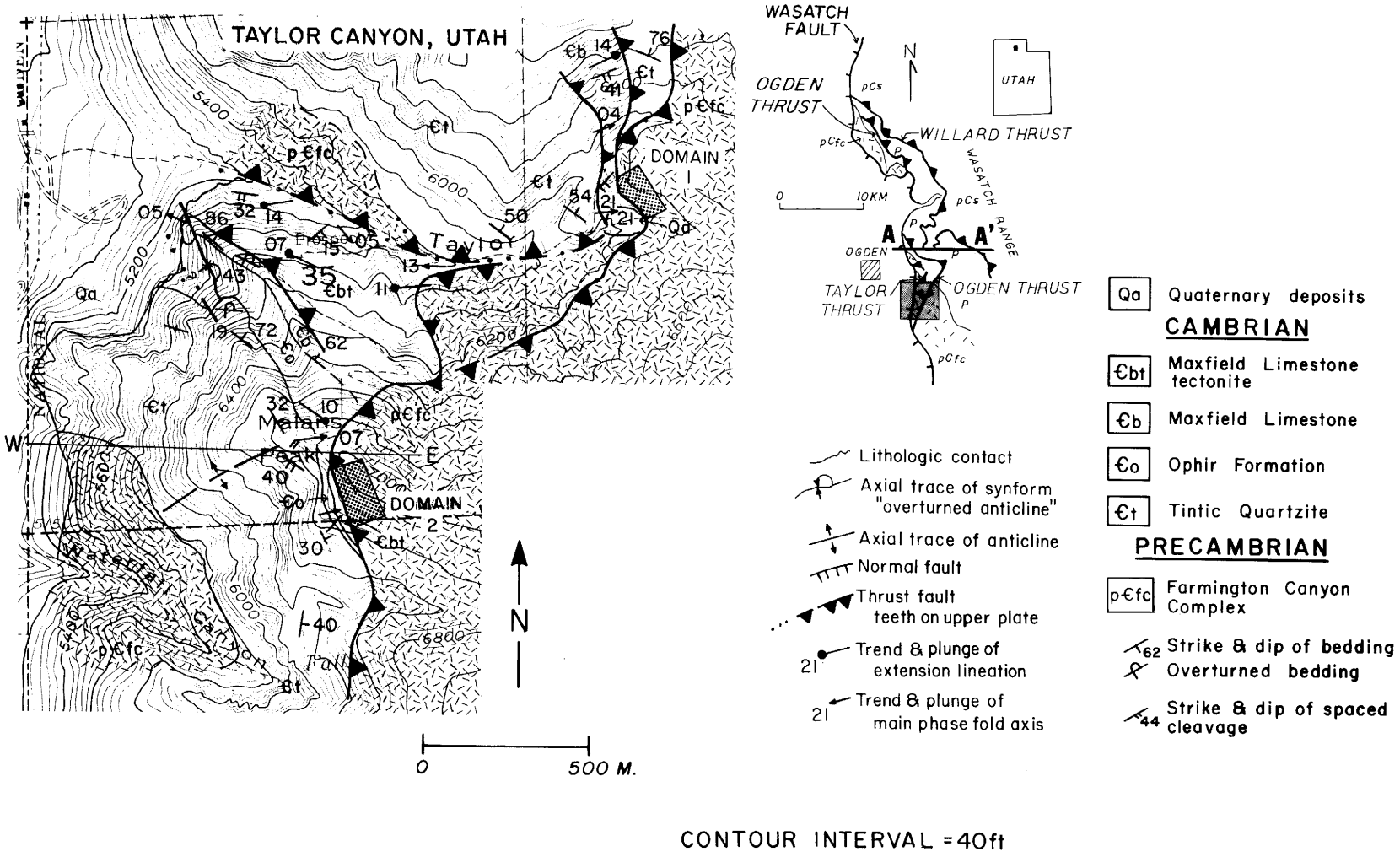

Figure 18. Geologic map of the Ogden and Taylor thrust faults.

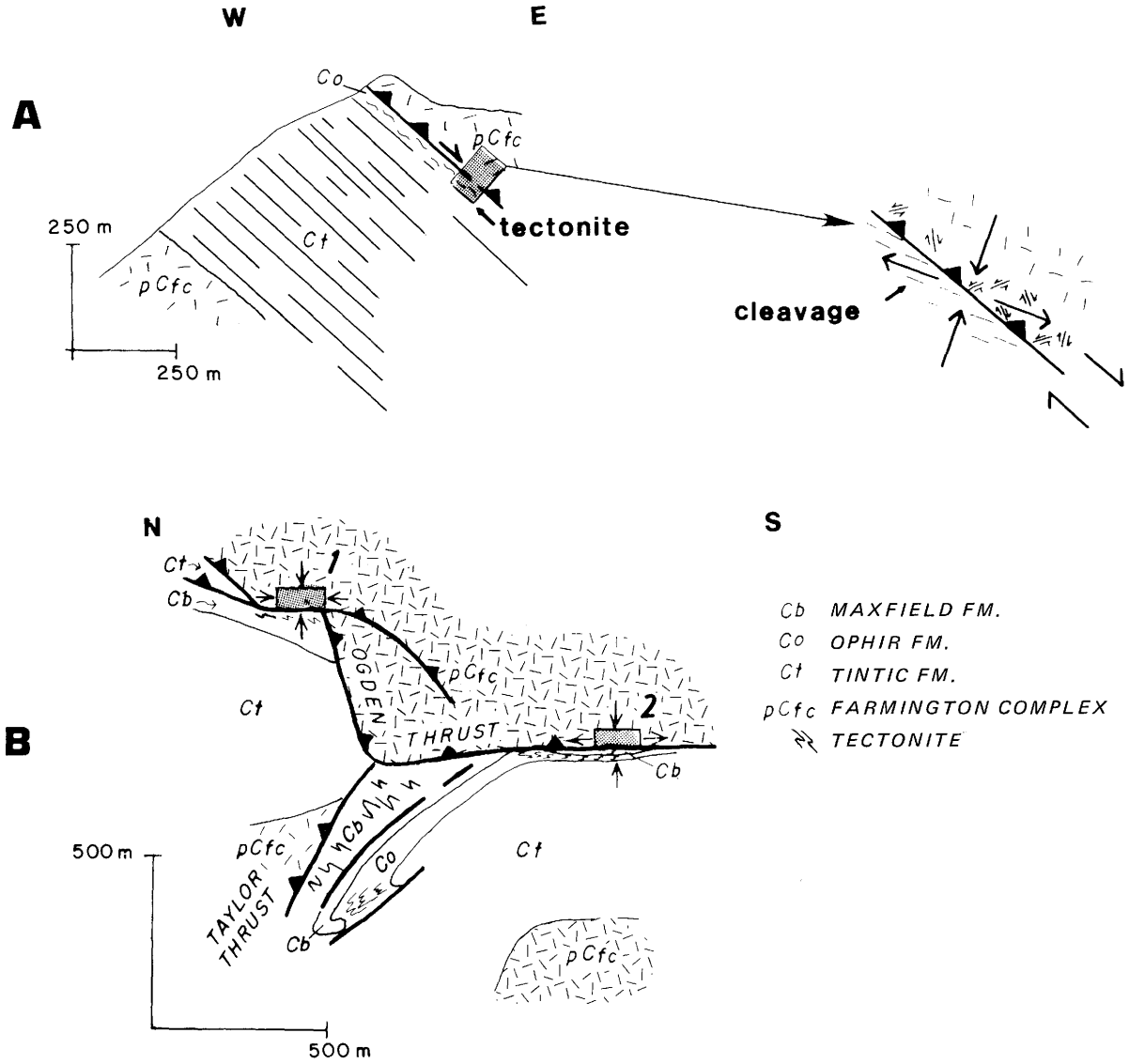

Figure 19. A. West to east cross-section of the Ogden thrust fault at Taylor Canyon. Location of section is indicated on Figure 19. B. Down-plunge cross-section of the structures in the map of Figure 19. The view is towards the east and shows the structural relation between the Ogden and Taylor thrust faults. Domains 1 and 2 are indicated on Figure 18. The arrows show the principal strain orientations in the altered gneiss at the base of the Ogden thrust plate (Bruhn and Beck, 1981).

crest region is disrupted by large, listric normal faults which border half-grabens filled with late Tertiary sedimentary and volcanic rocks in the northern Wasatch Mountains (Hopkins and Bruhn, 1982). The back-limb of the fold is down-faulted beneath Tertiary cover on the west side of the Wasatch fault along the Wasatch Mountain front.

This large fold is interpreted as a ramp-anticline that developed during faulting on the Absaroka thrust system in the Late Cretaceous (Royse and others, 1975). The Absaroka decollement is thought to occur at a depth of about 10 km beneath the northwestern Wasatch Mountains where it probably occurs in either basal Cambrian or late Precambrian strata. The fault ramp presumably was located just west of the present Wasatch Mountain front and marked the position where the basal decollement cut deep into crystalline basement towards the west. Movement on this decollement must have continued into the Paleocene after cessation of movement on the Absaroka thrust because the early to middle late Paleocene Hogsback thrust system is thought to merge into this decollement in the western part of the thrust belt (Royse and others, 1975; Dixon, 1982).

The Mesozoic thrust plates of the Wasatch Moun-

tains were folded into a large, north-verging anticline along the Uinta axis near Salt Lake City and represent a western continuation of Uinta Mountains structure (Figure 1; Crittenden, 1976). Folding on this east-trending axis may have commenced in latest Cretaceous and was certainly underway in the Paleocene based on the age of the regional unconformity that separates Paleocene to lower Eocene conglomerate of the Wasatch Formation from underlying, folded strata. This unconformity can be traced over a large distance from the core of the north-trending ramp-anticline of the northern Wasatch Mountains to the northern flank of the Uinta Mountains (Figure 1).

Several workers have discussed possible structural relationships between the Uinta Mountains and north-trending structures of the thrust belt in Utah and Wyoming (Sales, 1968; Beutner, 1977; Dixon, 1982). Most recently, Dixon (1982) pointed out that formation of the Uinta Mountains overlapped in space and time with eastward movement of the upper plate of the Hogsback thrust system. In particular, he suggested that complex structures should be expected in the region where transcurrent faulting along the Uinta Mountains intersected and presumably interacted with the Hogsback thrust.

Inspection of the regional geologic map of the central Wasatch Mountains and the Uinta Mountains reveals that the upper plate of the Hogsback thrust fault can be traced into the western end of the Uinta Mountains and Uinta axis. The Absaroka thrust fault is apparently folded into the Uinta axis at its southern end (Figure 1), exposing the upper plate of the Hogsback fault beneath the Absaroka thrust fault. East-striking faults on the north flank of the Uinta Mountains truncate the eastern part of the Hogsback thrust plate and then die out in the upper plate of the fault farther west in the Uinta axis. This geometry suggests that the western end of the Uinta Mountains was structurally part of the upper plate of the Hogsback thrust fault. In this area, the upper plate of the Hogsback fault moved eastward about 20 km in the Paleocene (Royse and others, 1975; Dixon, 1982); 20 km of sinistral-slip is therefore required on the Uinta axis and westernmost Uinta Mountains.

The Charleston thrust fault is the major thrust belt structure in the southern Wasatch Mountains (Figure 1). The fault has been folded and exposed along the southern edge of the Uinta axis (Figure 1). Here, the oldest rocks in the upper plate are late Precambrian. Crystalline basement is exposed in the upper plate at only one locality — Mount Nebo in the extreme southwestern end of the mountains. There, Precambrian gneiss occupies the core of a large, east to southeast-verging anticline that was disrupted by normal faulting during the Late Tertiary. The anticline is located above the Nebo thrust fault, an imbricate thrust that must root in the regional decollement of the Charleston thrust system. The presence of this basement-cored anticline at Mt. Nebo indicates that the basal decollement may have ramped down-section immediately west of the Wasatch Mountains where it rooted in crystalline basement. Significantly, normal faulting along the Wasatch fault occurs near the eastern edge of an inferred thrust-ramp in both the northern (Royse and others, 1975) and southern Wasatch Mountains. This suggests that ancient thrust belt structures may strongly influence the contemporary, extensional tectonics.

STRUCTURE OF THE UINTA MOUNTAINS

Following the explorations of John Wesley Powell, Clarence King, and Ferdinand Hayden in the 19th century, the Uinta Mountains attracted much attention. Since then the mountains have intrigued numerous geologists who have reflected upon the origin of their anomalous, east-west trend and contemplated the geometry of structures beneath the range. Such speculations have important economic implications for petroleum geologists; the geometry of "pet models" constrains visions of the petroleum potential.

Based on geological and geophysical data, we have constructed three cross-sections across the Uinta Mountains (Figure 20). Structurally, the Uinta Mountains are a north-verging anticline that trends eastward (Figure 1). On their eastern end, the mountains die out into a series of northwest striking folds and thrust faults in the Axial arch of Colorado which connect to the Grand Hogback monocline in the White River uplift. On their western end, the Uinta Mountains continue into the Uinta axis where late Mesozoic structures of the thrust belt are folded into a north-verging anticline (Crittenden, 1976).

Discussions of Uinta Mountains structure often center on the large, partly en-echelon series of reverse and thrust faults that extend along the north flank of the range. Indeed, significant displacements have occurred along some of these faults with estimates of stratigraphic offset as large as 10 km (Hansen, 1965; Ritzma, 1969). Hansen (1965) found up to 6 km of sinistral-slip along part of the

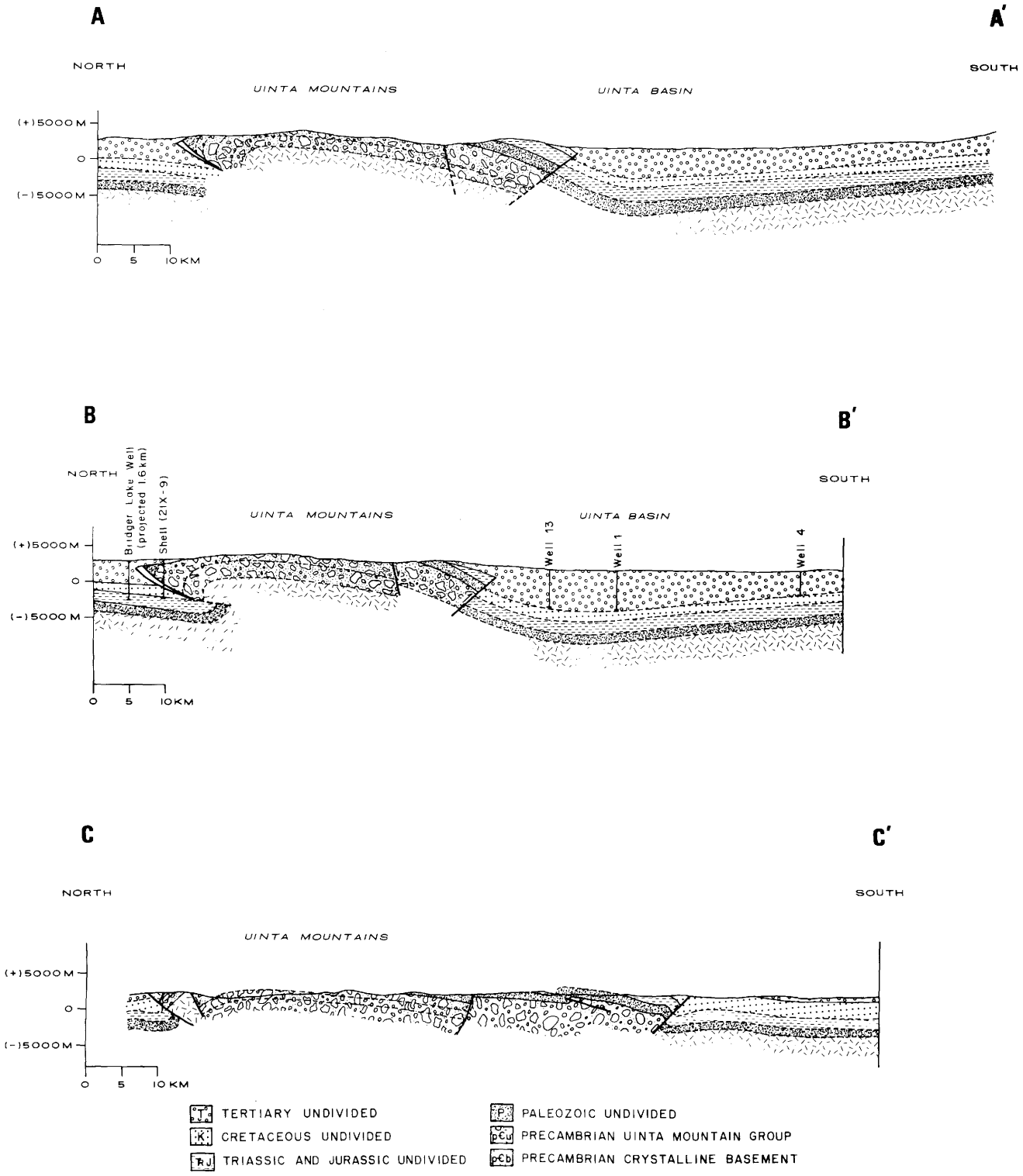

Figure 20. Geologic cross-sections of the Uinta Mountains. The locations of the three cross-sections are shown on Figure 1.

north flank. At least 20 km of sinistral-slip is required in the Uinta axis and westernmost part of the Uinta Mountains if our interpretation of the relation between the Hogsback thrust and Uinta axis is correct. Large, reverse faults also occur along most of the south flank of the mountains where they are buried by sedimentary deposits in the Uinta Basin (Figures 1, 20). These reverse faults apparently have displacements of several kilometers, but there is little published data on them (Campbell, 1976).

Although the faults are large, we consider the anticlinal geometry of the mountains to be even more significant and suggest that the fold geometry provides insight into the deep crustal structure. Our preliminary modelling of the deep structure is based on the following assumptions: 1) deformation in the crust occurred on discrete fault zones at depths above the brittle-ductile transition; 2) the long, gently dipping limb of a large anticline reflects the presence of a fault-ramp that extends from the brittle, sedimentary section downward to the brittle-ductile transition in the basement (Rich, 1934); 3) the ratio of vertical to horizontal displacement perpendicular to the mountain range is a reasonable estimate for the tangent of the ramp's dip; 4) we assume that the cross-sectional geometry is the result of crustal shortening across the mountain range. Undoubtedly, strike-slip movement has also occurred parallel to the strike of the range, but we assume this latter component of displacement did not strongly affect the cross-sectional geometry.

Crustal displacements are best calculated from section B-B′ (Figure 20) where well data are available. The vertical uplift between strata in the core of the Uinta fold and the same strata in the adjacent Green River Basin is about 12 km while the amount of horizontal shortening across the mountain range is at least 13 km. This latter figure is found by summing 6 km of horizontal translation on the thrust fault encountered in the Shell Dahlgreen Creek well with 7 km of shortening estimated from the geometry of the fold. The amount of movement on the thrust fault is probably greater than 6 km because the fault could extend at a low-angle for some distance south of the well. An additional 1 to 2 km of horizontal shortening occurred across the reverse fault on the southern flank of the mountains (Figure 20, B-B′).

Displacement estimates for the other two cross-sections (A-A′ and C-C′, Figure 20) are not constrained by well data. The overall geometry of section A-A′ is similar, however, to that of B-B′. Section C-C′ is located near the eastern end of the range, where uplift on the southern flank is greater than in areas to the west. The long, gently dipping southern limb of the Uinta fold is still present although the structure is more complicated than in the other two cross-sections and the north-dipping reverse faults may be more significant (Sears and others, 1982).

The model structure-section for the Uinta Mountains is shown in Figure 21. The thrust fault beneath the north flank of the mountains has been extended southward to the point where the south-dipping limb of the fold begins. A fault ramp is inferred to dip southward to a depth of 15 to 20 km — the estimated depth of the transition from discrete faulting to pervasive ductile deformation. This depth was chosen to coincide with temperatures of about 300 to 350°C, at which quartz-rich rocks should behave ductilely at geological rates of deformation (Beck and Bruhn, 1982). Extension of the north flank thrust fault to the south requires about 20 km of horizontal shortening across the Uinta Mountains. This is 7 km more than the minimum shortening estimate discussed previously, but it is reasonable in that several reflection profiles shown by exploration companies show this type of structure (Hamilton, 1981). Our geometric interpretation is broadly consistent with the ramp-anticline model of Rich (1934), although strict application of his model would require the fault ramp to parallel the south limb. Thrust-ramps are often complex structural zones rather than simple, discrete faults as originally proposed by Rich (1934). In particular, Serra (1977) — from observations of small-scale thrust systems — noted that the ramp region is often a wedge-shaped zone of complex strain, caused by imbrication, ductile flow, or extensive back-thrusting, depending on the physical properties of the rocks in the fault plates. The reverse fault in the south-flank of the mountains could intersect the south-dipping ramp at depth.

Figure 22 is a speculative drawing depicting our model for the evolution of the Uinta Mountains in the region just east of the Hogsback thrust system. We infer that the thick Uinta Mountain Group represents the fill of an east-trending trough or "aulacogen" that extended into the craton in late Precambrian time (Wallace and Crittenden, 1969; Sears and others, 1982). A thin and discontinuous section of strata accumulated in the Uinta Mountains region during the Paleozoic and Mesozoic (Herr and others, 1982) as deposition was interrupted by marine regressions.

Formation of the Uinta Mountains was certainly

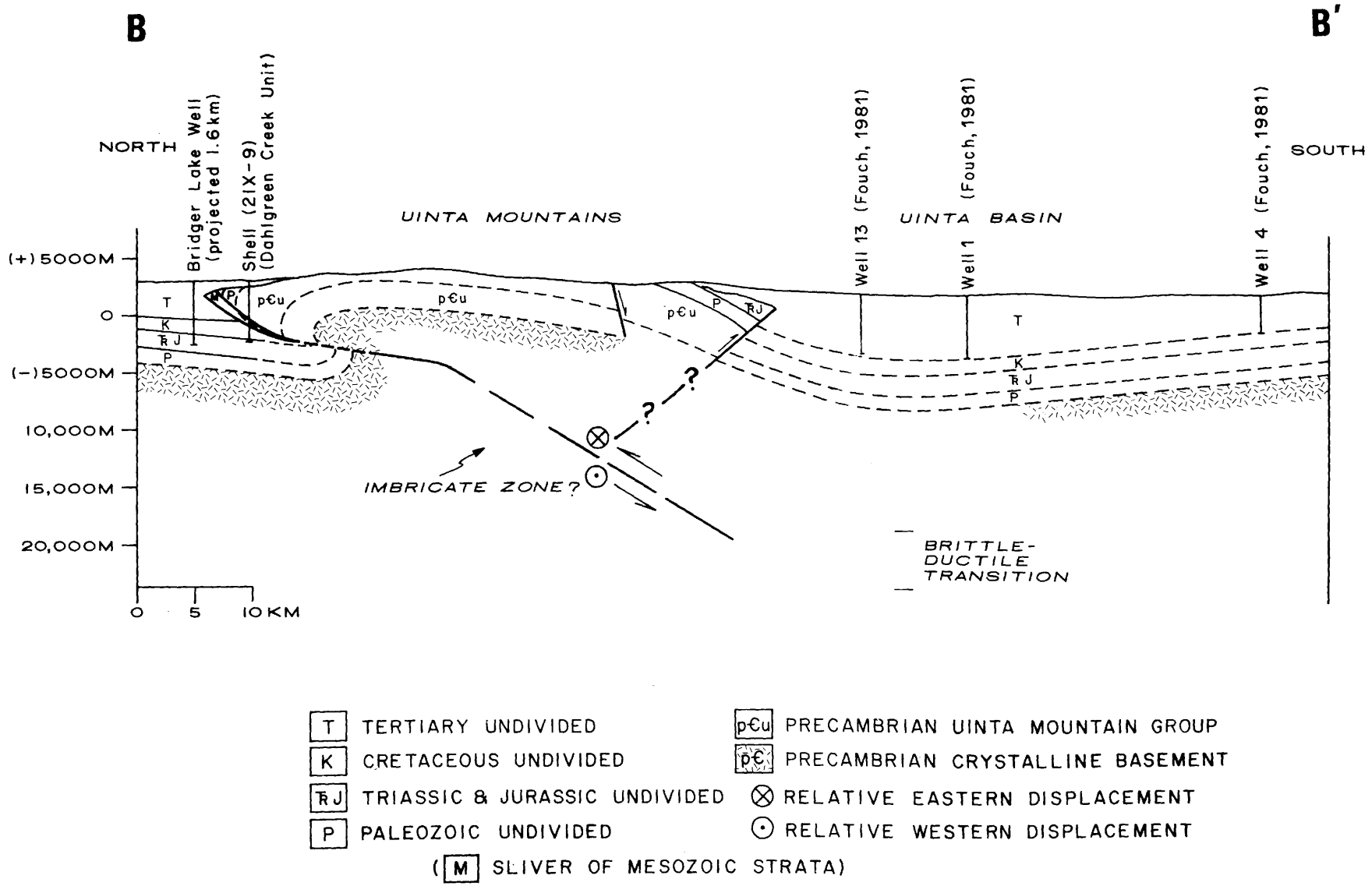

Figure 21. Inferred geometry of faulting beneath the Uinta Mountains along cross-section B-B' of Figure 20. The structural model is discussed in the text.

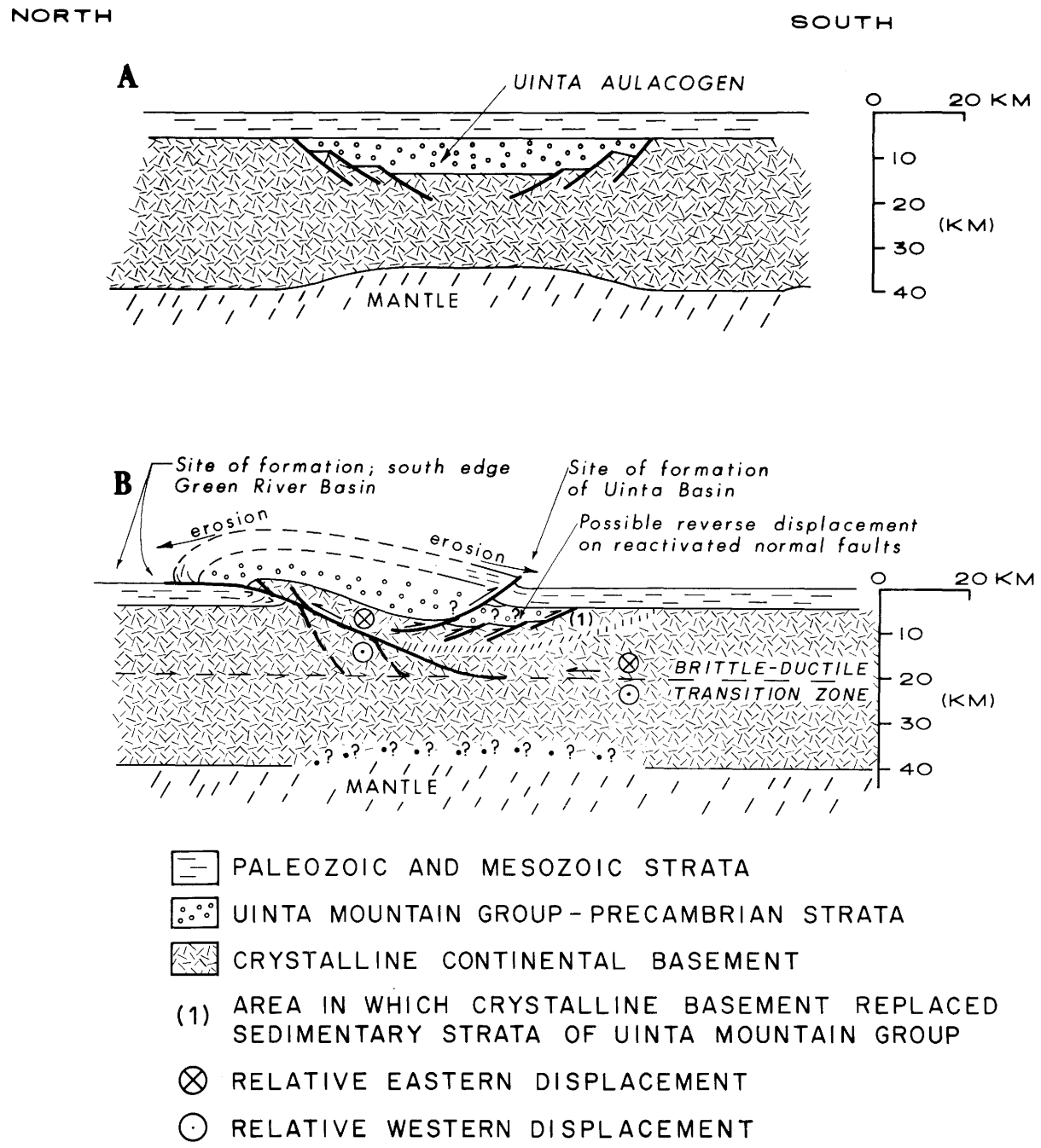

Figure 22. Schematic illustration of Uinta Mountains evolution in cross-section. A. Configuration of the Uinta Mountains region prior to Sevier-Laramide deformation. B. Structural model of deformation in the upper crust beneath the central Uinta Mountains.

underway in the early Paleocene and continued throughout the Eocene. We infer about 20 km of northward displacement of the mountains on a major thrust fault that dips southward to a depth of at least 15 to 20 km. Below this depth, the lower crust may have deformed ductilely, either by broadly distributed flow or perhaps by displacements on a complex system of ductile shear zones. We infer, as did Sears and others (1982), that some of the Precambrian faults along the edge of the aulacogen may have been reactivated during formation of the Uinta Mountains. Substantial sinistral-slip is inferred along the fault-ramp with at least 20 km of slip in the western part of the mountain range during the Paleocene. Thus, the crust beneath the Uinta Basin was translated eastward relative to that

of the Green River Basin. This eastward component of crustal shortening was presumably taken up in the Grand Hogback monocline and White River uplift in western Colorado. Such displacement is consistent with the regional tectonic models of Sales (1968) and Hamilton (1981).

SUMMARY

There are many salient problems and topics that require further research. Determining the history of synorogenic deposition is one key to understanding the relations between evolution of the Uinta Mountains and the thrust belt. We need better control on the age of synorogenic deposits and on the duration of time represented by regional unconformities. Comprehensive paleocurrent, stratigraphic and provenance studies are critical to refining the paleogeographic history. Such studies may also provide insights into the distribution and geometry of source and reservoir rocks in basins and fault plates. Specific examples: 1) regional unconformity at base of Wasatch Formation in Wasatch Mountains and its relation to unconformity on northeast flank of Uinta Mountains; 2) the Currant Creek Formation problem — age range of formation and provenance; 3) structural relief through critical times during the Late Cretaceous and early Tertiary; 4) history of White River uplift, Piceance Creek Basin, and tie to Uinta Mountains deformation; 5) study of early Tertiary deposits in mountains west of the Wasatch Front and tie to regions to the east; 6) sedimentology of Fort Union and Evanston Formations in the Uinta Mountains region.

Our preliminary model of basement structure in the Uinta Mountains is speculative. It requires testing by deep reflection profiling and by gravity modelling. The anticlinal geometry of the Uinta Mountains continues westward into the thrust belt along the Uinta axis, leading to the inference that the regional, south-dipping fault-ramp beneath the Uinta Mountains probably extended westward to at least the western edge of the Wasatch Mountains. The south-flank reverse fault apparently ends at the western edge of the thrust belt. It does not disrupt the upper plate of the Charleston thrust fault. This region is important to petroleum geologists and we suggest that judicious use of cross-sections — particularly downplunge sections made from the excellent published maps of the area — will provide insights into the structure and will place constraints on the interpretation of seismic reflection data.

The nature of deformation in the lower crust and upper mantle of the Rocky Mountain foreland remains a fundamental problem of Cordilleran tectonics. Evidence for large-scale transport of crystalline basement on low-angle thrust faults in the Wasatch Mountains is compelling (Royse and others, 1975; Beck, 1982). Certainly, by the Late Cretaceous, the basal decollement of the Sevier-Laramide thrust belt had cut deep into crystalline basement in the region immediately west of the Wasatch Mountains, probably reaching depths between 15 and 20 km — the level of the brittle-ductile transition in the crust (Beck, 1982). Excellent exposures of crystalline basement in the northern Wasatch Mountains provide opportunities to study characteristics of basement faulting (Bruhn and Beck, 1981).

What was the nature of deformation in the lower crust beneath the Uinta Mountains? Presumably, the position and orientation of the mountains was controlled by the presence of Precambrian features — crustal faults, compositional boundaries and, perhaps, differences in crustal thickness. Transcurrent displacement was significant. Possibly, the lower crust was deformed on steeply-dipping, ductile shear zones that extended into the mantle and the Uinta Mountains represent a "flower-type" structure as described by Lowell (1972). Alternatively, faulting in the brittle, upper crust of the Rocky Mountain foreland and Colorado Plateau region may have changed to pervasive, ductile flow in the lower crust at depths of 15 to 20 km. In this latter case, large faults in the upper crust would merge into a mid-crustal decollement of regional extent — partly decoupling the upper and lower crust. Satisfactory answers to this problem require advances in knowledge of the rheology of lower crustal rocks and the geometry of deep structures detected by seismic reflection profiling.

AKNOWLEDGEMENTS

Sandy Bruhn and Ginny Picard typed several drafts of the manuscript, and Michael DePangher gave important editorial suggestions. The help and advise of John Isby, Kadir Uygur, and Wm. Lee Stokes is greatly appreciated. We also wish to acknowledge Max Crittenden, Jr., Debbie Hopkins and Frank Royse, Jr. for discussions concerning thrust belt structures during the last several years. This work was partly supported by the Mineral Leasing Fund, University of Utah, and by a Research Corporation grant.

FIELD TRIP ROAD LOG: FIRST DAY

SEVIER-LARAMIDE STRUCTURE AND SEDIMENTOLOGY, CENTRAL WASATCH RANGE AND UINTA BASIN

M. Dane Picard, Ronald L. Bruhn, and Susan L. Beck

Geology of Wasatch Mountains between Salt Lake City and Brigham City

Mileage Incremental	Mileage Cumulative	Description
0.0	0.0	Salt Lake City — Union Pacific Railroad station (400 West, 1st South). Start of road log. Proceed north on 400 West, turn right at 500 North, then to 300 West and turn left.
1.4	1.4	Beck Street spa — warm springs because of circulation on Wasatch fault system.
1.2	2.7	Beck Street scarp of Wasatch fault. Gravel is faulted against Paleozoic carbonate sequence. Scarp is polished and striated, with most striae pitching downdip. Breathe infrequently — the air is sweeter north of here.
1.3	4.0	Intersection of Beck Street and I-15 North. Proceed north on freeway. Mountains on the east are metamorphic rocks of the Farmington Canyon Complex — highly deformed Archean and Proterozoic rocks that were metamorphosed to granulite (?) facies in the late Archean, then to amphibolite grade following quartz monzonite plutonism about 1,850 m.y.a. (Bryant 1980; Hedge and others, 1980). Numerous shear zones that contain retrograde, greenschist-facies, mineral assemblages cut the complex. The age of the shear zones is uncertain. It may be Precambrian or late Mesozoic. The Farmington Canyon Complex is in the core of a large, east-verging ramp-anticline that formed during the Sevier-Laramide orogeny. These rocks are also exposed on Antelope Island in the southern part of Great Salt Lake.
13.4	15.9	Turn onto U.S. Highway 89 — north toward Ogden.
2.6	18.3	Kaysville. This is the site of trenching of the Wasatch fault by Woodward-Clyde Consultants.
2.6	20.9	Crest of hill. On the left is Antelope Island surrounded by the Great Salt Lake. The Promontory Mountains on the northwest contain Precambrian and Paleozoic strata in a large thrust sheet that is structurally higher than the sheet that contains Antelope Island.
5.6	26.5	Intersection of U.S. Highway 89 and I-80 East. Note remnants of the Weber River delta system.
1.9	28.4	Intersection of U.S. Highway 89 and 203. Turn right on 203.
2.5	30.9	**STOP 1**. Entrance to Weber State College. Stop in access road with view of Wasatch Mountains. View of Farmington Canyon Complex thrust over Cambrian strata along the Ogden thrust fault. A clear example of basement involvement during the Sevier-Laramide orogeny. Continue north on Harrison Blvd.
3.0	33.9	Right turn onto A Street and

then an immediate left onto Valley Drive. Texaco station on right.

1.2 35.1 Right turn into South Ogden Canyon. Cross Wasatch fault into Precambrian Farmington Canyon Complex. Note perched river gravels — canyon up, base level down!

0.8 35.9 Unconformity of Cambrian basal Tinitc Quartzite on Farmington Canyon Complex. Nice view of east-dipping quartzarenite.

1.4 37.3 **STOP 2**. Tintic Quartzite is thrust over lower Cambrian limestone on the Ogden thrust fault. See South Ogden Canyon cross-section. Notice east-dip of strata and thrust fault (Figure 1).

3.8 41.1 **STOP 3**. Large "Z" fold in Mississippian strata (Figure 2). The fold is conical in that the amplitude decreases toward the south, where the fold dies out into an eastward dipping monocline. This fold was a focus of discussion between Max Crittenden Jr. and Armand Eardley concerning direction of movement during thrust faulting in the Wasatch Mountains.

0.2 41.3 Turn left and cross Pine View Dam. Cliff ahead is composed of Mississippian strata. (*I hate mountains, even from a spectacular point of view. . .* — George Orwell.)

0.4 41.7 **STOP 4**. Willard thrust fault. Precambrian "Z-age" strata thrust over Mississippian carbonate sequence. Traverse from lower to upper sheet reveals brecciated carbonate rocks overlain by phyllites in the base of the Willard thrust sheet. Mapping to the north and east reveals that the lower 1 to 2 km of the Willard sheet is penetratively deformed with large, isoclinal folds that were separated by ductile thrust faults or "tectonic slides." Penetrative deformation occurred under greenschist facies conditions. Deformation in the lower sheet was characterized by flexural-slip folding without regional cleavage development. Locally, spaced cleavage formed, however, and in some areas, thin discrete zones of tectonite marble occur. Transport of the upper sheet was from west to east. Once again, note the eastward dip of the thrust fault!

Small-scale folds just below the thrust fault and late-stage kink bands in the upper sheet suggest that north-south compression affected the thrust fault late in its history. The significance of these small-scale structures is unknown.

All of the hills on the east are formed by strata in the upper sheet of the Willard thrust.

Return to Intersection of South Ogden Canyon Road and Valley Drive.

1.3 43.3 Turn left onto Harrison Blvd.

7.5 55.8 Turn right onto I-84 East. Proceed east. Upon entering the canyon notice the cliffs of the Farmington Canyon Complex.

2.4 58.2 **STOP 5**. Shear zone in Farmington Canyon Complex. Amphibolite facies gneiss cut by retrograde, greenschist facies shear zone. Rocks are phyllonites and mylonite. The fabrics indicate eastward transport of the upper sheet relative to the

Figure 1. The Ogden thrust fault in the northern Wasatch Mountains. The Lower Cambrian section was repeated during faulting with basal Tintic Quartzite thrust over Lower Cambrian Limestone. The Tintic Quartzite (Ꞓt) forms the two large, resistant units in the photograph. View is towards the north, looking across south Ogden Canyon.

Figure 2. The large "Z" fold in the northern wall of south Ogden Canyon. The fold verges eastward and contains Mississippian strata of the Humbug Formation.

lower. The Farmington Canyon Complex is pervaded by these shear zones which vary in width from less than a meter to a kilometer. The age of the shear zones is uncertain. Bryant (1980) observed a shear zone on Antelope Island that did not cut the unconformity between gneiss and overlying Precambrian strata. He suggested therefore that the shear zones may be Precambrian. In contrast, Bell (1952) suggested that the shear zones developed during the Sevier orogeny and were the result of thrust faulting. Enough — we'll try to date the greenschist minerals in the shear zone.

1.3 59.5 **LUNCH STOP** at rest area by Weber River.

1.2 60.7 Entrance to Morgan Valley. Residential area on the left was built on tuffaceous strata of the Norwood Tuff, a widespread volcaniclastic sequence of Oligocene age. That was a mistake. Several houses have been damaged by creep of the tuff.

Morgan Valley is a large half-graben that is bounded by a listric normal fault on the eastern margin. Extension probably began in the Oligocene, during deposition of the Norwood Tuff, and has continued into the Quaternary. The faulting has partly disrupted the large, ramp-anticline that we are driving through.

10.8 71.5 Freeway exit to town of Morgan. Red beds along valley margins are Paleocene-Eocene strata of the Wasatch Formation. The Wasatch lies directly on the Farmington Canyon Complex on the skyline of the mountains to the west, indicating that crystalline basement was exposed in this area by Paleocene time. For the next several miles the highway proceeds eastward through the steeply dipping limb of the major ramp-anticline that forms this part of the Wasatch Mountains. Mountain side to the left is composed of Farmington Canyon Complex and Cambrian and Devonian strata. The fold is cored by Farmington Canyon Complex and we are driving up-section, toward the east through the entire Paleozoic section and part of the Mesozoic section. The fold is overlapped by conglomerate of the Evanston Formation, indicating that it formed during the Maestrichtian as the result of displacement on the Absaroka fault system.

1.0 72.5 Entering Mississippian sequence. We pass the following units in succession: Lodgepole Limestone, Deseret Limestone, Humbug Formation, and Donut Formation. Total thickness of the Mississippian is about 2,100 ft (640 m).

1.0 73.5 Approximate position of contact between Mississippian Donut Formation and Permian Round Valley Limestone. The Round Valley Limestone is about 400 ft (122 m) thick. It is overlain by the Pennsylvanian Morgan Formation. The Morgan Formation consists of up to 1,000 ft (305 m) of reddish-brown sandstone and siltstone with sparse limestone beds. Beds on the right side of the road belong to the Wasatch Formation.

0.8 74.3 Contact of Pennsylvanian-Permian Weber Formation with underlying Morgan Formation. We are driving through a large, second-order fold on the steeply dipping limb of the ramp-anticline. The Weber Quartzite consists of 1,200 to 1,500 ft (366 to 457 m) of fine-grained quartzarenite and interbedded limestone.

2.2 76.5 Taggert exit. Notice that the Weber Quartzite now dips steeply to the east. We have passed through the second-order fold and are once again in the main limb of the ramp-anticline. Driving eastward we pass through:

Park City Formation — 600 ft (183 m) of Permian limestone, shale and sandstone.

Dinwoody Shale — 100 ft (30 m) of Early Triassic red and green siltstone, claystone, and sandstone.

Woodside Formation — about 1,100 ft (330 m) of red siltstone, claystone and very fine grained sandstone. Early Triassic.

Thaynes Formation — 2,400 ft (732 m) of gray limestone, siltstone, and sandstone of Early Triassic age.

Ankareh Formation — 600 ft (180 m) of reddish brown siltstone that is Middle to Late Triassic in age.

Nugget Sandstone (Jurassic) — 1,100 ft (330 m) of reddish-orange, cross-bedded sandstone.

Twin Creek Limestone (Jurassic) — 2,600 ft (780 m) of limestone, sandstone, and siltstone. Lower part forms Devils Slide. The formation contains pale red siltstone and sandstone near the base. Reworking of the upper part of Nugget Sandstone.

Notice the numerous small folds and bedding-plane faults that disrupt beds. A nice example of intra-limb deformation during flexural slip folding.

3.1 79.6 Devils Slide viewpoint. Two resistant limestone beds in the lower part of the Twin Creek Limestone form the Devils Slide chute. Return to freeway.

0.4 80.0 **STOP 6**. Conglomerate of Evanston Formation rests unconformably on nearly vertical Twin Creek Limestone. The Evanston Formation is Maestrichtian in age. This unconformity dates the ramp-anticline as Maestrichtian.

0.9 80.9 Crossing trace of Croyden (East Canyon) fault. It is a normal fault with the downthrown block on the east. On the right, the Early Cretaceous Kelvin Formation is faulted against the Evanston conglomerate. For the next several miles we will drive through Cretaceous strata of the foreland basin.

6.9 87.8 Junction of I-84 with I-80 to Salt Lake City. Continue to the right, towards Salt Lake City. Roadside outcrops are Late Cretaceous in age. Notice the regional dip to the northwest. We are on a limb of the Coalville anticline.

0.8 88.6 Dam of Coalville Reservoir on left side of road.

0.8 89.4 Outcrops of Frontier Formation on the right. This Lower Cretaceous Formation is the oldest unit exposed in the core of the Coalville anticline.

2.9	92.3	Coalville exit. Crest of the large Coalville anticline.
7.4	99.7	Exit freeway to Rockport Reservoir — celebrated fishing. One of the authors — by choice unnamed — has managed to fish here many times without success. Take U.S. Highway 189 south to Wanship and Kamas.
1.9	101.6	Rockport Dam on the left. Good view of Frontier Formation in cliff at opposite side of the dam.
0.6	102.2	Frontier Formation in fault contact with the Kelvin Formation on the Dry Canyon fault. Fault dips steeply to the north-northwest.
0.4	102.6	Approximate position of contact of the Kelvin Formation with the Upper Jurassic Preuss Sandstone.
0.5	103.1	**STOP 7**. Preuss Sandstone is thrust over the Frontier Formation on the Crandall Canyon fault. Faulting occurred prior to deposition of the Upper Cretaceous Wanship Formation, which overlaps the faults and folds in the older rocks. The Wanship Formation is in turn folded and dips to the north-northwest in the area just northeast of Rockport Dam. We agree with the interpretation of Crittenden (1974) that the Dry Canyon and Crandall Canyon faults represent the folded trace of the Absaroka thrust fault. Folding of the thrust faults into their present attitudes probably occurred during latest Cretaceous (?) and Paleocene time, during formation of the Uinta Mountains and thrusting on the Hogsback thrust system.
1.0	104.1	Entrance to Rockport State Park. Roadside exposures are the Frontier Formation.
1.2	105.3	Approaching contact between Frontier Formation and Aspen Shale. We then drive downsection through the Kelvin Formation into the Jurassic Morrison, Stump, and Preuss Formations.
0.7	106.0	**STOP 8**. Contact of Lower Jurassic Twin Creek limestone with Preuss Sandstone. Traverse through Twin Creek Limestone into the underlying Nugget Sandstone.
0.4	106.4	Village of Peoa.
2.0	108.4	**STOP 9**. View of Uinta Mountains front towards the east. Notice the steep northward dips of strata. This structure continues westward into the Rockport area that we have just driven through.
1.1	109.5	Village of Oakley.
3.7	113.2	View of Uinta Mountains on the east. Notice how the beds are curving from east to north - striking in a large structural closure at the west end of the Uinta Mountains.
1.3	114.5	Entering village of Kamas.
3.0	117.5	Junction of U.S. Highway 89 South with Utah Highway 35. Turn right onto 89 South. Hills on the south and east are Keetley Volcanics, which are Oligocene in age and consist of andesite and rhyodacite flows, tuffs, and breccias.
1.4	118.9	Entering Wasatch County. We

		are in the central part of the Keetley volcanic field.
4.8	123.7	View to the west of the eastern edge of the Cottonwood mining district.
1.0	124.7	Junction of U.S. Highway 40 East and 189 South. Turn right towards Park City.
4.9	129.6	Chevron phosphorite plant. Ore comes from the Park City-Phosphoria Formation near Vernal, Utah, on the south flank of the Uinta Mountains.
5.6	135.2	Junction of Utah Highway 248 with U.S. Highway 40 East. Turn right to Park City. End of first day's trip. We thank Judy A. Long for careful typing of the road log through several versions. The help of Sandy Bruhn and Ginny Picard through the illegible rough drafts is also greatly appreciated. Have a good time in Park City, but set your alarm clock for 5:45 A.M. (*We'll use a signal I have tried and found far-reaching and easy to yell. Waa-hoo!* — Zane Grey.)

FIELD TRIP ROAD LOG: SECOND DAY

SEVIER-LARAMIDE STRUCTURE AND SEDIMENTOLOGY, CENTRAL WASATCH RANGE AND UINTA BASIN

M. Dane Picard, Ronald L. Bruhn, and Susan L. Bech

Geology Between Park City, Duchesne, Soldier Summit, Thistle Junction, Provo and Salt Lake City

Mileage Incremental	Mileage Cumulative	Description
0.0	0.0	Junction of Utah Highway 248 and U.S. Highway 40. Turn southeast and begin road log.
6.9	6.9	Junction with alternate U.S. Highway 189. Oligocene volcanic rocks west of highway to Heber City. Not as well exposed west of highway along this route.
4.4	11.3	Fine view of Mount Timpanogos on the skyline. At an elevation of 3,525 m, Mt. Timpanogos is one of the highest mountains in the Wasatch Range.
2.0	13.3	The mounds on the valley floor west of Heber City near Midway are calcareous tufa deposits that are associated with geothermal springs in the area.
0.5	13.8	Entering Heber City. Heber City is located on generally flat-lying Quaternary alluvium largely eroded from outwash glaciers which occupied the high Wasatch Range on the west and the Uinta Mountains on the east and north. The valley is drained by the Provo River through Deer Creek Reservoir — popular fishing reservoir — in the southwest part of the valley.
3.0	16.8	Junction with U.S. Highway 189. Highway runs past Deer Creek Reservoir down Provo Canyon to Provo, Utah. Remain east-bound on U.S. Highway 40.
3.0	19.8	Entering the mouth of Daniels Canyon. The trace of the Charleston thrust is concealed beneath alluvium near the mouth of the canyon. Paleozoic rocks have been carried from west to east for 25 km or more over the western margin of the Uinta Basin.
2.6	22.4	Entering Uinta National Forest. Route in Daniels Canyon

to the top of Daniels Summit — elevation 2,400 m — is through outcrops of Permo-Pennsylvanian Oquirrh Formation which is about 3,600 m thick. Oquirrh beds dip steeply and are overturned in places. Strongly jointed and fractured. Dark limestone weathers gray, tan, and brown; sandstone forms extensive slopes of dark brown talus.

9.7 32.1 Daniels Summit. Divide between the drainage of westward-flowing Daniels Creek and eastward-flowing streams that are tributaries to the Colorado River system.

5.4 37.5 West Strawberry Valley Junction. The Strawberry River once meandered across a flat-floored valley occupied in part by a glacial lake. The hills left and right above the valley floor are composed of the low-dipping Late Eocene Duchesne River Formation which was deposited over and conceals the leading edge of the Charleston thrust sheet. Road to south runs by the west side of Strawberry Reservoir. One fork leads west and then southwest along Diamond Fork to U.S. Highways 6 and 89. Travel along this route inspired the essay *Time in the Field* (Journal of Geological Education, 1982): *The distant peaks of the Wasatch Range had become small and undistinguishable. From our position, we could not tell if far-off mountains had turned into clouds or dark clouds had evolved into limestone peaks.*

1.3 38.8 Co-op Creek.

5.0 43.8 **STOP 1**. Strawberry Res. — one of the favorite fishing areas in Utah. Portal, Water Hollow Tunnel. Strawberry Reservoir is surrounded by synorogenic deposits of the Duchesne River Formation which record latest Laramide (latest Eocene) tectonic events in this part of the Rocky Mountains. A major north-south normal fault borders the reservoir on the east. Displacement is down to the west. The reservoir lies in a down-faulted block that is tilted slightly to the east. The fault is visible in the road cuts east of the reservoir, approximately where major landslides encroach on the highway.

4.2 48.0 Junction. Road to right (south) is to Soldier Creek Dam. The earthfill dam was built in 1973 as part of the Central Utah Project. The reservoir is still another popular fishing hole. (*As no man is born an artist, so no man is born an angler.* — Izaak Walton.)

5.2 53.2 Deep Creek Canyon. Fine drinking water. Alluvial Duchesne River beds are intensely jointed and many faults with small displacements cross the area. Strike of faults and joints is about N. to N. 20° E. Zone of intense fracturing apparently is a northern extension of the north-trending horst and graben structure of the Wasatch Plateau on the south.

2.1 55.3 Crossing Currant Creek. The Currant Creek Dam — Central Utah Project — is about 6.5 km upstream.

1.1 56.4 **STOP 2**. View of distal Duchesne River beds (Figure 3). Paleocurrent directions indicate south-flowing streams throughout the northern Uinta Basin. Coarse sediment accumulated as debris-flow deposits

Figure 3. Alluvial sandstone in Brennan Basin Member of Duchesne River Formation, western Uinta Basin.

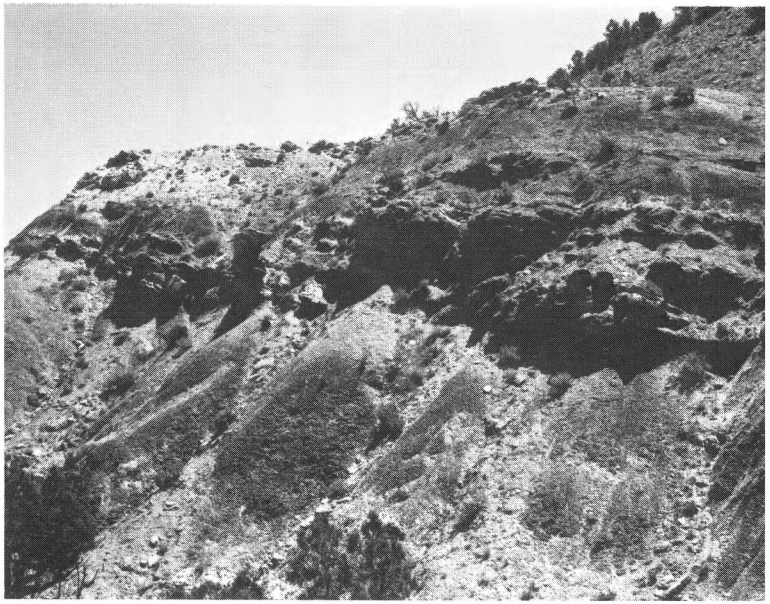

Figure 5. Floodplain facies interbedded with braided-stream channel sandstone in Currant Creek Formation.

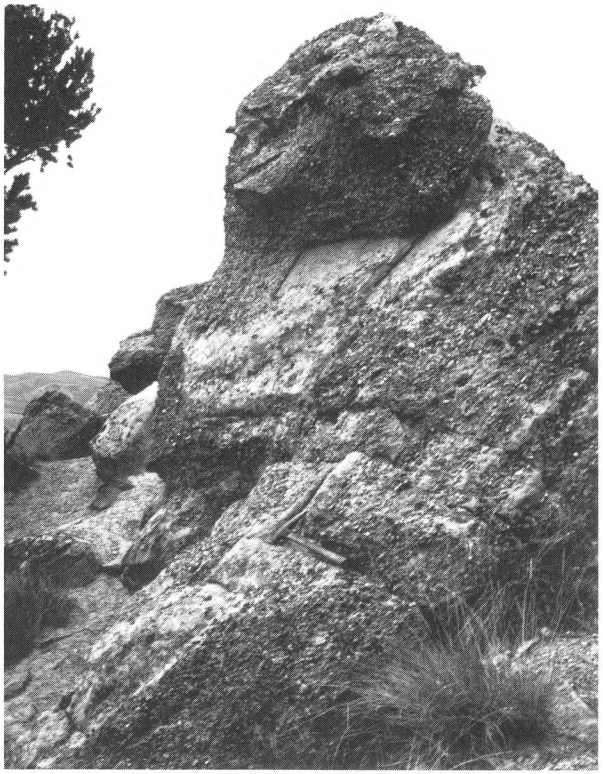

Figure 4. Currant Creek conglomerate and conglomeratic sandstone, northwest of Tabiona.

and as channel and floodplain deposits of relatively small, high-gradient, braided streams. Nearly all of the clastic material was derived from sedimentary and low-grade metamorphic source rocks of the Uinta Mountains. The formation contains altered volcaniclastic material that may represent intermediate volcanism in the Basin and Range Province.

3.0	59.4	Fruitland.
8.9	68.3	Junction of U.S. Highway 40 and Utah Highway 208. Turn north onto Utah 208 toward Tabiona.
12.9	81.2	Turn northwest onto Utah Highway 35 along the Duchesne River.
5.3	86.5	**STOP 3.** Unconformable contact of Cretaceous Mesaverde Group and the Cretaceous-Eocene (?) Currant Creek Formation northwest of Tabiona (Figure 4). Basal part of Currant Creek is Maestrichtian. The formation is a synorogenic conglomerate and conglomeratic sandstone deposit formed in braided streams. Varicolored claystone and siltstone beds are present (Figure 5). Paleocurrent directions in the basal sandstones are to the south and east.
18.2	104.7	Return to U.S. Highway 40 and turn east toward Duchesne.
9.4	114.1	Crossing structural axis of Uinta Basin.
1.0	115.1	Starvation Reservoir. (*We catched fish and talked, and we took a swim now and then to keep off sleepiness.* — Mark Twain.)
5.5	120.6	Duchesne.
0.8	121.4	Turn south onto Utah Highway 33.
0.4	121.8	Bridge over Strawberry River. Sandstone and limestone facies of Eocene Uinta Formation (Figure 6). As we drive through Indian Canyon across the south flank of the Uinta Basin we pass through Paleocene and Eocene rock units: sandstone and limestone facies of Uinta Formation (youngest), 600 m; saline facies of Uinta Formation, 350 m; Parachute Creek member of Green River Formation, 425 m; green shale facies (delta facies) of Green River Formation, 510 m; black shale facies of Green River Formation, 360 m. An alluvial tongue of unknown thickness is present in the lower part of the Eocene Green River Formation in the southwest part of Indian Canyon. The Green River and Uinta beds are mostly lacustrine except for the alluvial tongue and some sandstone beds that are alluvial and deltaic. In this area the Cretaceous-Paleocene Wasatch Group that underlies the Green River Formation is divided into three formations: North Horn Formation (oldest), Flagstaff Limestone, and the Colton Formation. Together they are from about 1,200 to 1,500 m thick.
4.9	126.7	Vertical jointing is well-developed in sandstone and limestone facies west of highway.
4.7	131.4	Right fork of Indian Canyon.
3.8	135.2	Alluvial channel sandstone on both sides of canyon in Uinta Formation.

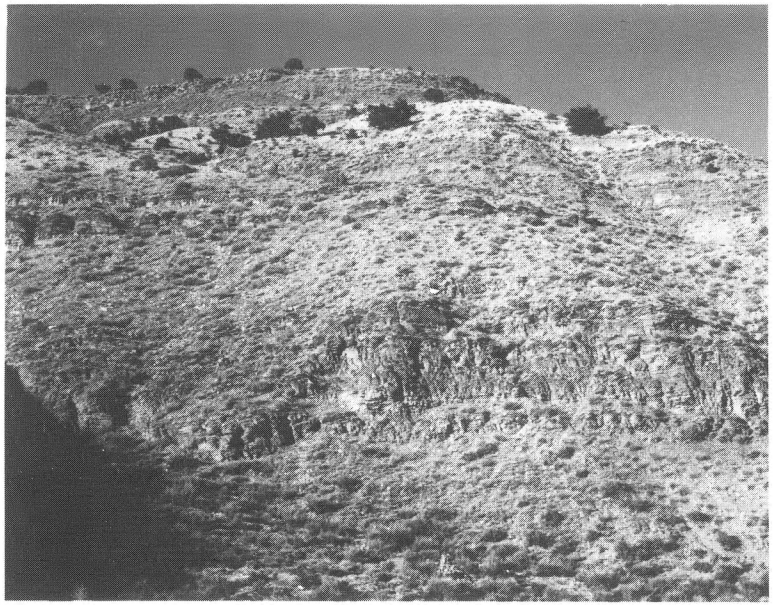

Figure 6. Sandstone and limestone facies of Uinta Formation, Indian Canyon.

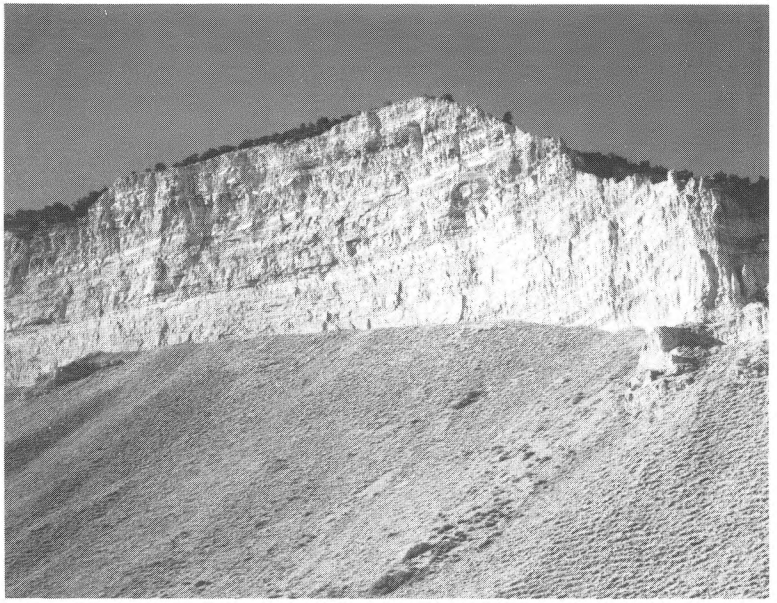

Figure 7. Saline facies of Uinta Formation, Indian Canyon.

Figure 8. Horse Bench Sandstone, Indian Canyon. Top of sandstone is about 150 m below the base of Dane's (1955) upper tuff zone. Paleocurrent directions are to the east and southeast.

2.2	137.4	Entering Ashley National Forest.
0.7	138.1	Obscure trail west of highway leads up hill to abandoned wurtzilite mine in saline facies.
1.6	139.7	White-weathering papery outcrops on west hillside are oil shale beds (kerogen-rich dolomicrite).
1.1	140.8	Thinly bedded, orange-colored, lacustrine carbonate beds in saline facies. Beds are persistent laterally.
0.7	141.5	Jones Hollow.
3.3	144.8	Just ahead is green shale facies.
0.4	145.2	Mill Hollow.
5.7	150.9	Pass. Cyclical sequence in Green River Formation (Figure 9).
0.9	151.8	**STOP 4**. Oil-impregnated deltaic sandstone bounded by stromatolites (Figure 10). **LUNCH**.
0.9	152.7	**STOP 5**. Alluvial tongue into Green River Formation. Nested channel deposits and associated floodplain beds (Figure 11).
1.7	154.4	Back in dark fine-grained beds of lacustrine origin — black shale facies of Green River Formation.
1.4	155.8	Contact of Green River and Colton Formations on right. Thick multi-story alluvial sandstones. Paleocurrent directions are to the northeast.
0.9	156.7	Traveling on Colton Formation. Light-colored dip slopes of Flagstaff Limestone at 12:00.
0.7	157.4	Entering Carbon County. (*The time to go there is when the machines are roaring and the air is black with coal dust, and when you can actually see what the miners have to do. At those times the place is like hell. . . .* — George Orwell.)
1.0	158.4	Contact of Flagstaff Limestone and Colton Formation.
0.1	158.5	Bear right at Y. Road is near contact of alluvial Colton Formation and lacustrine and alluvial Flagstaff Limestone.
9.4	167.9	Turn right onto U.S. Highway 6.
4.9	172.8	Junction with Utah Highway 96 (at Colton). Continue northwest on U.S. Highway 6. From here to Soldier Summit, route is entirely in Colton Formation.
3.2	176.0	Entering Wasatch County.
2.4	178.4	Soldier Summit. Strike valley is formed by less resistant Colton Formation rocks between more resistant Green River Formation on the north and Flagstaff Limestone on the south. Small dumps east of town are related to abandoned ozokerite mines and to processing plants. Ozocerite is a purplish to black, waxy, solid hydrocarbon that originated in the Green River Formation. Pockets were worked to 180 m between here and the town of Colton.
0.3	178.7	Entering Utah County.
6.0	184.7	Highway for next 12 to 13 km (7 to 8 mi) is through the Green River Formation.
1.0	185.7	Hummocky landslide and

Figure 9. Cyclical deposits in Green River Formation, Indian Canyon. Principal rocks are low-grade oil shale and carbonate beds.

Figure 10. Oil-impregnated foresets, Indian Canyon.

Figure 11. Nested channel deposits and associated floodplain beds.

creep topography on south side of canyon for several kilometers.

7.4 193.1 Faults with small displacements in Green River Formation. Light beds are carbonate rocks. Darker beds are low grade oil shale, claystone, and siltstone.

2.2 195.3 Well exposed outcrops of lower Green River Formation.

0.6 195.9 Contact of North Horn Formation and Flagstaff Limestone north of highway.

0.5 196.4 **STOP 6**. Cyclical, braided, alluvial beds in Cretaceous/Tertiary North Horn Formation — synorogenic deposits (Figures 12 and 13). Moussa's (1965) unpublished new formation name, Bennion Creek, may be applicable to this locality (W. L. Stokes, 1982, personal communication). Yet, the beds Moussa described have not been traced definitely into the area. According to Moussa (1965), the "Bennion Creek Formation" is certainly Late Cretaceous. Paleocurrent directions are to the east. Trace fossil locality. Large and small trails resemble *Scoyenia*. See abstract for this meeting by Picard and Bracken (1983).

5.0 201.4 **STOP 7.** Nearly flat-lying North Horn and Flagstaff Formations outcrop unconformably above Cretaceous formations (Figure 14).

1.6 203.0 Contact of Flagstaff Limestone with Twin Creek Formation.

0.3 203.3 **STOP 8**. Thistle Junction. Junction of U.S. Highways 89 and 6. Continue northwest on U.S. Highway 6.

Jurassic Twin Creek Formation — Nugget Sandstone contact (Figure 15). Cross-stratified facies of Nugget. Lowermost Twin Creek beds are reworked Nugget grains cemented with dolomite and Fe-rich carbonate.

1.6 204.9 Canyon Service.

0.9 205.8 Diamond Fork River. A Triassic sequence about 800 m thick outcrops here and on the northeast. The same formations — Woodside (oldest), Thaynes, Ankareh, Gartra, Popo Agie — are present on the southwest flank of the Uinta Mountains where they are only slightly thinner.

0.5 206.3 Permian sequence: Kirkman Limestone (oldest), Diamond Creek Sandstone, and Park City-Phosphoria Formation. Interval is about 1,100 m thick in the Spanish Fork Canyon area.

2.8 209.1 Pennsylvanian - Permian Oquirrh Formation.

7.4 216.5 Enter Interstate.

REFERENCES CITED

Andersen, D. W., and Picard, M. D., 1972, Stratigraphy of the Duchesne River Formation (Eocene-Oligocene?), northern Uinta Basin, northeastern Utah: Utah Geological and Mineralogical Survey Bulletin 97, 29 p.

————, 1974, Evolution of synorogenic clastic deposits in the intermontane Uinta Basin of Utah: *in* Tectonics and Sedimentation, Society of Economic Paleontologists and Mineralogists, Special Publication no. 22, p. 167-189.

Armstrong, F. C., and Oriel, S. S., 1965, Tectonic development of the Idaho-Wyoming thrust belt: American Association of Petroleum Geologists Bulletin, v. 49, p. 1807-1866.

Armstrong, R. L., 1968, Sevier orogenic belt in Nevada and Utah: Geological Society of America Bulletin, v. 79, p. 429-458.

Banks, E. Y., 1981, Petrographic characteristics and

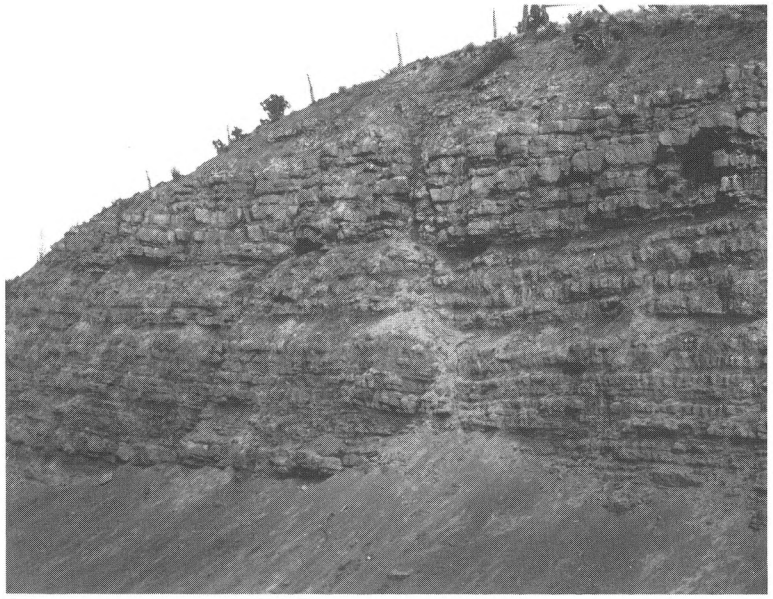

Figure 12. Cyclical distal facies of North Horn Formation, Spanish Fork Canyon.

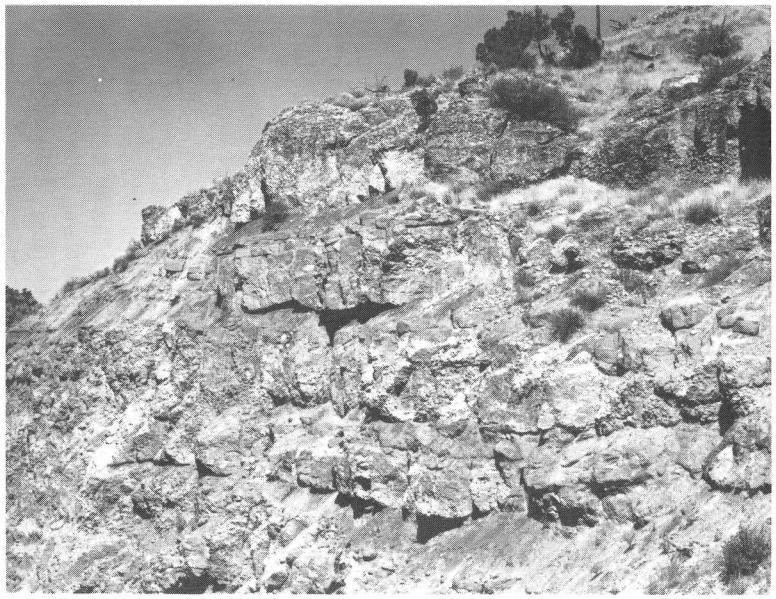

Figure 13. Proximal facies of North Horn Formation.

Figure 14. North Horn and Flagstaff on unconformity across Cretaceous beds.

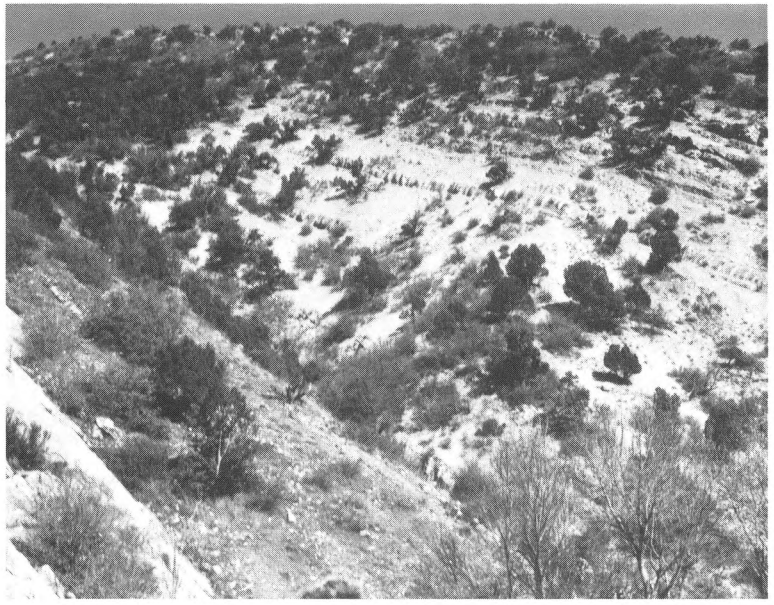

Figure 15. Uppermost Nugget Sandstone-lower part of Twin Creek Formation.

provenance of fluvial sandstone, Sunnyside oil-impregnated sandstone deposit, Carbon County, Utah: Unpublished M.S. thesis, University of Utah, 112 p.

Beck, S. L., 1982, Deformation in the Willard thrust plate in northern Utah and its regional implications: Unpublished M.S. thesis, University of Utah, 79 p.

Beck, S. L., and Bruhn, R. L., 1982, Geometry and mechanics of basement deformation beneath major Laramide folds in the Rocky Mountains, western U.S. (abs.): Transactions of the American Geophysical Union, v. 65, no. 9, p. 1115.

Beutner, E. C., 1977, Causes and consequences of curvature in the Sevier orogenic belt, Utah to Montana: *in* Rocky Mountain Thrust Belt Geology and Resources, Wyoming Geological Association, p. 353-365.

Birsa, D. C., 1974, The North Horn Formation, central Utah; sedimentary facies and petrography: Unpublished M.S. thesis, Ohio State University, 189 p.

Bruhn, R. L., and Beck, S. L., 1981, Mechanics of thrust faulting in crystalline basement, Sevier orogenic belt, Utah: Geology, v. 9, p. 200-204.

Bryant, B., 1980, Metamorphic and structural history of the Farmington Canyon Complex, Wasatch Mountains, Utah: Abstracts with Programs, Rocky Mountain Section of the Geological Society of America, 33rd Annual Meeting, p. 269.

Campbell, J. A., 1976, Structural geology and petroleum potential of the south flank of the Uinta Mountain Uplift, northeastern Utah: Utah Geology, v. 2, p. 129-132.

Crittenden, M. D., Jr., 1972, Willard thrust and the Cache allochthon, Utah: Geological Society of America Bulletin, v. 83, p. 2871-2880.

———, 1974, Regional extent and age of thrusts near Rockport Reservoir and relation to possible exploration targets in northern Utah: American Association of Petroleum Geologists Bulletin, v. 58, p. 2428-2435.

———, 1976, Stratigraphic and structural setting of the Cottonwood area, Utah: *in* Symposium on Geology on the Cordilleran Hingeline, Rocky Mountain Association of Geologists, p. 363-379.

Dickinson, W. R., Beard, L. S., Brakenridge, G. R., Erjavec, J. L., Ferguson, R. C., Inman, K. F., Knepp, R. A., Lindberg, F. A., and Ryberg, P. T., 1983, Provenance of North American Phanerozoic sandstones in relation to tectonic setting: Geological Society of America Bulletin, v. 94, p. 222-235.

Dixon, J. S., 1982, Regional structural synthesis, Wyoming salient of western overthrust belt: American Association of Petroleum Geologists Bulletin, v. 66, p. 1560-1580.

Eardley, A. J., 1944, Geology of the north-central Wasatch Mountains, Utah: Geological Society of America Bulletin, v. 55, p. 819-894.

Fouch, T. D., 1981, Distribution of rock types, lithologic groups and interpreted depositional environments for some lower Tertiary and Upper Cretaceous rocks from outcrops at Willow Creek-Indian Canyon through the subsurface of Duchesne and Altamont oil fields, southwest to north-central parts of the Uinta Basin, Utah: Oil and Gas Investigation Map, Chart/OC-81.

Garvin, R. F., 1969, Bridger Lake field, Summit County, Utah: *in* Geologic Guidebook of the Uinta Mountains, Intermountain Association of Geologists, 16th Annual Field Conference, p. 109-115.

Hamilton, W., 1981, Plate tectonic mechanism of Laramide deformation: Contributions to Geology, University of Wyoming, v. 19, p. 87-92.

Hansen, R. L., 1980, Analysis of the Willard thrust fault: Unpublished M.S. thesis, University of Utah, 81 p.

Hansen, W. R., 1965, Geology of the Flaming Gorge area Utah-Colorado-Wyoming: U.S. Geological Survey Professional Paper 490, 196 p.

Hedge, C. E., and Stacey, J. S., 1980, Precambrian geochronology of northern Utah: Abstracts with Programs, Rocky Mountain Section of the Geological Society of America, 33rd Annual Meeting, p. 275.

Herr, R. G., Picard, M. D., and Evans, S. H., Jr., 1982, Age and depth of burial, Cambrian Lodore Formation, northeastern Utah and northwestern Colorado: Contributions to Geology, University of Wyoming, v. 21, no. 2, p. 115-121.

Hopkins, D. L., and Bruhn, R. L., 1983, Extensional faulting in the Wasatch Mountains, Utah: Geological Society of America, Abstracts with Programs, v. 26, no. 5, p. 402.

Kauffman, E. G., 1977, special editor, Cretaceous facies, faunas, and paleoenvironments across the Western Interior basin: The Mountain Geologist, v. 14, p. 75-274.

Lawton, T. F., 1982, Lithofacies correlations within the Upper Cretaceous Indianola group, central Utah: *in* Overthrust Belt of Utah, Utah Geological Association. p. 199-213.

Lowell, J. D., 1972, Spitsbergen Tertiary orogenic belt and the Spitsbergen fracture zone: Geological Society of America Bulletin, v. 83, p. 3091-3102.

Moussa, M. T., 1965, Geology of the Soldier Summit quadrangle, Utah: Unpublished Ph.D. dissertation, University of Utah, 182 p.

Picard, M. D., 1971, Petrographic criteria for recognition of lacustrine and fluvial sandstone, P.R. Spring oil-impregnated sandstone area, southeast Uinta Basin, Utah: Utah Geological and Mineralogical Survey, Special Studies 36, 24 p.

———, 1980, Early Tertiary nonmarine basin deposits of northeast Utah; Record of late-orogenic molasse facies (abs.): Geological Association of Canada, Program with Abstracts, v. 5, p. 76.

Picard, M. D., and High, L. R., Jr., 1972, Paleoenvironmental reconstructions in an area of rapid facies change, Parachute Creek Member of Green River

Formation (Eocene), Uinta Basin, Utah: Geological Society of America Bulletin, v. 83, p. 2689-2708.

Pipiringos, G. N., and O'Sullivan, R. B., 1978, Principal unconformities in Triassic and Jurassic rocks, Western Interior United States — a preliminary survey: U.S. Geological Survey Professional Paper 1035-A, 29 p.

Rich, J. L., 1934, Mechanics of low-angle overthrust faulting as illustrated by the Cumberland thrust block, Virginia, Kentucky, and Tennessee: American Association of Petroleum Geologists Bulletin, v. 18, p. 1584-1596.

Ritzma, H. R., 1969, Tectonic resume, Uinta Mountains: *in* Geologic Guidebook of the Uinta Mountains, Intermountain Association of Geologists, 16th Annual Field Conference, p. 57-63.

Royse, F., Jr., Warner, M. A., and Reese, D. L., 1975, Thrust belt structural geometry and related stratigraphic problems, Wyoming-Idaho-northern Utah: *in* Rocky Mountain Association of Geologists Symposium on Deep Drilling Frontiers in the Central Rocky Mountains, p. 41-54.

Ryder, R. T., Fouch, T. D., and Elison, J. H., 1976, Early Tertiary sedimentation in the western Uinta Basin: Geological Society of America Bulletin, v. 87, p. 496-512.

Sales, J. K., 1968, Crustal mechanics of Cordilleran foreland deformation — a regional and scale-model approach: American Association of Petroleum Geologists Bulletin, v. 52, p. 2016-2044.

Sears, J. W., Graff, P. J., and Holden, G. S., 1982, Tectonic evolution of lower Proterozoic rocks, Uinta Mountains, Utah and Colorado: Geological Society of America Bulletin, v. 93, no. 10, p. 990-997.

Serra, S., 1977, Styles of deformation in the ramp regions of overthrust faults: Twenty-Ninth Annual Field Conference-1977 Wyoming Geological Association Guidebook, p. 487-498.

Sorensen, M. L., and Crittenden, M. D., Jr., 1972, Preliminary geologic map of part of the Wasatch Range near North Ogden, Utah: U.S. Geological Survey Miscellaneous Field Studies Map MF-428.

Stanley, K. O., and Collinson, J. W., 1979, Depositional history of Paleocene-lower Eocene Flagstaff Limestone and coeval rocks, central Utah: American Association of Petroleum Geologists Bulletin, v. 63, p. 311-323.

Van Houten, F. B., 1973, Origin of red beds: a review — 1961-1972: Annual Review Earth and Planetary Science, v. 1, p. 39-61.

Wallace, C. A., and Crittenden, M. D., Jr., 1969, The stratigraphy, depositional environment, and correlation of the Precambrian Uinta Mountain Group, western Uinta Mountains, Utah: *in* Geologic Guidebook of the Uinta Mountains, Intermountain Association of Geologists, 16th Annual Field Conference, p. 126-141.

NOTES

Utah Geological and Mineral Survey Special Studies 59, 1983
Guidebook Part 1 — GSA Rocky Mountain and Cordilleran Sections Meeting
Salt Lake City, Utah — May 2 - 4, 1983

STYLE OF MID-TERTIARY EXTENSION IN EAST-CENTRAL NEVADA

Phillip B. Gans and Elizabeth L. Miller
Department of Geology, Stanford University, Stanford, CA 94305

ABSTRACT

The northern Egan, Schell Creek, and Snake ranges in east central Nevada are characterized by low-angle, younger-on-older faults and by steep, westward dips of strata. The character of the early Oligocene unconformity and the ages of syntectonic intrusive and volcanic rocks suggest that most of the faulting and tilting occurred in the Oligocene. two types of "low angle" faults are present: 1) Originally high-angle (60° to bedding) normal faults that rotated domino-style to low angles; and 2) "Flat" ductile-brittle detachment faults that separate overlying rocks extended by high-angle normal faulting from underlying ductily deformed rocks. Conspicuously absent are large-displacement normal faults that initially formed at low angles to bedding. Apparent "bedding parallel" faults are generally the result of normal drag of incompetent strata along high-angle normal faults. The high-angle faults are typically "shovel-shaped" in three dimensions and may have fanning upward splays that document progressive rotation on the planar faults.

High-angle faults in the Egan and Schell Creek ranges penetrated to paleodepths of greater than 10 km without flattening significantly; the basal detachment of these faults is not exposed. In contrast, the ductile-brittle transition in the northern Snake Range developed at 6 to 7 km depth. Overlying rocks were drastically thinned by two generations of east-dipping high-angle normal faults that flattened abruptly into the Snake Range decollement. Each generation of upper plate faulting was accompanied by 40° of westward rotation such that first generation faults now dip gently westward, second generation faults dip gently eastward, and locally bedding is near vertical. Lower plate rocks beneath the Snake Range decollement were drastically thinned and extended co-axially with upper plate faulting. The comparable amount of extension recorded in the lower plate (350 percent) and upper plate (450 percent) together with the lack of stratigraphic omission across the Snake Range Decollement suggest that the upper "plate" need not have moved significantly with respect to the lower "plate."

The northern Egan, Schell Creek, and Snake ranges lie within and define a 120 km wide "belt" of mid-Tertiary extension. Both range-by-range palinspastic reconstructions and the dilation of older Mesozoic structures yield an average of approximately 250 percent extension across this corridor. Supracrustal extension in east-central Nevada was apparently accomodated by *in-situ* deep-seated ductile deformation and magmatism. "Rooted normal faults" and far-traveled "extensional allochthons" (Wernicke, 1982) are not important geometric elements. The presently high elevations suggest that extensional processes modified the entire lithospheric column.

INTRODUCTION AND OVERVIEW

Metamorphic core complexes of the U.S. Cordillera are thought to have evolved at least in part during the mid-Tertiary and represent uplifted areas of profound crustal extension (see, for example, reviews by Coney, 1979; Zoback and others, 1981; Eaton, 1982; Armstrong, 1982). In these complexes, gently folded detachment faults separate supracrustal rocks that have been thinned by normal faulting from underlying, variably deformed mid-crustal igneous and metamorphic rocks. To date, most studies have focused on the details of the core complexes themselves[1], such that the geologic

[1]An excellent collection of papers that describe the geology of many of the known metamorphic core complexes comprise GSA Memoir 153 by Crittenden and others (1980).

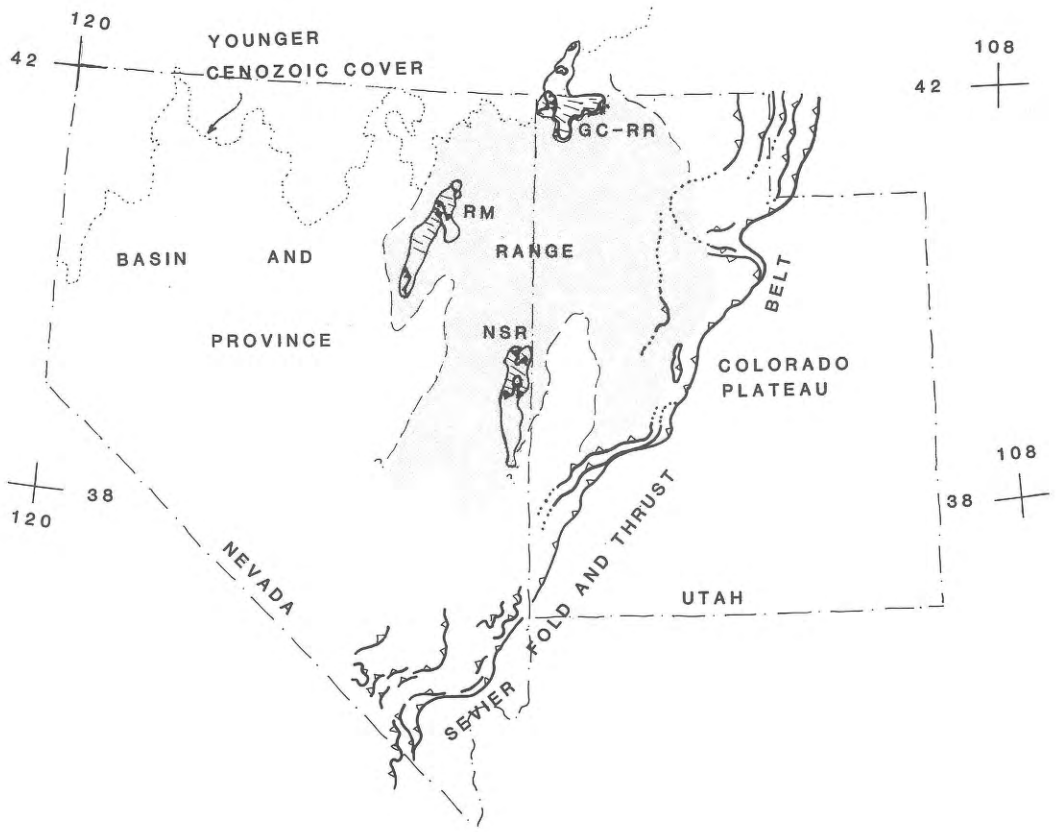

Figure 1. Location of the northern Snake Range (NSR), Ruby Mts (RM) and Grouse Creek - Raft River (GC-RR) metamorphic core complexes with respect to the Sevier fold and thrust belt. Lower plates of core complexes show lineations developed parallel to the direction of extension. Shaded region represents highly extended region in NE Nevada and adjacent Utah. From Compton (1980), Snoke (1980), and King (1969).

and geometric relationship of these apparently isolated culminations of metamorphic rocks to their surrounding areas is still poorly understood. However, in order to fully understand the extensional processes that bring deep-seated rocks to the surface, core complexes must be studied and evaluated in the context of the geology of adjacent areas that expose higher structural levels.

In this paper, we describe the geometric character of mid-Tertiary extension across three ranges in east-central Nevada. The northern Egan and Schell Creek Ranges, together with the Snake Range metamorphic core complex (Figure 1), lie within and define a 110 km wide corridor that was profoundly extended in the Oligocene. This extensional "belt" has sharp supracrustal boundaries with relatively unextended areas to the east and west.

Several unique characteristics of this region make it particularly well suited for the study of the kinematics of Tertiary extension: 1) east-central Nevada was not complicated by pre-Oligocene deformation except at very deep structural levels; 2) most of the bedrock consists of a well-defined and regionally persistent Paleozoic stratigraphy that allows accurate determination of fault offsets and palinspastic reconstructions; 3) scattered remnants of syntectonic volcanic and sedimentary rocks bracket the ages of various extensional episodes; and 4) variable amounts of later uplift has exposed a broad spectrum of earlier Tertiary paleodepths. This allows us to examine the three-dimensional geometry of normal faults and evaluate extensional processes at both supra and mid-crustal levels.

We preface our range-by-range descriptions of Tertiary extensional tectonics in east-central Nevada with a brief review of earlier ideas and a discussion of the pre-extensional evolution of this region.

REGIONAL SETTING

Introduction and Evolution of Ideas

The Egan, Schell Creek, and Snake Ranges (Figure 2) are located in the heart of the northern Basin and Range province. They are 10 to 25 km

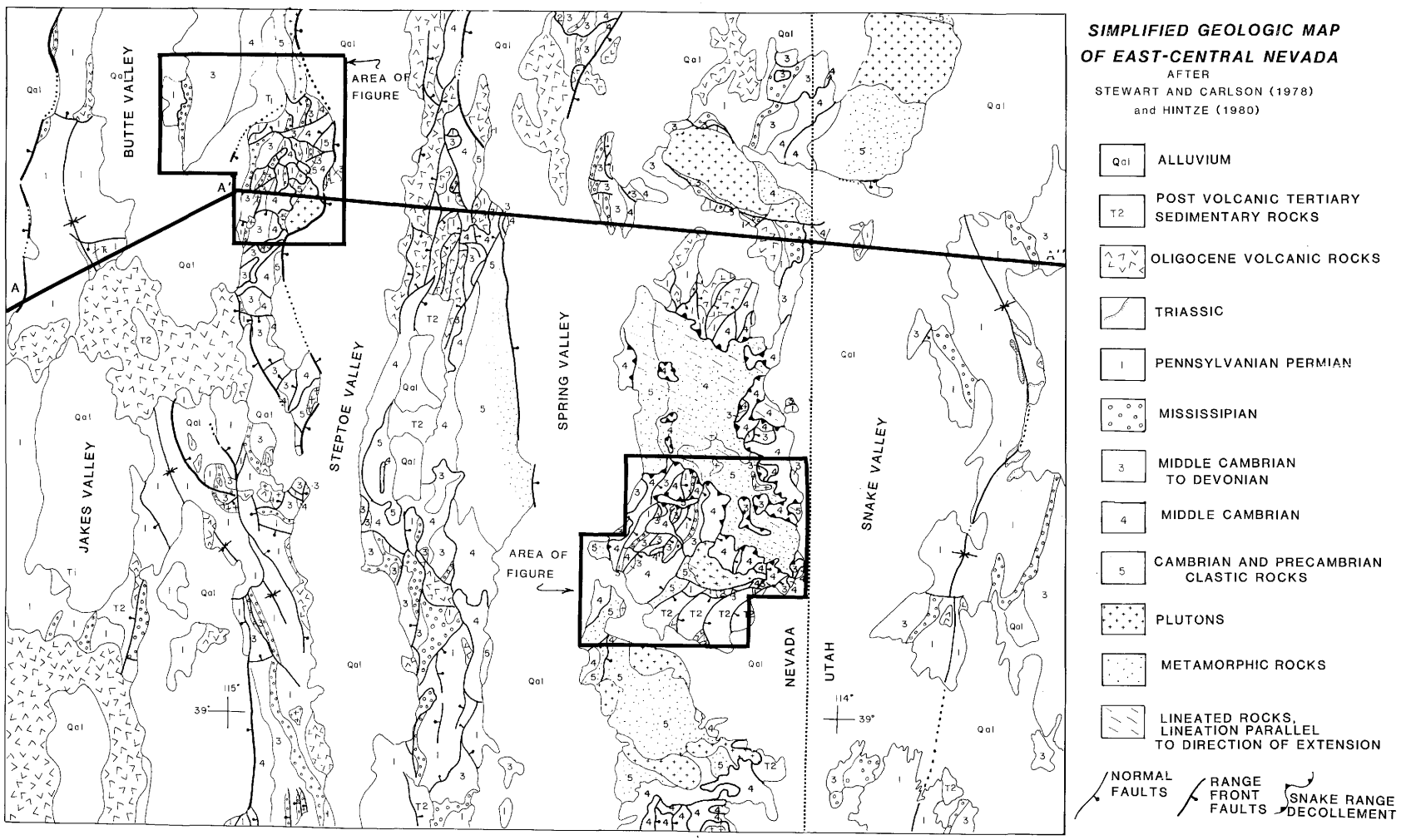

Figure 2. Simplified geologic map of east-central Nevada, modified from Stewart and Carlson (1978), Hintze (1980). Sources of data; Hose and Blake (1976), Hose (1977).

wide, N-S trending ranges that attain elevations in excess of 3,500 m and are separated by valleys of similar widths whose elevations average 1,800 m.

A striking aspect of the geology of this region is that some ranges are comprised of structurally simple homoclines or gentle folds that involve upper Paleozoic strata, whereas adjacent ranges are cut by imbricate low- and high-angle faults that typically place younger strata on older and expose rocks as old as upper Precambrian. The age and tectonic significance of these younger-on-older faults are the subjects of ongoing debate and the principal focus of this paper.

Misch (1960) and his students (Fritz, 1960; Avent, 1961; Woodward, 1962; Nelson, 1966; Cebull, 1967; Dechert, 1967) did much of the early mapping in east-central Nevada and interpreted the younger-on-older faults as decollements or "shearing-off" faults due to shortening during a mid-Mesozoic orogeny. In contrast, other early workers (Young, 1960; Playford, 1964; Kellogg, 1964; Moores and others, 1968) concluded that most of the faults were Tertiary normal faults and/or gravity slides. However, it was not until Armstrong (1972) reinterpreted some of the early mapping and highlighted the geochronologic and geometric evidence that a Tertiary age for the low-angle faulting of east-central Nevada received broader acceptance. Hose and Danes (1973), Hintze (1978), and Hose and Whitebread (1981) continued to argue for important Mesozoic, albeit extensional, deformation but most other references to this region (e.g., Coney, 1974; Proffett, 1977; Davis, 1979; Wernicke, 1981) have assumed a late Tertiary age and extensional origin for the younger-on-older faulting.

The Cordilleran Miogeocline

East-central Nevada was the site of relatively continuous shelf sedimentation from the late Precambrian through the early Triassic (Stewart and Poole, 1974). The miogeoclinal stratigraphy typically consists of an upper Precambrian and Lower Cambrian section of quartzite and shale, a Middle Cambrian to Lower Ordovician limestone section, a distinctive Middle Ordovician quartzite, an Upper Ordovician to Middle Devonian dolomite section, and an Upper Devonian to Lower Triassic section characterized by variable proportions of carbonate, shale, and sandstone (see compilation by Hose and Blake, 1976) (Figure 3).

Mesozoic Shortening and Plutonism

Mesozoic thrust faults are well documented to the east in the Sevier orogenic belt (Armstrong, 1968) and to the west in western Nevada (Speed, 1978). If thrust faults affected the intervening region, they were confined to deep structural levels and did not breach the surface (see Armstrong, 1972, and discussion below). At supracrustal levels, minor Mesozoic shortening is indicated by gentle folds such as in the Confusion and Butte synclinoriums of Hose (1977) (Figure 2). In contrast, at deep structural levels, upper Precambrian and locally Lower Cambrian strata were penetratively deformed during regional dynamothermal, greenschist to amphibole grade metamorphism (Misch, 1960; Misch and Hazzard, 1962). Structurally deepest rocks are polyphase deformed and commonly exhibit west-dipping, axial planar cleavages and N-S trending, bedding-cleavage intersections (refer to Road Log Stop no. 7). Metamorphism and deformation die out quickly up section.

Mesozoic plutons have been identified in east-central Nevada, but the magnitude and character of Mesozoic magmatism in this region is still poorly understood. In the southern Snake Range, several plutons that range in composition from two-mica granite to biotite granodiorite appear to be mid-Jurasic in age (Lee and others, 1968, 1980). Here metamorphism and deformation of the country rocks are synkinematic with pluton emplacement. In the southern Snake Range and in the Kern Mountains, strongly peraluminous two-mica granites are, most likely, latest Cretaceous in age (Best and other, 1974; Lee and others, 1980, in press). Other granitoid plutons in the northern Egan and Snake Ranges have yielded a scatter of Tertiary K-Ar dates (Lee and others, 1970, 1980), but their true ages are not certain.

Most of the better dated Mesozoic plutons intrude Middle Cambrian or older rocks and have tops that are roughly concordant to overlying strata. If any of these magmas vented, the correlative volcanic rocks must have been eroded prior to the deposition of Tertiary strata.

Early Oligocene Paleogeography Revisited

The Early Tertiary unconformity - The best indicator of pre-Tertiary supracrustal deformation is the character of the Tertiary unconformity. Young (1960), Kellogg (1964), and Moores and others (1968) were all impressed by the near conformity of the oldest Tertiary strata on exclusively upper Paleozoic rocks and suggested that pre-Tertiary structure must have been limited to gentle folds and small displacement faults. These views were cham-

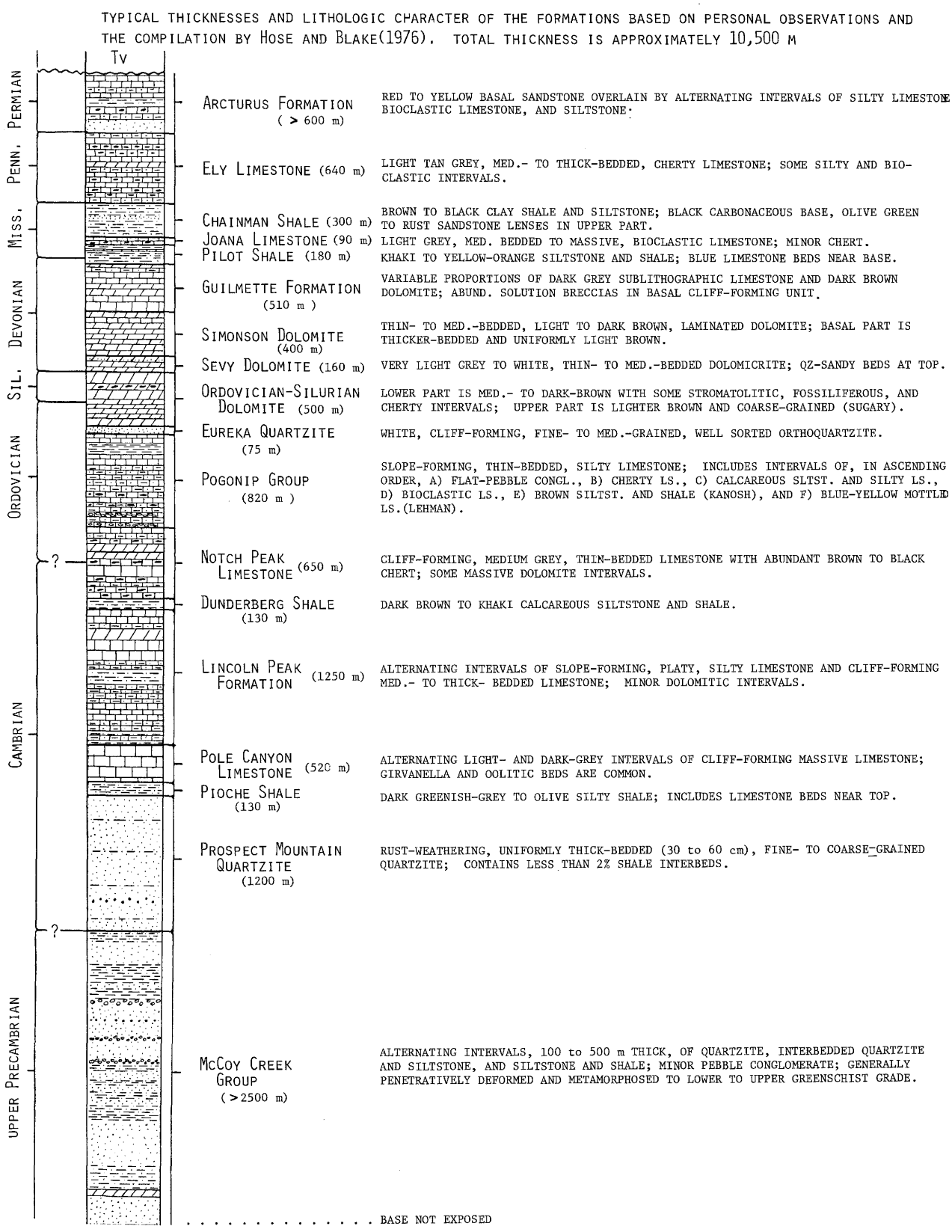

Figure 3. Representative miogeoclinal stratigraphic section for east-central Nevada.

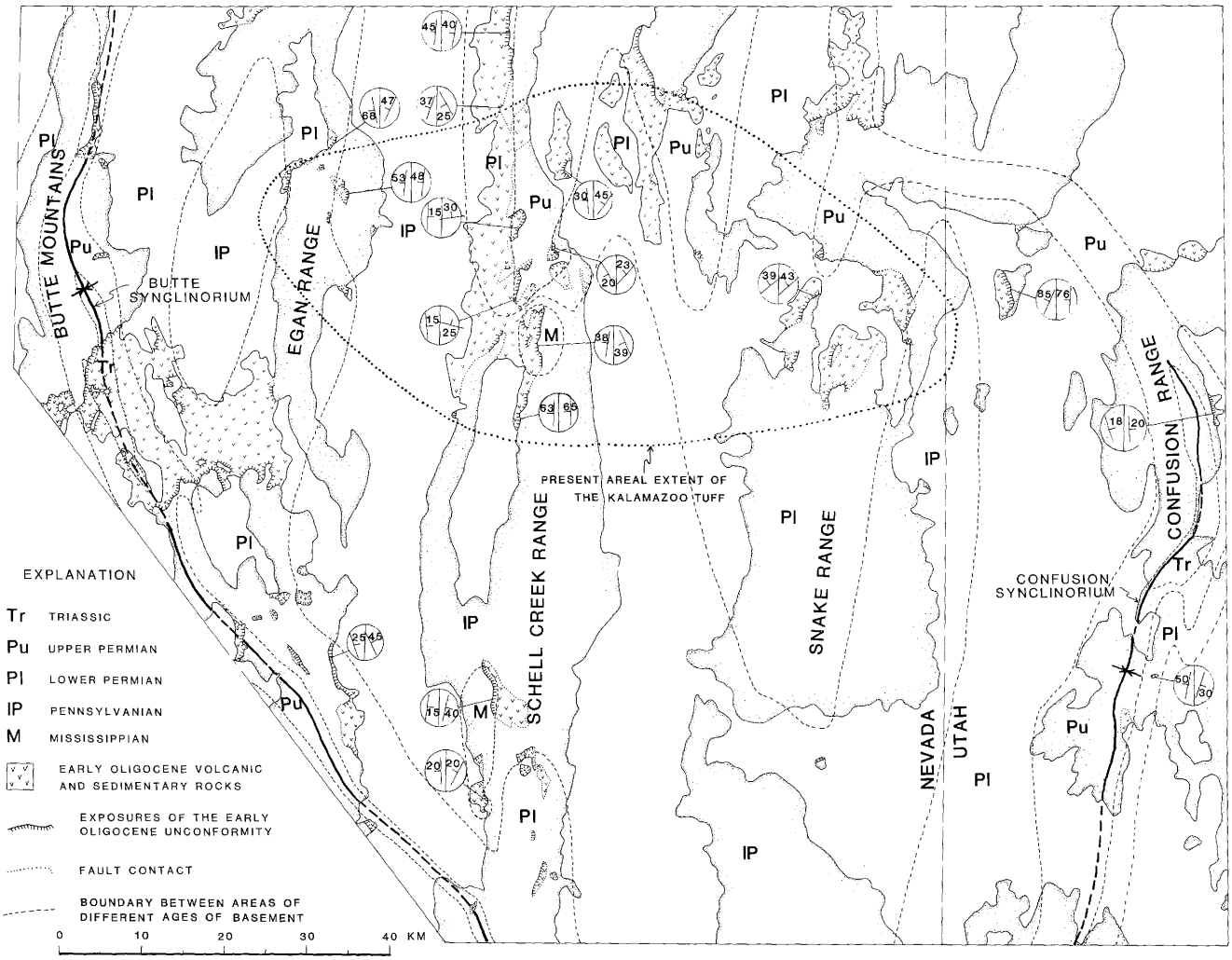

Figure 4. The early Oligocene unconformity. All known or inferred exposures of the early Tertiary unconformity in east-central Nevada are compiled. Dashed lines separate areas underlain by different ages of Paleozoic basement. Balloons enclose representative attitudes of the basal Tertiary units and of the directly underlying Paleozoic strata. Sources of data: Brokaw 1967; Brokaw and others, 1965, 1966, 1968, 1973; Dechert, 1967; Drewes, 1967; Fritz, 1968; Hintze, 1980; Hose, 1977; Hose and Blake, 1976; Kellogg, 1964; Moores and others, 1968; Nelson, 1966; Playford, 1961; Sides, 1966; Young, 1960.

pioned by Armstrong (1972) in his classic pre-mid-Tertiary reconstruction of eastern Nevada, although he left open the possibility of some Mesozoic faulting in this area.

We have re-examined many of the exposures of the Tertiary unconformity in east-central Nevada and western most Utah and compiled the pertinent structural and stratigraphic data (Figure 4). Only unconformities at the base of the earliest Oligocene volcanic rocks and pre-volcanic sedimentary sequences are included in our compilation. It is very clear from this data that early Oligocene rocks were deposited *exclusively* on Mississippian or younger strata. Exceptions described by Nelson (1959) and Dechert (1967) are actually fault contacts. In addition, the basal Tertiary deposits are remarkably conformable to the underlying upper Paleozoic strata. Local angular discordances are generally less than 15° and are not systematic.

Early Oligocene volcanic rocks were deposited on strata as old as Mississippian in only two small areas (Figure 4). However, even these occurrences may be a consequence of early Oligocene uplift rather than Mesozoic deformation. The basal Tertiary deposits in both of these areas consist of unusually thick, intracaldera(?), accumulations of ash-flow tuff. Regional tumescence (Smith and Bailey, 1966) may have preceded the eruption of tuff and caused preferential erosion of these near-vent areas.

Thin intervals of pre-volcanic conglomerate com-

monly define the base of the Tertiary sections. Unlike most later conglomerates in the exposed Tertiary sections, they contain only clasts of upper Paleozoic formations (Kellogg, 1960; Dechert, 1967; Grier, this volume). This strongly supports the inference that at the time of the early Tertiary unconformity, only upper Paleozoic rocks were exposed at the surface.

The early Tertiary erosion surface is underlain by roughly equal areas of Pennsylvanian and Lower Permian rocks and lesser Upper Permian and Triassic strata (Figure 4). Areas underlain by a single age strata are typically elongate in a N-S direction and give way laterally to areas underlain by successively older or younger basement. This topology is most compatible with very gentle N-S trending folds that had been beveled by erosion such that Pennsylvanian rocks were exposed in the cores of anticlines and Upper Permian or Triassic rocks were preserved in the cores of synclines. Two of these Mesozoic(?) folds are well exposed in the Butte and Confusion synclinoriums of Hose (1977) (Figure 4). The fold structure of the intervening area is largely obliterated by Tertiary faulting and tilting but is apparent in the palinspastic reconstruction we present in a later section.

Discussion - The amount of Mesozoic supracrustal deformation in east-central Nevada is severely constrained by the early Oligocene unconformity. Miogeoclinal strata had been gently folded, but only the uppermost units were exposed at the surface, and the total "stratigraphic relief" beneath the Tertiary unconformity was less than 2 km. Clearly, *no* significant Mesozoic faults breached the surface in this area. In contrast, the present ranges are underlain by complexly faulted and tilted rocks that encompass every geologic system from upper Precambrian to Quaternary.

Several authors (e.g., Dechert, 1967; Armstrong, 1968, 1972; Almendinger and Jordan, 1982) have suggested that large Mesozoic displacements may have occurred on low-angle or bedding-parallel "blind" faults without severely disrupting the surface. However, we find perfectly conformable sections that span the entire late Precambrian to late Paleozoic interval and effectively rule out regional Mesozoic decollements at any of the present levels of exposure. On geometric and geochronologic grounds, essentially *all* of the presently exposed faults in east-central Nevada are the product of post-early Oligocene extensional tectonics.

A direct consequence of this paleogeographic data is that "stratigraphic depth" within the miogeocline is an accurate estimate of Mesozoic to early Tertiary "structural depth." Several paleodepths derived in this fashion are particularly noteworthy:

1. In the northern Egan Range, Gans (in preparation, see Road Log Stop no. 1) describes early Oligocene rhyolitic dikes that can be traced from subvolcanic vents to depths of emplacement of approximately 10 km. However, even at their deepest levels the dikes are remarkably porphyritic and appear to have had glassy margins. Vigorous meteoric water circulation together with pressure quenching along deeply penetrating fractures apparently quenched the magmas such that "hypabyssal" textures were produced at mid-crustal levels.

2. The Cretaceous Tungstonia muscovite granite in the Kern Mountains (Best and others, 1974; Lee and others, 1980; in press) intrudes and metamorphoses Lower Ordovician to Upper Devonian strata (Nelson, 1959; Ahlborn, 1977) corresponding to depths of emplacent ranging from 4.5 to 2.0 km. Similarly, in the northern Snake Range, Miller and others (1983) describe swarms of muscovite pegmatite dikes that pervade Lower Cambrian rocks (paleodepth of 6 km). These depths are significantly less than the experimentally derived minimum depth for muscovite stability in granitic melts (e.g., Luth, 1976).

3. Miller and others (1983) describe uppermost Precambrian pelitic rocks in the northern Snake Range that were metamorphosed to kyanite-muscovite-biotite schists at a paleodepth of approximately 8 km. Lower Cambrian Pioche Shale was locally converted to staurolite-garnet-biotite-muscovite schist at a paleodepth of 6 km. Again, our reconstructed depths are much shallower than the experimentally derived minimum depths for these assemblages (e.g., Holdaway, 1971).

It is tempting to invoke a thick Mesozoic and/or early Tertiary sedimentary cover to explain the apparent shallow depths of these high pressure assemblages. However, it seems unlikely that the additional required thicknesses of strata could have been so neatly and uniformly removed from this entire area prior to the early Oligocene. For now, we prefer to stand by these geologically well-constrained depths, even if they go against accepted experimental wisdom.

Oligocene Magmatism

Intermediate to silicic volcanic rocks blanketed much of east-central Nevada between 38 and 30 m.y. ago (Hose and Blake, 1976). This is the *only* significant volcanism to have ever affected this area

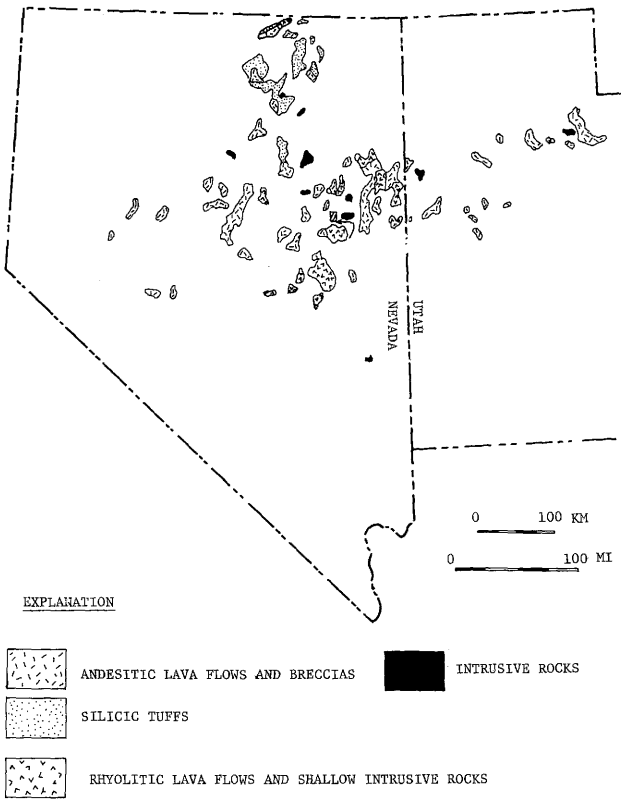

Figure 5. Map of Nevada and Utah showing generalized distribution of 43 to 34 m.y. old igneous rocks.

and it occurred within a broad, east-west trending belt that extends from central Nevada to central Utah (Figure 5). In the vicinity of the northern Egan, Schell Creek, and Snake Ranges, Oligocene volcanic rocks are predominantly lavas and locally derived tuffs that range in composition from potassium-rich andesite to high-silica rhyolite (Young, 1960; Dechert, 1967; Blake and others, 1968, 1969; Gans, 1982). A detailed field and petrologic investigation of these rocks is in progress by Gans and G.A. Mahood and some preliminary observations are provided in the Road Log Stops 1 and 5.

Intrusive and extrusive relations described below indicate that the onset of volcanism precisely coincided with the onset of extensional faulting in east-central Nevada and that much of the extension was synchronous with this brief pulse of volcanism. Because of their age and tectonic setting, these volcanic rocks are difficult to classify by traditional schemes. They form a high-potassium calc-alkalic "suite" (Blake and Hose, 1968) that was erupted during a time of continued subduction along the western margin of North America (Coney, 1978; Engebretson, 1982) and are generally included in compilations of "subduction-related" magmatism in the western United States (Snyder and others, 1976; Coney and Reynolds, 1977; Keith, 1978; Eaton, 1982). However, if east-central Nevada was part of the Oligocene continental arc, this arc was at right angles to the continental margin in Nevada and Utah. Conversely, although the volcanic rocks were erupted in a rapidly extending terrane, they resemble neither the "bimodal" basalt-rhyolite suite thought to be characteristic of Basin and Range extension (Christiansen and Lipman, 1972), nor the alkalic, silica-undersaturated rocks associated with extension in the African rift system (e.g., MacDonald, 1974).

STRUCTURAL EVOLUTION OF THE NORTHERN EGAN RANGE

Introduction

Most of the northern Egan Range was first mapped by Fritz (1960, 1968) and Woodward (1962). They divided the range into a mosaic of seven east-directed thrust sheets that they interpreted to have moved eastward during the Mesozoic. Armstrong (1972) and Wernicke (1981) reinterpreted parts of Fritz's (1968) map and suggested that at least some of the low-angle faults were Tertiary normal faults. The structural evolution of part of the northern Egan Range (Figure 6) was recently investigated by Gans (1982a, b, submitted) and these findings are synthesized below.

Geometric Relations

Low-angle faults and westward tilts - The architecture of the Egan Range is most apparent in cross section (Figure 7). Thin slices of steeply west-dipping upper Precambrian to Permian miogeoclinal rocks and Oligocene volcanic rocks are separated by low-angle normal faults that displace overlying sections eastward with respect to underlying rocks. Steeply west-dipping, older-on-younger thrust faults that were mapped by Fritz (1960), were remapped and are clearly east-dipping normal faults. Gently east-dipping faults typically merge downward with major, subhorizontal faults that span the entire width of the range. Individual faults can occasionally be traced eastward up to 10 km. The spacing of faults ranges from tens of meters to 0.5 km. Down-to-the-east displacements range from a few hundred meters to greater than 6 km. The larger displacements occur where several imbricate faults merge.

Bedding attitudes are remarkably consistent. Both miogeoclinal and Tertiary strata typically

strike NS to N 30 E and dip 35 to 75° NW (Figure 8). The average tilt is approximately 50° NW about a N 15 E axis. Attitudes do not vary systematically between different fault slices. Most of the variation occurs in less competent units near bends in faults, or because of differential movement within individual fault slices. Bedding-to-fault angles are 50 to 60° on the major, through-going faults and range from 60 to 90° on the steeper splays. Neither normal nor reverse drag along faults is common.

Many of the Egan Range faults are gently curved in a concave upward fashion. They dip 5 to 15° eastward on the west flank of the range and re-emerge on the east flank where they dip 5 to 20° westward (Figure 7). However, westward stratal rotations are also progressively steeper toward the east, such that bedding-to-fault angles do not decrease appreciably. The maximum original curvature or "listricity" that can be assigned to the normal faults in the Egan Range on the basis of decreasing bedding-to-fault angles with increasing stratigraphic depth is approximately 1°/km. (compare with Proffett, 1977). Differential uplift or doming, perhaps in some way related to the large intrusive mass on the east flank of the range, is responsible for most of the present curvature.

Three-dimensional geometry of fault surfaces - The rugged relief and near-horizontal faults of the northern Egan Range provide an ideal setting to study the three-dimensional geometry of normal fault surfaces. Here, NNE trending normal faults generally do not continue more than a few kilometers before they either: 1) bend abruptly into ESE-trending, "ramp-like" sides, 2) are cut by the side of an en-echelon fault, or 3) break into several strands whose combined offset equals that of the original fault (see Figures 6 and 7 for examples). The ESE trending "sides" dip 10 to 40° inward toward a subhorizontal "floor" that constitutes the main fault surface (compare cross sections B-B′ and Y-Y′, Figure 7). This geometry approximates that of a steep-sided shovel or platter and is similar to the "spoon-shapes" described by Proffett (1977). Both the corners and the edges on the fault surfaces are surprisingly sharp bends rather than smooth, curviplanar transitions. The width of the shovel-shaped scoops ranges from 0.5 to 5 km, and is generally less than the height (measured down the movement plane). The highly complicated map pattern of the northern Egan Range (Figure 6) is as much a consequence of the original discontinuous nature of the normal faults as it is of differential erosion.

Kinematic Interpretation

The relation of faulting to stratal rotation - Simple geometric considerations suggest that, as the faults moved, both bedding and faults must have rotated westward in a "domino" or "deck of cards" fashion (cf. Thompson, 1960; Morton and Black, 1975). Wernicke's (1981) reconstruction assumed that strata had first been tilted westward and later shuffled out to the east on the present, low-angle-faults. This interpretation requires that an unreasonably high, west-dipping homocline originally lay off to the west. In contrast, Armstrong (1972) implied that the combined, down-to-the-east displacements occurred while bedding was still horizontal and faults were steeply dipping. Untilting the Egan Range cross sections results in an equally unreasonable, 6 to 10 km high, east-facing scarp whose average dip is 50 to 60°.

Thus, the low-angle faults in the Egan Range must have originated as imbricate and en-echelon, high-angle (50 to 60°), shovel-shaped, normal faults that must have rotated to low angles as they moved. The faults penetrated to paleodepths of 10 km without flattening appreciably. However, at some greater depth, they must have flattened abruptly (?) into a ductile-brittle transition or detachment fault in order to produce the attendant rotation. The paleogeography at the time of normal faulting was probably characterized by narrow, arcuate ridges of bedrock separated by very small, discontinuous basins filled with synorogenic debris.

Fanning-Upward Splays - Short splays that merge downward with relatively planar, through-going normal faults are a common geometric element in the northern Egan Range (Figure 7). These splays typically fan upward such that bedding-to-fault angles increase systematically on structurally higher and steeper splays. By geometric necessity, movement on the splays must have been accompanied by movement on the main through-going faults.

A simple kinematic interpretation of these relations is: as blocks bounded by planar faults rotate to low angles, the faults attempt to steepen themselves by cutting successively deeper into the hanging-wall (Figure 9). Fanning-upward splays that bound upward-thickening wedges effectively chart the history of progressive rotation on a planar fault. Similar splays may also develop at depth, in order to alleviate space problems at the toes of tilted blocks (Figure 9). An implication of this model is that with continued rotation, the surface of movement

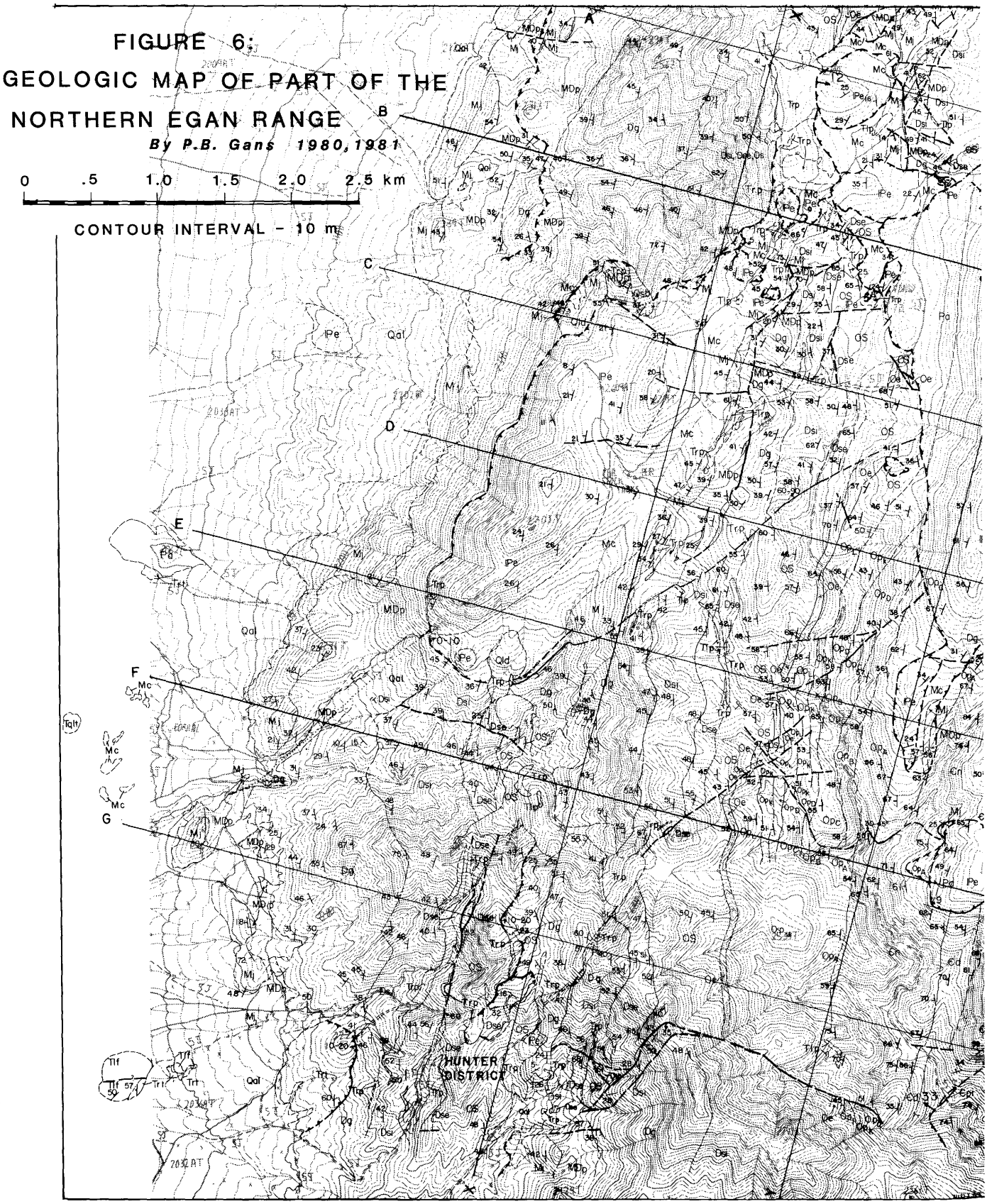

Figure 6. Geologic map of part of the northern Egan Range (for Explanation, see p. 118).

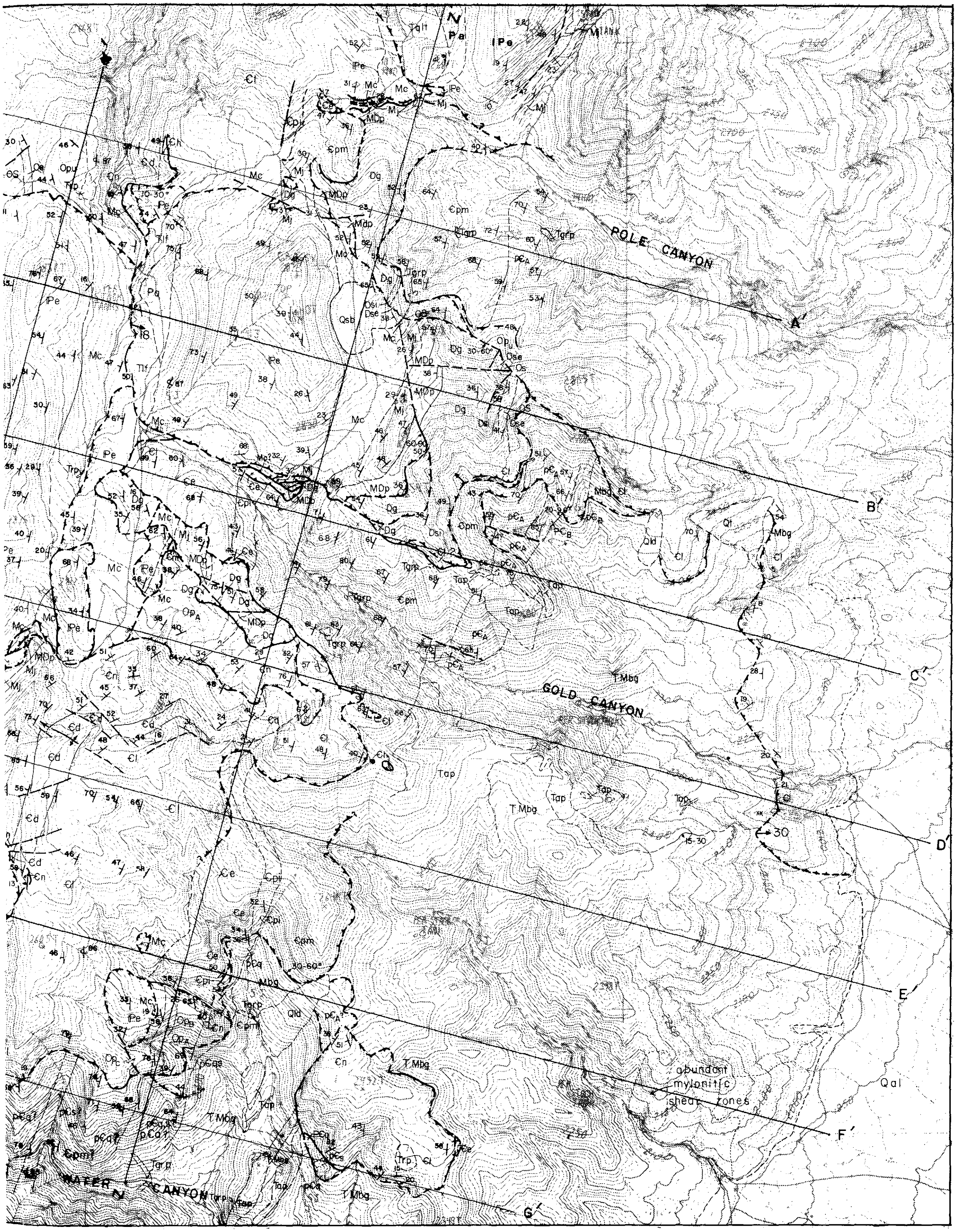
POLE CANYON
A′
B′
C′
GOLD CANYON
D′
E′
abundant
mylonitic
shear zones
Qal
F′
WATER CANYON
G′

EXPLANATION FOR FIGURE 6

Upper Precambrian and Paleozoic Clastic and Carbonate Rocks

Pennsylvanian–Permian

- Pa — ARCTURUS FORMATION — *sandstone, siltstone, and silty limestone*
- Pe — ELY LIMESTONE (650 m)

Mississippian

- Mc — CHAINMAN SHALE (310 m)
- Mj — JOANA LIMESTONE (60 m)
- MDp — PILOT SHALE (150 m)

Devonian

- Dg — GUILMETTE FORMATION (450 m) — *limestone and dolomite*
- Dsi — SIMONSON DOLOMITE (360 m)
- Dse — SEVY DOLOMITE (140 m)

Sil.

- OS — ORDOVICIAN–SILURIAN DOLOMITE (500 m)

Ordovician

- Oe — EUREKA QUARTZITE (50 m)
- Op_l — LEHMAN FORMATION (90 m) — *blue and yellow mottled silty limestone*
- Op_k — KANOSH SHALE (110 m)

Ordovician

- Op_d — POGONIP UNIT D (115 m) — *bioclastic limestone*
- Op_c — POGONIP UNIT C (100 m) — *red and yellow silty limestone*
- Op_u — POGONIP GROUP (undifferentiated)
- Op_b — POGONIP UNIT B (115 m) — *cherty, silty limestone*
- Op_a — POGONIP UNIT A (270 m) — *flat limestone pebble conglomerate*

Cambrian

- €n — NOTCH PEAK LIMESTONE (590 m) — *equiv. to Windfall Fm. + Ord. Fm. A of Fritz, 1960*
- €d — DUNDERBERG SHALE (150 m)
- €l — LINCOLN PEAK FORMATION (1250 m) — *limestone and shale: equiv. to Secret Canyon Sh. + Hamburg Ls. of Fritz(1960)*
- €e — ELDORADO LIMESTONE (660 m)
- €pi — PIOCHE SHALE (210 m)
- €pm — PROSPECT MOUNTAIN QUARTZITE (1175 m)

Upper Precambrian

- p€a — MCCOY CREEK UNIT A — *green to brown phyllitic siltstone*
- p€b — MCCOY CREEK UNIT B — *quartzite*

Tertiary Igneous Rocks

Tertiary

Volcanic Rocks

- Tlf — Latite to Trachyandesite Lava Flows — *phenocrysts of plag., rare hnbl. in a trachytic groundmass of plag. ± kspar ± opx ± cpx ± bio.*
- Tqlt — Quartz Latite Ash-Flow-Tuff — *plag., bio., hnbl, and qz crystals in a devitrified ash matrix*
- Trt — Rhyolite Ash-Flow-Tuff *(35.8 m.y. -K-Ar san, bio)* — *crystals of qz, san, plag, and bio*

Hypabyssal Rocks

- Tlp — Latite Porphyry — *phenocrysts of plag, bio, and hnbl in a fine grained, flow-banded groundmass*
- Trp — Rhyolite Porphyry — *4 generations of dikes: all contain qz, san, plag, and bio in an aphanitic groundmass:often argillically altered*

Plutonic Rocks

- Tgrp — Granite Porphyry — *contains kspar megacrysts, large qz eyes in a fine grained groundmass*
- Tap — Aplite Porphyry — *qz, feldspar, and bio phenocrysts in an aplitic to granophyric groundmass*
- TMbg — Biotite Granite — *equigranular, moderately deformed, may be Mesozoic*

Faults

- High angle normal fault showing dip (60)
- Low-angle normal fault showing strike and dip: teeth on hanging wall (17)
- Fault, located approximately (within 50 m)
- Buried fault

Contacts

- Lithologic (depositional or intrusive) contact showing dip (58)
- Contact located within 50 m
- Buried contact

Symbols

- 44 — Strike and dip of bedding
- 50 — Strike and dip of flow-banding or flattening fabric
- Age-date sample location
- Prospect pit
- Adit or drift
- Shaft
- Cabin

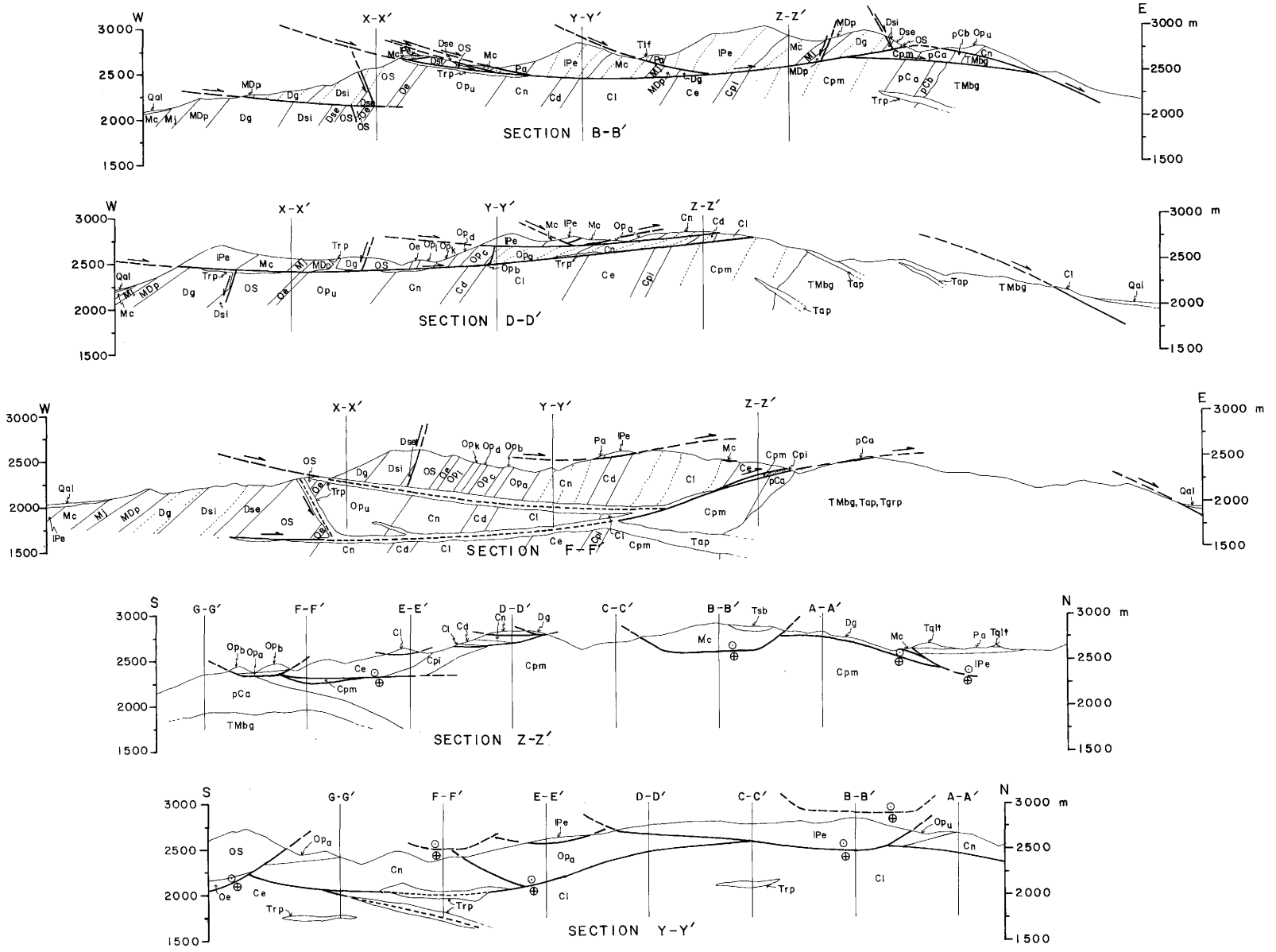

Figure 7. Geologic cross sections of the northern Egan Range (no vertical exageration) (see Figure 6 for explanation of symbols).

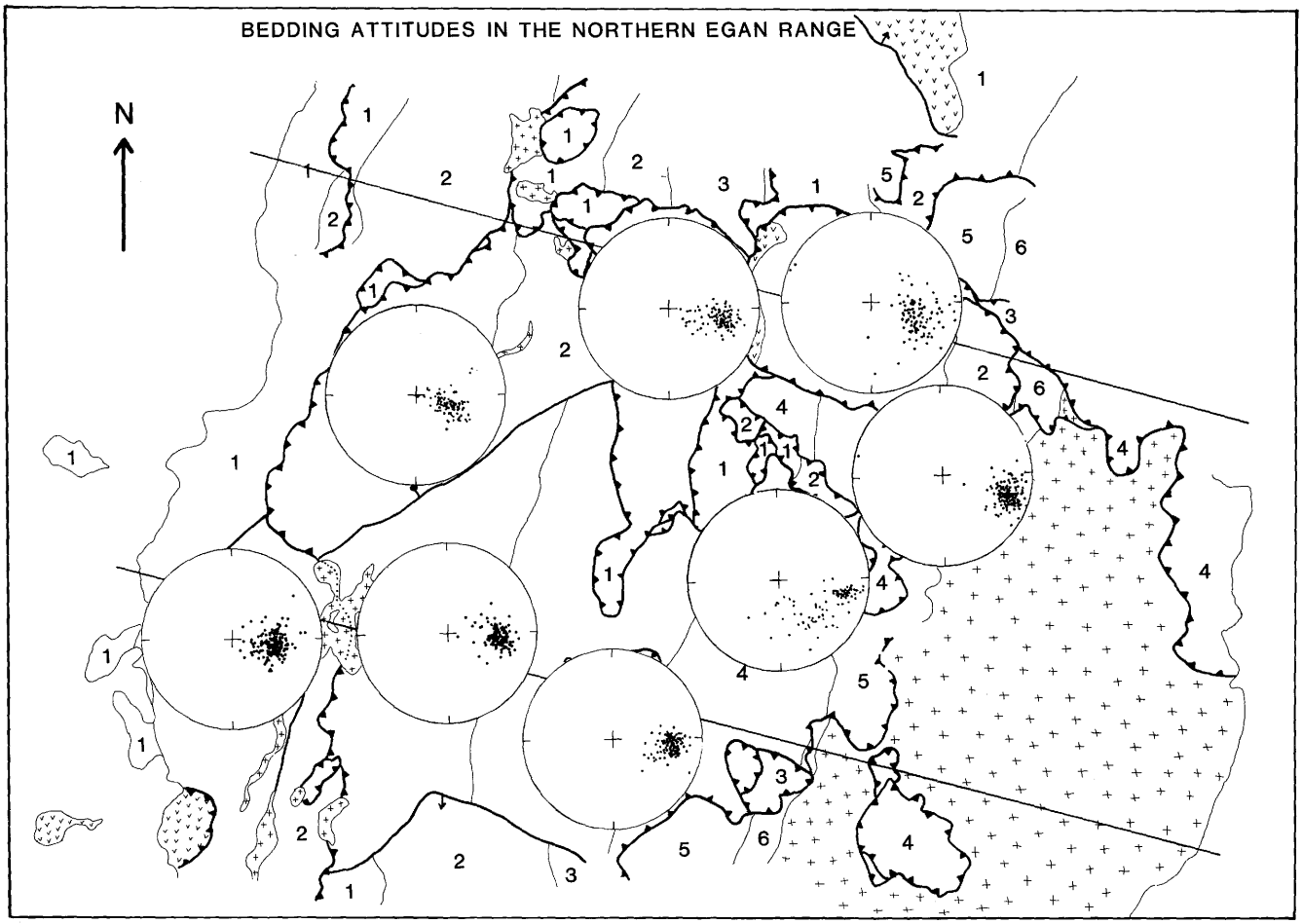

Figure 8. Representative bedding attitudes in the northern Egan Range. Stereonets are compiled from different fault slices and structural domains. Map area is the same as in Figure 6.

evolves from a planar, 60° fault to a curviplanar or listric fault.

A somewhat different interpretation for faults at very high angles to bedding was suggested by Colleta and Angelier (1982). They proposed that subvertical tension fractures develop within major blocks bounded by 60° normal faults. As the 60° (1st order) faults rotate, the tension fractures are eventually activated as (2nd order) normal faults and use the 1st order faults as detachment surfaces. However, their model does not explain 1) the progressively steeper bedding-to-fault angles observed on the fanning upward splays of the Egan Range, or 2) why both vertical and 60° fractures should develop concurrently and cospatially, as implied by their model.

The onset of extensional faulting - Our best evidence for when major extensional faulting began in east-central Nevada comes from the northern Egan Range. In the vicinity of the Hunter district (Figure 6), 35.8 m.y. old rhyolite dikes and small stocks intrude and are clearly guided by a low-angle fault whose down-to-the-east displacement is approximately 1 km (Gans, 1982) (see cross section F-F', Figure 7). However, shear zones are very common along the margins and within these dikes, and coeval volcanic rocks are displaced and tilted on geometrically identical faults (Figure 7). In keeping with the regional pattern, the oldest eruptive units rest disconformably on Upper Pennsylvanian or Lower Permian rocks - a paleosurface with less than 0.5 km of stratigraphic relief. These apparently contradictory relations suggest that extensional faulting in the northern Egan Range began 35.8 m.y. ago, precisely coincident with the onset of volcanism, and that faulting continued after volcanism had ceased.

Direction of extension - The movement direction on the low-angle faults, and hence, the direction of extension, was estimated by several methods: 1)

slickensides although very rare in the northern Egan Range, have azimuths that range from N 80 E to N 60 W; 2) if stratal rotation and faulting are antithetic, then the N 10 to 20 E average strike of beds (Figure 8) implies movement in a S 70 to 80 E direction; 3) the trends of the sides of shovel-shaped faults range from E-W to N 60 W and probably parallel the direction of movement. Taken together, these estimates suggest that the low-angle faults in the northern Egan Range are a product of extension oriented approximately N 75 W to S 75 E.

Palinspastic Reconstruction of the northern Egan Range and Vicinity.

The most accurate way to calculate the strain in a complexly faulted and tilted terrane is to systematically restore each fault and untilt the rocks to their previous attitude. We palinspastically restore a simplified cross section of the northern Egan Range and southernmost Cherry Creek Range by this method in Figure 10. The northern Egan Range is assumed to be in the hanging-wall of a gently dipping normal fault that separates it from the Cherry Creek Range. This fault or systems of faults is largely covered by alluvium but apparently cuts across the Egan Range north of the cross section line. Projecting the footwall units onto the line of cross section suggests that the total down-to-the-east offset on this fault(s) is approximately 8 km.

Our reconstruction is largely model independent. All of the normal faults probably developed concurrently and their attitudes are well constrained at a broad spectrum of paleodepths. Fault slices are simply slid back so that stratigraphic units match across the projected faults. The entire section is then rotated back to paleohorizontal. The behavior of the low-angle faults below the present levels of exposure is speculative, but it does not affect a palinspastic reconstruction of the upper 10 km of the crust. The 11.5 km increase in horizontal separation between two points on the Mississippian/Devonian boundary corresponds to exactly 200 percent extension. Wernicke (1981) attempted a similar reconstruction based on one of Fritz's (1968) cross sections, but failed to remove tilting or compensate for erosion. His estimate of 16.5 km or 300 percent extension is, in effect, a sum of the down-to-the-east displacements on rotated normal faults rather than a measure of the horizontal dilation between two points of known original separation.

Any model for the Tertiary evolution of east-central Nevada must account for abrupt boundaries

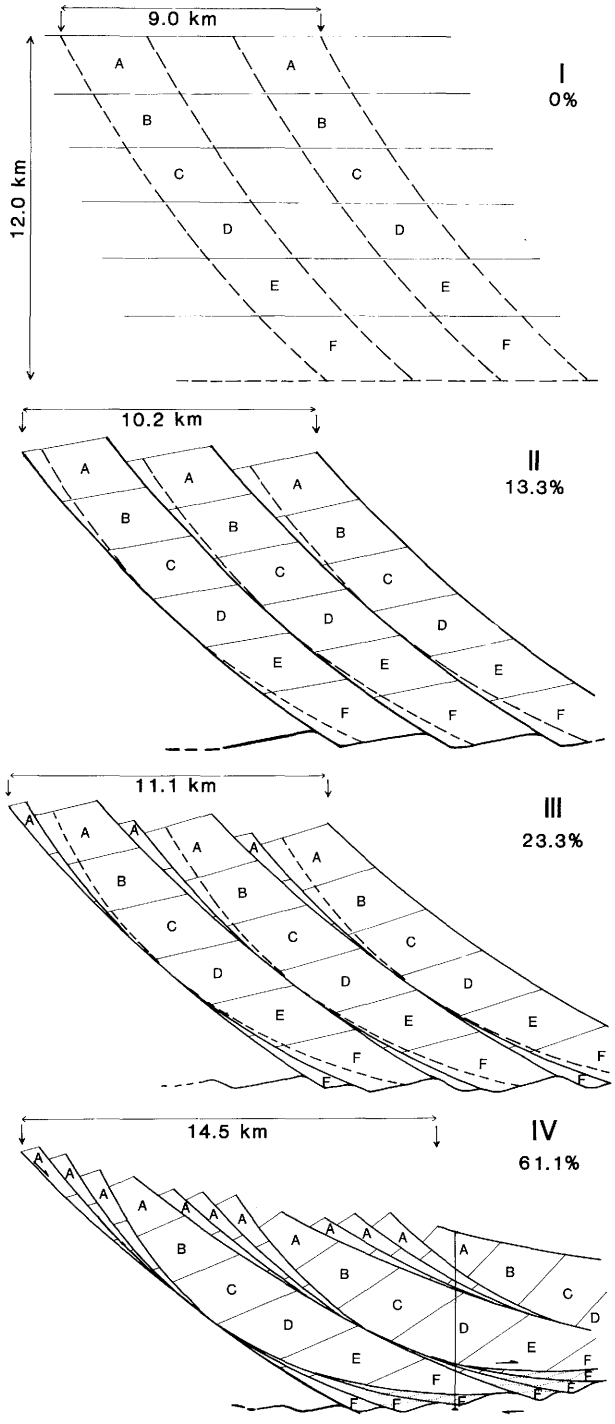

Figure 9. Kinematic model for fanning upward splays.

between areas that exhibit radically different structural styles and levels of exposure. For example, the Butte Mountains are immediately west of the Egan and Cherry Creek Ranges are underlain by essentially unfaulted, flat-lying upper Paleozoic rocks. In Figure 11 we present a series of balanced cross-

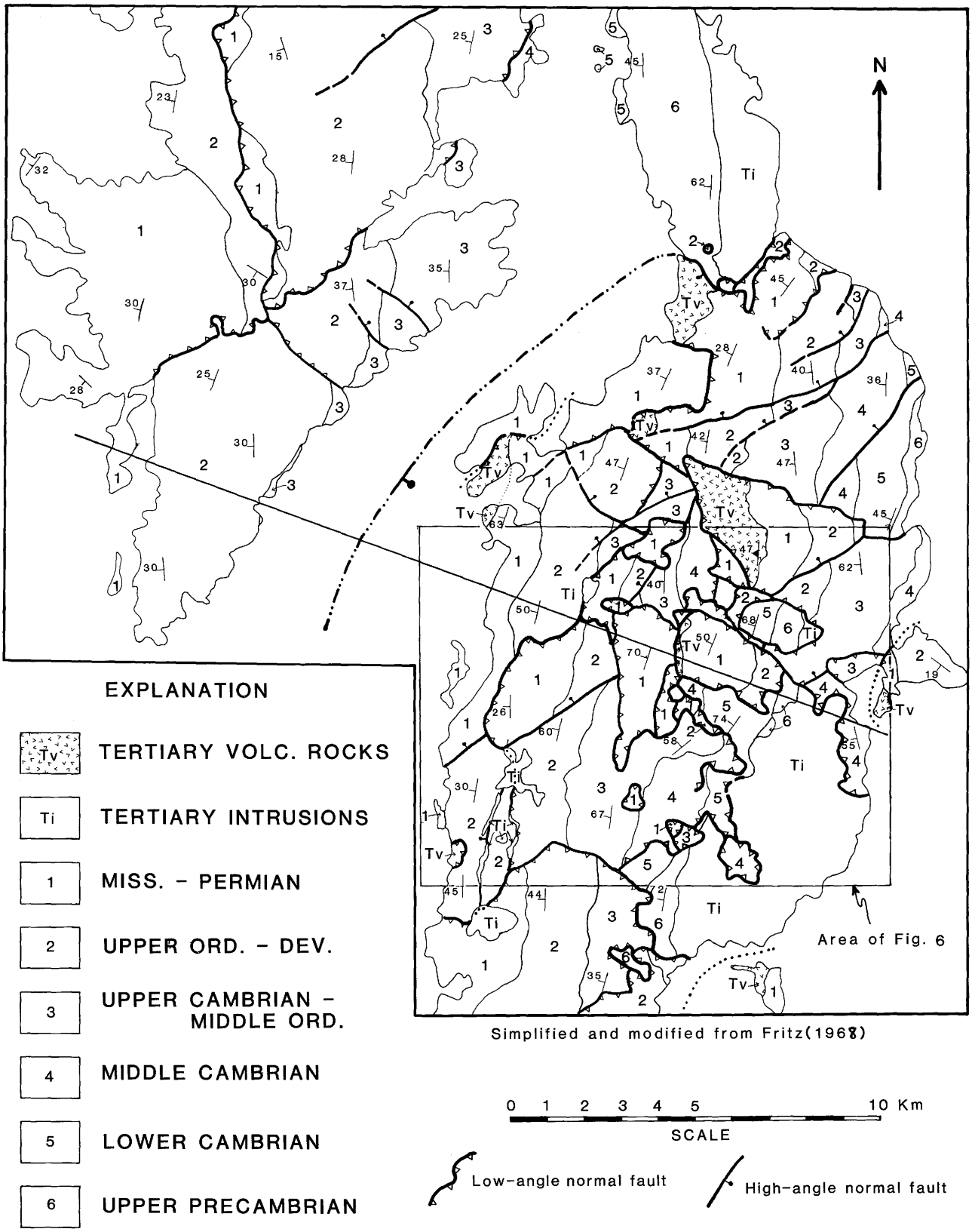

Figure 10a. Geologic map of the S. Cherry Creek Range and the N. Egan Range.

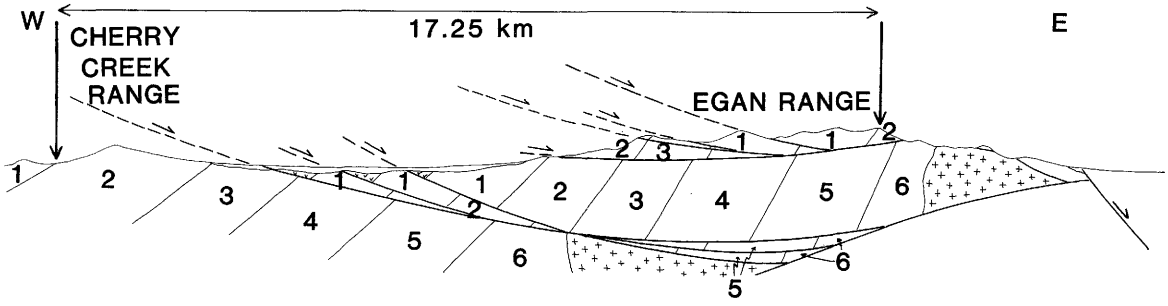

FIGURE 10(B). PALINSPASTIC RECONSTRUCTION OF THE S. CHERRY CREEK RANGE AND THE N. EGAN RANGE

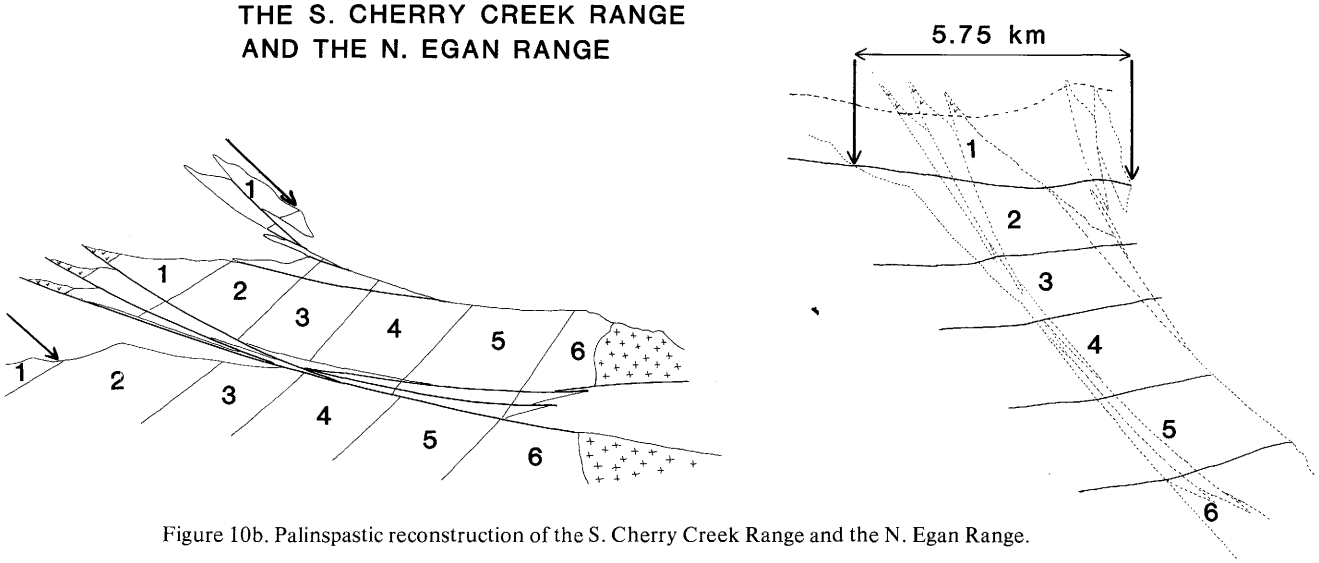

Figure 10b. Palinspastic reconstruction of the S. Cherry Creek Range and the N. Egan Range.

sections from the Butte Mountains to the northern Egan Range that chart the structural evolution of these ranges. Many of the relations shown at depth are entirely speculative, but are in accord with what is exposed in these and adjacent ranges. Several aspects of the structural evolution should be highlighted:

1. Upper Precambrian rocks that were at 8 to 10 km depth prior to the early Oligocene are presently exposed at the surface in the Egan Range, whereas they remain at mid-crustal levels beneath the Butte Mountains. This enormous differential uplift is a direct consequence of the much greater amount of extension toward the east.

2. Imbricate high-angle faults are shown to flatten abruptly into a subhorizontal, ductile-brittle detachment fault, beneath which extension is accomodated by penetrative stretching and pluton emplacement. This inference relies heavily on relations in the Snake Range that we describe below.

3. Differential uplift of the northern Egan Range with respect to the Butte Mountains has greatly accentuated westward tilts. Domino-style faults in the Egan Range probably rotated an additional 10 to 20° to their present position and the inferred basal detachment now dips gently west. Similarly, the east limb of the Butte synclinorium has been warped upward into a much steeper westward dip than is suggested by the early Tertiary paleogeography.

The duration of major extensional faulting in the Egan Range is not known. Regional considerations suggest that it is largely Oligocene. In any case, Basin and Range faults are clearly superimposed on the older low-angle faults.

SYNTECTONIC VOLCANISM AND SEDIMENTATION IN EAST-CENTRAL NEVADA

Introduction

The northern Schell Creek Range offers the best opportunity for constraining the timing of extension in east-central Nevada. Thick sections of mid-Tertiary volcanic and sedimentary rocks are well exposed and apparently span the duration of much of the extensional faulting. Work in this area by Gans

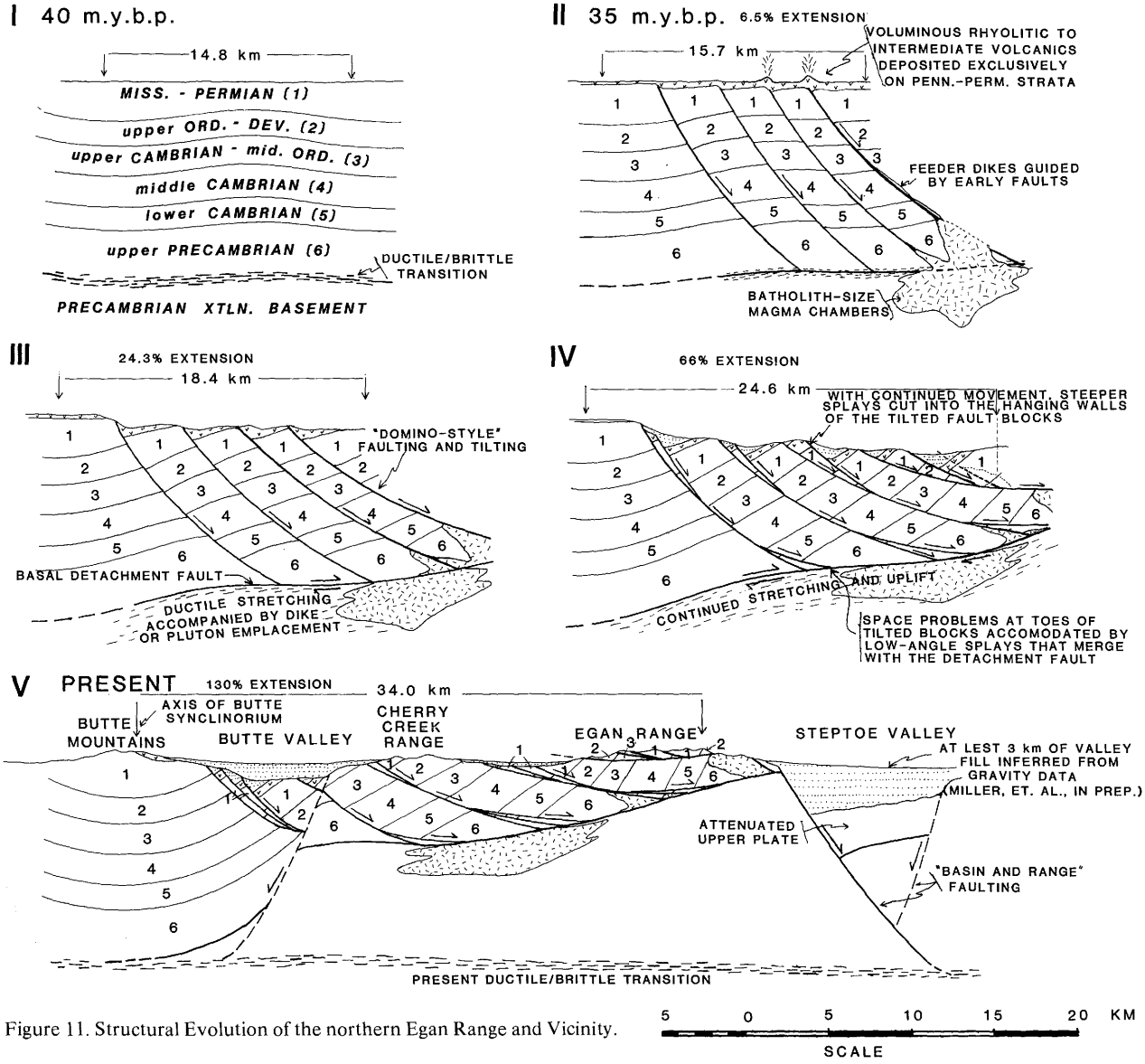

Figure 11. Structural Evolution of the northern Egan Range and Vicinity.

and G. Mahood has just begun so that here we discuss only a few initial observations within the context of previous work in this region.

Structural Summary

Young (1960) and Dechert (1967) mapped most of the northern Schell Creek Range, and described a complicated history of faulting for the area. The oldest faults in the range are low angle or gently west-dipping and consistently place younger strata on older. In places these faults appear to be bedding parallel whereas elsewhere they cut bedding at high angles. A younger system of predominantly east-dipping normal faults cut the older low angle faults. Both Paleozoic and Tertiary strata in the Schell Creek Range generally dip 30 to 70° westward although local domains of eastward tilts occur as well. The sequence and style of faulting in the Schell Creek Range is remarkably similar to faulting in the Snake Range which we describe in detail later in this paper.

Tertiary Stratigraphy

Tertiary rocks in the Schell Creek Range (Figure 12) consist from older to younger of: 1) thin, discontinuous intervals of pre-volcanic lacustrine limestone, sandstone, and conglomerate; 2) a thick section of intermediate to silicic lava flows and tuffs; and 3) post-volcanic conglomerates and monolithologic breccia blocks. The area immediate-

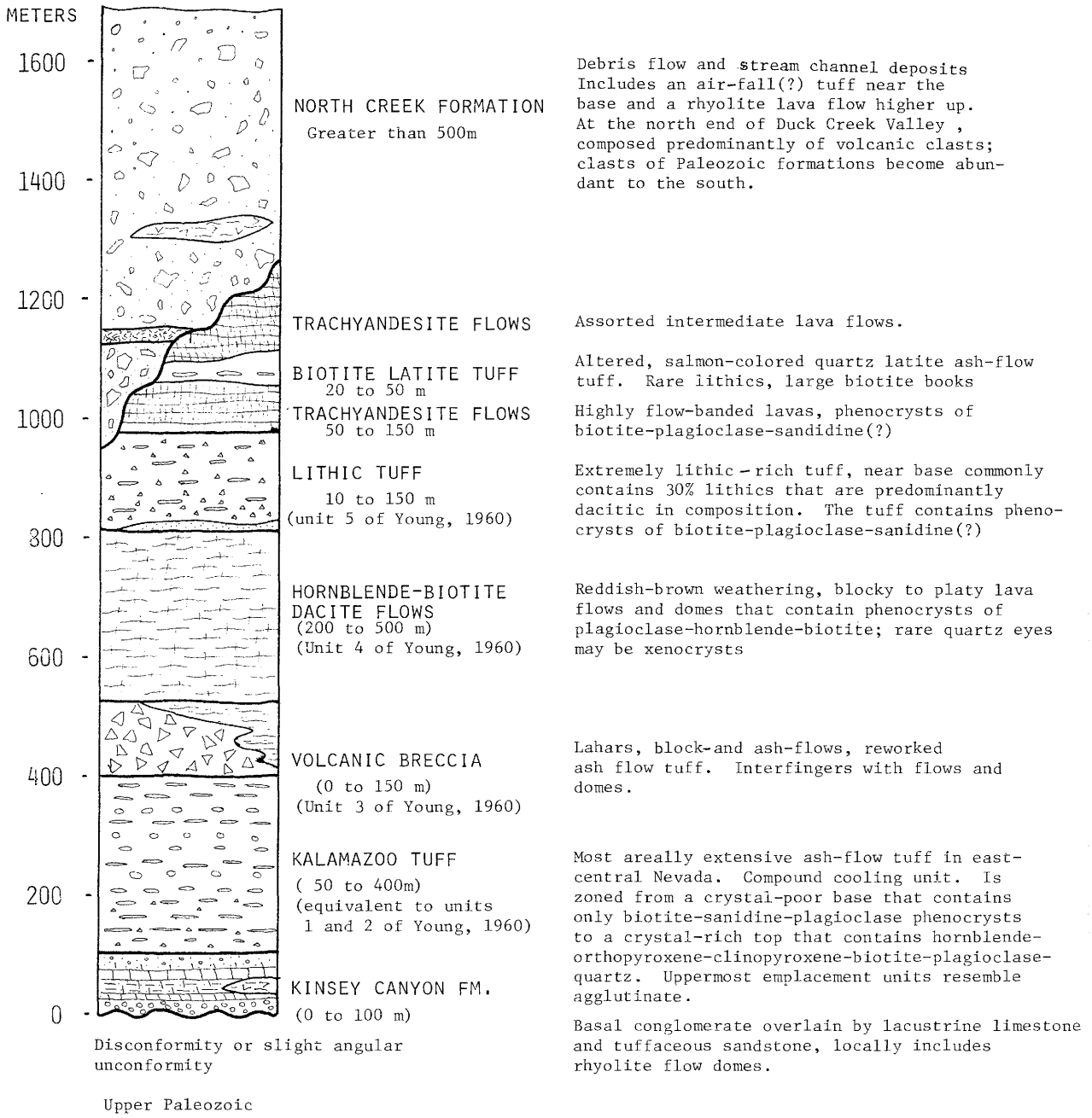

Figure 12. Tertiary stratigraphic section for the Schell Creek Range.

ly north of Duck Creek Valley is probably a major volcanic center from which most of the volcanic rocks were erupted. The total volume of erupted magmas is probably significantly greater than 100 cubic kilometers.

The volcanic units in the Schell Creek Range are 36 to 31 m.y. old (Blake, 1981 personal communication) and Anderson (in press) reports a 27.4 m.y. old airfall tuff from near the base of the younger conglomerates. We are presently dating more volcanic rocks in the range.

Timing of extensional faulting

As elsewhere in east-central Nevada, the Tertiary unconformity in the Schell Creek Range suggests little pre-Tertiary deformation. In contrast, angular unconformities within the volcanic sequence and particularly between the volcanic rocks and the

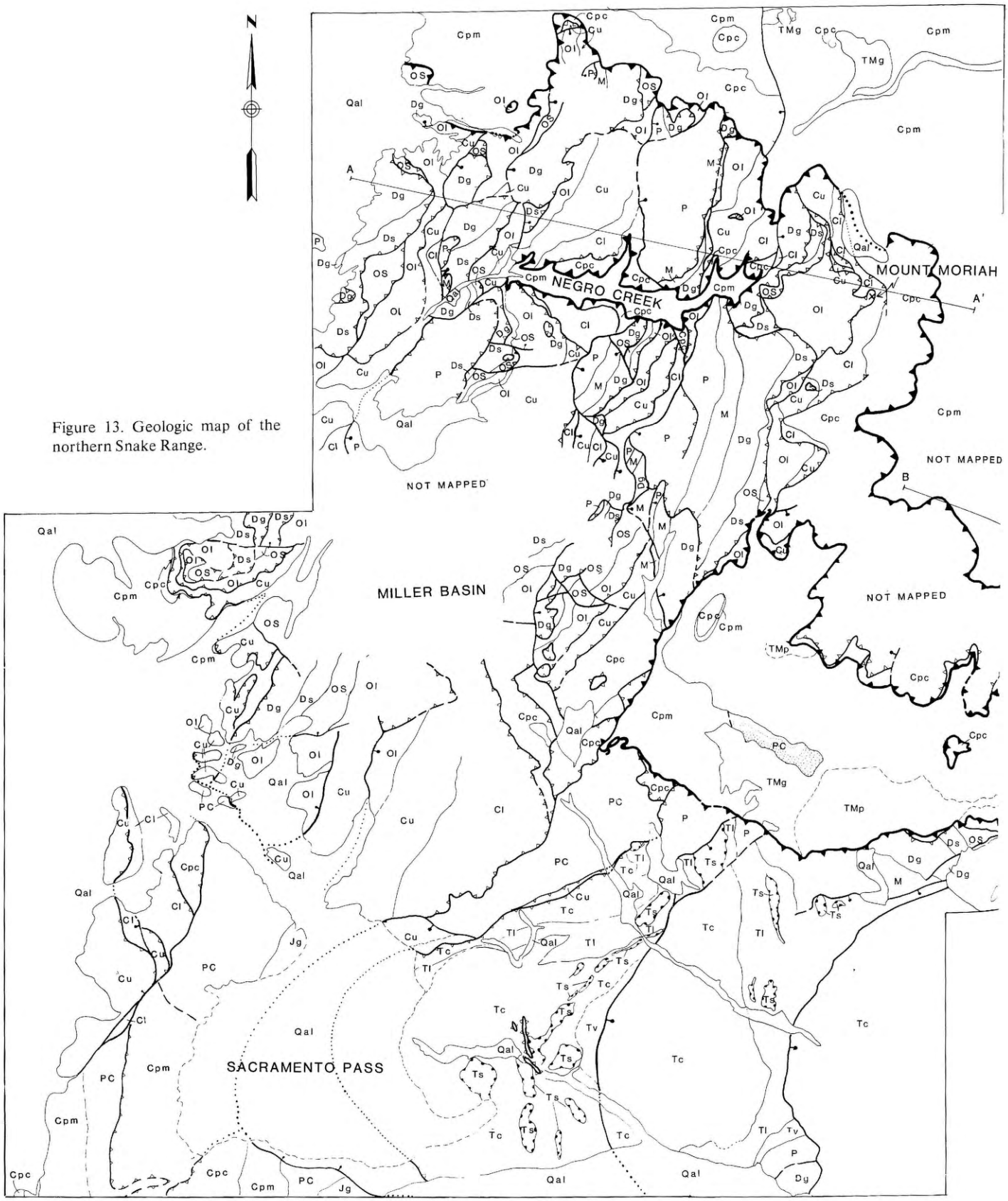

Figure 13. Geologic map of the northern Snake Range.

GEOLOGIC MAP OF PART OF THE NORTHERN SNAKE RANGE

STANFORD GEOLOGICAL SURVEY (1981, 82)

M.E. BAXTER, R. BEAMES, J. BLACK, J. BLANK, A. BOL, A. BRANHAM, C. CARLSON, A. CARVER, A. CHEN, L. CHIN, K. CHESICK, D. CLARK, M. DEBICHE, J. EABY, A.T. FAN, M. FITCH, P. GANS, J.D. GIBSON, W. GLOVER, T. GOODLIN, R. GREEN, S. GRIER, J. HARRIS, K. HESS, D. HRABIK, D. KIEHN, J. KOKINOS, J. LEE, C. MICHELL, C. MICHELSON, E.L. MILLER, M. MILLER, K. MORRIS, K. MORRISON, N. MORTIMER, M. NEUWELD, P. PEREZ, K. PHELPS, A. PRICE, R. REIMERS, D. RODGERS, L. ROWLES, M. SABISKY, S. SAXENIAN, P. SCHAEFER, E. SCHERMER, N. SCOTT, J. SEYMOUR, M. STALLARD, L. STERN, D. VOSHELL, H. WHELAN, W. WHITEFORD

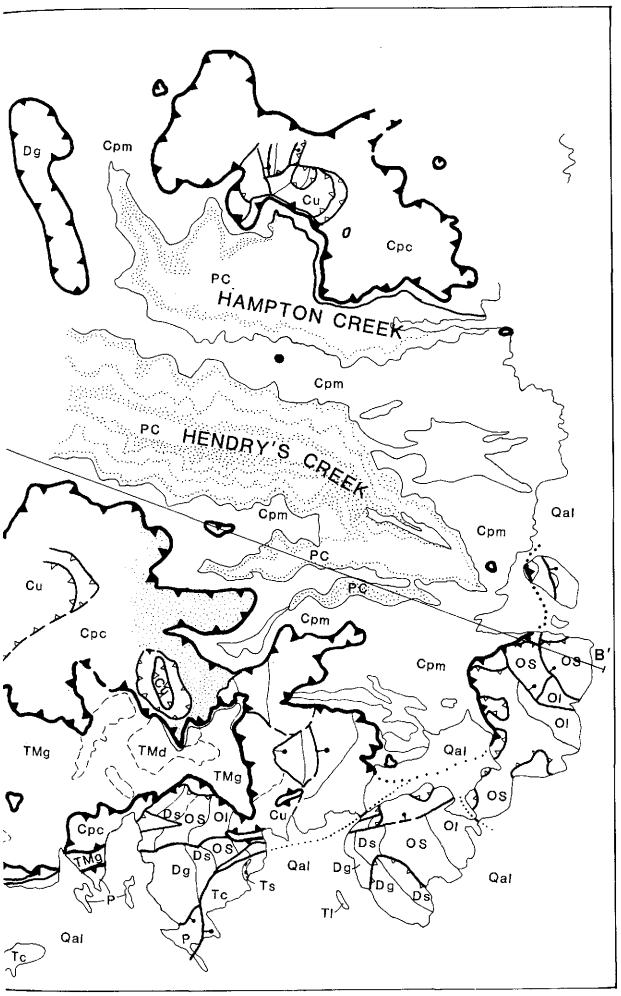

high angle or east-dipping normal fault bar and ball on downthrown side

low angle or gently west dipping faults

Northern Snake Range decollement

Tertiary slide blocks

1 .5 0 1 2 Kilometers

1 .5 0 1Mile

EXPLANATION

CENOZOIC

- Qal — QUARTERNARY ALLUVIUM
- Tc — TERTIARY CONGLOMERATE
- Tl — TERTIARY LACUSTRINE DEPOSITS
- Tv — TERTIARY VOLCANIC ROCKS (Includes rhyolite tuff and latite flows)
- Ts — TERTIARY SLIDE BLOCKS

UNCONFORMITY

MESOZOIC

- P — PENNSYLVANIAN and PERMIAN (Includes Ely Limestone and Arcturus Formation)
- M — MISSISSIPPIAN (Pilot Shale, Joana Limestone, and Chainman Shale)
- Dg — DEVONIAN GUILMETTE FORMATION
- Ds — DEVONIAN SEVY DOLOMITE and SIMONSON DOLOMITE
- Os — ORDOVICIAN-SILURIAN DOLOMITE
- Ol — LOWER ORDOVICIAN (Includes Pogonip Group and Eureka Quartzite)
- Cu — UPPER CAMBRIAN (Includes Dunderberg Shale and Notch Peak Formation)
- Cl — CAMBRIAN LINCOLN PEAK FORMATION
- Cpc — CAMBRIAN POLE CANYON LIMESTONE
- Cpm — CAMBRIAN PROSPECT MOUNTAIN QUARTZITE and PIOCHE SHALE

- PC — PRECAMBRIAN McCOY CREEK GROUP (Quartzite units are stipled)

PLUTONIC ROCKS

- Jg — JURASSIC GRANITIC ROCKS
- Tmg — TERTIARY?-MESOZOIC? GRANITIC ROCKS

younger overlying conglomerates suggest that significant faulting and tilting occurred during the time span of their deposition. The younger conglomerates contain clasts and slide blocks of formations as old as Middle Cambrian, thus clearly post-date faulting and the formation of major structural relief. However, they are in turn tilted and offset by younger faults.

Stratigraphic and geochronologic data available so far from the Schell Creek Range suggest that a significant proportion of the extensional faulting probably occurred strictly during the Oligocene, during the time of voluminous volcanism. At the time of the earliest eruptions (36 m.y. B.P.), only upper Paleozoic rocks were exposed at the surface, whereas by 30 to 27 m.y. ago, the older generation of faults had exposed rocks as old as Middle Cambrian. There are, however, no constraints on the upper age of faults that cut the youngest conglomerates in the Schell Creek Range.

AN EXHUMED DUCTILE-BRITTLE TRANSITION ZONE IN THE NORTHERN SNAKE RANGE

Introduction

Our best evidence for what happens to extensional fault mosaics at midcrustal depths comes from the northern Snake Range. Portions of this range were previously mapped by Nelson (1959), Hose and Blake (1976), and Hose (1981). The most prominent structural feature of the range, the Snake Range decollement, was first described by Hazzard and others (1953) and additional investigations and interpretations have been made by Misch (1960), Armstrong (1972), Coney (1974), Hose and Whitebread (1981), Wernicke (1981), and Rowles (1982). Miller and others (1983) describe in detail the structural evolution of the northern Snake Range based on two summers of mapping with the Stanford Geological Survey. The summary below is based largely on this work.

In the northern Snake Range (Figure 13), vast expanses of ductily deformed upper Precambrian and Lower Cambrian metasedimentary rocks and granitic intrusions of unknown age are exposed beneath the northern Snake Range decollement (NSRD). These rocks are structurally concordant to the gently arched NSRD, which generally follows the top of the Lower Cambrian Pioche Shale (Figures 13 and 14). In contrast, Middle Cambrian to Permian and Tertiary strata in the upper plate are broken up and tilted by imbricate normal faults that do not cut the decollement.

Along the southern flank of the northern Snake Range, the NSRD plunges abruptly southward beneath the Sacramento Pass area (Figures 13 and 15). Here, upper Precambrian and Lower Cambrian in the upper plate can be traced continuously into the southern Snake Range where they are in the lower plate of a decollement mapped by Whitebread (1969). As these two decollements are not structurally equivalent, the relations we describe below pertain only to the northern Snake Range.

Upper Plate Faulting

Geometric Relations - The geometry of upper plate faulting is best documented in the southwestern part of the northern Snake Range where the upper plate is largely preserved. Exposures of the NSRD to the north, east, and in a window along the Negro Creek drainage constrain its subsurface geometry and provide critical views of how upper plate faults interact with the decollement. Our description of upper plate faulting will focus specifically on the Negro Creek area (Figure 13).

Despite the extremely complex map pattern, a systematic structural style is evident in the upper plate. Structural sections that "young" to the west are repeated eastward on east-dipping faults (Figures 13 and 14). Older, west-dipping faults within these structural sections typically omit units. Two generations of faults are even more apparent in cross section (Figure 14). The younger faults are spaced approximately 1 km apart, dip 10 to 20° eastward, and apparently merge with the NSRD. The older faults are more closely spaced, dip 10 to 30° westward, and are truncated downward by either the NSRD or the younger faults.

Hanging-wall strata are displaced eastward relative to footwall strata on both generations of faults. The younger faults are clearly down-to-the-east normal faults, whereas the older faults presently have apparent reverse offset. The younger faults typically juxtapose upper Paleozoic formations on lower Paleozoic formations. Their actual offsets (0.2 to 2.0 km) are generally much less than their stratigraphic offsets (up to 4 km) because they displace sequences that were previously attenuated by the older faults.

Bedding attitudes in the upper plate are extremely variable. Most strata strike N 10 E to N 45 E and dip northwest, but the amount of tilting ranges from 0 to 90° or even overturned (Figure 16). Bedding in platy or shaly formations frequently parallels adjacent fault planes whereas more competent units tend to intersect the fault planes at high angles.

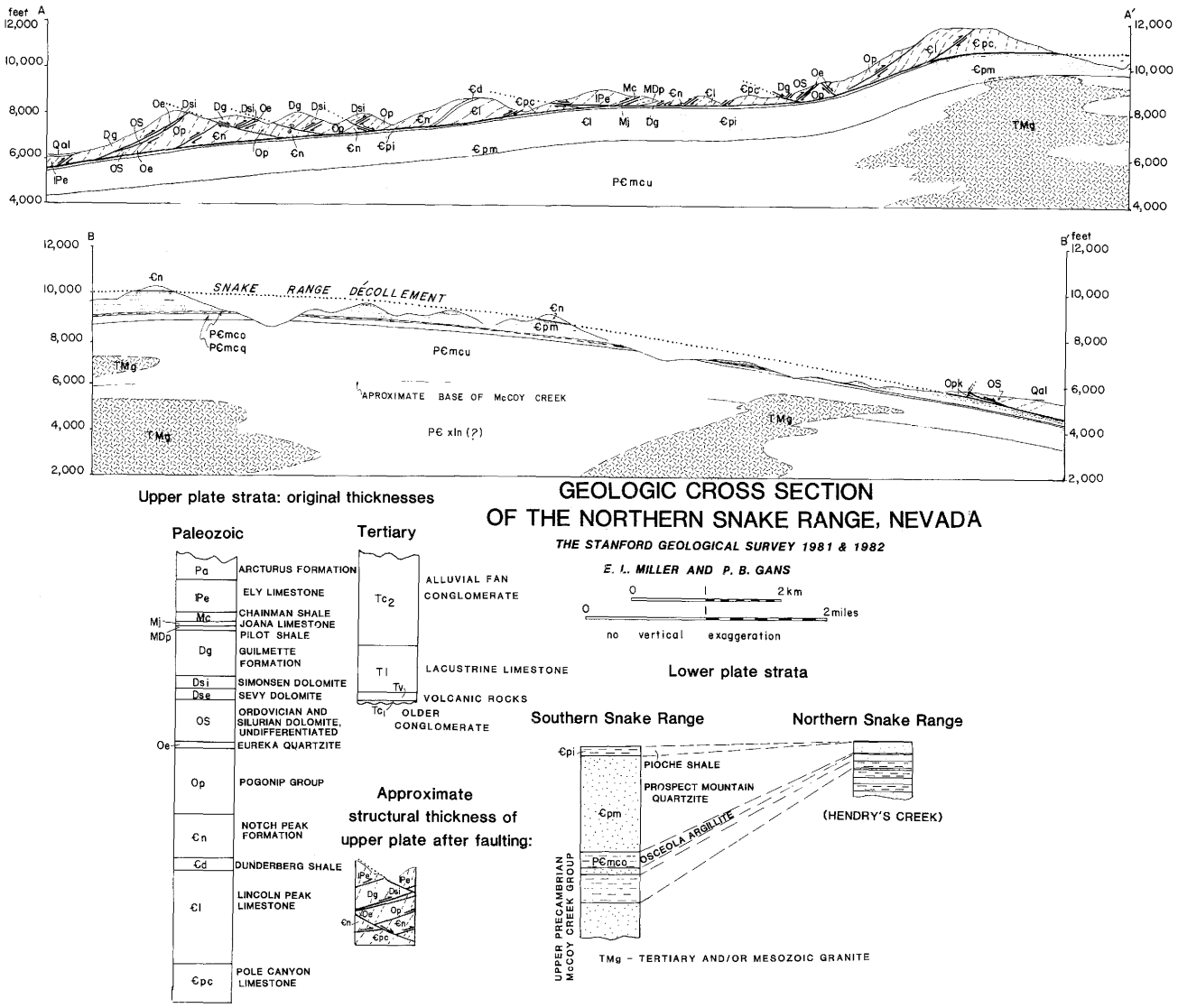

Figure 14. Geologic cross section of the northern Snake Range and a summary of upper and lower plate stratigraphy.

Classic "chaos structure" (Noble, 1941) is commonly developed along closely spaced low-angle faults directly above the NSRD. Bedding tilts get progressively steeper away from fault planes such that the steepest westward dips occur where faults are widely spaced and in the more massive limestone units. We emphasize that only these steepest dips reveal the true amount of westward rotation and the original bedding-to-fault angles. All lesser dips are demonstrably the result of normal drag on upper plate faults.

In three dimensions, the upper plate faults resemble faults in the Egan Range. They define shovel-shaped scoops that are 1.5 to 5 km across and have fairly planar bottoms. Bedding-to-fault angles do not decrease systematically with increasing stratigraphic depth on either generation of faults. However, unlike the Egan Range, all of the faults in the northern Snake Range are bounded below by an exposed detachment fault, the NSRD.

Kinematic Interpretations - The fact that faults in the upper plate flatten into a subhorizontal detachment plane requires that stratal rotation must have accompanied upper plate faulting. Figure 17 illustrates a sequence of faulting and tilting events that would result in the present bedding and fault attitudes. These simplified sequential cross sections do not attempt to show the effect of normal drag. First generation faults originated as *east-dipping*, high-angle (50 to 60°) normal faults that subse-

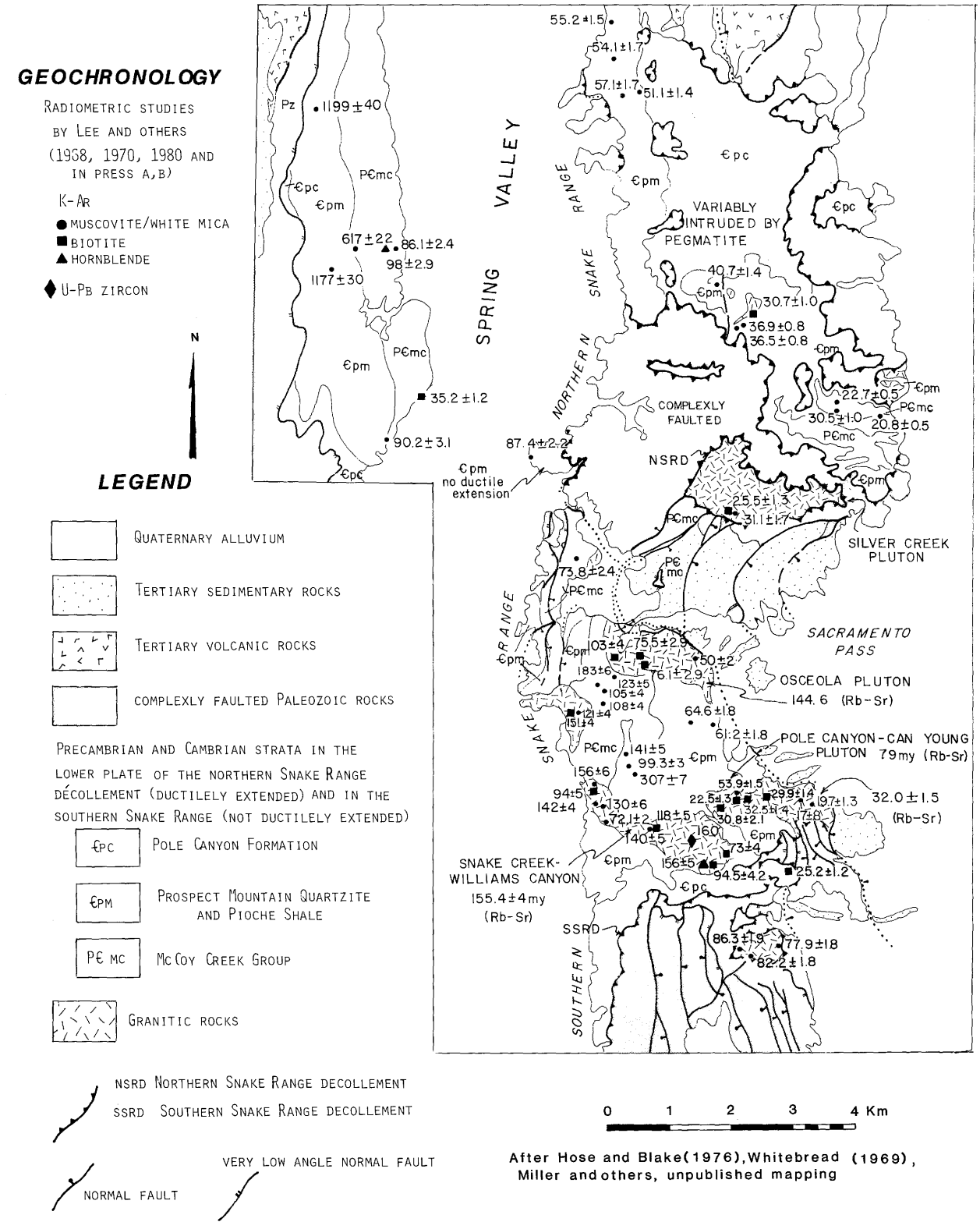

Figure 15. Index map of the northern and southern Snake Range, east-central Nevada, showing location of published radiometric dates.

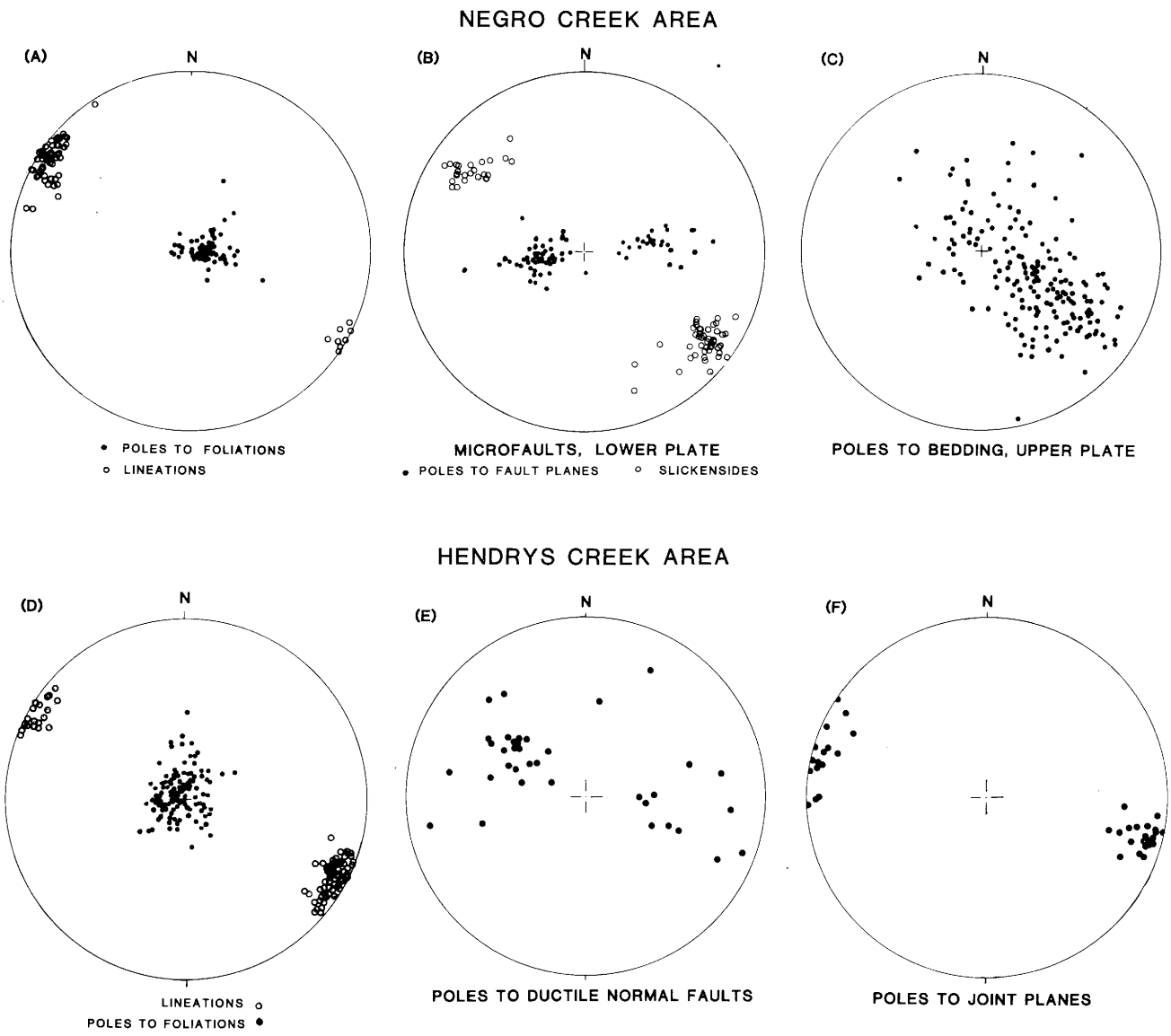

Figure 16. Structural data from the northern Snake Range (lower hemisphere equal area projection).
(a) Attitude of foliation and lineation in the lower plate of the NSRD, Negro Creek area.
(b) Late-stage ductile to brittle microfaults in the Prospect Mountain Quartzite, Negro Creek area.
(c) Poles to bedding upper plate, Negro Creek area.
(d) Attitude of level plate foliation and lineations in the Middle reaches of Hendry's Creek.
(e) Poles to closely spaced and penetrative micro-ductile normal faults in schist units along Hendry's Creek. East-dipping conjugate set is best developed.
(f) Poles to late-stage joints in Hendry's Creek.

quently rotated "domino-style" to low angles. Second generation faults also originated as high-angle faults and were superimposed on previously faulted and tilted strata. As the second generation faults rotated to low angles, the first generation faults were rotated through horizontal into westward dips and apparent reverse offsets. Note that the toes of the first generation faults were rotated away from the NSRD whereas higher segments were rotated downward and are presently truncated by the decollement. Nonetheless, the first generation faults must have interacted with the same basal detachment because they affect the entire range of stratigraphic levels in the upper plate. Later doming of the NSRD probably added an additional 5 to 10° of westward tilt to the Negro Creek area.

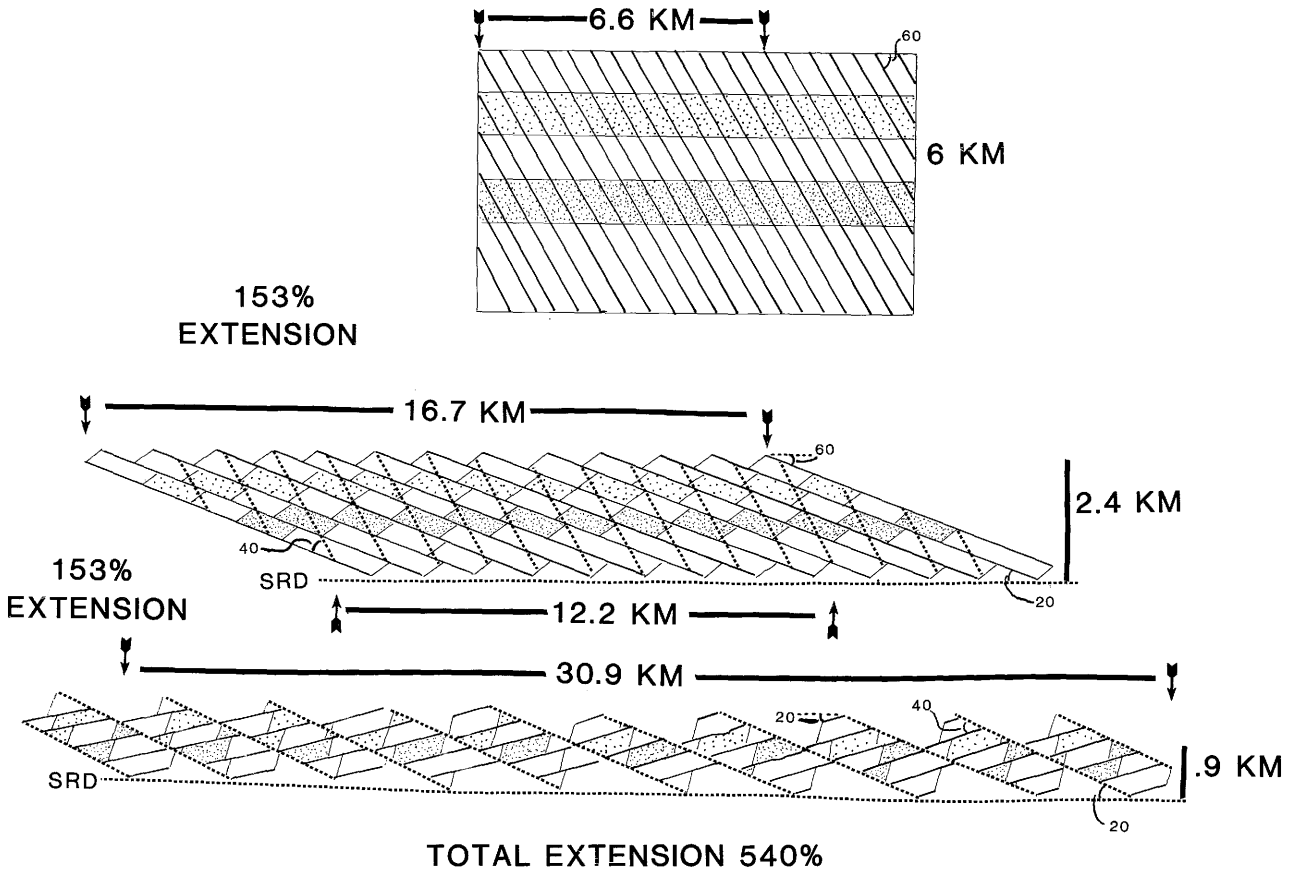

Figure 17. Simplified geometric model showing how two generations of upper plate faults interact with the decollement (SRD) to produce the bedding and fault attitudes observed in the Snake Range.

If both generations of faults originated at the same angle with respect to horizontal, then the average angular difference between them (40°) is precisely the amount of rotation that occurred on the older faults alone. Once these faults had rotated to dips as low as 20° the resolved shear stress on the fault planes apparently no longer exceeded the frictional resistance to movement, and a new generation of high-angle normal faults was developed.

The large bedding-to-fault angles at all stratigraphic levels in the upper plate suggests that both generations of faults must have flattened very abruptly into the NSRD. Space problems at the toes of fault blocks were relieved by several types of deformation: 1) brecciation was pervasive in the immediate vicinity of the NSRD; 2) warping and folding commonly "smeared out" less competent units along the decollement; 3) low-angle splays shaved off the sharp corners at the toes of major fault blocks (Figure 9). The third process was particularly important during movement on the younger, more widely spaced faults. Segments of rotated, first generation faults were apparently reactivated and served as splays at the toes of second generation faults. Evidence for this type of reactivation includes: 1) occasional, small-offset, high-angle faults that appear to bottom into the older rotated, low-angle faults; and 2) the imperfect match of hanging walls and footwalls on the younger faults. Renewed movement on older faults after they were at very low-angles (and subject to a larger resolved normal stress), may explain why frictional drag is so prevalent in the northern Snake Range.

The direction of extension in the upper plate was estimated to be N 55 W to S 55 E by the methods outlined previously for the Egan Range. The precise ages of normal faulting in the Snake Range are poorly constrained, but we assume that they coincide with faulting in the Egan and Schell Creek Ranges. The best constraints come from Tertiary rocks exposed in Sacramento Pass described by Grier (this volume). Here, a post-35 m.y. old lacustrine and fanglomerate sequence was deposited synchronously with nearby faulting and uplift. The se-

quence was then cut by imbricate normal faults that merge with the NSRD and geometrically resemble the second generation of faults in the Negro Creek area.

Amount of Extension in the Upper Plate - We have estimated the amount of extension in the upper plate for the Negro Creek area by three independent methods:

1. Sequentially restoring the faults along our line of cross section (Figure 18) yields approximately 125 percent extension by second generation faults and 155 percent extension by first generation faults for a total of 480 percent extension. This method has obvious problems because of the immense amount of small-scale faulting, brecciation, and folding that has changed the shape of the major fault slices.

2. Our best estimate of the average structural thickness of the upper plate after normal faulting but prior to erosion is approximately 1.1 km compared to an original stratigraphic thickness of 6 to 7 km. This change in thickness is equivalent to about 450 percent extension.

3. Calculation of the percent extension using bedding to fault angles and the amount of tilting (Thompson, 1960) yields 153 percent extension by both generations of faults for a total of 540 percent extension. This estimate is probably somewhat excessive because it does not account for deviations from two, simple generations of faults (e.g., fanning upward splays), or for internal deformation in fault blocks.

Considering the large uncertainties in all of these estimates, we are impressed by how closely they agree. We conclude that 450 to 500 percent is a reasonable, though perhaps conservative, estimate of the amount of extension in the upper plate of the northern Snake Range.

Lower Plate Deformation

Introduction - In marked contrast to the upper plate, rocks beneath the NSRD are relatively flat-lying and not appreciably faulted. Instead, they reveal a complex history of ductile deformation and magmatism that ended with a transition into a brittle regime.

Lower plate rocks in the northern Snake Range were metamorphosed to amphibolite grade and contain staurolite-garnet-biotite-muscovite and locally kyanite-muscovite-biotite schist. Metamorphic grade appears to increase both with increasing depth and to the north. Several plutons of biotite ± muscovite granite intrude the amphibolite grade rocks, but neither their absolute ages nor their relation to metamorphism is known. Both plutons and metasedimentary rocks are intruded by swarms of muscovite-garnet bearing pegmatite dikes (also of unknown age[s]) that locally comprise more than 80 percent of the lower plate.

Progressive (ductile to brittle) extension - Superimposed on all lower plate rocks is a penetrative subhorizontal foliation and lineation that increases in intensity both eastwards and upwards towards the NSRD. This deformation occurred at low greenschist grade and remarkably thinned all lower plate rocks. On the east flank of the northern Snake Range, stratigraphic sequences originally about 3 km thick have been ductily thinned to less than 0.5 km (Figure 14). The deformational fabric of lower plate rocks in the Hampton Creek area has been described by Rowles (1982).

Mesoscopic structures in the lower plate record ductile to brittle progressive extension (Figures 16 and 19). Stretched pebbles and mineral grains indicate extension in a NW-SE direction and flattening in a vertical direction. The direction of lower plate stretching varies from N 55 W on the west side of the range to N 70 W on the east side. Aspect ratios of stretched pebbles in McCoy Creek Group strata on the east flank of the range are commonly on the order of 8-10: 1:0.1. Late stage brittle structures such as closely spaced mesoscopic normal faults, ductile normal faults, and pervasive joints, cut earlier-formed ductile features and yield calculated directions of NW-SE-directed extension that are perfectly parallel to the direction of extension inferred from stretched pebbles (Figure 16). East-dipping mesoscopic normal faults are sometimes preferentially developed over their west-dipping conjugate sets. In general, however, the deformational fabric of lower plate rocks appears to have an orthorhombic symmetry. The ductile to brittle progressive deformation recorded in lower plate rocks of the Snake Range is similar to extensional fabrics described by G.H. Davis (1980) in many of the Arizona metamorphic core complexes and is markedly different from that typically developed in rocks during progressive compressional deformation (Figure 19).

The age of lower plate extension is not yet bracketed radiometrically, but we strongly suspect that it is Tertiary and synchronous with upper-plate normal faulting. Indirect arguments that support this age assignment incude: 1) the precise parallelism of lower and upper plate strain axes; 2) anomalously young Tertiary K-Ar mica ages from all rock

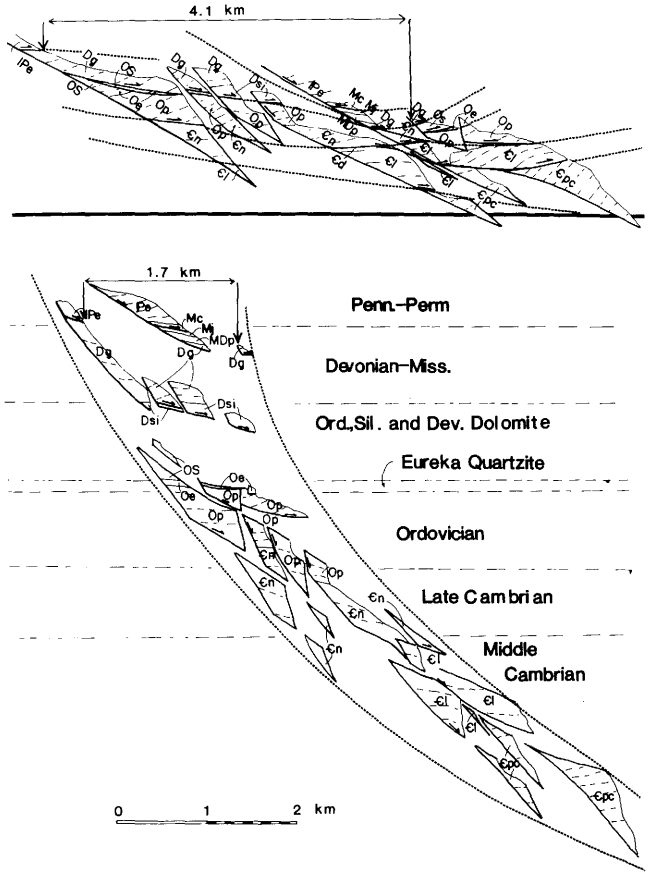

Figure 18. "Cut and paste" restoration of Snake Range upper plate faults along cross section A-A'. Unit symbols same as in Figure 14. Heavy solid lines are second generation faults, dashed lines are early generation faults.

types in the lower plate as compared to non-stretched but equivalent structural levels in adjacent ranges (Figure 15); and 3) well documented mid-Tertiary ages for identical fabrics in the nearby Raft River Range and Ruby Mountains (Compton and others, 1977; Snoke, 1982).

We have estimated the amount of extension in the lower plate by the amount of thinning of the Lower Cambrian Prospect Mountain Quartzite. Undeformed Prospect Mountain Quartzite sections in adjacent ranges are typically 1,200 m thick. On the east flank of the northern Snake Range, complete sections of this unit are generally only 100 to 200 m thick. On the west side of the range the base of the Prospect Mountain Quartize is not exposed. However the reduction in average bedding thickness suggests that it has been thinned to approximately one third its original thickness. An average of 330 percent extension across the range was derived by restoring the Prospect Mountain Quartzite to its original thickness while preserving its cross-sectional area (Figure 15).

Tectonic Significance of the Northern Snake Range Decollement

Models for detachment faulting in metamorphic core complexes fall in two general categories: 1) models that invoke a large amount of movement on the detachment faults (e.g., G.A. Davis and others, 1980; Wernicke, 1981); and 2) models that accomodate extension in the upper plate by *in-situ* extension below the detachment fault (e.g., G.H. Davis, 1980; Rehrig and Reynolds, 1981). The Snake Range, with its well constrained structural and stratigraphic relations, is particularly well suited for testing these models and deciphering the kinematics of detachment faulting.

The restored upper plate thickness (Figure 14 and 18) and the consistent stratigraphic position of the NSRD suggest that it originated at a depth of 6 to 7 km and was initially flat. Assuming that lower plate stretching was synchronous with upper plate faulting, then the NSRD represents an exhumed mid-Tertiary, ductile-brittle transition zone. Irregular zones of ductile deformation and recrystallization in the lower portions of upper plate fault slices suggest that, initially, the transition was fairly diffuse. As extension continued, the transition was rapidly localized within a narrow (probably less than 100 m) interval and ultimately evolved into a strictly brittle fault surface.

The precise amount and direction of movement of the upper plate with respect to the lower plate is not known as there are no offset markers. Although the NSRD presently juxtaposes rocks that represent radically different structural levels, this juxtaposition can be explained by two generations of normal faults that thin the upper plate and by the collapsing of isograds in the lower plate. We emphasize that there need not be a great amount of offset on the decollement as the amount of extension above and below is approximately the same! Thus, extension by normal faulting in the upper plate may have been largely accomodated *in-situ* by penetrative stretching and magmatism in the lower plate.

Several arguments can be made for at least some movement on the NSRD:

1. The metamorphic grade of the youngest units in the lower plate may locally be appreciably higher than that of the oldest units in the upper plate.
2. The amount of extension in the upper plate appears to be somewhat higher than the amount of extension in the lower plate.
3. The overall assymmetry of lower plate deformation (Figure 14) and the preferential development of down-to-the-east normal faults is compatible

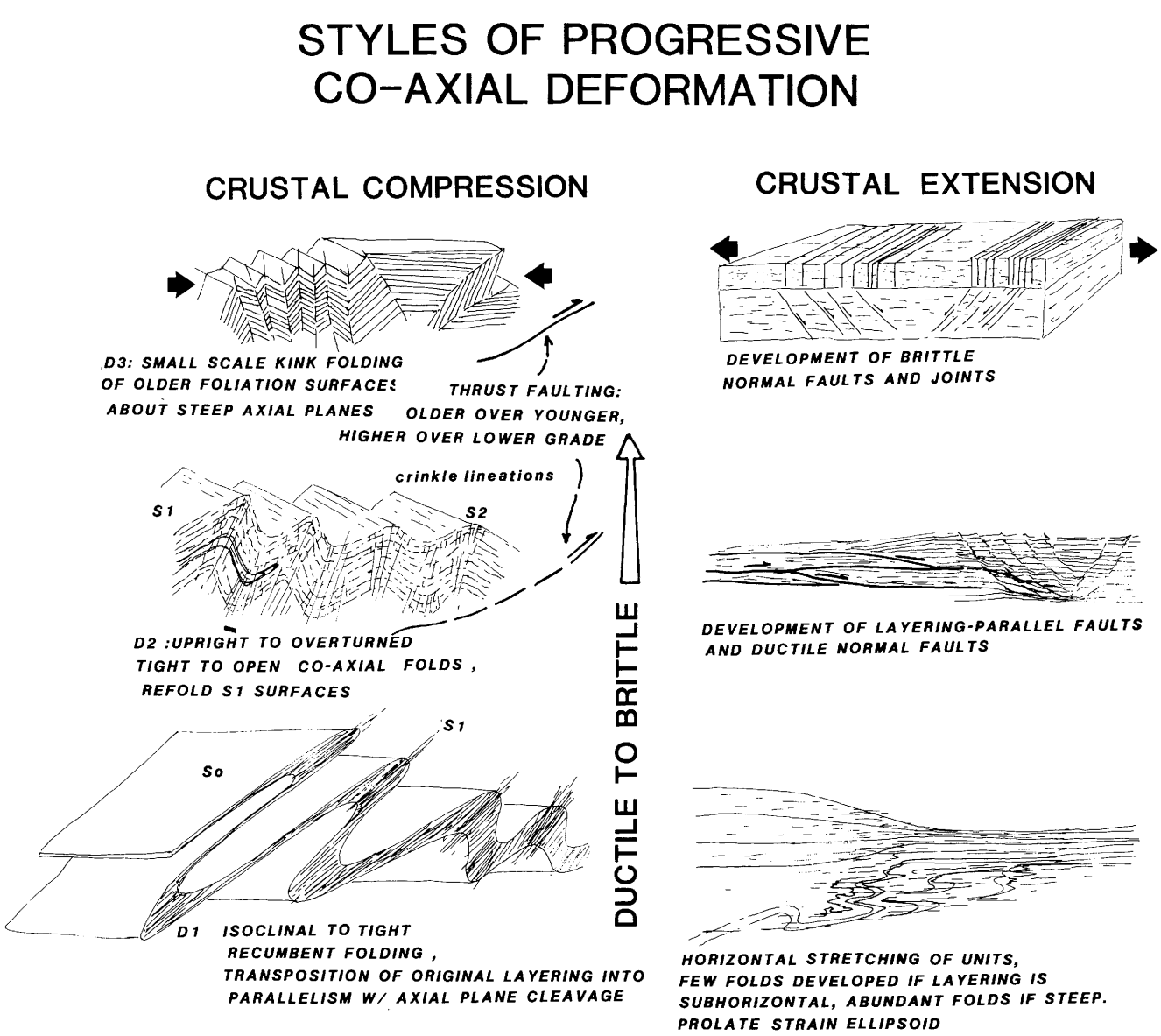

Figure 19. Comparison of ductile to brittle progressive, deformational fabrics produced during compression and extension.

with eastward movement of the upper plate with respect to the lower plate.

4. The observed strain gradient towards the decollement may indicate that lower plate deformation involved a component of simple shear. If so, upper plate rocks would be increasingly allochthonous with respect to progressively deeper horizons in the lower plate. Alternatively, the gradient in penetrative stretching may simply reflect increasing dilation by plutons with inceasing depth.

Wernicke (1981, 1982) interpreted detachment faults as very low-angle normal faults, or zones of simple shear, that may involve the entire crust. In his model, normal faults in the overlying "extensional allochthon" are "rooted" along a gently dipping surface to a laterally distant and much deeper area in the lower plate. Although some movement may have occurred on the NSRD, there is strong evidence that this surface was originally flat and did *not* cut down-section in the direction of movement of the upper plate. Across the entire width of the range, the oldest unit at the toes of upper plate fault slices (Middle Cambrian Pole Canyon Limestone) is in stratigraphic continuity with the youngest unit in the lower plate (Lower Cambrian Pioche Shale). The lack of stratigraphic (i.e., structural) omission across the decollement effectively rules out large amounts of movement on a

surface that originally cut down-section. It is interesting to note that a similar lack of stratigraphic omission is evident in the Ruby Mountains (Snoke and others, 1982) and in the Raft River Range (Compton and others, 1977) and may characterize metamorphic core complex detachment faults in general.

SYNTHESIS

A mid-Tertiary Extensional Belt

Imbricate low-angle faults and large stratal rotations are the characteristic geometric elements of the Egan, Schell Creek, and Snake Ranges. In each range, they are demonstrably the consequence of Oligocene-Miocene(?) extension oriented approximately N 65 W to S 65 E. Sharp supracrustal boundaries between ranges affected by this tectonism and relatively unfaulted ranges to the east and west delineate a north-northeast trending "belt" of mid-Tertiary extension (Figure 20). The northern Egan, northern Schell Creek, and northern Snake Ranges are dominated by down-to-the-east faults and westward dipping beds, whereas ranges to the south display the opposite polarity of faulting and tilting (Figure 20). These two structural domains are separated by a zone of complex block faulting and tilting rather than a discrete transform fault.

The total amount of extension across this corridor can be estimated from the offset of older structural trends. Southwest and northeast of the mid-Tertiary extensional belt the Butte and Confusion synclinoriums are subparallel and approximately 40 km apart (Figure 20). Where the northeast trending belt of extension intervenes between these older folds, they achieve a maximum separation of 135 km as first one, and then the other, is variably rotated, broken into segments, and "pulled" out to the west. This 95 km of dilation is equivalent to 250 percent extension and must be viewed as a minimum estimate because: 1) it does not allow for extension between the two synclinoriums outside the extensional belt; and 2) it is averaged over the non-extended limbs of the synclinoriums. Nonetheless, it is compatible with our reconstructions of individual ranges within the belt.

We have palinspastically restored part of east-central Nevada by shrinking the area between the Butte and Confusion synclinoriums to its original width of 40 km (Figure 21a). We assumed homogeneous extension across this corridor, but emphasize that, in fact, the strain is quite heterogeneous. Early Oligocene geologic contacts were obtained from the Tertiary unconformity data (Figure 4) and indicate a simple pattern of N-S trending, gentle anticlines and synclines (Figures 21a and 21b). The concave westward map pattern is a consequence of holding the Confusion synclinorium "fixed" during the reconstruction and may reflect differential extension east of the Confusion Range.

Other highly extended areas in the North Basin and Range (e.g., the Ruby Mountains and the Raft River Range) have not been reconstructed but probably represent a similar magnitude of extension as the 250 percent we have recorded in east-central Nevada. These highly extended domains are separated by regions of lesser extension (15 to 30 percent, Stewart, 1978). The total amount of extension across the northern Basin and Range province is probably close to or greater than the 100 percent estimated by Hamilton and Meyer (1966), and Proffett (1977).

Discussion: Models of Extension

Geologic relations in the Egan, Schell Creek, and Snake Ranges help constrain the kinematics of crustal extension. We present a simplified cross-section of east-central Nevada (Figure 21c) that is consistent with these relations and illustrates the key processes of crustal extension.

1. Supracrustal extension was accomplished by high-angle (50 to 60°), shovel-shaped normal faults that rotated to low angles as they moved. Fanning splays document progressive rotation of planar faults, and helped accomodate space problems at depth. Normal drag commonly obscures original bedding-to-fault angles and creates the illusion of "bedding-parallel" faulting. However, we find no evidence for large displacement normal faults that originated at low angles, even though this area has been repeatedly cited as a "type area" for this kind of deformation (Hintze, 1978; Wernicke, 1981, 1982; Wernicke and Burchfield, 1982).

2. Supracrustal high-angle faults flattened abruptly into mid-crustal ductile-brittle transition zones that evolved into brittle detachment faults. In the northern Snake Range the ductile-brittle transition originated at 6 to 7 km depth, whereas in the Egan and Schell Creek Ranges it was deeper than 10 km. Using the Snake Range as our example, the detachment faults need not have appreciable offset as the amount of extension above and below the Snake Range detachment fault is similar. We conclude that extensional detachment faults can be locally developed, have finite boundaries, and need not "surface" or "root."

3. At deeper levels, extension was accomplished

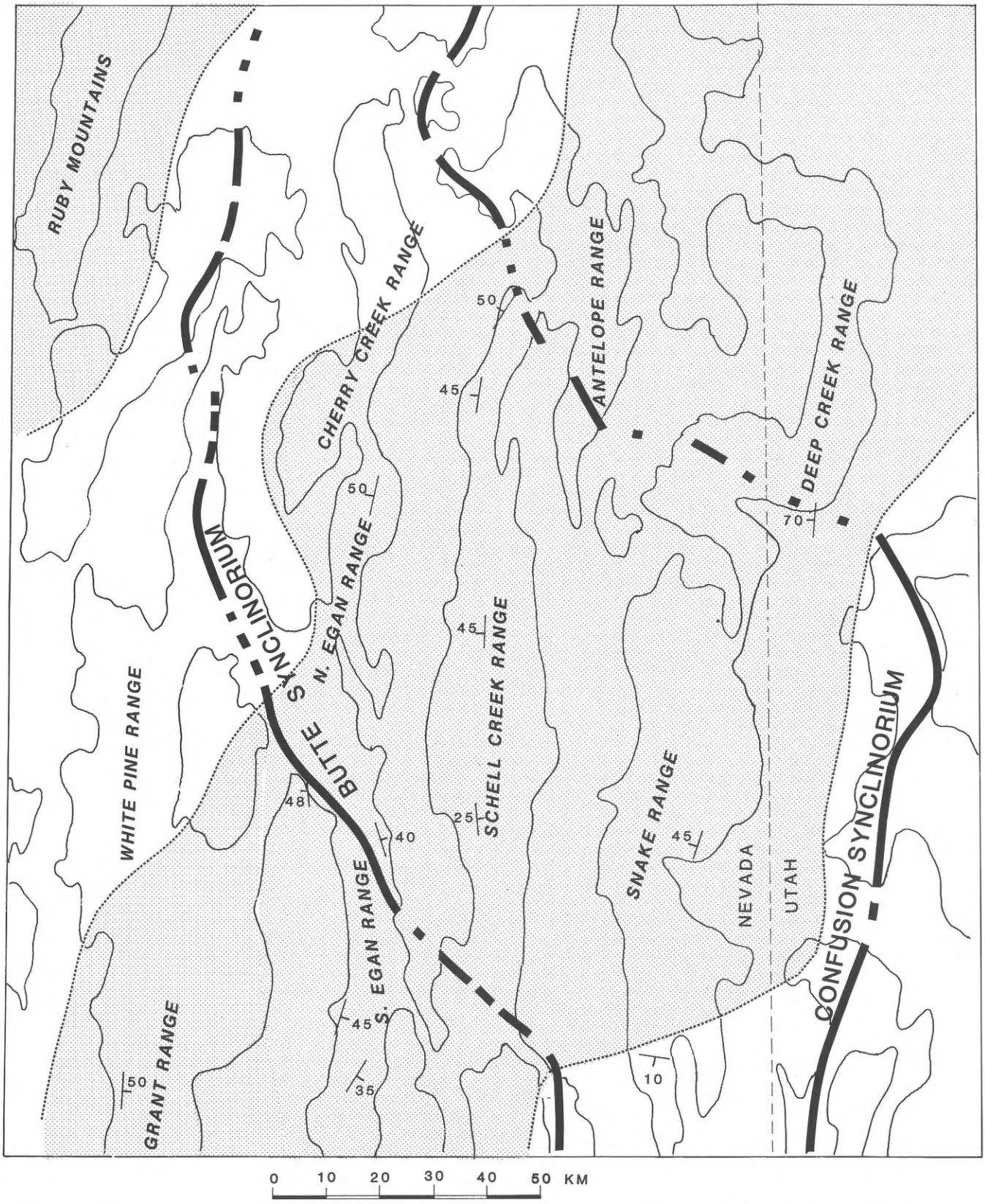

Figure 20. Mid Tertiary extensional belt in east-central Nevada. Highly extended areas characterized by imbricate normal faults and steep bedding dips are shaded. Intervening unpatterned areas display little supracrustal deformation bedding attitudes are on early Tertiary volcanic and sedimentary rocks but are representative of underlying Paleozoic rocks as well. Sources of data: Stewart and Carlson, 1976, and those listed for Figure 4.

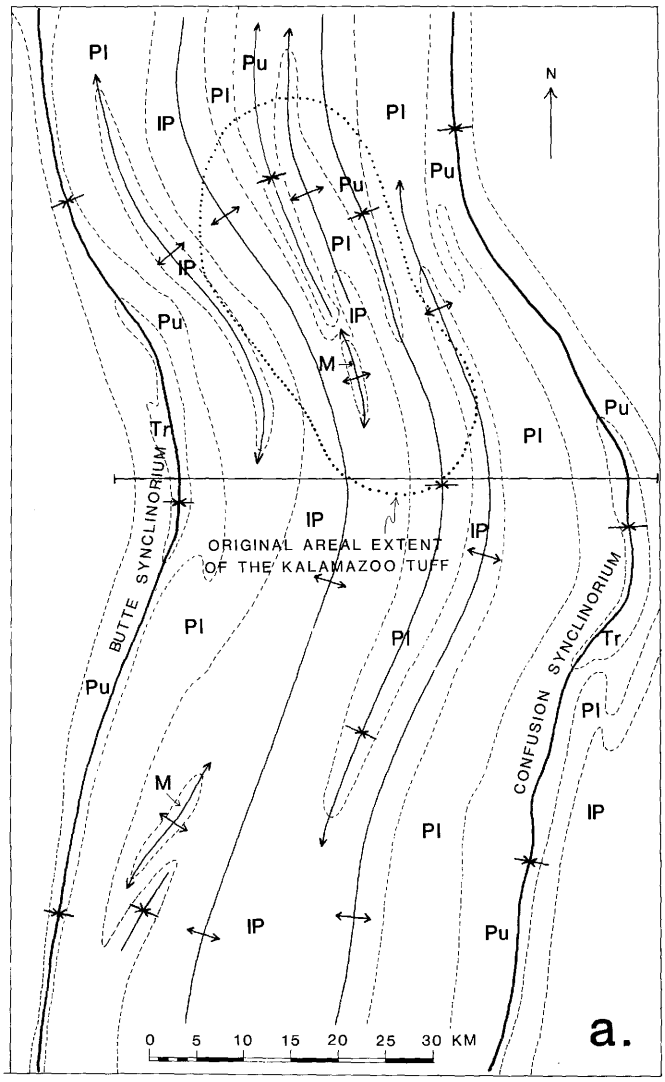

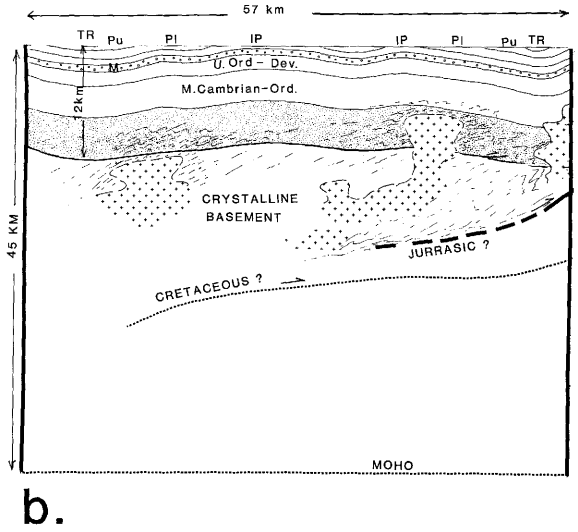

Figure 21. (a) Early Oligocene geologic map of east-central Nevada. Units the same as in Figure 4.
(b) Schematic cross section of east-central Nevada during the early Oligocene.
(c) Highly generalized present day cross section of east-central Nevada.

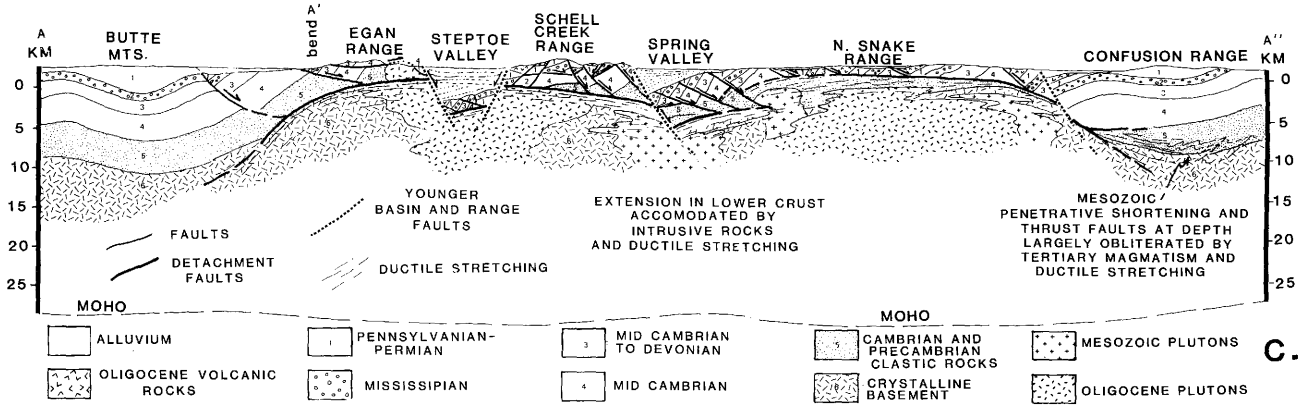

by penetrative stretching and intrusion, similar to models proposed by Rehrig and Reynolds (1980) and Eaton (1982). Large volumes of syntectonic volcanic rocks in the Schell Creek Range and Tertiary K-Ar ages in the Snake Range virtually require mid-Tertiary batholiths at depth and suggest that extensional processes were coupled with and/or triggered by a high thermal flux.

An enigmatic aspect of east-central Nevada, and many other core complex terranes, is that these highly extended areas are also topographically high. This cannot be explained by present day heat flow patterns nor by simple isostatic rebound due to supracrustal thinning, but instead sugests that the entire lithospheric column beneath the extended areas has been modified (e.g., Le Pichon and others, 1982). One possibility is that the underlying mantle lithosphere was thinned by a greater factor than the overlying crust.

The observed stretching factor of 250 percent and the present crustal thickness of 25 to 30 km in east-central Nevada (Saleeby and others, 1982) requires that either the crust was incredibly thick (85 to 100 km) prior to extension, or, more likely, large amounts of juvenile magma were added to the crust during extension. A present-day crust composed of up to 50 percent Oligocene plutons (Figure 21c) is compatible with our inference that extreme supracrustal extension in east-central Nevada was genetically linked to deep-seated magmatism and ductile deformation.

ACKNOWLEDGEMENTS

We appreciate the encouragement and financial support given to us by Shell Oil and Noranda Mining companies and the financial support of the Stanford University Earth Sciences McGee Fund in the beginning stages of our work in east central Nevada. Our work is presently funded by NSF Grant (EAR-82-06399) awarded to E. L. Miller and G. A. Mahood, which we gratefully acknowledge. Grier and Gans, in addition, acknowledge support of their studies by Tennecco Oil Company and Stanford AMAX funds. Many thanks go to the members and T.A.'s of the 1981 and 1982 Stanford Geological Survey for their enthusiasm and hard work in the Snake Range. We are extremely grateful to Sohio Oil Company for their recent funding of the Stanford Field Camp. Our understanding of the geology of east central Nevada has benefited from discussions with R. R. Compton, J. Garing, J. Hakkinen, R. K. Hose, G. A. Mahood, A. Snoke, B. Robinson, G. Thompson, and especially members of the Stanford Geological Survey. Finally, we thank Melina Whitehead for typing and helping us assemble this paper, and Jeff Lee for critical comments.

TERTIARY STRATIGRAPHY AND GEOLOGIC HISTORY OF THE SACRAMENTO PASS AREA, NEVADA

Susan Grier
Stanford University, Stanford, CA 94305

ABSTRACT

Tertiary strata in the Sacramento Pass region of the Snake Range, Nevada, accumulated in a NW-SE trending Oligocene-Miocene(?) basin between two areas with different extensional histories (see Miller and Gans, this volume). The 2 to 3 km thick sequence unconformably overlies Pennsylvanian-Permian rocks and consists of a basal conglomerate, latite flows, rhyolite tuff, lacustrine limestone, and a younger conglomerate. Paleocurrent indicators and lithotypes in the younger conglomerate indicate a southwestern source, implying that the earliest faulting occurred to the southwest of the basin where rocks as old as the Late Precambrian McCoy Creek Group were exposed. Large landslide blocks exist within the limestone and younger conglomerate section, also suggesting considerable structural relief in adjacent regions.

Four down-to-the-east normal faults that are curved in plain view repeat the Tertiary section and have tilted strata 30 to 50° westward. The faults occurred simultaneously with or prior to final movement on the Snake Range decollement; however, the deposition of the Tertiary section entirely predated the exposure of the lower plate rocks in the Northern Snake Range.

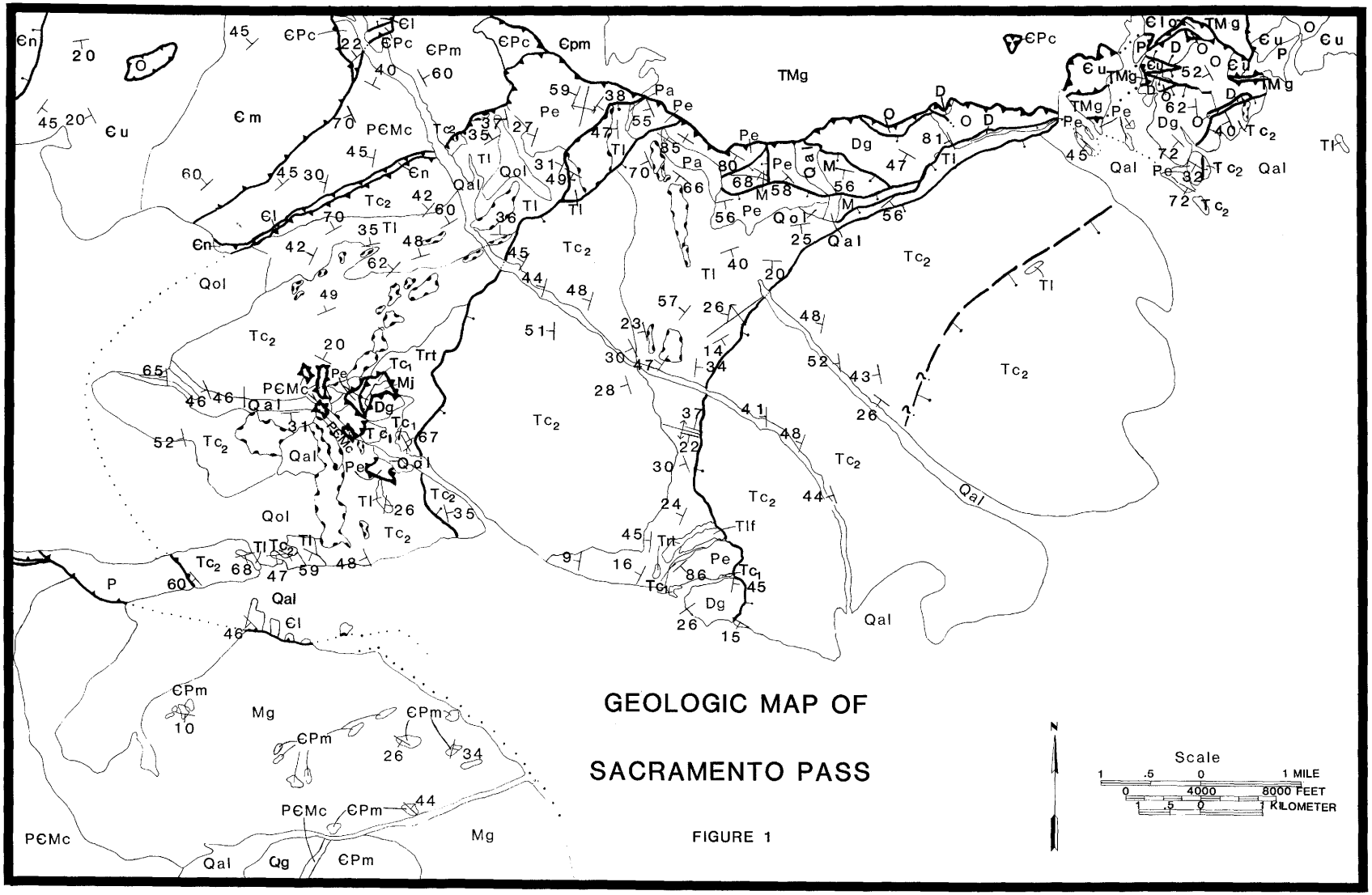

Figure 1. Geologic map of Sacramento Pass.

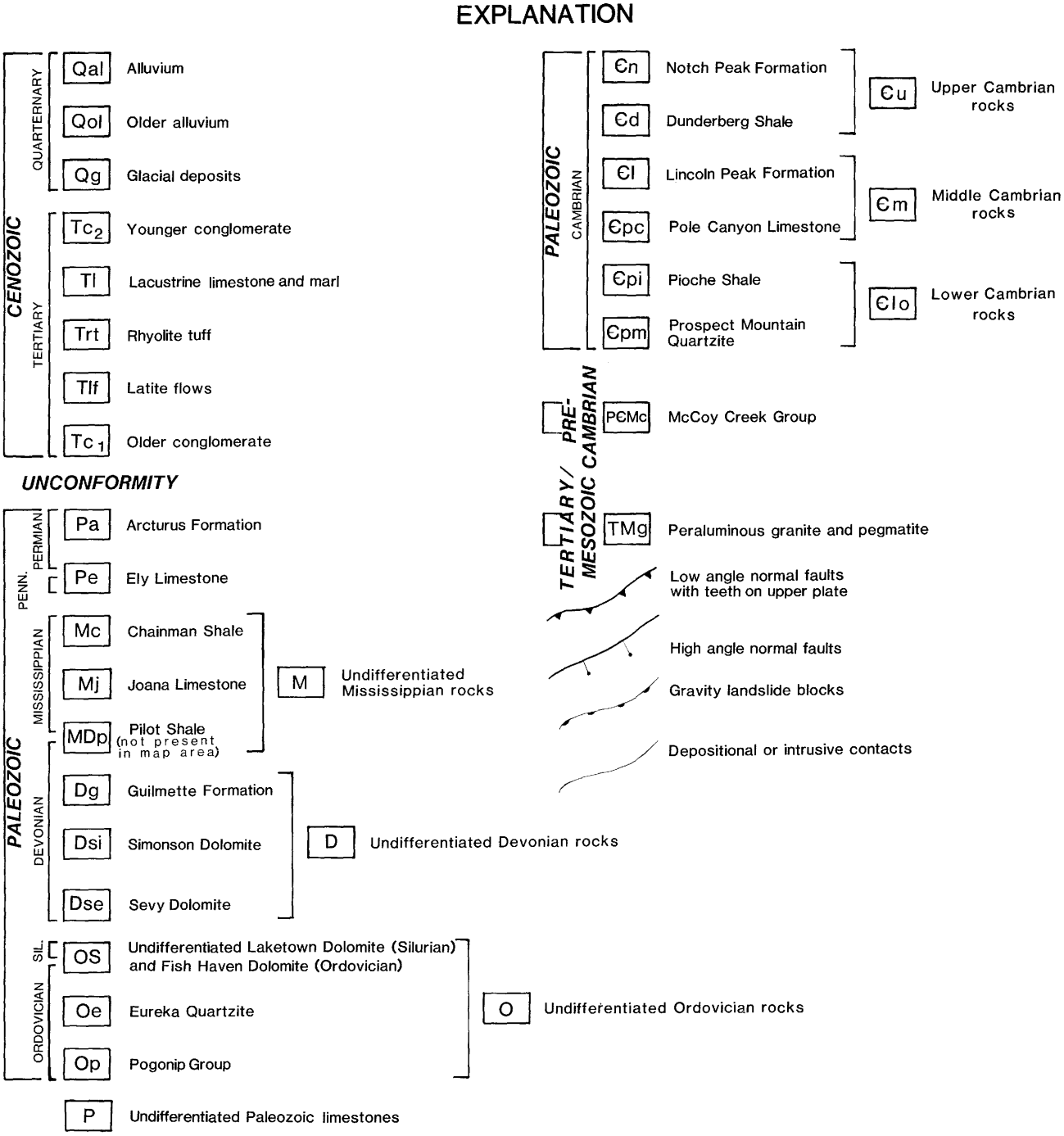

INTRODUCTION

The Tertiary section crops out along Weaver Creek and along a broad stretch from just north of Highway 50 to Miller Basin Wash (Figure 1). This area has been previously mapped by Hose and Blake (1976), Hose (1981), and the Stanford Geological Survey (1981, 1982). The present study was conducted to document the sedimentological characteristics of the Tertiary section, to examine the deformational history of the area, and to elucidate the structural evolution of adjacent regions.

STRATIGRAPHY

At the base of the Tertiary section, unconformably overlying Pennsylvanian-Permian rocks, is an older conglomerate (Tc_1). This poorly exposed con-

glomerate contains round to subround clasts derived exclusively from uppermost Paleozoic formations (Figure 2).

Conformably overlying the older conglomerate are Tertiary volcanic rocks dated at 35 m.y. old by Hose and Whitebread (1981). These consist of latite flows (Tlf) overlain by rhyolite tuff (Trt) (Figure 2). The latite flows form very dark red, knobby hills, are lavendar gray on fresh surfaces, and contain plagioclase, alkali feldspar, biotite, hornblende, augite, and some quartz and magnetite. The rhyolite ash-flow tuff is generally dark red to green-gray and contains 5 to 10 percent phenocrysts of quartz, alkali feldspar, plagioclase, biotite, and iron hornblende. The tuff is moderately to densely welded and contains abundant flattened pumice lumps, as well as lithic fragments of volcanic rocks and sandstone.

Tertiary lacustrine deposits (Tl) overlie the volcanic rocks and consist primarily of a brown to tan ledgy slope-forming, pisolitic, sandy limestone. Interbedded with this limestone is white, sandy tuffaceous marl (Figure 2). The limestone is well-bedded, generally with planar beds varying from 2 cm to 3 m in thickness; wavy beds are occasionally present. Common sedimentary features in the limestone include silicified stromatolites, mud cracks, silicified evaporites, fenestral fabrics, and chert beds and lenses. Toward the top of the section, thin beds of pebble conglomerate and sandstone are interbedded with limestone, and a rhyolite air fall tuff is exposed in trenches. The absence of marine fossils and the presence of detrital clasts support a shallow, ephemeral, saline lake as the depositional environment of the limestone. The stromatolites, pisolites, mud cracks, and silicified evaporites all indicate frequent dessication of this lake.

Interfingering with and overlying the lacustrine sediments is a younger conglomerate (Tc_2) (Figure 2). This conglomerate forms red to gray hills but is generally poorly exposed and concealed beneath a mantle of younger alluvium. Unlike the older conglomerate, the younger conglomerate contains clasts derived from the entire Paleozoic section (90 percent), as well as from Precambrian and Cambrian metasedimentary rocks (1 to 5 percent), Mesozoic(?) muscovite-biotite granite (1 percent), peraluminious pegmatite (1 percent), contact-metamorphosed schist (1 percent), and underlying Tertiary volcanic rocks and limestone (1 percent, locally 5 to 10 percent). The subangular to well-rounded clasts of the younger conglomerate are supported by a calcareous sandstone matrix and represent two distinct mechanisms of deposition: 1) interbedded debris flow deposits and; 2) stream channel deposits. The debris flow deposits are matrix supported, have very poor sorting, and contain boulders up to at least 2 m in diameter. A single debris flow unit may range from less than 3 to 6 m in thickness. Rarely, these deposits show crude channelling at the top of the flow. The stream channel deposits tend to be stratified by grain size, have subround to round clasts, and are better sorted. Some beds appear planar, while others are lenticular with well-developed lag deposits. Channel size averages at 3 to 4 m long and 1 m thick in cross section. The occasional scour features in the conglomerate include groove marks and cut and fill structures. Imbrication in the younger conglomerate measured along Miller Basin Wash indicate a northeasterly paleocurrent direction, thus signifying a southwest source area; these conclusions are consistent with the fact that conglomerate interfingers towards the northeast with underlying and coeval lacustrine sediments. The younger conglomerate is interpreted to have been deposited as part of a subareal fan complex upon which braided stream channelling was dominant with frequent debris flows.

Present in both the lacustrine limestones and the younger conglomerate are large landslide blocks, shown in Figure 1. These are monolithic or zoned polylithic, brecciated, yet coherent, masses of Paleozoic limestone, dolomite, and quartzite. The majority of these blocks consist of Ordovician-Silurian dolomites, Ordovician Eureka Quartzite, and the Ordovician Pogonip Group, but some blocks are composed of strata as old as the Cambrian Pole Canyon Limestone. The cement of each slide block appears to be derived from the constituents of the blocks themselves, for example, slide blocks of dolomite have dolomitic cement, while those of quartzite contain a silicious cement. This characteristic, coupled with the monolithic nature, suggests that brecciation and lithification either predated or occurred during the emplacement of the slide blocks. The slide blocks could, in part, represent fault breccias formed along a pre-existing scarp in adjacent regions. These olistostromal slide blocks probably traveled across the alluvial fan complex onto the soft lime mud in the lake. The Tertiary limestone by Willow Patch Spring show conical folds and convolute bedding beneath a large slide block of Ordovician Eureka Quartzite.

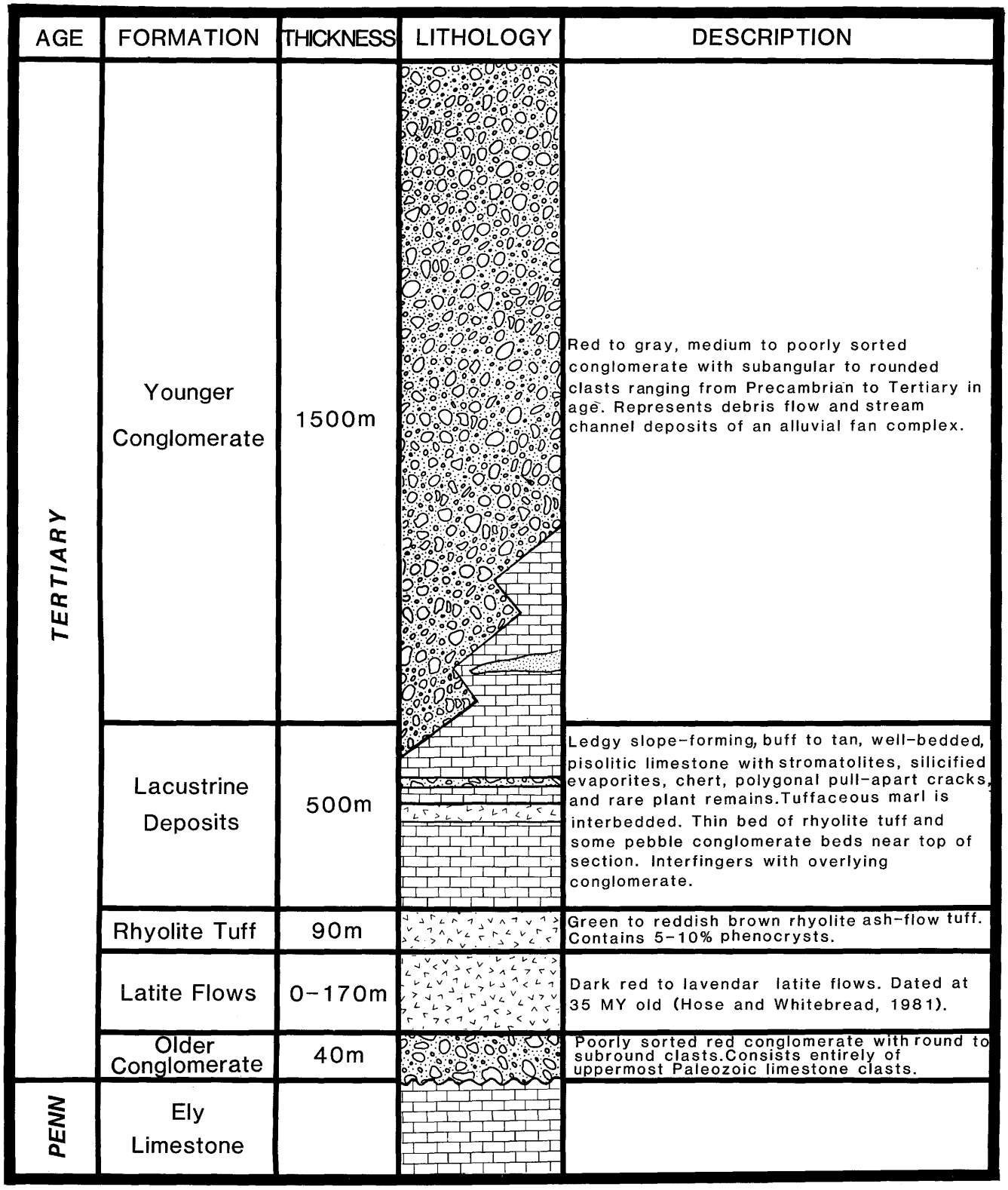

Figure 2. Stratigraphic Column.

STRUCTURE

The stratigraphic relations within the Tertiary section in Sacramento Pass provide important insight into the structural history of adjacent regions. The fact that the older conglomerate contains only uppermost Paleozoic clasts and rests on Pennsylvanian-Permian rocks, indicates that only minor structural relief existed prior to the deposition of the pre-35 m.y. old conglomerate. After or beginning with the period of volcanism, major faulting and uplift occurred in the adjacent areas, supplying clasts derived from strata as old as Precambrian. This uplift was synchronous with the deposition of the lacustrine sediments and of the younger conglomerate. Tectonic uplift is also evidenced by the presence of large slide blocks within the Tertiary sequence that range in age from Cambrian to Silurian. As indicated by clast imbrication, the source for the younger conglomerate was to the southwest, implying that the earliest faulting was along the southwest flank of the basin. Lithotypes in the younger conglomerate also support a southern source. The non-foliated and non-lineated Precambrian and Cambrian metasedimentary clasts and granitic clasts in the younger conglomerate are similar to lithologies presently exposed in the Southern Snake Range, while equivalent formations in the lower plate in the Northern Snake Range decollement are lineated and foliated (see Gans and Miller, this volume). Clasts of contact metamorphosed schist are similar to McCoy Creek Group schists in the contact aureole of the Strawberry Creek pluton in the Southern Snake Range. Faulting to the south and west of the Sacramento Pass Tertiary depocenter eventually migrated to the flanks of the basin itself, for clasts of Tertiary volcanic rocks and limestone were incorporated cannibalistically into the younger conglomerate.

Four down-to-the-east, arcuate, normal faults repeat the Sacramento Pass Tertiary sequence and tilt strata 30 to 50° westward. The faults apparently flatten abruptly with depth and merge with, but do not cut, the Northern Snake Range decollement (Figure 1). Thus, deformation of the Sacramento Pass basin occurred prior to or was coeval with the youngest movement along the Snake Range decollement; however, lower plate rocks were not exposed during the deposition of this entire sequence.

CONCLUSION

During the Tertiary, a saline lake flanked by an alluvial fan complex to the southwest occupied the Sacramento Pass area. Prior to 35 m.y. ago the topography in adjacent areas was only minor. Major faulting and tectonic uplift occurred to the southwest after the period of Tertiary volcanism and coeval with the deposition of the lacustrine sediments and the younger conglomerate. Faulting activity migrated into the Tertiary basin, and the resulting faults that cut the Tertiary section merge with, or are cut by, the northern Snake Range decollement.

FIELD TRIP ROAD LOG: FIRST DAY

Style of Mid-Tertiary Extension in East-Central Nevada

Elizabeth L. Miller, Phillip B. Gans, and Susan Grier

Mileage		Description
Incremental	Cumulative	
0.0	0.0	The roadlog starts at the junction of Highways 50 and 93 in Ely, Nevada (Figure 1). Proceed north on Highway 93 towards McGill.
8.8	8.8	Turn left on graded dirt road immediately past the Club 50 Cafe.
1.1	9.9	At pavement turn left and drive due west across Steptoe Valley. Straight ahead is Heusser Mountain, part of the northern Egan Range. A biotite granite pluton (white outcrops in lower foreground) intrudes upper Precambrian McCoy Creek Group (reddish outcrops and talus at the crest of the ridge and to the right). Woodward (1962) describes polyphase deformation and metamorphism of the country rocks that resemble what you will see in the McCoy Creek area tomorrow.
2.0	11.9	Pavement ends. Turn right on graded dirt road. You are now

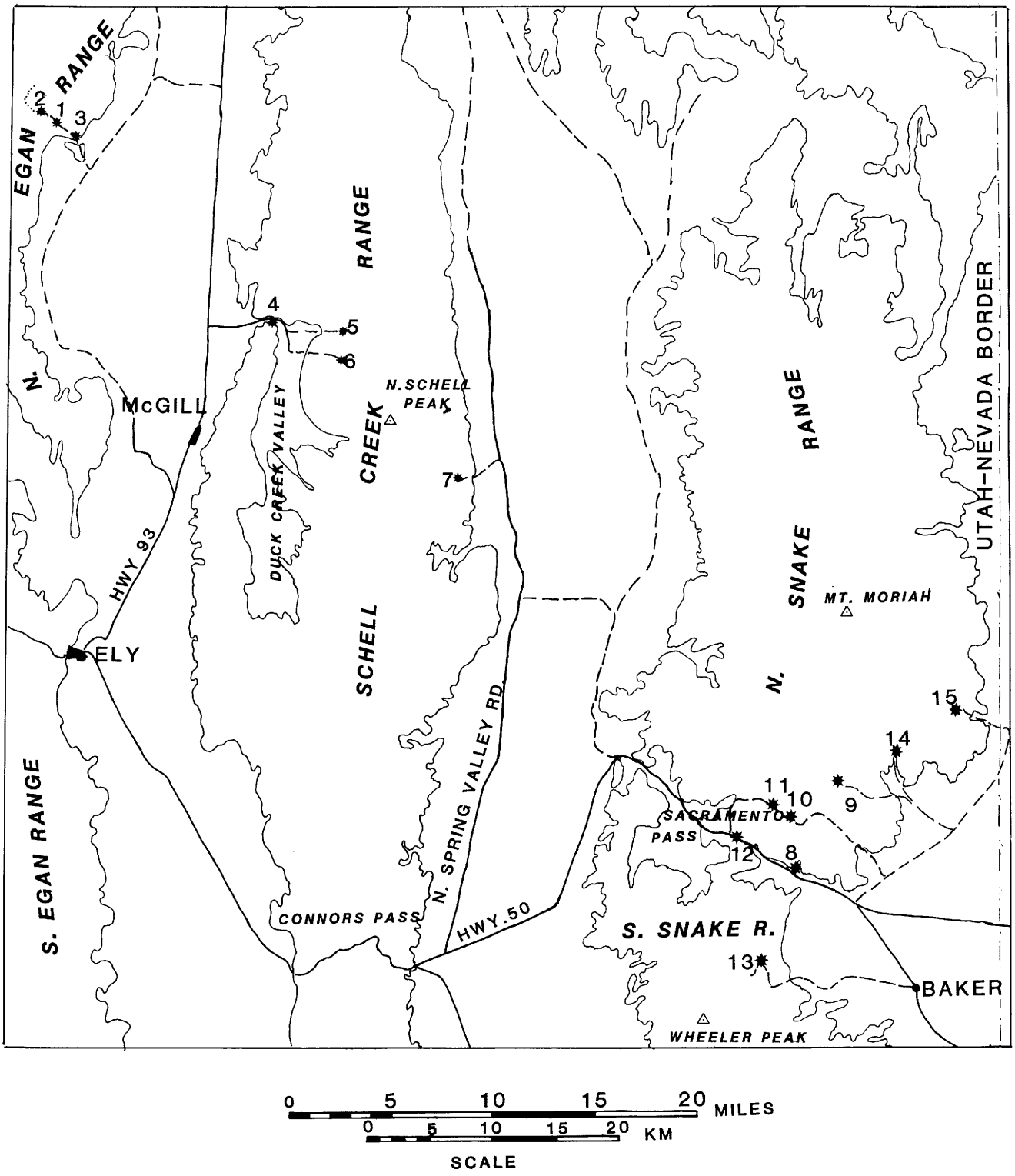

Figure 1. Field trips stops.

headed north on the west Steptoe Valley Road. On the left is the Egan Range. The high ridgeline of the Schell Creek Range is now visible on the right, behind the Duck Creek Range. McGill's tailings ponds are in the foreground.

5.9 17.8 Straight ahead, the prominent white band is one of the most distinctive Paleozoic formations, the Ordovician Eureka quartzite. Tree covered slopes below are underlain by the Pogonip Group, overlying cliffy units up to the ridgeline are the Ordovician and Silurian dolomites.

6.2 24.0 Steptoe Ranch on the right.

4.6 28.6 Turn left on road to Water Canyon: unmarked but look for mound of dirt by the turnoff.

The low, yellowish brown hills at the mouth of Water Canyon consist of Pennsylvanian-Permian strata overlain by Oligocene volcanic rocks. These units are downdropped against a large biotite-granite pluton along a major, east dipping fault (refer to Stop 3).

1.5 30.1 Concrete pillar with black arrow. Follow the arrow by taking the right fork in the road and then continue straight up Water Canyon and into the pluton.

1.3 31.4 Continue straight, road off to right.

0.2 31.6 Spring on the right.

0.4 32.0 Road off to right. Park here.

Introductory remarks by E. L. Miller and overview of the geology of the Egan Range by P. B. Gans. **STOP 1**. Oligocene Magmatism at Mid-Crustal Depths.

The thick stack of upper Precambrian to Permian strata in the northern Egan Range was intruded at its base by several large composite plutons. At this stop, you will examine the textural variations in one of these plutons at a depth of emplacement of 10 km[1].

The main phase of the Water Canyon pluton is an equigranular biotite granite with K-spar megacrysts. It is coarse-grained right up to its intrusive contacts and contact metamorphoses the wall rocks. It has yielded a K-Ar date on biotite of 36.2 ± 0.7 m.y. (Armstrong, 1970) but may be significantly older. The main phase is weakly deformed as evidenced by polygonized and strained quartz and broken feldspars. Locally, mylonitic shear zones are abundant.

The main phase of the pluton is intruded by at least two varieties of porphyritic dikes, here informally named Aplite Porphyry and Granite Porphyry. Both have similar mineralogy (qz-ksp-plag-bio) but are differentiated on the basis of texture. Aplite Porphyry has relatively small quartz and feldspar phenocrysts in a groundmass that grades from aphanitic at the margins of dikes to aplitic in the interiors. Granite porphyry has a fine- to coarse-grained, seriate groundmass and is characterized by extremely large phenocrysts of K-spar (up to 10 cm). Granophyric textures are common in the groundmasses of both types of dikes.

The dikes presently dip 10 to

[1]The companion paper to this roadlog describes how we derive paleodepths.

40° eastward because of westward tilting. Both sets of dikes can be traced continuously westward and upward out of the pluton and into the overlying country rocks where they commonly intrude low-angle normal faults. In the Hunter district, they are exposed at depths of emplacement of 1 to 3 km, and, on compositional and textural grounds, are clearly feeders for nearby crystal-rich rhyolite tuffs (Gans, 1982). Relations in the Hunter district suggest that the onset of extensional faulting precisely coincided with the emplacement and venting of these silicic dikes. The dikes and the tuffs yield indistinguishable K-Ar biotite dates of 35.8 m.y. (Gans, 1982).

Thus, steep westward tilting in the northern Egan Range has rotated an early Oligocene magmatic system over on its side and allowed us to examine it from the original surface down to mid-crustal depths. At this stop, the equigranular main phase of the pluton may represent an early crystallized top of a magma chamber that was subsequently fractured and injected with feeder dikes from a deeper level. Perhaps most surprising is the "hypabyssal" texture of these mid-crustal dikes. They are always strongly porphyritic and appear to have had glassy margins. We explain this by: 1) pressure quenching, as magmas were injected along active fractures and vented to the surface, coupled with 2) incursion of meteoric water down the same system of fractures that were guiding the magmas.

Continue up the main Water Canyon Road

1.0	33.0	End of Water Canyon Road. Turn around and park. **STOP 2**. Structural Overview of the Northern Egan Range.

We will be gone from the vehicles for approximately 2½ hours so bring lunch and water. From the end of the road, we will hike up Water Canyon into the interior of the Egan Range. Part of this walk will be through brush so it is imperative that we stick together.

A detailed account of the structural evolution of the northern Egan Range is provided by Gans and Miller (this volume). The range is composed of thin slices of steeply west-dipping upper Precambrian to Permian rocks and Oligocene volcanic rocks that are separated by low-angle normal faults. Each fault displaces overlying sections eastward with respect to underlying sections such that younger strata always rest on older. We will begin in Lower Cambrian Prospect Mountain Quartzite in the lowest structural slice, cross a low-angle fault into Upper Cambrian Dunderberg Shale and Notch Peak Limestone in the next higher slice, and finally cross another fault onto a klippa of Pennsylvanian Ely Limestone. From here we can get a broad overview of the internal structure of the northern Egan Range and discuss in detail the kinematics of normal faulting.

Return to the vehicles and drive back out the Water Canyon Road.

2.6	35.6	Turn left at mouth of Water Canyon on road that curves up to a road cut.
0.2	35.8	Park on road that bears to the right. **STOP 3**.

Here we will quickly examine an exhumed fault surface that dips 25 to 30° eastward and parallels the eastern flank of the northern Egan Range. Here a thin fault sliver of Pogonip Group separates Oligocene volcanic rocks from the lowest exposed level in the pluton - a total offset of greater than 10 km. This is *not* a detachment fault! Several high angle normal faults have merged and rotated to low angles to produce the observed juxtaposition. This fault appears to be warped over the pluton in a convex upward fashion. Continuous exposures of the fault to the north roll over from 25 to 30° eastward dips on the flank of the range to subhorizontal on top.

Continue straight on this road.

1.5 37.3 Back to main Steptoe Valley Road. Turn left.

On the left, the white outcrops on the low flank of the Egan Range consist of silicified and brecciated granite - part of the same fault zone we examined at Stop 3.

4.5 41.8 Turn right. You are now headed east across Steptoe Valley. Straight ahead is the Schell Creek Range. Reddish outcrops are exposures of the Oligocene Kalamazoo volcanic sequence (Young, 1960).

3.5 45.3 Intersect Highway 93; turn right (south).

12.0 57.3 Turn right at paved road turnoff to Duck Creek Valley (sign).

2.9 60.2 Pull over along side of road and park. **STOP 4**. Introduction to the Schell Creek Range.

Brief overview of the geology of the Schell Creek Range by P. B. Gans.

This part of the northern Schell Creek Range was mapped in detail by Young (1960). He described a sequence of faulting and tilting events that closely matches what we see in the Egan and Snake Ranges. Young (1960) was one of the first workers in east-central Nevada to document that Tertiary rocks were extensively faulted and tilted and that essentially all of that faulting in this area was Tertiary. Although he called low-angle, younger-on-older faults "thrusts," he was unsure as to their origin.

This stop provides a good view of some typical fault geometries in the northern Schell Creek Range. A low-angle fault displaces Ordovician-Silurian Dolomite eastward and drags Eureka Quartzite in the footwall into parallelism with the fault plane. This fault is then cut by a younger moderately east-dipping fault.

Continue straight on the paved road into Duck Creek Valley.

Overview of Duck Creek Valley.

Duck Creek Valley is a peculiar basin within a range. It is underlain by a thick section of predominantly west-dipping conglomerates called the North Creek Formation (Young, 1960). They unconformably overlie Oligocene volcanic rocks and Paleozoic rocks on the eastern margin of the valley and are in fault contact with Cambrian rocks on the west side. Young (1960) believed that these conglomerates were Mio-Pliocene in age and that Duck Creek Valley was

formed by relatively young Basin and Range faulting. In contrast, Anderson (1982) documented that at least the base of North Creek Formation is Oligocene and proposed that Duck Creek Valley formed as a consequence of preferential erosion of weak clastic sediments from an uplifted Oligocene basin.

1.1 61.3 Turn left onto dirt road and take right fork immediately after the turnoff.

1.9 63.2 Road off to left, cattle guard; bear right.

0.7 63.9 Outcrops of debris flows near the base of the North Creek Formation on the left; take left branch at fork.

1.2 65.1 Park on saddle. **STOP 5.** Volcanic Stratigraphy of the Schell Creek Range.

A detailed mapping and analytical investigation of the volcanic rocks in the Schell Creek Range is currently in progress by Gans and G. Mahood. We hope to use the volcanic rocks to bracket the age(s) and rate(s) of extensional deformation in this area and ultimately understand the interplay between volcanism and extension.

At this stop we will briefly examine some of these syntectonic volcanic rocks. We will start near the bottom of the Tertiary section and hike up through a basal sequence of lacustrine limestone and tuffaceous sandstones and then the three lower units of the Kalamazoo volcanic sequence. The lowest volcanic unit is a fairly distal outflow sheet of the Kalamazoo Tuff. It is overlain by a thin interval of lahars and volcanic breccias which in turn, is overlain by biotite-hornblende dacite lava flows. These units were probably all derived from a major volcanic center immediately north of Duck Creek Valley.

Return back out to the paved Duck Creek Valley Road.

3.8 68.9 Turn left on the Duck Creek Valley Road.

1.1 70.0 Turn left on gravel road toward Bird Creek (sign).

2.5 72.5 Pull into the circle and park at the Bird Creek Campground. **STOP 6.**

If time permits, we will quickly examine some excellent exposures of the North Creek Formation. The conglomerates here contain predominantly Paleozoic carbonate clasts whereas to the north the clasts are mostly derived from the Oligocene volcanic rocks. At this stop the conglomerates include clasts of Ordovician and Cambrian limestones suggesting that major structural relief had been formed by the time they were deposited. We are presently dating a rhyolite flow that overlies these conglomerate beds.

2.5 75.0 Return out to the Duck Creek Valley Road and turn right.

5.1 80.1 Return out to Highway 93 and turn left back to Ely.

17.2 97.3 Arrive Ely.

FIELD TRIP ROAD LOG: SECOND DAY

Mileage		Description
Incremental	Cumulative	
0.0	0.0	Intersection Highways 50 and 93, downtown Ely. Drive east on Highway 50.

17.8	17.8	Ascent to Connor's Pass, Schell Creek Range. Miogeoclinal strata in the Connor's Pass quadrangle (mapped by Drewes, 1967) are complexly faulted and tilted but not in a consistent direction. Both east and west tilts occur as this part of the Schell Creek Range lies within a diffuse boundary separating a northern domain of westward tilting from a southern terrane of eastward tilting (Figure 20). Most of the rocks we are driving through are Pennsylvanian-Permian limestones.
4.0	21.8	Connor's Pass. Wheeler Peak of the southern Snake Range at 2:00 in the distance (elevation 13,067 ft).
2.8	24.6	Here we cross a low-angle fault (the "Schell Creek Thrust" of Drewes [1967]) that separates brecciated Devonian rocks from metamorphosed and complexly folded middle Cambrian silty limestones. It is not clear whether this fault is a regionally extensive detachment fault or is simply a tilted normal fault. Drewes (1967) interpreted the Schell Creek Thrust as Mesozoic, but Armstrong (1972) suggested a Tertiary age as it involves Tertiary strata.
1.8	26.4	Junction of Highways 93 and 50, take left fork and continue east on 50. Mt. Moriah, the highest peak in northern Snake Range lies in the distance at 11:00.
2.0	28.4	Turn left on North Spring Valley Road. To the west, view of Cleve Creek drainage in the Schell Creek Range. Reddish talus slopes on right are underlain by Cambrian Prospect Mountain Quartzite; white cliffs are Middle Cambrian limestone. North of here, the entire eastern flank of the Schell Creek Range consists of a west-tilted section of late Precambrian and Early Cambrian clastic rocks. Up to 8,800 ft of structural section of late Precambrian McCoy Creek Group rocks (Misch and Hazzard, 1962) are exposed along this flank of the range. The high crest line of the range is underlain by Lower Cambrian Prospect Mountain Quartzite.
20.2	48.6	The light bands at the base of the first hills to the left are carbonate intervals within the lower part of the McCoy Creek Group.
3.5	52.1	Turn left on dirt road up McCoy Creek (marked with sign).
2.7	54.8	Campsite to left; turn around and park. **STOP 7.** Mesozoic Penetrative Deformation at Deep Structural Levels. At this stop, we will look at phyllites and quartzite in structurally lower exposures of the McCoy Creek Group. The attitude of deformational fabrics at this stop is typical of Mesozoic deformation elsewhere in east-central Nevada in that the prominent cleavage is west-dipping and axial planar to rare east-vergent mesoscopic folds (Figure 2). Here this cleavage crenulates an older (S1) surface that is subparallel to bedding. Both cleavages die rapidly up section and are restricted to phyllitic intervals. Sedimentary structures are very well preserved except near the bottom of the sequence and are always upright; folds are scarce to absent. Bedding-cleavage inter-

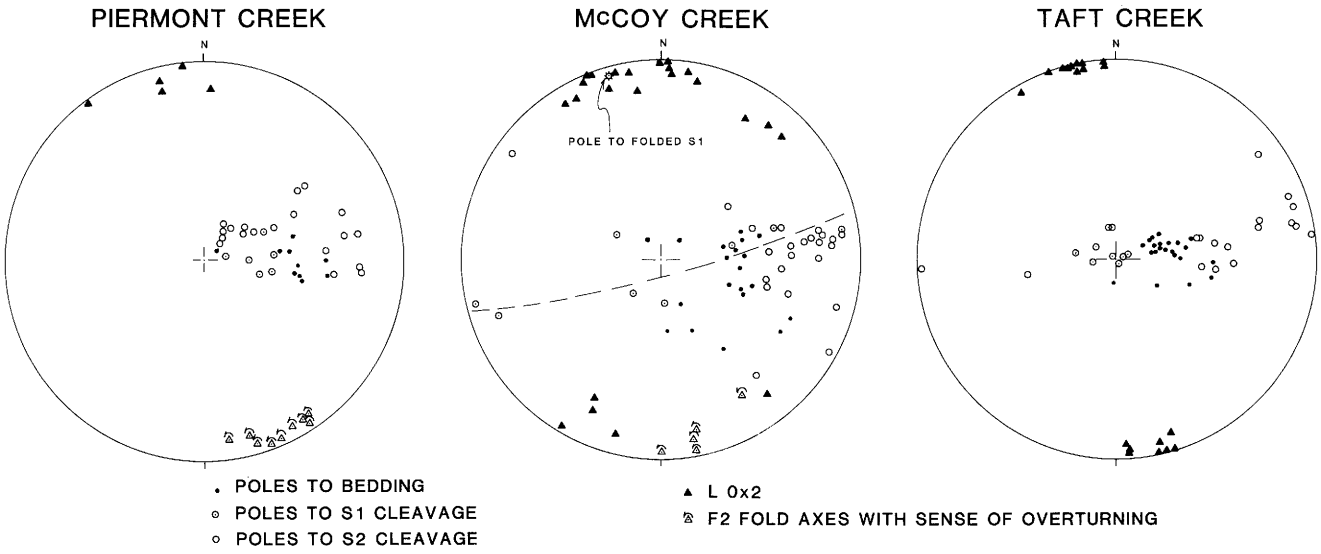

Figure 2. Structural data (lower hemisphere equal area project) from the McCoy Creek Group on the east flank of the Schell Creek Range.

section lineations are oriented north-south and are subhorizontal.

Across the Snake, Schell Creek, and Egan Ranges, deep structural levels (generally Precambrian McCoy Creek Group but locally as high as the Middle Cambrian) are variably metamorphosed (greenschist to amphibolite grade) and polyphase deformed. This deformation and metamorphism is well dated in the southern Snake Range by syn- to late-kinematic plutons that are about 160 m.y. old (Misch, 1960; Lee and others, 1968, 1980). Although deformation and metamorphism is as yet undated in the other ranges, the similarity in structural style between these three ranges suggests a similar age.

As described by Misch (1960), deformation and metamorphism across east-central Nevada increases gradually down-section and is more intense near the margins of Jurassic plutons. We feel that mid-Jurassic differential shortening with depth in the hinterland of the Sevier thrust belt may be associated with the formation of, and/or a deep-seated expression of earliest thrust movement to the east. Thus the Jurassic part of the Sevier thrust belt could root at depth here in east-central Nevada; however this entire region may be allochthonous above younger (Cretaceous) thrusts. Any such thrusts, however, would have to lie at structurally deeper levels than those exposed today, most likely within crystalline basement.

Return to paved road with possible view stop of Snake Range, depending on sun angle.

0.9 55.7 **View Stop:** The Snake Range decollement is gently domed across the northern Snake Range and separates variably metamorphosed and ductilely extended Cambrian Prospect Mountain Quartzite and Pioche Shale from faulted Cambrian Pole Canyon Limestone and younger units in the upper plate. From this vantage

point you can see the nearly flat decollement project beneath Mount Moriah, a klippe of Cambrian and Ordovician carbonate rocks. The decollement gives the northern Snake Range its flat-topped physiography; the forested bumps on this smooth surface are klippes of upper plate rocks. Along the west flank of the range, the decollement bends abruptly down towards us; the small rugged hills at 10:00 to 11:00 are klippes of upper plate Cambrian limestone resting on lower plate Prospect Mountain Quartzite.

1.6 57.3 North Spring Valley Road, head south (right).

5.8 63.1 Just before cattle guard, take a left on good graded dirt road and head east across Spring Valley towards the Snake Range.

5.1 68.2 Cross roads, turn right and drive south.

7.1 75.3 On the left is the Negro Creek - Miller Basin region of the northern Snake Range, where the best exposures of upper plate rocks are preserved. Negro Creek is an erosional window into the lower plate and is an ideal place to study the geometry of upper plate faulting and the interaction of the upper plate faults with the decollement (refer to Gans and Miller, this volume).

Unfortunately, roads into the Miller Basin-Negro Creek area are inacessible this time of year.

The bare, rolling hills further south on the left are underlain by Cambrian Prospect Mountain Quartzite. Here it is locally shattered and folded but *not* penetratively stretched as it is elsewhere in the northern Snake Range. A gently east-dipping fault separates this exposure of Prospect Mountain from faulted and tilted Paleozoic carbonate rocks (forested slopes). It is unclear whether this fault is a continuation of the Snake Range decollement, or just an "upper plate" normal fault. If it is the Snake Range decollement, "lower plate" ductile stretching must die out to the west. Alternatively, if it is an upper plate fault, the NSRD must cut down-section to the west.

0.8 76.1 Highway 50 turn left (east).

3.8 79.9 Sacramento Pass. On the right, Wheeler Peak in the southern Snake Range is near the apex of a broad dome underlain by Cambrian Prospect Mountain Quartzite, Precambrian McCoy Creek Group rocks, and Jurassic plutons (Whitebread, 1969).

2.2 82.1 The red outcrops on the left side of highway are alluvial fan deposits of the Sacramento Pass Tertiary sequence.

0.9 83.0 Bouldery exposures in the Tertiary sequence on both sides of highway are slide blocks of Eureka Quartzite and Ordovician-Silurian dolomite.

3.3 86.3 Left turn on graded dirt road and park. **STOP 8.**

From this vantage point, we can view the northern Snake Range decollement (NSRD) in the background, and the Sacramento Pass Tertiary sequence in the foreground. The NSRD is defined by a thin, subhorizontal white ledge of marble tectonite above which are

prominent cliffs of variably tilted Paleozoic limestone. The lower plate in this view consists of the Silver Creek granite which we will see at the next stop. The NSRD dives abruptly south over the southern edge of the pluton and beneath the Tertiary section in the foreground.

The Tertiary sequence consists primarily of alluvial fan conglomerates and lacustrine limestone that are syntectonic with normal faulting in the Snake Range. A detailed description of this sequence is provided by Grier (this volume). The depositional base of the Tertiary section is exposed in the foreground; Pennsylvanian-Permian Ely limestone on the right is overlain roughly conformably by a thin conglomerate followed by 35 m.y. old latite flows and rhyolite tuff (Hose and Whitebread, 1981) which form the knobby red ridge and small adjacent mounds. The pre-35 m.y. old conglomerate contains only clasts of uppermost Paleozoic formations suggesting that there was very little structural relief in this region prior to volcanism. The volcanic rocks are in turn overlain by the yellowish, well-bedded, lacustrine limestone on the right. Less resistant marl forms the slopes between the ridges.

The Sacramento Pass Tertiary section in part obscures the relationship between the northern and southern Snake Range structural domains (Figure 16). At one locality along the southwest flank of the northern Snake Range, the NSRD juxtaposes unstretched McCoy Creek and Prospect Mountain Quartzite in an *upper plate* position against ductilely stretched Middle Cambrian and older rocks in a lower plate position. These upper plate units can be traced into the southern Snake Range, where they are flat-lying beneath Wheeler Peak. Thus, if the NSRD continues southward, it must cut to deeper stratigraphic levels and lie beneath the southern Snake Range "decollement" mapped by Whitebread (1969).

Continue east on Highway 50.

3.8	90.1	Moriah's Great Basin Inn.
0.2	90.3	Junction in highway, take left fork (U.S. Highway 50 East). Take immediate left on good graded dirt road and head north.
2.1	92.4	Dip-Ranch GO SLOW.
3.1	95.5	Turn left on dirt road marked by a tire.
1.5	97.0	Great view of NSRD - we will hike up there tomorrow morning.
0.3	97.3	Road to right, continue straight.
1.5	98.8	Fork - take right.
0.1	98.9	Road to right, continue straight.
0.9	99.8	Fork, take left.
0.1	99.9	Road to right, continue straight.
0.1	100.0	Gate.
0.8	100.8	Fork - take right.
0.1	100.9	Take sharp turn to right. Just before road drops down into the drainage, turn around and park. **STOP 9**. Southernmost

Exposure of the NSRD.

Bring lunch and water with you On this hike. We will walk down the road, turn left and walk up the canyon. At the mouth of this narrow canyon, near-vertically dipping Devonian Guilmette limestone and dolomite constitute a small scrap of the upper plate along the southern flank of the northern Snake Range. As you walk in the canyon, you cross the decollement into the main biotite granite phase of the Silver Creek pluton. Here the granite has been pervasively injected by swarms of muscovite pegmatite dikes and sills. Both rock types have been variably stretched into concordance with the decollement. We will veer right and look at exposures of 1) ultra mylonitic plutonic rocks immediately beneath the decollement, and 2) thin slivers of assorted Paleozoic formations or "chaos" like structure in the upper plate.

Return to cars and head out the same way we came in.

5.5	106.4	Back at main dirt road - go right.
3.0	109.4	Ranch - slow down.
0.2	109.6	200 yards past ranch take a right on Silver Creek Road.
0.7	110.3	Reservoir turnoff to right - continue straight.
0.4	110.7	Fork - turn left and continue on the main road.
3.4	114.1	Cattle guard and turn off to right, continue straight.

At about 3:00 you see well-bedded Tertiary lacustine limestone that contains large slide blocks of Paleozoic limestone. Brown lumps on far ridge crests are slide blocks of Paleozoic dolomite and the grey ridge is a slide block of Cambrian Pole Canyon Limestone.

0.7	115.5	Cavernous outcrops on the right are more Paleozoic slide blocks.
0.3	115.8	Just beyond fence, pull over and park. **STOP 10**. Tertiary Lacustrine Limestone and Conglomerate.

Here we will examine the top of the lacustrine limestone and marl where it is interbedded with and overlain by fanglomerates. The Tertiary section here is approximately 1.8 km thick (Grier, this volume) and is repeated by at least 3 down-to-the-east, arcuate, normal faults which have rotated the sections 30° to 50° westward. The presence of enormous slide blocks of rocks as old as Middle Cambrian and clasts as old as Precambrian indicate that this sequence was deposited during active faulting and the formation of considerable structural relief. Clasts of lineated and foliated rocks such as those present in the lower plate of the NSRD are conspicuously absent in the Tertiary sequence here and elsewhere.

Back to cars and continue up the road as we drive west up Miller Basin wash, note the enormous thickness of alluvial fan deposits, and also the fact that the dip of beds remains approximately constant up section.

1.7	117.5	Small road turn off to left, pull over and park. **STOP 11**. Slide Blocks and Monolithologic Breccia.

We have just crossed a major NE-trending arcuate normal fault that downdrops alluvial fan deposits against the lacustrine limestone; the throw on this fault is about 1.6 km. We will look at slide blocks and monolithologic breccia of Paleozoic dolomite and Ordovician Eureka quartzite. They rest on alluvial fan conglomerate and are overlain by lacustrine limestone.

Back to cars and continue along road through lacustrine limestone and more dark brown dolomite slide blocks.

0.5	118.0	Intersection. Turn left and go back out to highway.
3.1	121.1	Highway 50 - turn left to Baker.
0.2	121.3	**STOP 12** (if time permits) - Roadside Rest. Here, brecciated Precambrian or Cambrian (?) quartzite lies beneath steeply dipping Tertiary deposits along an almost flat fault which apparently surfaces to the north where it dips about 30° (Figure 13). It is unclear how this fault relates geometrically to the Snake Range decollement.
6.8	128.1	Moriah's Great Basin Inn, take right fork to Baker (5 miles).
5.3	133.4	Dinner and spend the night in Baker.

FIELD TRIP ROAD LOG: THIRD DAY

Mileage Incremental	Mileage Cumulative	Description
0.0	0.0	Beginning in downtown Baker, take paved road (488) to Lehman Caves National Monument.
4.9	4.9	Turn right on Wheeler Peak Road.
3.3	8.2	**STOP 13**. View Stop of the Northern Snake Range. From this point we have a good view northward towards the Snake Range decollement and the faulted Tertiary section in Sacramento Pass. Behind you, about 3,000 ft of Prospect Mountain Quartzite is exposed on the face of Wheeler Peak. Here this impressively thick sequence of quartzite consists of beds about 1 to 3 ft thick. Remember what these rocks look like as this afternoon we will walk through a section of Prospect Mountain Quartzite that has paper-thin beds and is only a few hundred feet thick.
3.5	11.7	Serene overlook, turn around, view of mighty Wheeler Peak. Go back down 488 to Baker.
12.0	23.7	At Baker, turn left on 487 and drive north.
5.1	28.8	100 yards before Highways 50 and 487 merge, turn right on cross path, cross 50 and head north on graded Snake Valley Road.
2.1	30.9	Ranch - slow up.
3.1	34.0	Turn left at tire.
1.8	35.8	Cowpond on left, take road to right. Spectacular view of the NSRD as we drive into our next stop. Marble mylonite beneath the NSRD forms a conspicuous ledge halfway up the mountain. Tilted and faulted Paleozoic strata above the marble tectonite ledge are clearly truncated by the NSRD. The dark rocks beneath the marble mylonite are biotite granite of the Silver Creek pluton.
1.5	37.3	Sharp right turn.

0.6 37.9 Cattle pond, Y in road, bear left. As we drive into Old Man Canyon, the low hills on either side of the drainage consist of upper plate Devonian to Pennsylvanian carbonates. The decollement dips beneath us.

1.6 39.5 Park. **STOP 14**. Snake Range Decollement in Rock Canyon.

This is the type locality of the SRD as described by Misch (1960). We will hike through the deformed Silver Creek pluton up to the SRD. The Silver Creek pluton is variably deformed and chloritized; it ranges in composition from hornblende diorite to biotite granite, and contains occasional aplite dikes (also deformed). The pluton intrudes Middle Cambrian (?) marbles and calc-silicate rocks. Towards the decollement, both the pluton and pendants become mylonitized. You can actually put your finger on the decollement surface at this stop, but it is a fairly subtle fault; Pole Canyon Limestone above the decollement is recrystallized and brecciated whereas the same limestone beneath it is ductily deformed.

On the way down from the decollement, we will look at a large pendant of intricately folded calc-silicate and limestone that has "escaped" ductile stretching.

Perhaps by the time you read this guide book, we will have a U-Pb date for the Silver Creek pluton. So far, it has yielded a K-Ar biotite age of 25.5 ± 1.3 , a K-Ar white mica age of 31.1 ± 1.7 (Lee and others, 1970) and a hornblende age of 215 m.y. (R.K. Hose, personal communication).

Back to cars and return to main Snake Valley Road.

9.1 48.6 Turn left (north) on Snake Valley Road. As we drive north along the east flank of the Snake Range, the rugged brown hills you see in the foreground are upper plate klippen of mid-Paleozoic dolomite and Ordovician Eureka Quartzite. Behind the klippen are light grey-yellow, smooth slopes underlain by stretched lower plate Prospect Mountain Quartzite. The NSRD projects above the smooth hills and beneath the vegetated cliffs of upper plate in the background.

1.0 49.6 Welcome to Utah.

1.2 50.8 Main road veers to right, take left fork for 100 yards and then bear left into Hatch Rock Quarry.

3.0 53.8 Take left fork. Cavernous, brecciated Ordovicia-Silurian dolomite in the upper plate forms the ridge line to the south. The SRD is defined by a thin ledge at 10:00. The light-colored slopes below the thin ledge and straight ahead are stretched, lower plate Prospect Mountain Quartzite. The decollement dips about 15° towards us so that it barely clips the top of the hill at 2:00 where there is a little klippe of Devonian Guilmette Limestone, and projects under brecciated Cambrian limestone to our right.

0.1 53.9 Take right fork.

0.3 54.2 Take left fork.

0.5 54.7 Cattle gate. The cliffs to the left and in front of us expose impressively thinned Prospect Mountain Quartzite (uppermost quartzite unit). Quartzite and schist units beneath the

Prospect Mountain belong to the Precambrian McCoy Creek Group. The distinctive steel blue-grey schist beneath the Prospect Mountain is the Osceola Argillite, the upper-most unit of the McCoy Creek Group.

0.1 54.8 Creek crossing-Hendry's Creek. If road conditions are bad we will stop here and walk.

0.4 55.1 Bog. Park cars here and we will hike about ½ mile up the road to the first pine trees on right, then up the side of the canyon to the high ridge. **STOP 15.** Lower Plate Ductile Extension, and Discussion of the Nature and significance of the Snake Range Decollement.

Exposures of metasedimentary rocks in the deeply incised canyons along the eastern flank of the Snake Range best exhibit the ductile thinning of lower plate strata. Here, Precambrian McCoy Creek Group quartzite, schist, and overlying Cambrian Prospect Mountain and Pioche Shale are involved in a progressive ductile to brittle extensional deformation (Figures 17 and 20). The section we will hike through up the canyon wall is now less than .5 km thick, but represents an original thickness of about 3 km (Figure 15), corresponding to more than 500 percent extension. Strain is parallel to and increases towards the decollement, strain axes are oriented N 60 to 70 W(X), Z subvertical and perpendicular to the foliation and Y subhorizontal. Stretched pebbles in the McCoy Creek Group commonly have aspect ratios of 10:1:.1. Beds in the Prospect Mountain Quartzite originally 1 to 3 ft thick are now only a few inches thick, and the 4,000 ft thick Quartzite is in places only several hundred ft thick. Ductile stretching was followed by coaxial brittle extension that successively formed: 1) small-scale ductile normal faults and spaced "extensional cleavage", 2) micro and mesoscopic conjugate brittle normal faults, and 3) subvertical joints perpendicular to the earlier direction of ductile extension.

This progressive extensional deformation affected amphibolite grade rocks, but apparently occurred at lower greenschist grade conditions, as exhibited by the synkinematic growth of retrograde chlorite and white mica. Older metamorphic minerals such as biotite and muscovite have been mechanically rotated into parallelism with the new stretching fabric, but quartz has behaved ductilely. Where the older metamorphic fabric was steep with respect to the new strain axes, it was kinked about subhorizontal axial planes. Older synkinematic metamorphic fabrics are preserved in rotated, bent, broken, and twisted porphyroblasts.

From the top of the ridge between Hendry's and Hampton Creek drainages there is an excellent view of the Snake Range decollement and of the lower plate units. The view to the east towards the Confusion Range is approximately parallel with the new COCORP line and an opportune location for discussing the subsurface extent of the Snake Range decollement.

Return to cars and go back to Snake Valley Road.

Turn right and go back to Highway 50.

Highway 50, go east back to Delta and Salt Lake City.

REFERENCES CITED

Ahlborn, R. C., 1977, Mesozoic-Cenozoic structural development of the Kern Mountains, eastern Nevada and western Utah: Brigham Young University Geology Studies, v. 24, pt. II, p. 117-131.

Allmendinger, R. W., and Jordan, T. E., 1981, Mesozoic evolution, hinterland of the Sevier orogenic belt: Utah Geology, v. 9, p. 308-313.

Anderson, R. E., in press, Cenozoic structural history of selected areas in the eastern Great Basin, Nevada-Utah: U.S. Geologic Survey Open-File Report.

Armstrong, R. L., 1968, Sevier orogenic belt in Nevada and Utah: Geological Society of America Bulletin, v. 79, p. 429-458.

———, 1972, Low-angle (denudational) faults, hinterland of the Sevier Orogenic Belt, eastern Nevada and western Utah: Geological Society of America Bulletin, v. 83, Earth Science Bulletin, p. 1729-1754.

Avent, J. C., 1961, Geologic map of the Antelope Range, northeastern White Pine County, Nevada: M.S. thesis, Washington University.

Best, M. G., Armstrong, R. L., Graustein, W. C., Embree, G. F., and Ahlborn, R. C., 1974, Mica granites of the Kern Mountains pluton, eastern White Pine County, Nevada: Remobilized basement of the Cordilleran miogeocyncline?: Geological Society of America Bulletin, v. 85, p. 1277-1286.

Blake, M. C., Jr., and Hose, R. K., 1968, Petrology of Tertiary volcanic rocks, southern Antelope Range, White Pine County, Nevada (abs.): Geological Society of America Special Paper 101, p. 388.

Blake, M. C., Jr., Hose, R. K., and McKee, E. H., 1969, Tertiary volcanic stratigraphy of White Pine County, Nevada (abs.): Geological Society of America, Rocky Mountain Section, 22nd Annual Meeting, Salt Lake City, Utah Program, pt. 5, p. 8.

Brokaw, A. L., 1967, Geologic map and section of the Ely quadrangle, White Pine County, Nevada: U.S. Geological Survey Geologic Quadrangle Map GQ-697.

Brokaw, A. L., Bauer, H. L., and Beitrick, R. A., 1973, Geologic map of the Ruth quadrangle, White Pine County, Nevada: U.S. Geological Survey Map GQ-1085.

Brokaw, A. L., and Barosh, P. J., 1968, Geologic map of the Riepetown quadrangle, White Pine County, Nevada: U.S. Geological Survey Geologic Quadrangle Map GQ-758.

Brokaw, A. L., and Heidrick, T., 1966, Geologic map and sections of the Giroux Wash quadrangle, White Pine County, Nevada: U.S. Geological Survey Geologic Quadrangle Map GQ-476.

Brokaw, A. L., and Shawe, D. R., 1965, Geologic map and sections of the Ely 3 SW quadrangle, White Pine County, Nevada: U.S. Geological Survey Miscellaneous Geological Investigations Map I-449.

Cebull, S. E., 1970, Bedrock geology and orogenic succession in the southern Grant Range, Nye County, Nevada: American Association of Petroleum Geologists Bulletin, v. 54, p. 1828-1842.

Christiansen, R. L., and Lipman, P. W., 1972, Cenozoic volcanism and plate-tectonic evolution of the western United States. II. Late Cenozoic: Royal Society of London Phil. Trans. A 271, p. 217-248.

Colletta, B. and Angelier, J., 1982, Sur les systems de blocs failles bascules associes aux fortes extensions: etude preliminaire d'exemples ouest-americains (Nevada, U.S.A. et Basse-Californie, Mexique), Comptes Rendus Acad. Science Paris t. 294, s. 11, p. 467-469.

Compton, R. R., Todd, V. R., Zartman, R. E., and Naesser, C. W., 1977, Oligocene and Miocene metamorphism, folding, and low angle faulting in northwestern Utah: Geological Society of America Bulletin, v. 88, p. 1237-1251.

Coney, P. J., 1974, Structural analysis of the Snake Range decollement, east-central Nevada: Geological Society of America Bulletin, v. 85, p. 973-978.

———, 1978, Mesozoic-Cenozoic Cordilleran plate tectonics, *in* Smith, R. B., and Eaton, G. P., eds., Cenozoic tectonics and regional geophysics of the western Cordillera, Geological Society of America Memoir 152, p. 33-50.

———, 1979, Tertiary evolution of Cordilleran metamorphic core complexes, *in* Armentrout, J. W., and others, eds., Cenozoic Paleogeography of the Western United States: Society of Economic Paleontologists and Mineralogists, Pacific Section Symposium III, p. 15-28., Geological Society of America Memoir 153, p.7-31.

Coney, P. J., and Reynolds, S. J., 1977, Cordilleran Benioff zones: Nature, v. 270, p. 403-406.

Crittenden, M. D. Jr., Coney, P. J., and Davis, G. H., 1980, Cordilleran Metamorphic Core Complexes, Geological Society of America Memoir 153, 490 p.

Davis, G. A., 1979, Problems of intraplate extensional tectonics, western U.S. with special emphasis on the Great Basin; *in* Newman, G. W., and Goode, H. D., 1979, eds., Basin and Range Symposium and Great Basin field conferences: RMAG-UGA, p. 41-54.

Davis, G. A., Anderson, J. L., Frost, E. G., and Shackelferd, T. J., 1980, Mylonitization and detachment faulting in the Whipple-Buckskin-Rawhide Mountains terrane, southeastern California and western Arizona, *in* Cordilleran Metamorphic Core Complexes, Crittenden, M. D., Jr., Coney, P. J., and David, G. H., eds., Geological Society of America, Inc., Memoir 153, p. 79-130.

Davis, G. H., 1980, Structural characteristics of metamorphic core complexes, southern Arizona; *in* Crittenden, M. D., Jr., Coney, P. J., and Davis, G. H., eds., Cordilleran Metamorphic core complexes: Geological Society of America, Inc., Memoir 153, p. 35-78.

Dechert, C. P., 1967, Bedrock geology of the northern Schell Creek Range, White Pine County, Nevada: Ph.D. dissertation, University of Washington.

Drewes, H., 1967, Geology of the Connors Pass quadrangle, Schell Creek Range, east-central Nevada: U.S. Geological Survey Professional Paper 557.

Eaton, G. P., 1982, The Basin and Range Province: Origin and tectonic significance: Annual Review of Earth and Planetary Sciences, 1982, v. 10, p. 409-440.

Engebretson, D. C., and Cox, A., 1982, Plate interactions in the NE Pacific since the Oxfordian, EOS, v. 63, no. 45, p. 910.

Fritz, W. H., 1960, Structure and stratigraphy of the northern Egan Range, White Pine County, Nevada: Ph.D. dissertation, Washington University.

Fritz, W. H., 1968, Geologic map and sections of the southern Cherry Creek and northern Egan Ranges, White Pine County, Nevada: Nevada Bureau Mines, Map 35.

Gans, P. B., 1982, Geometry of mid-Tertiary extensional faulting, northern Egan Range, east-central Nevada, Abstract, submitted to Geological Society of America Cordilleran Section Meeting.

———, 1982b, Mid-Tertiary magmatism and extensional faulting in the Hunter district, White Pine County, Nevada: M.S. thesis, Stanford University.

Hamilton, W., and Meyers, W. B., 1966, Cenozoic tectonics of the western U.S.: Rev. Geophysics, v. 4, p. 509-549.

Hazzard, J. C., Misch, P., Wieses, J. H., and Bishop, W. C., 1953, Large-scale thrusting in northern Snake Range, White Pine County, north-eastern Nevada (abs.): Geological Society of America Bulletin, v. 64, p. 1506-1508.

Hintze, L. F., 1980, Geologic map of Utah: Utah Geological and Mineral Survey, scale 1:500,000.

———, 1978, Sevier orogenic attenuation faulting in the Fish Springs and House Ranges, western Utah: Brigham Young University Geology Studies, v. 25, pt. 1, p. 11-24.

Holdaway, M. J., 1971, Stability of andalusite and the aluminum silicate phase diagram: American Journal of Science v. 271, p. 97-131.

Hose, R. K., 1977, Structural geology of the Confusion Range, west-central Utah: U.S. Geological Survey Professional Paper 971, 9 p.

———, 1981, Geologic map of the Mount Moriah further planning (Rare II) area, eastern Nevada: U.S. Geological Survey Map MF-1244A (in press).

Hose, R. K., and Danes, Z. E., 1973, Development of late Mesozoic to early Cenozoic structures of the eastern Great Basin; *in* DeJong, K. A., and Scholten, R., eds., Gravity and Tectonics: New York, John Wiley and Sons, p. 429-441.

Hose, R. K., and Blake, M. C., Jr., 1976, Geology and mineral resources of White Pine County, Nevada: Part I, Geology: Nevada Bureau of Mines and Geology Bulletin 85, 105 pp.

Hose, R. K., and Whitebread, D. H., 1981, Structural evolution of the central Snake Range, eastern Nevada during the mid-to-late Tertiary: Geological Society of America Abstract with Programs, v. 113, p. 62.

Jordan, T. E., and Allmendinger, R. W., 1982, Mesozoic evolution, hinterland of the Sevier orogenic belt: Comment and Reply, Geology, v. 10, p. 5-6.

Keith, S. B., 1978, Paleosubduction geometries inferred from Cretaceous and Tertiary magmatic patterns in southwestern North America: Geology, v. 6, p. 516-521.

Kellogg, H. E., 1964, Cenozoic stratigraphy and structure of the southern Egan Range, Nevada: Geological Society of America Bulletin, v. 75, p. 949-968.

King, P. B., 1969, Tectonic map of North America, U.S. Geological Survey, scale 1:5,000.000.

Lee, D. E., Marvin, R. F., Stern, T. W., Mays, R. E., and Van Loenen, R. E., 1968, Accessory zircon from granitoid rocks of the Mount Wheeler mine area, Nevada *in* Geological Survey Research, 1968: U.S. Geological Survey Professional Paper 600-D, p. D197-D203.

Lee, D. E., Marvin, R. F., Stern, T. W., and Peterman, Z. E., 1970, Modification of K-Ar ages by Tertiary thrusting in the Snake Range, White Pine County, Nevada, *in* Geological Survey Research, 1970: U.S. Geological Survey Professional Paper 700-D, p. D93-D102.

Lee, D. E., Marvin, R. F., and Mehnert, H. H., 1980, A radiometric age study of Mesozoic-Cenozoic metamorphism in eastern White Pine County, Nevada and nearby Utah, U.S. Geological Survey Professional Paper 1158C, p. C17-C28.

Lee, D. E., Kistler, R. W., and Robinson, A. C., (in press), The strontium Isotope Composition of Granitoid Rocks of the southern Snake Range, Nevada, Shorter Contributions to Isotope Research, U.S. Geological Survey, Professional Paper.

Lee, D. E., Stacey, J. S., and Fischer, L., (in press), Muscovite-phenocrystic two-mica granites of northeastern Nevada are late Cretaceous in age: Shorter Contributions to Isotope Research, U.S. Geological Survey Professional Paper.

Le Pichon, X., Angelier, J., and Sibuet, J. C., 1982, Plate boundaries and extensional tectonics: Tectonophysics, v. 81, p. 239-256.

Luth, W. C., 1976, Granitic Rocks; *in* Bailey, D. K., and MacDonald, R., eds., The evolution of crystalline rocks: New York, Academic Press.

MacDonald, R., 1974, Tectonic settings and magma associations, *in* Bailey, D. K., Barbeiri, F., and MacDonald, eds., Oversaturated peralkaline rocks: Bulletin, Volcanologique Fiftieth Anniversary Volume, v. 38.

Miller, E. L., Gans, P. B. and Garing, J. D., 1983, An ex-

humed ductile-brittle transition in the Snake Range, Nevada, Tectonics, (in press).

Misch, P., 1960, Regional structural reconnaissance in central-northeast Nevada and some adjacent areas: observations and interpretations: Intermountain Association of Petroleum Geology 11th Annual Field Conference Guidebook, p. 17-42.

Misch, P., and Hazzard, J. C., 1962, Stratigraphy and metamorphism of Late Precambrian rocks of central northeast Nevada and adjacent Utah: American Association Petroleum Geologists Bulletin, v. 46, p. 289-343.

Moores, E. M., Scott, R. B., and Lumsden, W. W., 1968, Tertiary tectonics of the White Pine-Grant Range region, east-central Nevada, and some regional implications: Geological Society of America Bulletin, v. 79, p. 1703-1726.

Morton, W. H., and Black, R., 1975. Crustal attenuation in Afar; *in* Pilger, A., and Resler, A., eds., Afar depression of Ethiopia, Inter-union commission on Geodynamics: International Symposium on the Afar Region and Related Rift Problems, E. Schweizerbart'sche Verlagsbuchhandlung, Stuttgart, Germany. Proceedings, Scientific Report no. 14, p. 55-65.

Nelson, R. B., 1959, The stratigraphy and structure of the northernmost part of the northern Snake Range and Kern Mountains in eastern Nevada and the southern Deep Creek Range in western Utah: Ph.D. dissertation. Washington University.

Nelson, R. B., 1966, Structural development of the northernmost Snake Range, Kern Mountains, and Deep Creek Range, Nevada and Utah: American Association Petroleum Geologists Bulletin, v. 50, p. 921-951.

Noble, L. F., 1941, Structural features of the Virgin Spring area, Death Valley, California, Geological Society of America Bulletin, v. 52, p. 941-999.

Playford, P. E., 1961, Geology of the Egan Range, near Lund, Nevada: Ph.D. dissertation, Stanford University.

Proffett, J. M., Jr., 1977, Cenozoic geology of the Yerington district, Nevada, and implications for the nature and origin of basin and range faulting: Geological Society of America Bulletin, v. 88, p. 247-266.

Rehrig, W. A., and Reynolds, S. J., 1980, Geologic and geochronologic reconnaissance of a northwest-trending zone of metamorphic complexes in southern Arizona; *in* Tectonic significance of metamorphic core complexes of the North American Cordillera, Crittenden, M. D., Jr., Coney, P. J., and Davis, G. H., eds., Geological Society of America Memoir 153, p. 157.

Rowles, L., 1982, Deformational history of the Hampton Creek Canyon Area, N. Snake Range, Nevada: M.S. thesis, Stanford University.

Smith, R. L. and Bailey, R. A., 1966, The Bandalier Tuff: A study of ash-flow eruption cycles from zoned magma chamber: Bulletin Volcanol., v. 29, p. 83-104.

Snoke, A. W., Durgin, S. L., and Lush, A. P., 1982, Structural Style variations in the northern Ruby Mountains- East Humbolt Range, Nevada: Geological Society of America Abstracts with Programs, v. 14, no. 4, p. 235.

Snyder, W. S., Dickinson, W. R., and Silberman, M. L., 1976, Tectonic synthesis of space-time patterns of Cenozoic magmatism in the western United States: Earth Planet, Science Letters, v. 32, p. 91-106.

Speed, R. C., 1978, Paleogeographic and plate tectonic evolution of the early Mesozoic marine province of the western Great Basin; *in* Mesozoic Paleogeography of the western United States, Howell, D. G., and McDougall, K. A., eds., Pacific Coast Paleogeography Synposium 2: Society of Economic Paleontologists and Mineralogists, Pacific Section, p. 253-270.

Stewart, J. H., and Poole, F. G., 1974, Lower Paleozoic and uppermost Precambrian of the Cordilleran Miogeocline, Great Basin, western United States; *in* Dickinson, W. R., ed., Tectonics and Sedimentation, SEPM Special Publication no. 22, p. 28-57.

Stewart, J. H., and Carlson, J. E., 1978, Geologic map of Nevada, U.S. Geological Survey, scale 1:500,000.

Stewart, J. H., and Carlson, J. E., 1976, Cenozoic rocks of Nevada-Four maps and brief description of distribution, lithology, age, and centers of volcanism: Nevada Bureau Mines Geological Map 52, 4 sheets, text, 5 p., scale 1:1,000,000.

Thompson, G. A., 1960, Problems of late Cenozoic structure of the Basin Ranges: International Geological Congress 21st, Copenhagen, pt. XVIII, p. 62-68.

Wernicke, B., 1981, Low Angle Normal Faults in the Basin and Range Province: map tectonics in an extending orogen: Nature, v. 291, p. 645.

_____, 1982, Mesozoic evolution, hinterland of the Sevier orogenic belt: Comment and Reply, Geology v. 10 p. 3-5.

_____, 1982, Cenozoic Dilation of the Cordilleran orogen and its relation to plate tectonics: EOS, v. 63 no. 45, p. 914.

Whitebread, D. H., 1969, Geologic map of the Wheeler Peak and Garrison quadrangles, Nevada and Utah: U.S. Geological Survey Map I-578.

Woodward, L. A., 1962, Structure and stratigraphy of the central Egan Range, White Pine County, Nevada: Ph.D, dissertation, University of Washington.

Young, J. C., 1960, Structure and stratigraphy in the north central Schell Creek Range, eastern Nevada: Ph.D. dissertation, Princeton University.J.

Zoback, M. L., Anderson, R. E., and Thompson, G. A., 1981, Cainozoic evolution of the state of stress and style of tectonism of the Basin and Range province of the western U.S.: Phil. Trans. R. Society of London (in press).

UTAH GEOLOGICAL AND MINERAL SURVEY

606 Black Hawk Way
Salt Lake City, Utah 84108-1280

THE UTAH GEOLOGICAL AND MINERAL SURVEY is a Division of the Utah Department of Natural Resources and Energy and operates under the guidance of a Governing Board appointed by the Governor from industry and the public-at-large. The Survey is instructed by law to collect and distribute reliable information concerning the mineral resources, topography, and geology of the state, to investigate areas of geologic and topographic hazards that could affect the citizens of Utah, and to support the development of natural resources within the state. The *Utah Code annotated, 1953 Replacement Volume 5, Chapter 36, 53-36-1 through 12,* describes the Survey and its functions.

The Survey publishes bulletins, maps, a quarterly newsletter, and other publications that describe the geology of the state. Write for the latest list of publications available.

THE SAMPLE LIBRARY is maintained to preserve well cuttings, drill cores, stratigraphic sections, and other geological samples. Files of lithologic, electrical, and mechanical logs of oil and gas wells drilled in the state are also maintained. The library's collections have been obtained by voluntary donation and are open to public use, free of charge.

THE UTAH GEOLOGICAL AND MINERAL SURVEY adopts as its official policy the standard proclaimed in the Governor's Code of Fair Practices that it shall not, in recruitment, appointment, assignment, promotion, and discharge of personnel, discriminate against any individual on account of race, color, religious creed, ancestry, national origin, or sex. It expects its employees to have no interest, financial or otherwise, that is in conflict with the goals and objectives of the Survey and to obtain no personal benefit from information gained through their work as employees of the Survey. For permanent employees this restriction is lifted after a two-year absence, and for consultants the same restriction applies until publication of the data they have acquired.

Archive Approval No. 1830079
Account No. 016103